UNIVERSITEIT GENT

IDENTIFICATION AND CHARACTERIZATION OF MONOCLONAL ANTIBODY 14C5

A potential agent for radioimmunodetection and –therapy

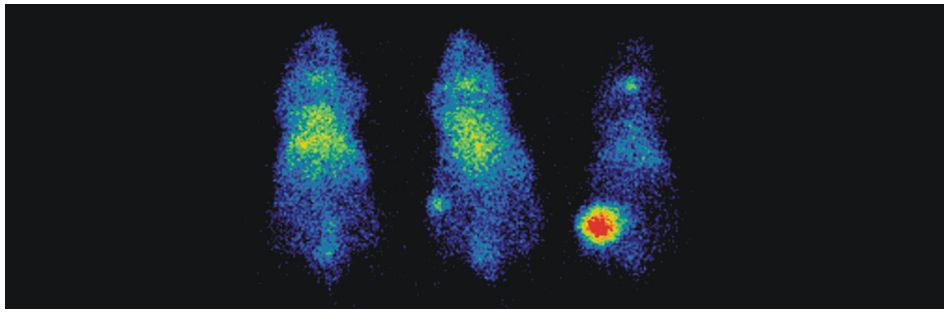

PROEFSCHRIFT

Voorgelegd tot het verkrijgen van de graad van

Doctor in de Farmaceutische Wetenschappen

aan de

Faculteit Farmaceutische Wetenschappen
Laboratorium voor Radiofarmacie
Universiteit Gent,

Door:

Ingrid Burvenich

Promotor : Prof. Dr. G. Slegers
Co-promotors : Prof. Dr. N. Mertens
Prof. Dr. F. De Vos

2007

Front cover : Radioimmunodetection with ^{123}I-labeled monoclonal antibody 14C5 in A549 non-small cell lung tumour-bearing mice. From left to right: tumour weight 7 mg, 140 mg and 1 g

UNIVERSITEIT GENT

IDENTIFICATION AND CHARACTERIZATION OF MONOCLONAL ANTIBODY 14C5

A potential agent for radioimmunodetection and –therapy

PROEFSCHRIFT

Voorgelegd tot het verkrijgen van de graad van

Doctor in de Farmaceutische Wetenschappen

aan de

Faculteit Farmaceutische Wetenschappen
Laboratorium voor Radiofarmacie
Universiteit Gent,

Door:

Ingrid Burvenich

Promotor : Prof. Dr. G. Slegers
Co-promotors : Prof. Dr. N. Mertens
Prof. Dr. F. De Vos

2007

LEES- EN EXAMENCOMMISSIE

Prof. Dr. Jean Paul Remon
Decaan en voorzitter
Vakgroep Geneesmiddelenleer, UGent

Prof. Dr. Jan Van Bocxlaer
Secretaris
Vakgroep Bioanalyse, UGent

Prof. Dr. Guido Slegers
Promotor
Vakgroep Farmaceutische Analyse, UGent

Prof. Dr. Nico Mertens
Co-promotor
Moleculaire Immunobiotechnologie, VIB-UGent

Prof. Dr. Filip De Vos
Co-promotor
Vakgroep Farmaceutische Analyse, UGent

Prof. Dr. Daisy Vanrompay
Vakgroep Moleculaire Biotechnologie, UGent

Prof. Dr. Marleen Praet
Vakgroep Pathologische Anatomie, UZ-UGent

Prof. Dr. Dieter Deforce
Vakgroep Geneesmiddelenleer, UGent

Prof. Dr. John Mertens
Dienst Nucleaire Geneeskunde / BEFY, VUB

Prof. Dr. Stefaan De Smedt
Vakgroep Geneesmiddelenleer, UGent

Prof. Dr. Otto Boerman
Departement Nucleaire Geneeskunde
Radboud Universiteit, Nijmegen, Nederland

ACKNOWLEDGEMENTS

DANKWOORD

Al wist ik het toen nog niet, dit doctoraat startte zes jaar geleden op het N. Goormaghtigh Instituut, toen ik daar mijn thesisjaar voor het behalen van mijn bio-ingenieursdiploma, kon beginnen bij wijlen Prof. Christian De Potter. Er zat een antilichaam in een ijskast (met een bizarre naam 14C5) dat mogelijks interessant kon zijn als geneesmiddel tegen kanker en er waren geen garanties tot wetenschappelijk succes (zijn er ooit?). Ondertussen zijn we zes jaar verder, heeft het onderzoek naar het antilichaam 14C5 zowel geleid tot het behalen van mijn ingenieursdiploma als tot het afwerken van dit doctoraatswerk. Hoog tijd voor een oprecht woord van DANK.

Mijn eerste dank gaat uit naar mijn *promotor Prof. Guido Slegers* die het voor mij heeft mogelijk gemaakt om dit doctoraatswerk te verwezenlijken. Dank u wel voor de leerrijke kansen, de kritische geest en de vele mogelijkheden tot samenwerking. Ook *Prof. Filip De Vos* wil ik alvast bedanken voor het overnemen van de fakkel en de springplank naar een boeiend vervolg van het 14C5 project.

Mijn *co-promotor Prof. Nico Mertens* wil ik bedanken voor het helpen creëren van een breder onderzoekskader. De biotechnologische wereld werd hierdoor geopend voor 14C5 en leidde tot het identificeren van het antilichaam en het antigeen. Grote dank ook om mij voor te stellen aan *Ir*. *Steve Schoonooghe*.

Steve, we hebben vele boeiende jaren achter de rug. Jij betekende voor mij 'een partner in crime'. Bedankt voor de vele hulp en wetenschappelijke bijdrage bij dit doctoraat, maar ook voor het plezier en de vriendschap, de onverstaanbare dubbele negaties en de soms West-Vlaamse klank in mijn hedendaags taalgebruik. Ik heb echt genoten van onze samenwerking en hoop op een mogelijkheid om dit 'dream team' in de toekomst verder te zetten!

Prof. Claude Cuvelier en *Prof. Marleen Praet* van het N. Goormaghtigh Instituut wil ik bedanken om me er na mijn thesisjaar thuis te mogen blijven voelen op de dienst en er gebruik te mogen maken van de vele faciliteiten. *M.D. Lieve Vanwallegem* en *M.D. Jacques Vanhuysse* wil ik in het bijzonder bedanken voor de intense hulp bij de immunohistochemie!

Mijn 'geestelijke' mentoren wil ik oprecht bedanken vanuit mijn hart. De ooievaar die me mAb 14C5 bracht en hij die me leerde dat "*het onderzoek altijd moet doorgaan*" (wijlen *Prof. Christian De Potter*), hij die in mij al een doctoraatsstudent zag toen ik het nog niet kon zien (thesisbegeleider *Dr. John Van Emmelo*) en mijn toenmalige thesiscoaches *Dr. Lic. Elisabeth Coene* en *Ir. Anouk Waeytens*, die van in het begin voor mij een voorbeeld waren van gedrevenheid,

doorzettingsvermogen en werklust en me steeds vanachter de schermen bleven steunen. Dank je wel!

De *collega's* van op het *labo Radiofarmacie* (Bart, Christophe, Elke, Frank, Katia, Leonie, Liesbet, Magalie, Marleen, Fidu, Peter, Rien, Ruth, Sylvie, Thomas, Veerle), *de Routine* (Davy, Dirk, Elke, Fijo, Joeri, Lieve, Nico, Patricia, Valerie), *secretaresse* Ghilaine (die me verloste van het SAP) en *Unit 11* (An, Els, Miek, Rudy, Stefaan, Yannick): bedankt voor het delen van plezier en leed! We hebben ons dikwijls geamuseerd, we hebben ook samen gevloekt,…maar we hebben vooral memorabele jaren beleefd vol fantastische herinneringen, die me voor de rest van mijn leven zullen bijblijven!

Mijn hardwerkende thesisstudenten (*Karen, Vicky, Katelijn, Ellen, Jelle, Caroline en Veerle*) wil ik bedanken voor jullie volledige inzet. Jullie hebben vaak mee tot de late uren het vele wetenschappelijke werk geleverd. Jullie betekenden voor mij veel energie en motivatie, en ik wens jullie nog veel succes toe met alles wat jullie later doen! Caroline en Veerle wens ik in het bijzonder nog veel sterkte bij het schrijven van hun thesis op het einde van dit academiejaar.

Mijn familie, vrienden en Peter wil ik bedanken voor hun geduld, voor de vele steun en voor mijn rijkelijk leven los van stress en werkalcoholisme. Jullie betekenen heel veel voor mij en zijn een bron van kracht bij alles wat ik doe.

Bedankt!

Ingrid Burvenich

TABLE OF CONTENTS

LIST OF ABBREVIATIONS

Å	Angstrom, 1×10^{-10} meters
ABL	Abelson murine leukaemia oncogene
ADCC	antibody-dependent cellular cytotoxicity
ADEPT	antibody-directed enzyme prodrug therapy
AML	acute myeloid leukaemia
APL	acute promelotic leukaemia
ATP	adenosine triphosphate
ATRA	all-*trans*-retinoic acid
BFC	bifunctional chelating agents
bFGF	basic fibroblast growth factor
BCR	breakpoint cluster region
C	constant domain of antibody
C1q	complement component 1q
C3bR	complement 3b receptor
CAF	cancer-associated fibroblasts
CDC	complement-mediated cytotoxicity
CDR	complementarity-determining regions
CEA	carcinoembryonic antigen
CLL	chronic lymphocytic leukaemia
CML	chronic myeloid leukaemia
CRC	colorectal cancer

CHOP	Cyclophosphamide, Doxorubicin or Hydroxydaunorubicin, Vincristine, Prednisolone
Col	collagen
CT	computed tomography
DNA	deoxyribonucleic acid
Dr	death receptor
DTPA	diethylenetriaminepentaacetic acid
EDTA	ethylenediaminetetraacetic acid
EMEA	European Medicines Agency
EGFR	epidermal growth factor receptor, ERBB1
EGP-1	epidermial glycoprotein 1
ER	estrogen receptor
Fab	antigen binding fragment
FAP	fibroblast activation protein
Fc	Fragment crystallisable
Fd	VH-CH1 chain
FDA	Food and Drug administration
FDG	[18F]fluorodeoxyglucose
Fg	fibrinogen
FLT3	fetal liver (or Fms-like) tyrosine kinase 3
Fn	fibronectin
GIST	gastrointestinal stromal tumour
HACA	human anti-chimer antibody
HAMA	human anti-mouse antibody response
HCC	hepatocellular carcinoma
HER2/neu	herceptin receptor, ERBB2
HNSCC	head and neck squamous-cell carcinoma
ID	injected dose
IgG	immunoglobulin G
i.p.	intraperitoneally
iTLC	instant thin layer chromatography
K_d	dissociation constant
k_{off}	off rate constant
k_{on}	on rate constant
KIT	stem cell factor receptor, C-KIT

L	VL-CL chain
LET	linear energy transfer
Ln	laminin
mAb	monoclonal antibody
MAC	membrane attack complex
MAPK	mitogen-activated protein kinase, MEK
MMP	matrix metalloproteinase
MMPI	matrix metalloproteinase inhibitor
MRI	magnetic resonance imaging
mTOR	mammalian target of rapamycin
NHL	non-Hodgkin's lymphoma
NFκB	nuclear factor kappa B
NK	natural killer cell
NRI	near infrared optical imaging
NSCLC	non-small cell lung cancer
Opn	osteopontin
PCL	perlecan
PDGFR	platelet derived growth factor receptor
PET	positron emission tomography
p.i.	post injection
PI3K	phosphatidyl inositol-3-kinase
PKB/Akt	protein kinase B
PKC	protein kinase C
PML	promyelotic
PSMA	prostate specific membrane antigen
pY	phosphorylated tyrosine
RARα	retinoic acid receptor-alpha
RCC	renal cell carcinoma
RET	neurotrophic factor receptor
RGD	arginine-glycine-aspartate peptide motive
RID	radioimmunodetection
RIT	radioimmunotherapy
RTK	receptor tyrosine kinase
s.c.	subcutaneous(ly)
scFv	single chaine veraible fragment

SMKI	small molecule kinase inhibitor
SPECT	single photon emission computed tomography
$t_{½}$	half-life
TAG-72	tumour-associated glycoprotein 72
TK	tyrosine kinase
TKI	tyrosine kinase inhibitor
Tn	tenascin
TRAIL R1	tumour necrosis factor-related apoptosis-inducing ligand receptor 1
TRAIL R2	tumour necrosis factor-related apoptosis-inducing ligand receptor 2
Tsp	thrombospondin
V	variable domain of antibody
VEGF	vascular endothelial growth factor
Vn	vitronectin
vWF	von Willebrand factor

Chapter 1

INTRODUCTION

1.1 Use of monoclonal antibodies in targeting cancer

Surgery and external radiation therapy are the major treatment modalities for primary tumours and large metastases (Fig. 1.1). Chemotherapy is used for disseminated tumour diseases and may be curative in cases of lymphomas, testicular tumours and tumours in the paediatric group.

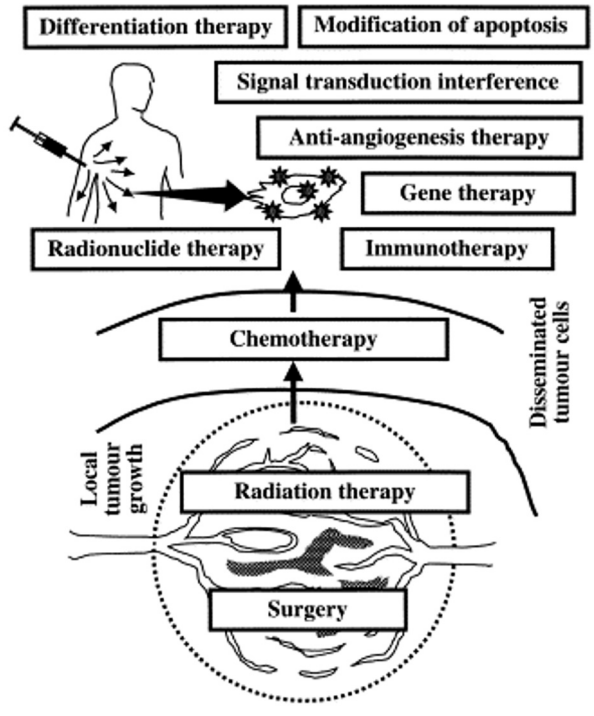

Fig. 1.1. Schematic illustration of strategies for tumour therapy. Surgery and external radiation therapy form the basis when locally growing tumour masses are treated. Chemotherapy in various forms is applied when there is tumour cell dissemination. New therapy approaches will be tried when chemotherapy is not effective in its present forms and these can be based on e.g. signal transduction interference with kinase inhibitors or modification of apoptotic processes. Some general and `biology-based´ concepts are immunotherapy, differentiation therapy, anti-angiogenesis therapy and gene therapy. Radionuclide therapy is based on the same effect mechanism as external radiation therapy, namely induction of severe DNA-damage, and is therefore a form of radiotherapy. However, radionuclide therapy is placed among the new forms of `biology-based´ therapies because it is dependent to a large extent on antigen and receptor expression and the biological factors that regulate them. (Carlsson et al., 2003)

Table 1.1 FDA-approved agents and the spectrum of targeted cancers (Abou-Jawde et al., 2003; Imai and Takaoka, 2006)

		Targeted cancer												
		Solid tumours						**Haematological tumours**						
Agent	**Target for agent and mechanism of action**	**NSCLC**	**Breast Cancer**	**CRC**	**GIST**	**Renal cancer**	**Pancreatic cancer**	**HNSCC**	**AML**	**APL**	**B-cell CLL**	**CML**	**B-cell lymphoma**	**Multiple myeloma**
mAbs														
Cetuximab (Erbitux)	EGFR (ERBB1)			√‡				√§						
Trastuzumab (Herceptin)¶	HER2 (ERBB2)		√											
Bevacizumab (Avastin)#	VEGF			√										
Rituximab (Rituxan)**	CD20												√	
Ibritumomab tiuxetan (Zevalin)* $^{111}In/^{90}Y$	CD20												√	
Tositumomab (Bexxar)* ^{131}I	CD20												√	
Gemtuzumab ozo-gamicin (Mylotarg)‡‡	CD33								√					
Alemtuzumab (Campath-1H)	CD52										√			
Small-molecule inhibitors														
Imatinib mesylate (Gleevec)	TKs (BCR-ABL, KIT, PDGFR)				√							√		
Gefitinib (Iressa)	TK (EGFR)	√												
Erlotinib (Tarceva)	TK (EGFR)	√					√§§							
Sunitinib (Sutent)	TKs (VEGFR, PDGFR, KIT, FLT3, RET)				√	√								
Sorafenib (Nexavar)	Kinases (B-Raf, VEGFR2, EGFR, PDGFR)					√								
Bortezomib (Velcade)	20S proteasome													√
All-trans-retinoic acid (ATRA)	Induces promyelotic differentiation (PML-RARα)									√				
Arsenic trioxide	Direct effect on the mitochondria, apotosis (PML-RARα)									√				

Agents are shown as generic names with trade names in parentheses. The table lists cancers to which each targeted agent is approved. *Radiolabeled with Yttrium-90 or Iodine-131. ‡In combination with irinotecan or administered as a single agent. §In combination with radiation therapy or administered as a single agent. ¶In combination with paclitaxel or administered as a single agent. #In combination with 5-fluorouracil-based chemotherapy. **In combination with CHOP (cyclophosphamide, doxorubicin, vincristine and prednisolone) or other anthracycline-based chemotherapy regimens. ‡‡This mAb is linked to N-acetyl- calicheamicin, a bacterial toxin. After internalization of the mAb, the released toxin binds to DNA and causes double-strand DNA breaks. §§In combination with gemcitabine. AML, acute myeloid leukaemia; APL, acute promyelotic leukaemia; CLL, chronic lymphocytic leukaemia; CML, chronic myeloid leukaemia; CRC, colorectal cancer; EGFR, epidermal growth factor receptor; FLT3, fetal liver (or Fms-like) tyrosine kinase 3; GIST, gastrointestinal stromal tumour; KIT, stem cell factor receptor; NSCLC, non-small-cell lung cancer; HNSCC, head and neck squamous-cell carcinoma; PDGFR, platelet-derived growth factor receptor; RAR, retinoic acid receptor-alpha; RET, neurotrophic factor receptor; TK, tyrosine kinase; VEGFR, vascular endothelial growth factor receptor.

Currently, there is no curative treatment in the quantitatively large groups of patients with disseminated adenocarcinomas (e.g. breast, prostate, colorectal, lung and ovarian tumours) and squamous cell carcinomas (e.g. lung, oesophagus and head-neck tumours), where a palliative effect and/or prolonged survival can at best be achieved with chemotherapy. This is also true for malignant gliomas and various other types of disseminated tumours, e.g. malignant melanomas and neuroendocrine tumours (Carlsson et al., 2003).

Successes of targeted strategies against the big killers (lung, breast and colorectal cancer) have been reported. These strategies have in common that they start from a target that has been identified as playing an important role in tumour biology and oncogenesis. The agents include monoclonal antibodies (mAbs), small molecules, peptide mimetics and antisense oligonucleotides. The different targeted strategies have been intensively reviewed over the past five years and include modification of apoptosis, differentiation, signal transduction interference, anti-angiogenesis, gene therapy, immunotherapy and radiotherapy (Carlsson et al., 2003; Kim, 2003; Abou-Jawde et al., 2003; Brannon-Peppas, 2004; Mariani, 2005; Koppe et al., 2005; Newell, 2005; Lambert, 2005; Reubi et al., 2005; Wu et al, 2005; Sharkey and Goldenberg, 2005; Larson et al., 2005; Imai and Takaoka, 2006) (Fig.1.1).

Two classes of agents have been FDA-approved including monoclonal antibodies and small molecules. Table 1.1 shows the today's FDA-approved agents and the spectrum of targeted cancers. Categorization of the different strategies is difficult, since there are many overlaps in use of agents as well as mechanism of action. In this overview, we will discuss the potential role of immunotherapy, and more specifically discuss the different mechanisms of action of antibody targeted therapies. Where possible, the use of antibodies will be compared with the use of smaller molecules, e.g. peptides and non-peptides,

and successes of these different agents will be briefly mentioned for reason of comparison.

The concept of immunotherapy is based on the body's natural defence system. One immediate research goal in cancer immunology is the development of methods to harness and enhance the body's natural tendency to defend itself against malignant tumours. Antibodies have now become part of standard cancer treatment. Other examples of immunotherapy remain experimental, e.g. cancer vaccines (Scott, 1997; Pardoll, 2002), or involve certain cytokines (Hutson, 2005), but are out of the scope of this thesis.

1.1.1 Monoclonal antibodies

Köhler and Milstein developed the hybridoma technology in 1976, leading to today's approval of twelve monoclonal antibodies for detection or therapy of cancer (Table 1.2) and more than 150 mAbs under clinical investigation. Six monoclonal antibodies are used for other diseases than cancer, including chronic inflammatory diseases, transplantation and infectious diseases, and for cardiovascular medicine (Carter, 2006).

Monoclonal antibodies, with immunoglobulin G (IgG) the most commonly used immunoglobulin, are unique proteins with dual functionality. All naturally occurring antibodies are multivalent, with IgG having two binding 'arms.' Antigen-binding specificity is encoded by three complementarity-determining regions (CDRs), while the Fc-region is responsible for binding to serum proteins (e.g., C1q complement factor) or cells such as macrophages and natural killer (NK) cells (Sharkey and Goldenberg, 2006b) (Fig. 1.2).

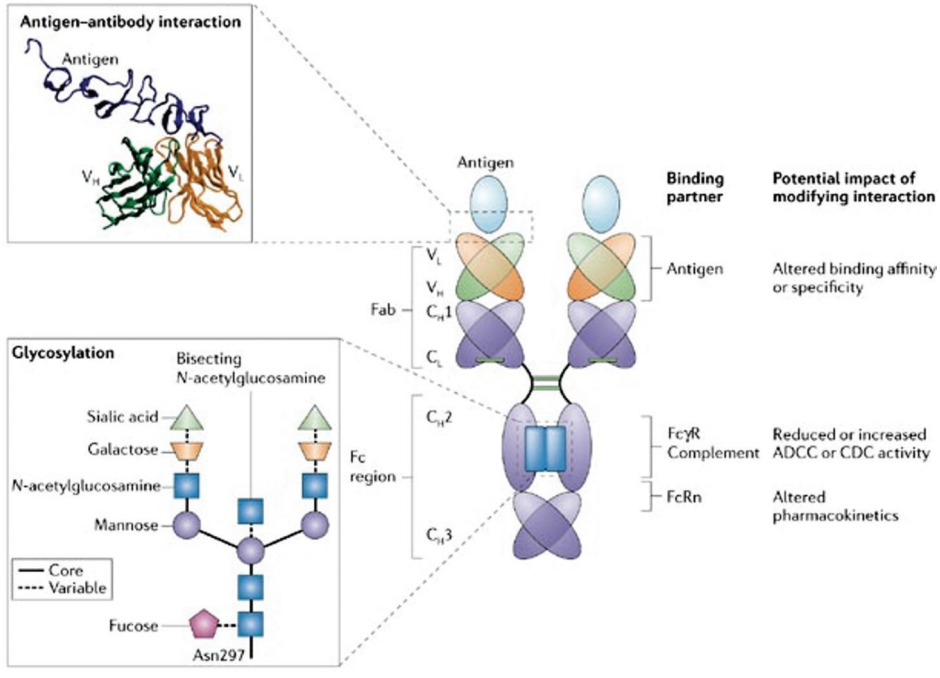

Fig. 1.2. IgG molecules are tetramers of ~150 kDa, which comprise a pair of identical heavy and light chains linked by disulphide bonds (green bars). The heavy chains contain a variable (V) domain (the V_H domain; green) and three constant (C) domains, the C_H1 domain, C_H2 domain and C_H3 domain (purple). By contrast, the light chains contain a V domain (the V_L domain; orange) and a single C domain (the C_L domain; purple). Highly selective binding of antigen (light blue) is a common hallmark of antibodies. This is mainly mediated by six loops, which are known as the complementarity-determining regions (CDRs), three of which are present in each of the V_H and V_L domains. The interaction of antibody with antigen is exemplified in this figure by the Fab of trastuzumab (Herceptin; Genentech, Inc. and F.Hoffman-LaRoche Ltd) in complex with HER2. For clarity, only the V domains of trastuzumab and domain IV of HER2 are shown (see inset). The remaining portion of the V domains, which are known as framework regions, function mainly as a structural scaffold to support the CDRs. Human IgG bound to an antigen on a target cell, particularly IgG1 and IgG3, can subsequently interact through its Fc region with IgG receptors FcγRs) expressed by effector cells or with complement component 1q (C1q), potentially supporting the destruction of target cells through antibody-dependent cell-mediated cytotoxicity (ADCC) or complement-dependent cytotoxicity (CDC), respectively. In addition, the Fc region of IgG can bind the salvage receptor FcRn after fluid-phase uptake by vascular endothelial cells and other cells, an interaction that contributes to the long (21 day) half-life of human IgG. Effector functions (that is, ADCC and CDC) require the presence of the Fc-region glycan (dark blue) and are crucially influenced by its structure. The N-linked glycan that is attached to the conserved asparagine (Asn) residue at position 297 comprises a core structure of N-acetylglucosamine and mannose, plus additional carbohydrate residues, which can vary, including fucose, galactose, sialic acid and bisecting N-acetylglucosamine. (Cho et al., 2003; Carter, 2006)

Table 1.2 FDA- and EMEA-approved antibodies for parental use in therapy and detection of cancer and mechanism of action (Sharkey and Goldenberg et al., 2006b)

Name	mAb	Mechanisms of action/Application	Indication	Approval
Unconjugated antibodies				
Rituximab (Rituxan)	CD20 Chimeric IgG1	Sensitization of cells to chemotherapy, induction of apoptosis, ADCC and CDC	Non-Hodgkin's lymphoma	1997 (US) 1998 (EU)
Trastuzumab (Herceptin)	HER2 Humanized IgG1	Sensitization of cells to chemotherapy, inhibition of angiogenesis, induction of ADCC	HER2/neu positive metastatic breast cancer	1998 (US) 2000 (EU)
Alemtuzumab (Campath)	CD52 Humanized IgG1	Induction of ADCC and CDC	B-cell CLL	2001 (US/EU)
Bevacizumab (Avastin)	VEGF Humanized	Ligand binding and receptor antagonism, inhibition of angiogenesis, and metastatic disease progression	Metastatic colorectal cancer	2004 (US) 2005 (EU)
Cetuximab (Erbitux)	EGFR Chimeric IgG1	Receptor binding and antagonism, inhibition of cell proliferation, induction of apoptosis, sensitization of cells to chemotherapy and radiotherapy, inhibition of angiogenesis, invasion and metastasis; induction of ADCC	Metastatic colorectal cancer Head and neck cancer	2004 2006 (US/EU)
Conjugated antibodies				
Satumomab pendetide (Oncoscint)	TAG-72 ^{111}In-murine IgG	Imaging, SPECT	Colorectal, ovarian	1992 (US)
Nofetumomab merpentan (Verluma)	EGP-1 ^{99m}Tc-murine Fab	Imaging, SPECT	SCLC	1996 (US)
Arcitumomab (CEA-scan)	CEA ^{99m}Tc-murine Fab	Imaging, SPECT	Colorectal	1996 (US/EU)
Capromab pendetide (Prostascint)	PSMA ^{111}In-murine IgG1	Imaging, SPECT	Prostate	1996 (US)
Gemtuzumab ozogamicin (Mylotarg)	CD33 Humanized IgG4	Drug delivery: induction of double-strand DNA breaks and cell death	ACL that expresses CD33	2000 (US)
Ibritumomab tiuxetan (Zevalin)	CD20 ^{90}Y-murine IgG1	Induction of cell death by radiation, induction of apoptosis	Non-Hodgkin's lymphoma	2002 (US) 2004 (EU)
^{131}I-Positumomab (Bexxar)	CD20 ^{131}I-murine IgG2a	Induction of cell death by radiation, induction of apoptosis, ADCC and CDC	Non-Hodgkin's lymphoma	2003 (US)

ACL, Acute myelogenous leukaemia; ADCC, antibody-dependent cellular cytotoxicity; CDC, complement-mediated cytotoxicity; CLL, chronic lymphocytic leukaemia; SCLC, small cell lung cancer; SPECT, single photon computed tomography

1.1.2 Unconjugated antibodies

1.1.2.1 Enhancing cytolytic mechanisms

There are many different mechanisms of action using monoclonal antibodies in cancer patients (von Mehren, 2003). The early models of mAb-based therapies focused on enhancing the cytolytic mechanisms against tumour cells (Adams and Weiner (2005).

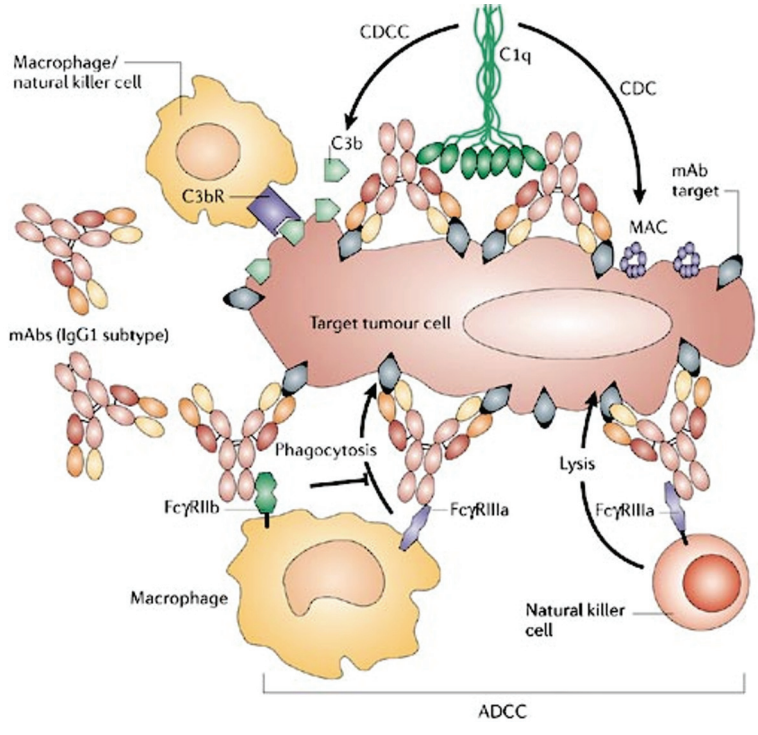

Fig. 1.3. Schematic model of indirect antibody action by immune mechanisms. Antibody-dependent cellular cytotoxicity (ADCC) involves the recognition of the C_H3 constant region of the antibody by immune effector cells such as macrophages and natural killer (NK) cells through FcγRIIIa receptors expressed by both effector cells. Target tumour cells become phagocytosed by macrophages or undergo cytolysis by NK cells. Complement-dependent cytotoxicity (CDC) involves the recognition of the C_H2 region of the antibody by the C1q complement factor, which leads to activation of a proteolytic cascade of the classical complement pathway and consequently induces the formation of a membrane-attack complex (MAC) and lysis of the tumour cell. C3b, which is generated during this cascade reaction, functions as an opsonin to facilitate phagocytosis and cytolysis through its interaction with the C3b receptor (C3bR) on a macrophage or natural killer (NK) cell; this activity is termed complement-dependent cell-mediated cytotoxicity (CDCC). (Imai and Takaoka, 2006)

An antibody itself usually is not responsible for killing target cells, but instead marks the cells. In that way, other components or effector cells of the body's immune system attack the marked cells. These attack mechanisms are referred to as antibody-dependent complement-mediated cytotoxicity (CDC) and antibody-dependent cellular cytotoxicity (ADCC) (Sharkey and Goldenberg, 2006b) (Fig. 1.3). IgG1 and IgG3 can activate the classical complement pathway and interact with Fc receptors more potently than IgG2 or IgG4. In particular, IgG4 cannot activate the classical complement pathway (Imai and Takaoka, 2006).

The anti-tumour effect of Rituxan (anti-CD20) (Table 1.2) was initially attributed to CDC and ADCC. Shan et al. (1998) showed that the anti-CD20 mAb Rituxan provides also pro-apoptotic signals to B-cell lymphomas, offering another mechanism of action of this antibody (Kim, 2003).

1.1.2.2 Signal transduction interference

The increasing knowledge of molecular pathways that underlie the cancer process has resulted in the use of antibodies in a direct way. These modes of action involve blocking the function of target signalling molecules or receptors (e.g., blocking ligand binding, inducing regression of angiogenesis, increasing internalization of receptors), and stimulating function of target signalling molecules or receptors (e.g., inducing apoptosis). Based on these mechanisms of action, several monoclonal antibodies as well as small molecules have been FDA approved for clinical use (Table 1.2).

Signal transduction in cancer cells is a sophisticated process involving receptor tyrosine kinases (RTKs) that eventually trigger multiple cytoplasmic kinases, which are often serine/threonine kinases. Three major signalling pathways that have been identified as playing important roles in cancer include the phosphatidyl inositol-3-kinase (PI3K)/Akt, protein kinase C (PKC) family, and

mitogen-activated protein kinase (MAPK)/Ras signalling cascades (Fig. 1.4) (Faivre et al., 2006). Targeting signal transduction involves blocking or interfering with the RTKs (C-KIT, EGFR (ERBB1), HER2 (ERBB2), PDGFR, VEGFR, FLT3 and RET) or molecules downstream the signal transduction cascade (Ras, Raf, MAP, MEK, mTOR, PKC, BCR-ABL) (Faivre, 2006).

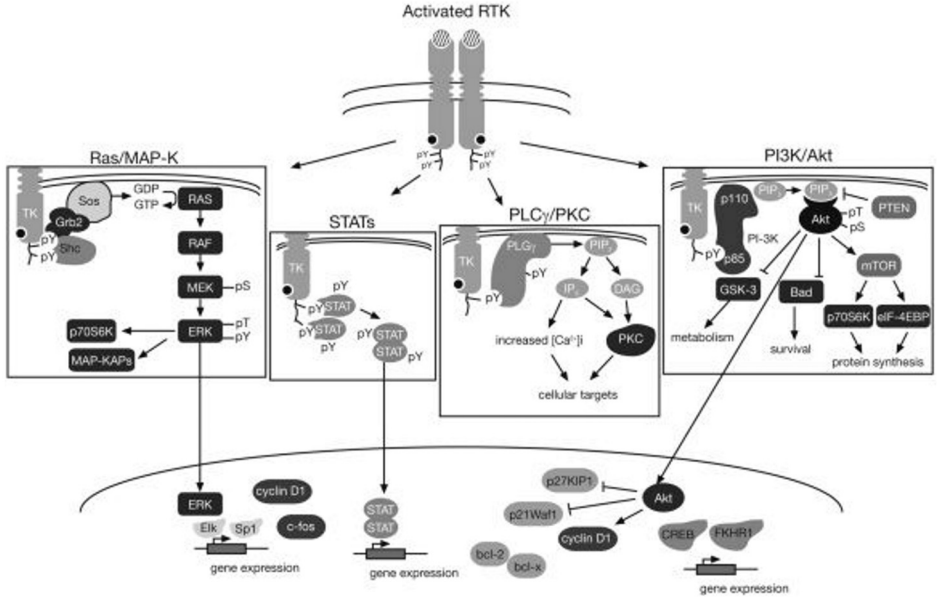

Fig. 1.4. Schematic diagram of key signalling pathways leading from receptor tyrosine kinase (RTK) activation to cancer development. pY, phosphorylated tyrosine (Marmor et al., 2004; Faivre et al., 2006)

Small-molecule tyrosine kinase inhibitors (TKIs), such as gefinitib, function as adenosine triphosphate (ATP) analogues and inhibit the epidermal growth factor receptor (EGFR) signalling by competing with ATP binding within the catalytic kinase domain of RTKs (Fig. 1.5). As a result, the activation of various downstream signalling pathways is blocked. Each TKI has a different selectivity for RTKs, and some are dual- or multi-selective, which might provide a therapeutic advantage. By contrast, therapeutic monoclonal antibodies (mAbs) bind to the ectodomain of the RTK with high specificity (for example, cetuximab binds to the L2 domain of EGFR), and thereby inhibits its

downstream signalling by triggering receptor internalization and hindering ligand-receptor interaction.

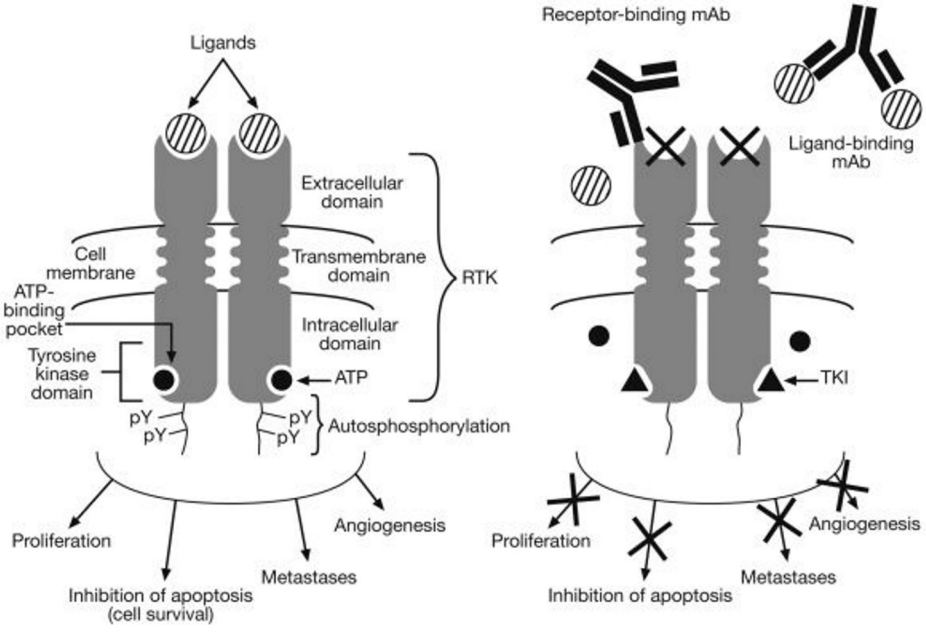

Fig. 1.5. Schematic diagram of the structure of receptor tyrosine kinases and the mechanism of action of monoclonal antibodies (mAbs) and tyrosine kinase inhibitors (TKIs) inhibiting these receptors. pY, phosphorylated tyrosine kinase (Faivre et al., 2006)

Both gene amplification and overexpression of EGFR and HER2 are frequently observed in breast, lung and colorectal cancers, and the deregulated activation of intracellular mitogenic signalling by the ErbB family has been implicated in various cancers. Table 1.3 gives an overview of the main clinical investigations currently available on targeted signal transduction agents in the treatment of non-small cell lung cancer (NSCLC), colon and breast cancer, and other solid tumours (Allen et al., 2003; Gridelli, 2004; Maione et al., 2004; Vanhoefer, 2005; Isobe et al., 2005; Mendelsohn and Balsega, 2006; Massarelli and Herbst, 2006).

Table 1.3 Main clinical investigations currently available on targeted signal transduction agents in the treatment of non-small cell lung cancer, colon and breast cancer, and other solid tumours (Allen et al., 2003; Gridelli, 2004; Maione et al., 2004; Vanhoefer, 2005; Isobe et al., 2005; Mendelsohn and Balsega, 2006; Massarelli and Herbst, 2006; Steeghs et al., 2006)

Agents		Characteristic	Tumourtype	Stage
Receptor tyrosine kinase inhibitors				
ErbB-1 (EGFR)				
Antibody	Cetuximab (Erbitux)	IgG1κ, chimeric	Colon, H&N	Marketed
			NSCLC, pancreas	Phase II/III
	Panitumumab (ABX-EGF)	IgG2, human	Colon, renal, H&N	Phase III
	Matuzumab (EMD-72000)	IgG, humanized	H&N, ovarian, colon, cervix	Phase II
TKI	Gefitinitib (Iressa, ZD1839)	Quinozaline, reversible	NSCLC	Marketed
			Breast, colon and other types	Phase II
	Erlotinib (OSI-774, Tarceva)	Quinazoline, reversible	NSCLC, pancreas	Marketed
			Ovarian, H&N, glioblastoma	Phase II
	EKB-569	Reversible	colon	Phase II
ErbB-2 (HER2)				
	Trastuzumab (Herceptin)	IgG1κ, humanized	Breast	Marketed
			NSCLC	Phase II
	Pertuzumab	IgG, humanized	Breast, ovarian, prostate, NSCLC	Phase III
Panerb-B				
	Canertinib (CI-1033)	Quinazoline, irreversible	NSCLC, breast	Phase I/II
			SCC, skin	Phase II
	Lapatinib (GW-572016, Tykerb)	EGFR/HER2, irreversible	Breast	Phase III
Cytoplasmic inhibitors				
Protein kinase C				
	Affinitak (ISIS3521, LY900003)	Antisense oligonucleotide	NSCLC	Phase I/II/III
Ras pathway				
	ISIS2503	Antisense oligonucleotide	NSCLC	Phase II
	Lonafarnib (SCH-66336)	Non-peptidomimetic, reversible	NSCLC	Phase III
	Tipifarnib (R115777)	Non-peptidomimetic quinolone FTI	NSCLC	Phase III
	BMS214662	Benzodiazepine FTI	NSCLC	Phase II

CML, chronic myelogenous leukaemia; GIST, gastrointestinal stromal tumours; H&N, head and neck; NSCLC, non-small cell lung cancer; PDGFR, platelet-derived growth factor receptor; SCC, squamous cell carcinoma; VEGFR, vascular endothelial growth factor receptor

Tabel 1.4 Main clinical investigations currently available on targeted anti-angiogenesis agents in the treatment of NSCLC, colon and breast cancer and other solid tumours (Gridelli, 2004; Maione et al., 2004; Rüegg et al., 2004; Isobe et al., 2005; Vanhoefer et al., 2005; Steegh et al., 2006)

Agents		Characteristic	Tumortype	Stage
VEGF inhibitors				
Antibody	Bevacizumab	IgG1, humanized	Colon	Marketed
			NSCLC	Phase II/III
SMKI	Zactima (ZD6474)	VEGFR, EGFR	NSCLC	Phase I/II/III
	Sunitib (Sutent, SU11248)	VEGFR-1, PDGF, KIT, FLT-3	RCC, GIST	Marketed
			NSCLC	Phase II
	ZD6474	VEGFR-2 and EGFR inhibitor	NSCLC	Phase II/III
	Vatalanib (PTK787, ZK 222584)	VEGFR, PDGFR, c-KIT	colon	Phase II/III
	Sorafanib (Bay 43-9006, Nevaxar)	VEGFR, PDGFR, Raf-1	RCC	Marketed
			Melanoma, HCC	Phase II/III
Angiogenesis				
	Endostatin	Cleavage product of plasminogen, natural anti-angiogenic protein	NSCLC	Phase III
Integrin				
Antibody	Vitaxin	αvβ3 (IgG1, humanized)	Melanoma, prostate	Phase II
	CNTO95	αv (IgG1, humanized)	Melanoma	Phase II
Peptide	Cilengitide	Cyclic RGD peptide	Glioma	Marketed
			Prostate	Phase II
MMP				
	Prinomastat	MMPI (MMP-2, MMP-9)	NSCLC	Phase III (early closure)
	BMS275291	MMPI (MMP-1, -2, -8, -9, -13, -14)	NSCLC, prostate	Phase II/III
	Neovastat	Anti-VEGF and MMPI	NSCLC	Phase III

EGFR, epidermal growth factor receptor; GIST, gastrointestinal stromal tumours; HCC, hepatocellular carcinoma; IgG, immunoglobuline G; MMPI, matrix metalloproteinase inhibitor; NSCLC, Non-small cell lung cancer; PDGF, platelet derived growth factor; RCC, renal cell carcinoma; RGD, arginine-glycine-aspartate peptide motive; SMKI, small molecule kinase inhibitor; VEGF, vascular endothelial growth factor

1.1.2.3 Anti-angiogenesis therapy

Tumour cells will continue dividing until they reach the diffusion-limited maximum size (~2 mm^3). At that point, the outer cancer cells have access to nutrients, while the inner cells of the tumour will perish because the amount of nutrients is insufficient. A steady state tumour size forms.

To grow beyond this size the tumour must start the process of angiogenesis, i.e. new blood vessels must be formed to provide the tumour with nutrients essential for expansion. The factors involved in angiogenesis present new therapeutic targets (Brannon-Peppas, 2004). Table 1.4 shows some of the most important factors under investigation including the vascular endothelial growth factor (VEGF), basic fibroblast growth factor (bFGF), platelet-derived growth factor (PDGF), integrin $\alpha_v\beta_3$ and certain matrix metalloproteinases (MMPs) (Kerbel, 2006).

1.1.2.4 Inducing apoptosis

Apoptosis, or programmed cell death, is a gene-directed control mechanism by which cells die if DNA damage is not repaired (Lowe et al., 2000). Apoptosis is also important in controlling cell number and proliferation as part of normal development. The genetic basis of apoptosis implies that it can be disrupted by mutation. The results of defects in apoptosis lead to immortal clones of cells. Defects in the apoptotic regulatory pathways such as p53, the nuclear factor kappa B (NFκB), or phosphatidylinositol 3-Kinase (PI3K)/Akt lead to new treatments that target them.

When tumour cells detect DNA damage beyond the repair capabilities of the cell, programmed cell death pathways are triggered. Apoptotic cell death can be initiated through an extrinsic pathway involving activation of cell surface death receptors or by an intrinsic pathway via the mitochondria (Fig. 1.6).

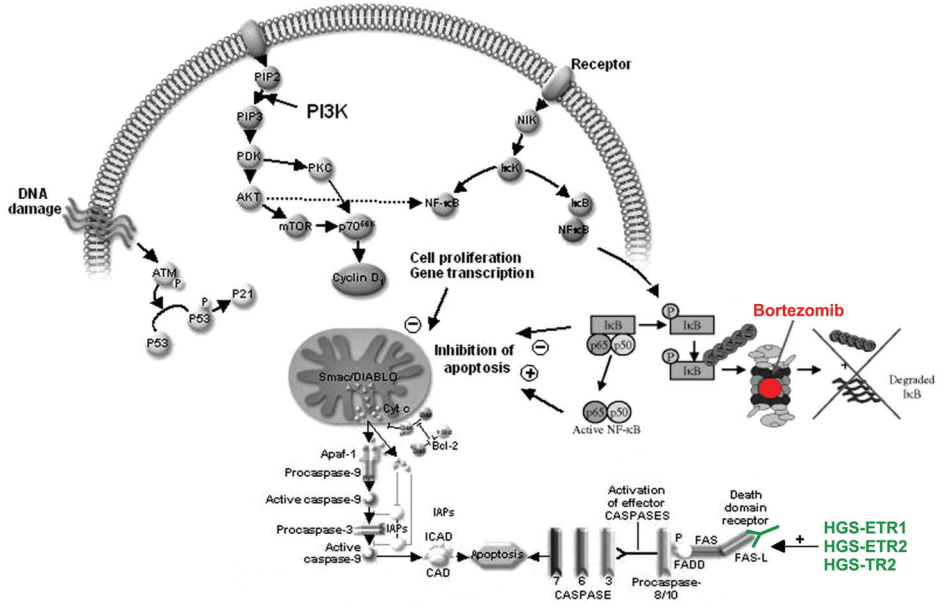

Fig. 1.6. Extrinsic (cytoplasmic) and intrinsic (mitochondrial) apoptotic pathways. These are regulated by proteins such as p53, the PI3K pathway, NFκB, and the ubiquitin/proteasome system. Influence of FDA-approved proteosome inhibitor bortezomib on the nuclear factor (NF) κB survival pathway is indicated. Bortezomib (red) binds to the 20S β-subunit, thereby blocking the proteasome. As a result, IκB will not be degraded into small peptides. It remains bound to the survival protein NFκB, thereby inhibiting NFκB action. Action of antibodies HGS-ETR1, HGS-ETR2, and HGS-TR2 (green) stimulate apoptosis by binding the death receptors Dr4 (TRAIL R1, tumour necrosis factor-related apoptosis-inducing ligand receptor 1) and Dr 5 (TRAIL R2, tumour necrosis factor-related apoptosis-inducing ligand receptor 2) receptor. (Vink et al., 2006 and Ghobrial 2006 – modified)

Both pathways lead to activation of effector caspases that trigger a proteolytic cascade resulting in fragmentation of intracellular components. Many of these are p53 dependent; the p53 gene is mutated in the majority of human cancers, resulting in inhibition of apoptosis.

Monoclonal antibodies (HGS-ETR1 (mapatumumab), HGS-ETR2, and HGS-TR2) with agonist function at the death receptor (Dr) Dr4 (TRAIL R1, tumour necrosis factor-related apoptosis-inducing ligand receptor 1) and Dr5 (TRAIL R2, tumour necrosis factor-related apoptosis-inducing ligand receptor 2) sites may also induce apoptosis and caspase activation and have shown tumour regression in colon tumour xenograft models. Phase I and Phase II trials in

patients with advanced non-small cell lung cancer, colon cancer, and non-Hodgkin lymphoma are in progress (Ghobrial et al., 2005). Other examples of agents active on apoptotic proteins in the extrinsic, intrinsic and common pathways or indirect modulators of apoptosis, are given by Ghobrial et al. (2005).

1.1.2.5 Future targets

Stroma cells contribute to the cancer microenvironment and are essential for cancer growth, invasion and metastatic progression. Fibroblasts, often termed myofibroblasts or cancer-associated fibroblasts (CAFs), represent the most abundant cell type in the tumour stroma. The demonstrated tumour-promoting capacities of CAFs have increased the interest to exploit them as drug targets for anticancer therapy. Single factors, such as platelet-derived growth factor, transforming growth factor-β1, hepatocyte growth factor and matrix metalloproteinases have been identified as mediators in the fibroblast tumour interaction (Micke et al., 2005). The cell surface serine protease known as fibroblast activation protein (FAP) emerges as a promising candidate for specifically targeting CAFs (Rettig et al., 1993). FAP is not expressed by mature somatic tissues except for activated fibroblasts during wound healing and within stroma (Wang et al., 2005). A phase I dose-escalation study with sibrotuzumab (an anti-FAP antibody) in patients with advanced colorectal carcinoma and non-small cell lung carcinoma showed that sibrotuzumab bound specifically to the tumour sites without apparent site effects (Scott et al., 2003). Targeting CAFs as therapeutic strategy against cancer is an intriguing concept and needs further study (Kalluri and Zeisberg, 2006). Other promising unconjugated antibodies or agents in advanced clinical trials are discussed by Sawyers (2004) and, Sharkey and Goldenberg (2006b).

1.1.3 Conjugated antibodies

Other modes of action of antibodies are the specific delivery of radioisotopes (Goldenberg et al., 2006; Koppe et al., 2005; Milenic et al., 2004; Tolmachev et al., 2004; Goldenberg, 2003; Goldenberg, 2002), toxins (Pastan et al., 2006; Ross et al., 2003) or drugs (Carter, 2001; Lambert, 2005) to target tumour sites. Today, two radioimmunoconjugates and one drug-immunoconjugate are FDA-approved (Table 1.2). New approaches involve pretargeting strategies and the use of immune-modulating bispecific antibodies or recombinant ligand-antibodies (Pardoll, 2002; Holliger and Hudson, 2005; Waldmann, 2006). Pretargeting approaches have been applied to radionuclides (Goldenberg, 2002; Boerman et al., 2003; Sharkey and Goldenberg, 2005; Goldenberg et al., 2006) and drugs termed antibody-directed enzyme prodrug therapy (ADEPT) (Goodwin and Meares, 2001; Sharma et al., 2005). In all these cases, the antibody acts as a homing device to carry its payload to the target where the latter precipitates a biologic activity with minimum side effects to non-target tissue (Kim et al., 2005; Sanz et al., 2005). In the scope of this thesis we will only focus on radioimmunotherapy as part of radionuclide therapy.

Radionuclide therapy differs from radiotherapy in the mechanism of radiation delivery to the target tissue, i.e. systemic versus external beam-radiation. In radionuclide therapy, specific delivery of radiotoxic agents to tumour lesions while sparing normal tissues, depend on physicochemical events (e.g., ^{131}I-NaI concentration in thyroid) or is receptor based (interaction of peptides and antibodies with tissue-specific receptors). The principal target for ionizing radiation is DNA. Several lesions are produced (e.g., single-strand or double-strand DNA breaks, base damage, DNA-protein cross-links, and multiple damage sides) by direct ionization of DNA (direct effect) or by interaction of free radicals (mostly hydroxyl radicals). In general, these lesions are repaired with high precision by the control mechanisms within each cell. Exceptions are

the double strand breaks and multiple damaged sides. After a delay in the progression of dividing cells, non repairable cells will undergo apoptosis (Kassis and Adelstein, 2005).

Today, ^{131}I-NaI is the only FDA-approved agent for a solid tumour (thyroid) based on targeted radionuclide therapy. Ibritumomab tiuxetan (Zevalin ^{111}In/^{90}Y) and ^{131}I-tositumomab (Bexxar) are both monoclonal antibodies approved for the localization and treatment of non-Hodgkin's lymphoma (NHL) (Larson and Krenning, 2005).

An overview of representative radioimmunotherapy trials in NHL and solid tumours is given by Koppe et al. (2006). For solid tumours, the most targeted malignancies in Phase I/II clinical RIT are epithelial cancers, e.g. colorectal cancer, ovarian cancer, medullary thyroid cancer, and to a lesser extent breast, prostate and renal cell cancer. The most commonly targeted antigens are the carcinoembryonic antigen (CEA, mainly in colorectal, medullary thyroid and breast cancer), tumour-associated antigen-72 (TAG-72, mainly in colorectal, ovarian and breast cancer), and G250 (renal cell cancer). ^{131}I or ^{90}Y were the radionuclides commonly applied, although in some trials ^{186}Re, ^{188}Re, or ^{177}Lu were used. In most cases, the radiolabeled antibodies were administered in dose-escalating steps to determine the maximum tolerable dose. As a result, in most studies suboptimal doses were administered. Most of these patients had metastatic, bulky disease, and had been heavily pretreated with chemotherapy and/or radiotherapy. Compared to haematological disease, complete responses in patients with solid cancers have rarely been reported, although in many studies a few patients still experienced minor, partial or mixed responses or stabilization of previously progressive disease.

1.2 Use of monoclonal antibodies in molecular imaging

Molecular imaging may be defined as the spatially localized remote sensing of molecular and physiological processes in vivo. An alternative definition might be that molecular imaging is the minimally invasive depiction, characterization, and measurement of biological processes at the cellular and molecular levels in living organisms (Hillman and Neiman, 2002). Molecular imaging can be useful in four broad categories of applications: screening and early detection, diagnosis and staging, guidance for less invasive treatments, drug development, and monitoring of treatment response.

Medical imaging modalities most relevant to cancer research and clinical care include ultrasound, x-ray computed tomography (CT), magnetic resonance imaging (MRI), nuclear imaging (single photon emission computed tomography (SPECT) and positron emission tomography (PET)), and near infrared optical imaging (NRI) (Hillman, 2006). A brief and clear overview of the principles underlying these modalities is given by Schnall and Rosen (2006). Over the past decades, each of these techniques have undergone increasing interest for research and improvements regarding sensitivity and the development of contrast agents (Bloch et al., 2004; Nelson SJ, 2004; Blankenberg, 2004; Pomper and Hammoud, 2004; Mahmood, 2004; Kelloff et al., 2005). Previous and today's clinical practice measures the effect of anticancer treatment mainly on the basis of the morphological changes that are imaged using structural imaging using CT and MRI. As the size of the tumour after therapy is not directly related to the viability of the tumour, these imaging techniques have limitations in assessing therapeutic effects. In addition, neoadjuvant chemoradiotherapy can produce severe mucositis, edema, scarring and granulation tissue, which might interfere with the detection of persistent disease using conventional diagnostic methods (Kitagawa et al., 2003). Also, with these techniques, sensitivity for early disease is poor. Many diseases are

initiated at the molecular and cellular levels, and usually do not cause gross abnormalities for an extended period. As a result, functional imaging techniques such as PET and SPECT can complement anatomical modalities and overcome some of the deficiencies of structural imaging (Alavi et al., 2004). Nuclear medicine techniques have the capability to detect and serially monitor a variety of biologic and pathophysiologic processes, but PET and SPECT lack the high anatomical spatial resolution of CT and MRI. The development of PET/CT (Townsend et al., 2003), SPECT/CT (von Schulthess, 2005), and PET/MRI (Gaa et al., 2004; Seemann, 2005) research and clinical scanners provide the combination of functional and structural images. Four monoclonal antibodies have been approved for imaging including Oncoscint, Verluma, Prostascint, and CEA-scan (Table 1.2).

1.2.1 PET and SPECT: basic principles

Positron emission tomography (PET) imaging begins with the injection of a biological molecule that carries a positron-emitting isotope (e.g., ^{11}C, ^{13}N, ^{15}O, or ^{18}F). As the tracer accumulates in an area of the body for which it has a high affinity, the isotope decays by positron emission, i.e. a positively charged antiparticle of the electron. After travelling a short distance the positron combines with an electron to annihilation. As a result, two gamma rays of 511 keV each are emitted in opposite direction at a 180° angle (Fig. 1.7A). By detecting those photons that travel in opposite directions in coincidence within several nanoseconds, the projection data required for tomographic reconstruction are obtained. If two detectors are in coincidence, the assumption is that the positron was emitted along the line that connects them, referred to as the line of response (Pomper and Hammoud, 2004).

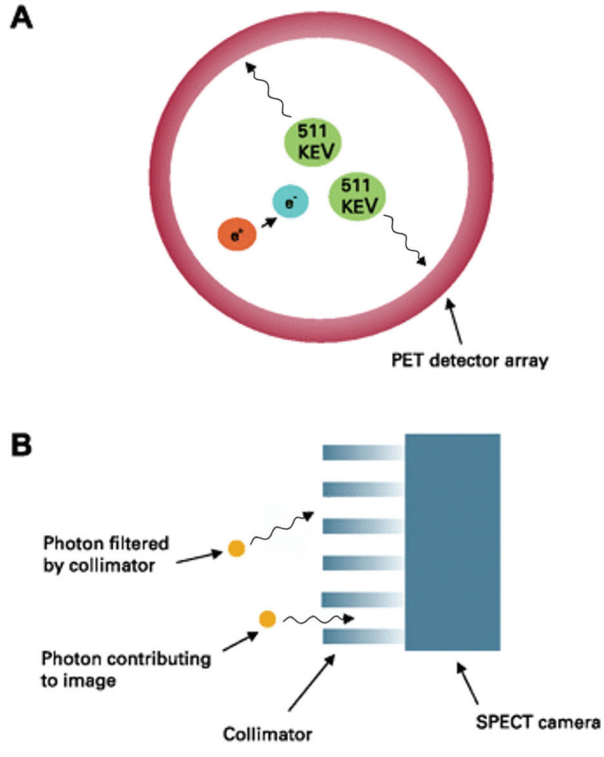

Fig. 1.7. (A) Positron emission tomography (PET) and (B) single-photon emission computed tomography (SPECT) detection. The trajectory of the photon is determined by the coincidence detection of two photons emitted 180 degrees apart, whereas for SPECT, the collimator determines the trajectory of the photons that contribute to the image by filtering out unwanted photons, resulting in only a fraction of the possible photons contributing to the image. (Schnall and Rosen, 2006)

Single photon emission computed tomography (SPECT) relies on the emission of a single photon (e.g. ^{99m}Tc, $^{123/131}$I, ^{111}In, or ^{67}Ga) by a decaying isotope. The origin of the single photon needs to be located. Therefore, a perforated metal filter (a collimator) is used to filter out the photons from all but the prescribed direction (Fig. 1.7B). This is an inefficient process that results in the majority of photons not reaching the detector and less sensitivity compared to PET (Schnall and Rosen, 2006). The advantages and disadvantages of PET and SPECT are summarized in Table 1.5.

Tabel 1.5 Characteristics of human PET and SPECT imaging

	PET	**SPECT**
Cost	Expensive	Less expensive
Isotopes	Cyclotron isotopes: short $t_{½}$ (2 min-2 hrs)	Generator or purchased isotopes: long $t_{½}$ (6 hrs – 8 days)
Chemistry	Physiologic radiotracers	Direct or chelation
Emission energies	511 keV	70-364 keV
Quantification	Semi-quantitative/quantitative	Quantitative?
Resolution	High (4-5 mm)	Lower (8-10 mm)
Sensitivity	No collimators: higher sensitivity	Collimators: lower sensitivity

SPECT enables imaging of biological processes with long half-lives because of longer physical half-lives of the radionuclides, has more readily available radiotracers, employs less expensive equipment and, can simultaneously detect isotopes with different emission energies. PET employs physiologic radiotracers which can be identical to the biological molecule of interest, lends itself more easily to quantification, and is approximately two orders of magnitude higher in sensitivity than SPECT. The high resolution of PET is limited because of the positron range and the photon non-colinearity effects (Pomper and Hammoud, 2004). Further improvement in SPECT resolution is possible using high resolution pinhole collimators. Unfortunately, this is not generally practical for human imaging (Meikle et al., 2005).

1.2.2 Molecular imaging targets and probes

An important application in molecular imaging in oncology is to design and implement better drug development. This includes differentiation (i.e. inflammation vs. recurrence, sensitive vs. drug resistant) and prediction (i.e. selection of patients who are more likely to respond to therapy). The imaging probes can facilitate early clinical pharmacokinetic and/or pharmacodynamic evaluation particularly in patients where no direct measures of pharmacokinetics and/or pharmacodynamics throughout the tissues of the body and at the target are available.

Tabel 1.6 Imaging probes used to visualize molecular targets and processes in cancer (Kelloff et al., 2005)

Molecular target/process	Imaging probes (phase of development)
Small-molecule probes	
Proliferation	2-[^{11}C]Thymidine, [^{18}F]-FLT, [^{18}F]FFEAU, [^{124}I]-IdUrd (clinical testing)
Apoptosis	[^{99m}Tc]Annexin V, [^{18}F]Annexin V (clinical testing)
Hypoxia	[^{18}F]FMISO, [^{18}F]-EF5, [^{18}F]FETNIM, [^{18}F], [^{64}Cu]ATSM, [^{124}I]-IAZG, [^{123}I]-arabinoside, [^{18}F]FAZA (clinical testing)
Pharmacokinetics	[^{18}F]5-FU, [^{11}C]DACA, [^{11}C]BNCU, [^{11}C]temozolomide, [^{13}N]cisplatin (FDA approved)
Multidrug resistance	[^{99m}Tc]sestamibi, [^{11}C]verapamil, [^{11}C]daunorubicin, [^{11}C]colchicine, [^{99m}Tc]MIBI (FDA approved)
Breast cancer (ER)	[18F]FES (clinical testing)
Prostate cancer (androgen receptor)	[18F]FDHT (clinical testing)
Peptide probes	
Somatostatin/somatostatin receptor	[^{90}Y] DOTATOC, [^{111}In]DTPA-D-Phe-1-octreotide, [^{90}Y]DOTALAN, [^{90}Y]DOTAVAP (FDA approved)
Vasoactive intestinal peptide/vasoactive intestinal peptide receptor-1	[^{123}I]VIP, [^{99m}Tc]TP3654 (clinical testing)
Bombesin, gastrin-releasing peptide/gastrin-releasing peptide receptor	[^{99m}Tc]Bombesin (clinical testing)
Cholecystokinin, gastrin/cholecystokinin receptor	[^{111}In]DTPA-minigastrin (clinical testing)
Angiogenesis	[^{18}F]RGD peptide targeted to $\alpha_V\beta_3$ integrin (preclinical testing)
Antibody probes	
Angiogenesis	Paramagnetic nanoparticles using antibodies to integrin $\alpha_V\beta_3$, the integrin $\alpha_V\beta_3$ ligand, vascular cell adhesion molecule 1, E-selectin (preclinical testing)
CEA	[^{99m}Tc]-Arcitumomab (CEAscan), [^{111}In] Satumomab (FDA approved)
Prostate-specific membrane antigen	[^{111}In]-Capromab pendetide (ProstaScint) (FDA approved)
CD20	[^{131}I]-tositumomab (Bexxar), [^{90}Y]-ibritumomab tiuxetan (Zevalin) (FDA approved)
CD22	[^{99m}Tc]-Bectumomab (clinical testing)

ATSM, diacetyl-bis(N^4-methylthiosemicarbazone); BNCU, 1,3-bis(chloroethyl)-1-nitrosourea; CEA, carcinoembryonic antigen; DACA, *N*-[2-(dimethylamino)ethyl]acridine-4-carboxamide; DOTALAN, 1,4,7,10-tetraazacyclododecane-1,4,7,10-tetraacetic acid lanreotide; DOTATOC, DOTA-Tyr^3-octreotide; DOTAVAP, DOTA-vapreotide; EF5, 2-(2-nitro-1H-imidazol-1-yl)-N-(2,2,3,3,3-pentafluoropropyl) acetamide; ER, estrogen receptor; FAZA, fluoro-azomycin-arabino-furanoside; FDHT, 16β-fluoro-5α-dihydrotestosterone; FES, 16α-fluoroestradiol-17β; FETA, fluoroetanidazole; FETNIM, fluoroerythronitroimidazole; FFEAU, 2′-fluoro-2′-deoxy-1-β-D-arabinofuranosyl-5-(2-fluoroethyl)-uracil; FLT, 3'-deoxy-3'-fluorothymidine; FMISO, fluoromisonidazole; 5-FU, 5-fluorouracil; IAZG, iodo-azomycin-galactoside; IdUrd, iododeoxyuridine, MIBI, methoxyisobutylisonitrile; RGD, arginine-glycine-aspartic acid peptide,VIP, Vasoactive intestinal peptide

An application of this strategy can be comparing lead candidates interacting with the same target in an early phase of drug development. Also, imaging probes can act as biomarkers of tumour response; imaging end points at the molecular level (i.e., apoptosis, proliferation, angiogenesis, etc.) can speed up the evaluation of therapeutic success (Smith-Jones et al., 2004; Kelloff et al., 2005).

Although the introduction of [^{18}F]-fluorodeoxyglucose (FDG)-PET has offered a revolution in oncology imaging (Alavi et al., 2004), the complexity of cancer progress and unique capabilities of PET and SPECT, lead to the increased development of new tracers, both for PET and SPECT applications. The most important molecular imaging targets and probes are given in Table 1.6. Analogously to targeted therapeutics, the target of choice in molecular imaging plays an important role in tumour biology or the physiological mechanisms of oncogenesis. Prominent examples of targets include specific kinases, cellular receptors, and signalling molecules. Imaging of neoplastic processes includes proliferation, angiogenesis, apoptosis and, hypoxia (Table 1.6). The probes used are small molecules, peptides and monoclonal antibodies labeled with radionuclides (e.g., ^{11}C, ^{18}F, ^{99m}Tc, and ^{123}I) or magnetic ligands (Kelloff et al., 2005). Each category has been intensively investigated and reviewed over the last decade (Blankenberg et al., 2000a-b; Welch and Redvanly, 2003; Alavi et al., 2004; Blankenberg, 2004; Schuster and Halkar, 2004; Czernin et al., 2006; Yang et al., 2006).

CEA was one of the earliest targets for radioimmuodetection and radiotherapy. Extensive work in the late 1970s and early 1980s used a variety of antibodies primarily labeled with iodine radionuclides (Goldenberg et al., 1978; Mach et al., 1980). Despite high rates of detection, and a lot of improvements over the years (e.g., genetic engineering, pretargeting) radioimmunodetection is still not

considered a routine procedure in the clinic. Table 1.7 lists some of the factors discussed by Bischof Delaloye (2000) possibly impeding its overall acceptance.

Tabel 1.7 Factors impeding overall acceptance of radioimmunodetection (Bischof Delaloye, 2000)

Costs
Complexity of procedure
Difficulty of penetration
Human anti-mouse antibodies
Lack of interest from clinicians
Lack of large clinical trials
Lack of pertinence of the method
Lack of support from the industry
Competing methods

Two of the most important factors are the success of FDG-PET and the refinement of the anatomic imaging methods, which have reduced the unclear cases in which functional imaging often allows a clarification of the diagnosis. However, one limitation of FDG is that its uptake is related to increased glucose metabolism and not a specific metabolic feature. False positive results have been described in cases of active inflammatory/infection lesions (Sugawara et al., 1998; Lim et al., 2005; Jacene et al., 2006). Improved imaging methods, such as immuno-PET, offer possible advantages (Larson et al., 1992, Lovqvist et al., 2001; Sundaresan et al., 2003), and rapid imaging using pretargeting and other techniques could enable application of PET radionuclides with short half-lives (e.g., ^{18}F and ^{68}Ga) labeled to antibodies. A spectrum of antibodies and antibody derivatives, including minibodies and diabodies (Sundaresan et al., 2003; Olafsen et al., 2004), are now available based on advanced molecular engineering techniques, and these forms are likely to have targeting advantages when optimized. These new antibody forms are also likely to lack immunogenicity, permitting repeated diagnostic use, or therapeutic administration (Winter and Harris, 1993).

These diverse advances in the technology of imaging and radiolabeling, and in molecular engineering of antibodies, will together provide opportunities to develop increasingly effective molecularly agents for imaging.

1.3 Advances in radioimmunodetection and -therapy

Monoclonal antibodies account for an increasing portion of marketed human, biological therapeutics. Since the mid-1990s, antibodies have emerged as an important new drug class.

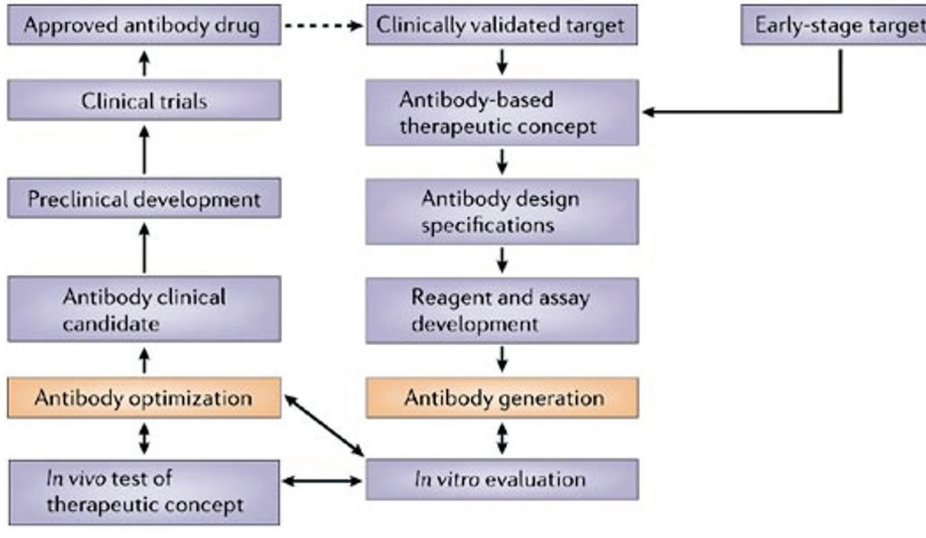

Fig. 1.8. The first step in the generation of antibody therapeutics, which is one of the most difficult steps, is the selection of a target antigen. A concept for therapeutic intervention using an antibody is then devised, ideally on the basis of knowledge about the target, including its role in the pathobiology of disease. This therapeutic concept leads to the antibody design specification: that is, a list of crucial or desirable properties that are predicted to achieve the desired clinical outcome. The design specification guides the method of antibody generation, as well as the reagents and assays that are needed to identify antibodies with the desired properties. Panels of antibodies are evaluated in vitro and then in vivo to test the therapeutic concept and to rank the antibodies for potency and safety. Antibody optimization might be necessary or desirable to meet the design goals and can be guided by existing antibody drugs, in terms of favourable attributes to emulate and limitations to overcome. Revision of the design specifications might be required in light of in vitro and in vivo data. The antibody clinical candidate is then subjected to further preclinical and, if warranted, clinical development. Clinical-trial data — particularly if they validate the target through to the drug-approval stage — might provide the impetus for the whole process to begin again, to generate an improved drug (Carter, 2006).

Eighteen antibodies have now been approved (17 have been marketed, and 1 withdrawn) for imaging and therapeutic use. Twelve of these antibodies are used in oncology of which half of them are radioimmunoconjugates. The other antibodies are used in chronic inflammatory diseases, transplantation, infectious diseases and cardiovascular medicine (Carter, 2006). Selection, design, and engineering of these antibodies not only expanded in the past two decades but are now becoming important competitive factors. In his latest review, Carter (2006) depicts the development of an antibody drug as an iterative design process (Fig. 1.8). From this design process, it is clear why antibody drugs are expensive. One of the many factors includes the large expense of drug development in general and high costs of intellectual property associated with the generation, optimization and production of antibodies.

The success of both radioimmunodetection (RID) and radioimmunotherapy (RIT) depends on intrinsic factors of the antibody, the radionuclide, and the target. A key strength of antibodies is that their clinical potential can readily be increased by improving their existing properties, as will be discussed below. Many authors review the pros and contras concerning these evolving steps made in the past five years. Most progresses have been made in the field of genetic engineering and pretargeting (Bischof Delaloye, 2000; Blankenberg, 2000; Illidge and Brock, 2000; Maynard and Georgiou, 2000; Verhaar-Langereis et al., 2000; Banerjee et al., 2001; Carter, 2001; Reff and Heard, 2001; Todorovska et al., 2001; Allen, 2002; Batra et al., 2002; Carlsson et al., 2002; Goldenberg, 2002; Boerman et al., 2003; Brekke and Sandlie, 2003; Carlsson et al. 2003; Goldenberg, 2003; von Mehren et al., 2003; Bethge and Sandmaier, 2004; Carter 2004; Huchalov and Chester, 2004; Mertens et al., 2004; Milenic et al., 2004; Mirick et al., 2004; Penichet and Morrison, 2004; Robinson et al., 2004; Tolmachev et al., 2004; Van De Wiele et al., 2004; Adam and Willbur, 2005; Adams and Weiner, 2005; Kelloff et al., 2005;

Koppe et al., 2005; Pavlou and Belsey, 2005; Sharkey and Goldenberg, 2005; Wu et al., 2005; Carter, 2006; Goldenberg et al., 2006; Pohlman et al., 2006; Sharkey and Goldenberg, 2006a; Sharkey and Goldenberg, 2006b; Weiner, 2006).

1.3.1 Antibody parameters

1.3.1.1 Binding affinity

The longer the time the radionuclides stay in or near the targeted cell the higher the fraction of the total radioactivity that can be utilised for imaging or therapy, and the higher the dose will be delivered per targeting event. Increased retention can be achieved by a targeting process that gives a high affinity and stable binding (Carlsson et al., 2003). Affinity is often expressed by the dissociation constant ($K_d = k_{off}/k_{on}$). In general a high affinity antibody is one which requires a very low concentration (typically 10^{-7} – 10^{-12} mol/l) of free antibody to acquire half of the saturating antibody level (Morris, 1995).

However, it remains an interesting question whether the affinity of the antibody for its receptor should be high or low. There is some evidence that with solid tumours, decreased tumour penetration can occur when the affinity is too high because of the 'binding site barrier' (Weinstein and van Osdol, 1992). Consequently, high affinity antibodies bind to the first targets encountered but fail to diffuse further into the tumour (Adams et al., 2001). On the contrary, with readily accessible cancer cells, e.g. tumour vasculature and haematological malignancies, high binding affinity might be desirable (Allen, 2002).

Ong and Mattes (1993) demonstrate that an antibody has a spectrum of functional affinities depending on the experimental conditions applied.

1.3.1.2 Antibody fragments

The long persistence of monoclonal antibodies in circulation exhibits toxic radiation to normal tissues with limited quantities delivered to the tumours (Carter, 2006). Furthermore, intact mAbs show poor diffusion from the vasculature into and through the tumour (Jain, 1987; Goel et al., 2000). While micrometastases offer an interesting target for RIT, these lesions often show high interstitial pressure and low vascularization, in which only low sensitivities have been observed (Bock et al. 1992; Vijayakumar et al. 1993, Goldenberg et al. 2002). To minimize these limitations of intact mAbs, many efforts of various groups have been undertaken in increasing the tumour-to-background ratio and increase tumour penetration. A common approach is the development of smaller antibody fragments by enzymatic cleavage (papain, pepsin or ficin) and genetically engineered single-chain Fv (scFv) constructs of antibody molecules (Reff ME, 2001; Goldenberg DM, 2002; Batra SK et al., 2002).

Enzymatic derived bivalent $F(ab')_2$ and monovalent Fab fragments have shown promising tumour penetration and good therapeutic results in animals (Wahl et al., 1983; Sharkey et al., 1990; Hansen et al., 1990; Blumenthal et al., 1992; Behr TM , 2000) and clinical studies (Murray et al., 1994; Willkomm et al., 2000; Libutti et al., 2001; Goldenberg, 2002). Disadvantages seen with these fragments are lower tumour uptake and high renal uptake particularly when a radiometal is used, which raises concern for renal toxicity. However, studies have shown that a high predose of cationic amino acids (e.g. L-lysine) could significantly reduce renal tubular reabsorption of radiometal-labeled Fab (Behr et al., 1995; Behr et al., 1998).

Genetic engineering provides powerful tools for manipulating the structure and pharmacokinetic properties of antibodies. One useful strategy has been the production of single chain fragments (scFv) containing the variable regions of

the immunoglobulin heavy chain and light chain, covalently connected by a flexible peptide linker (Colcher et al., 1990). Several scFvs have been evaluated for their specific *in vivo* tumour targeting to antigens such as TAG-72, carcinoembryonic antigen (CEA) and the HER2/neu receptor. They demonstrated more rapid clearance and higher tumour-to-normal tissue ratios than the corresponding IgG or Fab fragments (Milenic et al., 1991; Adams et al., 1993; Wu et al., 1996). Furthermore, penetration of scFv into a tumour from the vasulature demonstrated with autoradiography, was superior to that of corresponding intact IgG, $F(ab')_2$ or Fab (Yokota et al., 1993).

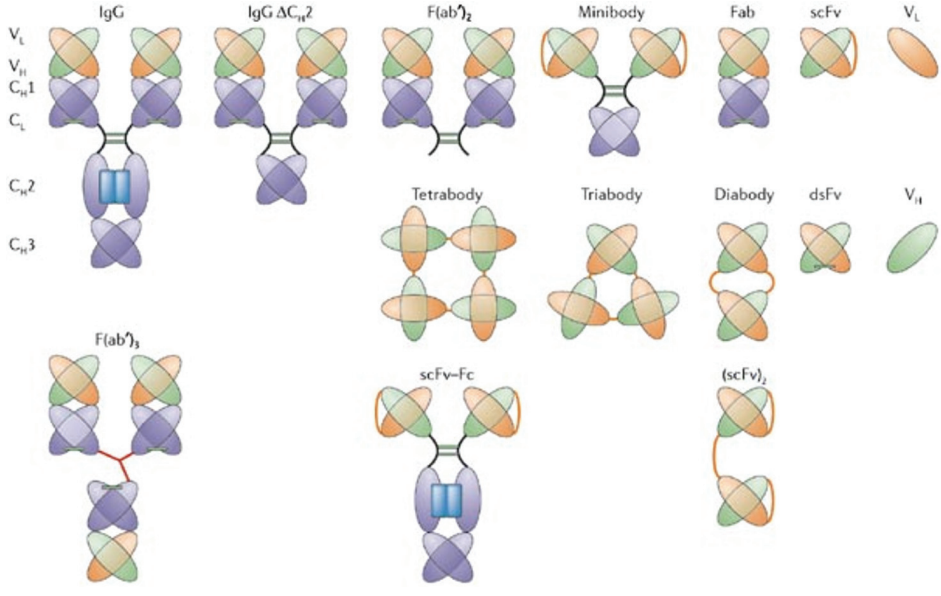

Fig. 1.9. Alternative antibody formats with a molecular-weight range of at least 12–150 kDa and a valency (n) range from monomeric (n = 1), dimeric (n = 2) and trimeric (n = 3) to tetrameric (n = 4). The building block that is most frequently used to create novel antibody formats is the single-chain variable (V)-domain antibody fragment (scFv), which comprises V domains from the heavy and light chain (V_H and V_L domain) joined by a peptide linker of up to ~15 amino-acid residues. Constant (C) and V domains, inter-chain disulphide bonds (green bars) and glycosylation are depicted. Peptide and chemical linkers are shown as orange and red lines, respectively. C_H, C domain of immunoglobulin heavy chain; C_L, C domain of immunoglobulin light chain; dsFv, disulphide-stabilized scFv. (Carter, 2006)

Because of the rapid clearance of 25 kDa proteins from the blood pool, the absolute tumour uptake of a monomeric scFv is limited. Multivalent antibody constructs have demonstrated improved tumour uptake with the corresponding form and demonstrate intermediate blood clearance ratios compared with scFv and intact antibodies. Different strategies have been described in literature for the formation of multivalent antibodies with altered pharmacokinetics and improved tumour uptake. Adams et al. (1993) described an improvement in *in vivo* tumour targeting using divalent forms of anti-*neu*-scFv with a C-terminal Gly_4Cys joined by a disulfide bond (Huston et al., 1994). Another antibody fragment, a minibody, was produced by fusion of T84.66 anti-CEA scFv to the human IgG1 CH3 domain (Hu et al. 1996). Others have fused scFvs to protein domains capable of multimerization, e.g., leucine zipper proteins (Kostelny et al., 1992), streptavidin (Dubel et al., 1995), or the κ-constant region (McGregor et al. 1994). The easiest approach for the production of dimeric scFvs is based on spontaneous formation of noncovalent dimers such as 50 kDa diabodies (Holliger, 1993). Figure 1.9 shows a recent overview of alternative antibody formats based on the scFv as building block given by Carter (2006).

Tabel 1.8 Targeting properties of monoclonal antibody and alternative antibody formats (Goldenberg et al., 2006)

	IgG	$F(ab')_2$	CH2-deletion	Minibody	Fab	Diabody	scFv
Physical properties							
Approximate molecular weight (kDa)	150	100	120	80	50	40-50	20-25
Biological properties							
Approximate biological $t_{½}$ blood[†]	2-3 d	1 d	Hours	Hours	Hours	Hours	Hour
Target organ	Liver	Liver	Liver	Liver	Kidney	Kidney	Kidney
Tumour binding properties							
Relative uptake[‡]	1	2	2-3	2-3	3	3	4
Time to optimum accumulation	Day(s)	Day	Hours	Hours	Hours	Hours	Hour
Relative duration[‡]	1	2	2-3	2-3	3	3	4

[†] Estimated time for 50% of the antibody to clear from the blood
[‡] From the highest (1) to the lowest (4)

Table 1.8 shows the changes in targeting properties of some engineered antibody fragments. New molecular constructs are being developed with properties that enable good uptake in tumours, with minimal accumulation and retention in normal tissue, but it is possible that at least for some of these constructs, the choice of radionuclide may be limited.

1.3.1.3 Immunogenicity

Except for altering pharmacokinetics, genetic engineering has another advantage. Mouse monoclonal antibodies have shown limited use as therapeutic agents in humans as a result of the production of human anti-mouse-antibodies (HAMA response).

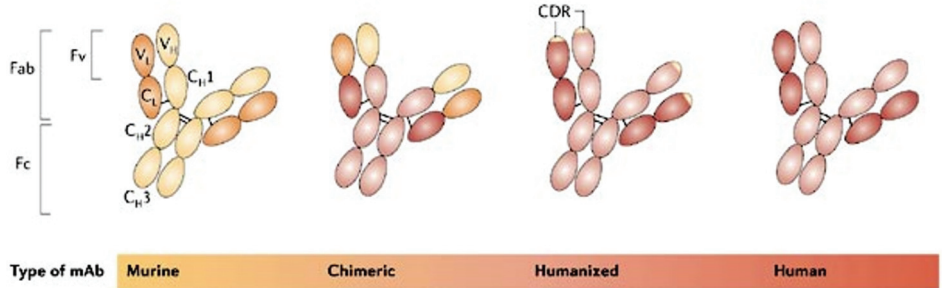

Fig. 1.10. Advances in genetic engineering techniques have contributed to the development of humanized therapeutic mAbs. The fundamental structure of an intact, single immunoglobulin G (IgG) molecule has a pair of light chains (orange/red) and a pair of heavy chains (yellow/pink). Light chains are composed of two separate regions (one variable region (VL) and one constant region (CL)), whereas heavy chains are composed of four regions (VH, CH1, CH2 and CH3). The complementarity-determining regions (CDRs) are found in the variable fragment (Fv) portion of the antigen-binding fragment (Fab). Chimeric mAbs such as cetuximab and rituximab are constructed with variable regions (VL and VH) derived from a murine source and constant regions derived from a human source. Humanized therapeutic mAbs are predominantly derived from a human source except for the CDRs, which are murine. There are currently four approved humanized mAbs. Both murine and human mAbs are entirely derived from mouse and human sources, respectively. Panitumumab (ABX–EGF) is a fully human anti-epidermal growth factor receptor (EGFR) mAb, but has not yet been approved. (Imai and Takaoka, 2006)

In an attempt to reduce the immunogenicity of mouse antibodies, genetic engineering was also used to generate chimeric antibodies, that is, antibodies with human constant regions and mouse variable regions. However, anti-chimeric antibody responses (HACAs) have been observed. Further minimization of the mouse component of antibodies can be achieved through complement determining region (CDR) grafting. In these humanized antibodies, only the CDR loops are inserted into the human variable framework (Fig. 1.10) (Imai and Takaoka, 2006).

1.3.1.4 Pretargeting

Pretargeting is a process in which the antibody and radionuclide targeting steps are separated. Recently, Sharkey (2006a) and others (Goodwin and Meares, 2001; Boerman et al., 2003) reviewed the advances made in pretargeting strategies. There are basically 3 types of pretargeting methods used for radionuclides: those that use a bispecific antibody (bsMAb); those based on streptavidin/avidin and biotin; and a new model that is evaluating the possibility for using complementary DNA analogues. The steps commonly used in these pretargeting methods are illustrated in Figure 1.11.

Pretargeting procedures permit a very rapid uptake of radioactivity in tumours, thereby increasing the radiation dose rate, which could be important for improving therapeutic responses. Data from animal models and recent clinical studies suggest that pretargeting can deliver more radioactivity to tumours than a directly radiolabeled whole IgG. All pretargeting procedures could be adapted for use with different radionuclides that would be best suited for a variety of clinical indications and settings. Therefore, pretargeting has potentially important advantages over directly radiolabeled antibodies for future therapeutic applications.

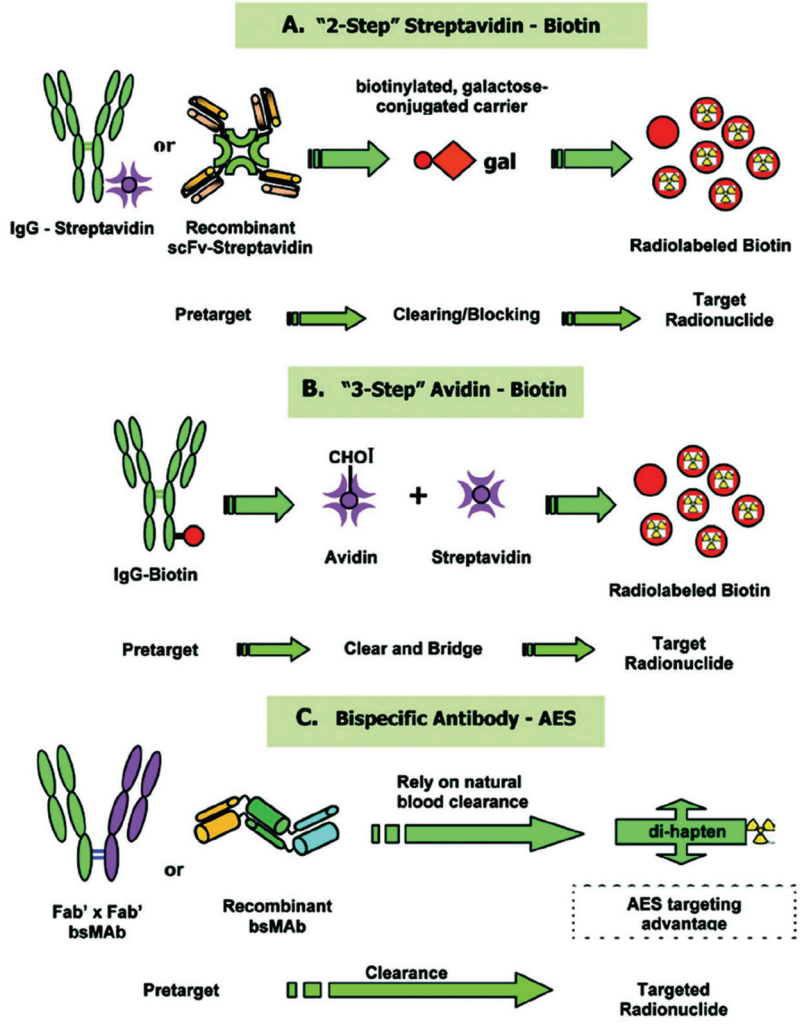

Fig. 1.11. Most commonly used pretargeting methods for radioimmunotherapy (Sharkey and Goldenberg, 2006a) *AES, affinity enhancing system; gal, galactose; IgG, immunoglobulin G*

1.3.2 Choice of Radionuclides

1.3.2.1 Radionuclides for radioimmunotherapy

In RIT, potentially therapeutic radionuclides are transported to the desired site of action by target-selective vehicles. As a consequence, any consideration of the optimal properties of such nuclides must take into account the nature and *in*

vivo behaviour of the respective vehicle. Despite this obvious limitation, some generalizations can be made about the required physical characteristics of therapy nuclides, and these have formed the basis of numerous publications (e.g. Wessels and Rogus (1984) and Andres and Schubiger (1987)). Several types of radionuclides are suitable for therapy. Table 1.9 lists some of the more commonly used radionuclides conjugated to antibodies for RIT.

Tabel 1.9 Physical properties of some radionuclides of therapeutic interest in RIT

Radionuclide	Emission	Half-life	Range	Approximate # Cell Diameters
^{131}Iodine	β	8.0 d	0.08–2.3 mm	10 to 230
^{90}Yttrium	β	64.1 h	4.0–11.3 mm	400 to 1100
^{177}Lutetium	β	6.7 d	0.04–1.8 mm	4 to 180
^{188}Rhenium	β	17.0 h	1.9–10.4 mm	200 to 1000
^{67}Copper	β	61.9 d	0.05–2.1 mm	5 to 210
^{211}Astatine	α	7.2 h	60 µm	6
^{213}Bismuth	α	46 min	84 µm	8
^{125}Iodine	Auger	60.5 d	<100 nm	(1)
^{111}Indium	Auger	3.0 d	<100 nm	(1)

The three major groups are those emitting therapeutically adequate amounts of β particles, Auger electrons or α particles. Important factors influencing the choice of an isotope are the nature of the associated radiation, the penetration range, the physical half-life ($t_{1/2}$) of the nuclide, the stability of any daughter nuclides formed, cost, availability, linear energy transfer (LET), specific activity, feasibility of radiochemistry, substitution index, internalization and cellular metabolism. Tumour size is the primary consideration (Goldenberg, 2002; Carlsson et al., 2003; Adam et al., 2005; Milenic et al., 2004; Sharkey and Goldenberg, 2006b).

High energy β particles (e.g., ^{90}Y, E_{max} 2.3 MeV; ^{188}Re, E_{max} 2.1 MeV) are not efficient for killing single disseminated cells or small metastases, since only a small fraction of the electron energy will be deposited in such small targets. Most of the energy will instead be absorbed in surrounding tissues. On the other hand, they might be important for treatment in case of a non-uniform

radioactivity distribution in larger tumour areas to kill across several hundred cells, referred to as 'bystander effect' or 'crossfire effect'. Irradiation from the targeted cells will then enable a more uniform dose-distribution and give therapeutic effect also to non-targeted tumour cells (O'Donoghue et al., 1995). This is considered a significant attribute for radioconjugates compared with other immunoconjugates, since they can be therapeutically active even if heterogeneous antigen expression, tumour architecture, or other factors impede targeting of every cell (Carlsson et al., 2003; Sharkey and Goldenberg, 2006b).

Radionuclides emitting α particles are more appropriate for metastatic disease or applications where single cells are targeted. These high-energy particles (4-9 MeV) travel short distances (40-100 μm). They are characterized by dense emission path lengths of high LET, which is approximately 400 times greater than β^- emitters (80 versus 0.2 keV per μm). While it is estimated to take several hundred β^- particle emitting radionuclides (e.g., > 400) on a single cell to kill that cell, only few hits of α particles (e.g., 1-14) are necessary (Mattes, 2002; Milenic et al., 2004).

The low energy Auger electrons deposit their energy in a very short distance (e.g. a few Å), which makes it high LET. Auger electron emitters are only suitable if nuclear localisation is possible (Hofer, 2000). Despite this limitation, studies have demonstrated that Auger emitters might have a significant role as therapeutics, even if their clinical use might be limited to eradication of microscopic residual disease (Mattes, 2002; Michel et al., 2003; Milenic et al., 2004).

The physical half-life of the radionuclides should preferably be in the same order of magnitude as the biological half-life. A too long physical half-life increases the necessary amount of radionuclides to be delivered to the tumour cells to allow for reasonable amounts of decays before excretion. A too short physical half-life will not give enough time for the targeting process to take

place. It seems reasonable to assume that the most suitable physical half-life ranges from a few hours up to some days when targeting of disseminated cells is considered. Longer physical half-lives (up to one or a few weeks) might be desirable if high uptakes in solid tumour masses are needed (Carlsson et al., 2003).

1.3.2.2 Radionuclides for radioimmunodetection

The most studied radionuclides for radioimmunodetection are iodine-131 (^{131}I), indium-111 (^{111}In), iodine-123 (^{123}I), and technetium-99m (^{99m}Tc) (Table 1.10). Early studies were performed with ^{131}I (364 keV), but gamma rays emitted by ^{123}I (159 keV) or ^{99m}Tc (140 keV) are superior for imaging with a conventional gamma camera or SPECT. ^{99m}Tc is the most widely used radioisotope for diagnostic imaging.

Tabel 1.10 Most common radionuclides used in radioimmunodetection

Radionuclide	Emission	Half-life
SPECT		
^{131}Iodine	γ	8.0 d
^{123}Iodine	γ	13.1 h
^{99m}Technetium	γ	6.0 h
^{111}Indium	γ	62 h
PET		
^{64}Copper	β^+	12.7 h
^{18}Fluorine	β^+	1.8 h
^{89}Zirconium	β^+	3.27 d
^{124}Iodine	β^+	4.18 d

Labeling strategies for radiometals require bifunctional chelating agents (BFC), which consist of a chelator to complex the radiometal and a functional group for linkage with amine or thiol groups on proteins and peptides (Schubiger et al., 1996). The first BCFs were analogues of (ethylenediaminetetraacetic acid) EDTA and diethylenetriaminepentaacetic acid (DTPA) (Hnatowich et al., 1983). Many improvements have been made and commonly used BCFs for copper, technetium and indium have been reviewed (Hnatowich, 1994;

Schubiger et al., 1996; Zalutsky and Lewis, 2003; Yang et al., 2006). Several review articles discuss the various direct protein labeling methods for ^{99m}Tc and rhenium isotopes (Griffiths et al., 1992; Hnatowich, 1994). The labeling strategies for radiohalogen radionuclides were recently reviewed by Adam and Wilbur (2005). Different labeling strategies with radioiodine isotopes are reviewed by Zalutsky and Lewis (2003). The most frequently used methods for generating the electrophilic radioiodinating species involve the oxidants Iodo-Gen (Fraker and Speck, 1978) or chloramine-T (Hunter and Greenwood, 1962). Feasibility of immuno-PET has been established with ^{124}I- or ^{64}Cu-labeled monoclonal antibodies and more alternative PET tracers have been examined (Pagani et al., 1997; Lewis et al., 2003; Verel et al., 2004). Increased sensitivity has been documented relative to CT or magnetic resonance imaging (MRI). Limited availability of antibodies labeled with these isotopes has hindered development of immuno-PET and much effort has focused on the more readily available ^{18}F-labeled reagents. Due to the short half-life of ^{18}F, studies have been limited to small antibody fragments that can be rapidly cleared from the circulation. A possible solution to the search of a long-lived metallic PET isotope in the form of ^{89}Zr for labeling antibodies is described by Verel et al. (2003a-b). A possible limitation of this tracer can be the concomitant high gamma emission at 909 keV, which may limit the radioactive dose that can be administered and affect image quality and quantitative aspects of imaging (Eary, 2001).

1.3.3 Antigen parameters

1.3.3.1 Antigen/Receptor expression

Identifying a molecular or cellular target critical to the pathophysiology of cancer is a basic step in drug development. It is anticipated to be a necessary but not sufficient condition for successful tumour targeting with an antibody.

An ideal expression profile is abundant and homogeneous on the external surface of all tumour cells for multiple tumour types, with the majority of patients for each tumour type, and absent from normal tissue. It is not necessary to fully satisfy all of these criteria as evidenced by clinical approval of antibodies targeting HER2 (Herceptin), CD20 (Rituxan, Zevalin and Bexxar), CD33 (Mylotarg), CD52 (Campath) and epidermal growth factor receptor (EGFR) (Erbitux). Table 1.11 gives an overview of the most important antigen expression characteristics that need to be investigated during identification and validation of new antibody targets (Carter et al., 2004).

Tabel 1.11 Antigen expression characteristics suitable for antibody targeting (Carter et al., 2004)

- Associated with advanced disease; present in tumours at all stages of disease, including metastatic foci; causally involved in disease pathogenesis; no downregulation
- Homogeneous expression; heterogeneous expression may necessitate bystander effect
- Lower limit and upper limit of antigen expression are not known; dependent non-solid tumour versus solid tumour; dependent conjugated versus unconjugated; 5 000 to 1 000 000 copies
- Limited, preferably no expression on vital normal tissue; less problematic on non-vital tissue e.g. CD20, CD33 and CD52
- Target is not shed or shed at low levels (<500 ng/ml)

Ideally, the target is preferentially expressed and/or activated in cancer cells at all stages of disease, including metastatic foci. Minimally, it should be present in advanced disease and preferentially causally involved in the pathogenesis to reduce the probability that tumours will escape from antibody therapy by down regulation. Target cells should not show a high degree of heterogeneity in antigen expression. However, using radionuclides, the targeted treatment might lead to toxicity against antigen-negative cells, called the bystander effect, which are in close proximity of the actual target. In that case, some heterogeneity might be tolerated (Carter, 2001; Milenic, 2002; Presta, 2002; Ross et al., 2003). The targeted antigen should ideally have a high density (100 000 targets/cell) on the tumour cell, although it depends on several parameters

such as treatment of non-solid tumour versus solid tumour, use of immunoconjugates versus non-conjugates (Tanimoto et al., 1989). The antigen should not be shed or downregulated. Circulating shed antigen will compete with targets at the cancer cells for binding of the targeted therapeutics, resulting in acceleration of antibody clearance and decrease of antibody localization. Using radioimmunoconjugates this might lead to increasing the toxicity to normal tissues. Ideally the target antigen is not shed (e.g. CD20, Einfeld et al. 1988) or shed at only low (<500 ng/ml) and antibody-titratable levels in the majority of patients (e.g. HER2, Baselga et al. 1996, Cobleigh et al. 1999). Genomic instability is sometimes referred to as a consequence of the multistep carcinogenesis in which defect onco-, supressor-, cell cycle- and apoptosis regulating genes allow the tumour cells to pass the cell cycle and divide in spite of non-repaired DNA damage. The genomic instability may give rise to unique tumour cell epitopes suitable for targeting. However, if an efficient therapy based on targeting of new epitopes is carried out, a selection will be created and new subclones with no or only low amounts of the epitope might appear.
Furthermore, the treatment with radioactivity itself will create DNA damages and thereby possibly make the selection process more extensive. By choosing appropriate targets for radionuclide therapy it might be possible to minimise the risk for adverse effects due to genomic instability. For example, it is known that the expression of the oncogene HER2 is surprisingly stable when comparing primary tumours with the corresponding metastases (Niehans et al., 1993; Tewari et al., 2000; Carlsson et al., 2003).
Tumour progression depends upon a variety of non-cancerous cells (e.g. endothelial cells, stromal cells) and factors associated directly or indirectly with them (e.g., matrix metalloproteinases, growth factors). Consequently, non-cancerous cells and these associated factors should also be considered as a source of cancer therapy targets. The recent approval of an anti-VEGF

antibody, bevacizumab (Avastatin), as anti-angiogenic treatment is an example of such approach.

1.3.3.2 Internalization

The binding of some ligands to their receptor can cause receptor-mediated internalization and influence the metabolism of radiolabeled antibodies (Sands and Jones, 1987). Depending on the type of radiotargeted therapy, this may be desired or should not at all occur. One critical factor is the high cellular retention of the radionuclides. For therapies with radiolabeled antibodies, internalization might be advantageous for α-emitting radionuclides. Because of the very short range of α-particles, they should ideally be produced in the proximity of the DNA. For radioiodinated tracers, internalization may lead to metabolization and also excretion of iodo-tyrosine from the lysosomes. Hereby, cell-associated radioiodine decreases rapidly from the cells followed by diffusion and elimination of the radionuclide (Geissler et al., 1991; Shih et al., 1994a; Shih et al., 1994b).

Different approaches have been developed for residualizing radioiodine activity in tumour cells after mAb internalization: oligosaccharide conjugates, positively charged templates, and D-amino acid peptides (Ram and Buchsbaum, 1994; Thorpe et al., 1993; Reist et al., 1995; Stein et al., 1995; Reist et al., 1996; Mattes et al., 1997; Govindan et al., 1999; Foulon et al., 2000; Zalutsky and Lewis, 2003; Stein et al., 2003; Govindan et al., 2004; Schaijk et al., 2005).

Radiometals, e.g. indium and technetium, are trapped within the lysosomes after catabolization (Duncan and Welch, 1993; Mattes et al., 1994). Therefore, tumour uptake can be increased when using radiometals instead of halogens when internalization of mAb-receptor occurs. However, kidney uptake of radiometals is increased by the same internalization effect, especially when

smaller antibody fragments are used. Therefore, different strategies have been tested to reduce kidney uptake of radiometals using basic amino acids (e.g., Lysine), amino sugars, and basic polypeptides. The effect seems to rely essentially on the presence of a positively charged amino group (Behr et al., 1998).

Some evidence is given that multivalency is required for internalization, e.g. when monovalent Fab fragments of several anti-HER2 antibodies were tested for internalization, the monovalent Fab fragments were not internalized (Srinivas et al., 1993).

1.3.3.3 Haematological cancers versus solid tumours

Despite the success of RIT in the treatment of non-Hodgkin's lymphoma, therapeutic success in solid tumours has been modest. Immunotherapeutics are often administrated via intravenous injection and distribution to the target cells occurs by the bloodstream. Therefore, haematological cancers are more accessible than solid tumours, e.g. malignant B or T cells, metastatic cells distributed in the bloodstream, or the cells of the tumour vasculature. Targeted therapeutics can rapidly bind these cells and long circulation times may not be necessary. On the contrary, in the case of solid tumours it is important that the radioimmunoconjugates circulate for sufficient time to obtain sufficient tumour uptake. Higher penetration is obtained when smaller antibody fragments are used, however, their size need to be above the exclusion limit for kidney filtration in order to circulate enough time in the bloodstream (Allen, 2002).

Solid tumours have substantial physical barriers composed by the microvascular endothelium, the tumour stromal and interstitial structures as well as the excessive interstitial pressure associated with a high cell density (Christiansen and Rasjeskaran, 2004). The affinity of the antibody is probably critical, and if it is too high, its ability to penetrate a tumour mass will be

further restricted (Adams et al., 2001; Graff and Wittrup, 2003). Various solutions to these problems have been considered, including the use of smaller antibody fragments, intratumour injection of antibody and the targeting of tumour vasculature with agents that increase permeability such as TNFα (Hale, 2006).

1.3.4 Future challenges

One of the initial goals of targeted strategies is defining targets early in cancer development, to intervene in early stages of cancer. Has radioimmunotherapy potential in targeting early steps of cancer development? Carter (2004) suggests that antigen expression restricted to early stage cancer appears impractical for antibody drug development for the following reasons. First, there is a risk that diagnosis of cancer will not occur until after antigen expression has been lost. Secondly, patients with early stage disease will often have established treatment options that preclude the use of an unproven experimental drug (Carter et al., 2004). However, very encouraging results of first-line treatment of lymphoma patients with radiolabeled antibodies were published (Kaminski et al., 2005). Seventy-six previously untreated patients received Bexxar. The overall response rate was as high as 95%, of which fifty-seven patients achieving a complete response (Kaminski et al., 2005). On the contrary, in solid cancers patients eligible for phase I/II RIT trials almost invariably have metastatic and bulky disease, and have been heavily pretreated with chemotherapy and/or radiotherapy (Koppe et al., 2005).

Perhaps the most challenging problem with RIT remains its inability to deliver a sufficient amount of radioactivity to kill solid tumours, especially when >5 cm, at tolerable doses to other organs. Interestingly, Sharkey (2006) discusses the potential of RIT in targeting the tumour vasculature, rather than to breach the tumour vasculature to deliver the radiotoxicity to the individual tumour cells. Vascular targets have received increasing attention over the past decade,

with a variety of agents, including antibodies, being used to inhibit neovascularization (Cardones and Banez, 2006; Folkman, 2006; Mitra et al., 2006). Some of these agents act on substances found on the endothelial cells of the blood vessels, but others, such as inhibitors of the vascular endothelial growth factor, act indirectly by binding to substances required to activate blood vessel formation (Folkman, 2006). Tijink et al. (2006) used a recombinant engineered antibody, L19-SIP, that binds to an isoform of fibronectin found primarily on blood vessels formed within the tumour, and thus the antibody does not have to overcome the barriers that inhibit migration to the individual tumour cells (Borsi et al., 2002). In addition to revaluating the conditions where RIT should be best applied, careful consideration also needs to be given to choosing solid tumours that, like NHL, will be more susceptible to radiation. In this regard, head and neck cancers are noted for their relative sensitivity to radiation, and therefore this would be an excellent indication for the development of a targeted radionuclide therapy (Sharkey, 2006).

Exploring the combinations of all new targeted strategies and optimizing the role of RIT in these combinations offers another big challenge for the future. Enhancement of immunotherapy and radioimmunotherapy has recently been demonstrated by the use of combined molecular targeting. The efficacy of radioimmunotherapy with an anti-LewisY monoclonal antibody was enhanced by the use of a tyrosine kinase that inhibited signalling of the epidermal growth factor receptor during RIT in animals (Lee et al., 2005). Several other studies support the possibility of synergy when combining targeted strategies (Burke and Denardo, 2001; Burke et al., 2002; Denardo, 2006). Also, in clinical trials highly selective or specific blocking of only one of the kinases involved in the signalling pathways has been associated with limited or sporadic responses. Many authors suggest that optimal targeting may involve targeting multiple molecules found in both the tumour and supportive tissue (Faivre et al., 2006;

Imai and Takaoka, 2006). Agents that target multiple pathways may increase the treatment-related toxicities (Kim, 2003). Also, the combination of small molecules and monoclonal antibodies may enhance the therapeutic efficacy, e.g. Bortezomib (PS-341, Velcade) increases the efficacy of trastuzumab (Herceptin) in HER-2-positive breast cancer cells in a synergistic manner (Cardoso et al., 2006).

1.4 References

Abou-Jawde R, Choueiri T, Alemany C, Mekhail T. An overview of targeted treatments in cancer. Clin Ther. 2003;25:2121-37.

Adam MJ, Wilbur DS. Radiohalogens for imaging and therapy. Chem Soc Rev. 2005;34:153-63.

Adams GP, McCartney JE, Tai MS, et al. Highly specific in vivo tumor targeting by monovalent and divalent forms of 741F8 anti-c-erbB-2 single-chain Fv. Cancer Res. 1993;53:4026-34.

Adams GP, Schier R, McCall AM, et al. High affinity restricts the localization and tumor penetration of single-chain fv antibody molecules. Cancer Res. 2001;61:4750-5.

Adams GP, Weiner LM. Monoclonal antibody therapy of cancer. Nat Biotechnol. 2005;23:1147-57.

Alavi A, Kung JW, Zhuang H. Implications of PET based molecular imaging on the current and future practice of medicine. Semin Nucl Med. 2004;34:56-69.

Allen LF, Eiseman IA, Fry DW, et al. CI-1033, an irreversible pan-erbB receptor inhibitor and its potential application for the treatment of breast cancer. Semin Oncol. 2003;30:65-78.

Allen TM. Ligand-targeted therapeutics in anticancer therapy. Nat Rev Cancer. 2002;2:750-63.

Andres RY, Schubiger PA. Radiolabelling of antibodies: methods and limitations. Nuklearmedizin. 1986;25:162-6.

Banerjee S, Pillai MR, Ramamoorthy N. Evolution of Tc-99m in diagnostic radiopharmaceuticals. Semin Nucl Med. 2001;31:260-77.

Baselga J, Tripathy D, Mendelsohn J, et al. Phase II study of weekly intravenous recombinant humanized anti-p185HER2 monoclonal antibody in patients with HER2/neu-overexpressing metastatic breast cancer. J Clin Oncol. 1996;14:737-44.

Batra SK, Jain M, Wittel UA, et al. Pharmacokinetics and biodistribution of genetically engineered antibodies. Curr Opin Biotechnol. 2002;13:603-8.

Behr TM, Blumenthal RD, Memtsoudis S, et al. Cure of metastatic human colonic cancer in mice with radiolabeled monoclonal antibody fragments. Clin Cancer Res. 2000;6:4900-7.

Behr TM, Goldenberg DM, Becker W. Reducing the renal uptake of radiolabeled antibody fragments and peptides for diagnosis and therapy: present status, future prospects and limitations. Eur J Nucl Med. 1998;25:201-12.

Behr TM, Sharkey RM, Juweid ME, et al. Reduction of the renal uptake of radiolabeled monoclonal antibody fragments by cationic amino acids and their derivatives. Cancer Res. 1995;55:3825-34.

Bethge WA, Sandmaier BM. Targeted cancer therapy and immunosuppression using radiolabeled monoclonal antibodies. Semin Oncol. 2004;31:68-82.

Bischof Delaloye A. Radioimmunoimaging and radioimmunotherapy: will these be routine procedures? Semin Nucl Med. 2000;30:186-94.

Blankenberg FG, Eckelman WC, Strauss HW, et al. Role of radionuclide imaging in trials of antiangiogenic therapy. Acad Radiol. 2000;7:851-67.

Blankenberg FG, Tait J, Ohtsuki K, et al. Apoptosis: the importance of nuclear medicine. Nucl Med Commun. 2000;21:241-50.

Blankenberg FG. Molecular imaging with single photon emission computed tomography. How new tracers can be employed in the nuclear medicine clinic. IEEE Eng Med Biol Mag. 2004;23:51-7.

Bloch SH, Dayton PA, Ferrara KW. Targeted imaging using ultrasound contrast agents. Progess and opportunities for clinical and research applications. IEEE Eng Med Biol Mag. 2004 ;23:18-29.

Blumenthal RD, Sharkey RM, Haywood L, et al. Targeted therapy of athymic mice bearing GW-39 human colonic cancer micrometastases with 131I-labeled monoclonal antibodies. Cancer Res. 1992;52:6036-44.

Bock E, Becker W, Scheele J, et al. Diagnostic accuracy of 99mTc-anti-CEA immunoscintigraphy in patients with liver metastases from colorectal carcinoma. Nuklearmedizin. 1992;31:80-3.

Boerman OC, van Schaijk FG, Oyen WJ, et al. Pretargeted radioimmunotherapy of cancer: progress step by step. J Nucl Med. 2003;44:400-11.

Borsi L, Balza E, Bestagno M, et al. Selective targeting of tumoral vasculature: comparison of different formats of an antibody (L19) to the ED-B domain of fibronectin. Int J Cancer. 2002;102:75-85.

Brannon-Peppas L, Blanchette JO. Nanoparticle and targeted systems for cancer therapy. Adv Drug Deliv Rev. 2004;56:1649-59.

Brekke OH, Sandlie I. Therapeutic antibodies for human diseases at the dawn of the twenty-first century. Nat Rev Drug Discov. 2003;2:52-62.

Burke PA, DeNardo SJ, Miers LA, et al. Cilengitide targeting of alpha(v)beta(3) integrin receptor synergizes with radioimmunotherapy to increase efficacy and apoptosis in breast cancer xenografts. Cancer Res. 2002;62:4263-72.

Burke PA, DeNardo SJ. Antiangiogenic agents and their promising potential in combined therapy. Crit Rev Oncol Hematol. 2001;39:155-71.

Cardones AR, Banez LL. VEGF inhibitors in cancer therapy. Curr Pharm Des. 2006;12:387-94.

Cardoso F, Durbecq V, Laes JF, et al. Bortezomib (PS-341, Velcade) increases the efficacy of trastuzumab (Herceptin) in HER-2-positive breast cancer cells in a synergistic manner. Mol Cancer Ther. 2006; Epub ahead of print.

Carlsson J, Forssell Aronsson E, Hietala SO, Stigbrand T, Tennvall J. Tumour therapy with radionuclides: assessment of progress and problems. Radiother Oncol. 2003;66:107-17.

Carlsson J, Forssell-Aronsson E, Glimelius B, et al. Therapy with radiopharmaceuticals. Acta Oncol. 2002;41:623-8.

Carmeliet P , Jain R . 2000. Angiogenesis in cancer and other diseases. Nature 2000;407:249–57.

Carter P, Smith L, Ryan M. Identification and validation of cell surface antigens for antibody targeting in oncology. Endocr Relat Cancer. 2004;11:659-87.

Carter P. Improving the efficacy of antibody-based cancer therapies. Nat Rev Cancer. 2001;1:118-29.

Carter PJ. Potent antibody therapeutics by design. Nat Rev Immunol. 2006;6:343-57.

Chabner BA, Roberts TG Jr. Timeline: Chemotherapy and the war on cancer. Nat Rev Cancer. 2005;5:65-72.

Cho, H. S. et al. Structure of the extracellular region of HER2 alone and in complex with the Herceptin Fab. Nature 2003;421,756–60

Christiansen J, Rajasekaran AK. Biological impediments to monoclonal antibody-based cancer immunotherapy. Mol Cancer Ther. 2004;3:1493-501.

Cobleigh MA, Vogel CL, Tripathy D, et al. Multinational study of the efficacy and safety of humanized anti-HER2 monoclonal antibody in women who have HER2-overexpressing metastatic breast cancer that has progressed after chemotherapy for metastatic disease. J Clin Oncol. 1999;17:2639-48.

Coene E, Schelfhout AM, De Ridder L, De Potter C. Generation of a monoclonal antibody directed against a human cell substrate adhesion molecule and the expression of the antigen in human tissues. Hybridoma. 1997;16:77–83.

Colcher D, Bird R, Roselli M, et al. In vivo tumor targeting of a recombinant single-chain antigen-binding protein. J Natl Cancer Inst. 1990;82:1191-7.

Czernin J, Weber WA, Herschman HR. Molecular imaging in the development of cancer therapeutics. Annu Rev Med. 2006;57:99-118.

Dameron KM, Volpert OV, Tainsky MA, Bouck N. Control of angiogenesis in fibroblasts by p53 regulation of thrombospondin-1. Science 1994;265:1582–4.

De Potter C, Schelfhout AM, De Smet FH, et al. A monoclonal antibody directed against a human cell membrane antigen prevents cell substrate adhesion and tumor invasion. Am J Pathol. 1994;144:95–103.

DeNardo SJ. Combined molecular targeting for cancer therapy: a new paradigm in need of molecular imaging. J Nucl Med. 2006;47:4-5.

Dubel S, Breitling F, Kontermann R, et al. Bifunctional and multimeric complexes of streptavidin fused to single chain antibodies (scFv). J Immunol Methods. 1995;178:201-9.

Duncan JR, Welch MJ. Intracellular metabolism of indium-111-DTPA-labeled receptor targeted proteins. J Nucl Med. 1993;34:1728-38.

Eary JF. PET imaging for planning cancer therapy. J Nucl Med. 2001;42:770-1.

Einfeld DA, Brown JP, Valentine MA, et al. Molecular cloning of the human B cell CD20 receptor predicts a hydrophobic protein with multiple transmembrane domains. EMBO J. 1988;7:711-7.

Faivre S, Djelloul S, Raymond E. New paradigms in anticancer therapy: targeting multiple signaling pathways with kinase inhibitors. Semin Oncol. 2006;33:407-20.

Folkman J. Angiogenesis. Annu Rev Med. 2006;57:1-18.

Foulon CF, Reist CJ, Bigner DD, et al. Radioiodination via D-amino acid peptide enhances cellular retention and tumor xenograft targeting of an internalizing anti-epidermal growth factor receptor variant III monoclonal antibody. Cancer Res. 2000;60:4453-60.

Fraker PJ, Speck JC Jr. Protein and cell membrane iodinations with a sparingly soluble chloroamide,1,3,4,6-tetrachloro-3a,6a-diphrenylglycoluril. Biochem Biophys Res Commun 1978;80:849-57.

Gaa J, Rummeny EJ, Seemann MD. Whole-body imaging with PET/MRI. Eur J Med Res. 2004;9:309-12.

Geissler F, Anderson SK, Press O. Intracellular catabolism of radiolabeled anti-CD3 antibodies by leukemic T cells. Cell Immunol. 1991;137:96-110.

Ghobrial IM, Witzig TE, Adjei AA. Targeting apoptosis pathways in cancer therapy. CA Cancer J Clin. 2005;55:178-94.

Giffels P, Köhler S, De Potter C, et al. MAb 14C5 against a human cell substrate adhesion molecule for inhibition of tumor growth in-vivo. Eur J Cancer. 1997;33.(suppl 5):96.

Goel A, Colcher D, Baranowska-Kortylewicz J, et al. Genetically engineered tetravalent single-chain Fv of the pancarcinoma monoclonal antibody CC49: improved biodistribution and potential for therapeutic application. Cancer Res. 2000;60:6964-71.

Goldenberg DM, DeLand F, Kim E, et al. Use of radiolabeled antibodies to carcinoembryonic antigen for the detection and localization of diverse cancers by external photoscanning. N Engl J Med. 1978;298:1384-6.

Goldenberg DM, Sharkey RM, Paganelli G, et al. Antibody pretargeting advances cancer radioimmunodetection and radioimmunotherapy. J Clin Oncol. 2006;24:823-34.

Goldenberg DM. Advancing role of radiolabeled antibodies in the therapy of cancer. Cancer Immunol Immunother. 2003;52:281-96.

Goldenberg DM. Targeted therapy of cancer with radiolabeled antibodies. J Nucl Med. 2002;43:693-713.

Goodwin DA, Meares CF. Advances in pretargeting biotechnology. Biotechnol Adv. 2001;19:435-50.

Govindan SV, Mattes MJ, Stein R, et al. Labeling of monoclonal antibodies with diethylenetriaminepentaacetic acid-appended radioiodinated peptides containing D-amino acids. Bioconjug Chem. 1999;10:231-40.

Govindan SV, Stein R, Qu Z, et al. Preclinical therapy of breast cancer with a radioiodinated humanized anti-EGP-1 monoclonal antibody: advantage of a residualizing iodine radiolabel. Breast Cancer Res Treat. 2004;84:173-82.

Graff CP, Wittrup KD. Theoretical analysis of antibody targeting of tumor spheroids: importance of dosage for penetration, and affinity for retention. Cancer Res. 2003;63:1288-96.

Gridelli C. Targeted therapies in the treatment of non small cell lung cancer: reality and hopes. Curr Opin Oncol. 2004;16:126-9.

Griffiths GL, Goldenberg DM, Jones AL, et al. Radiolabeling of monoclonal antibodies and fragments with technetium and rhenium. Bioconjug Chem. 1992;3:91-9.

Hale G. Therapeutic antibodies--delivering the promise? Adv Drug Deliv Rev. 2006;58:633-9.

Hansen HJ, Jones AL, Grebenau R, et al. Labeling of anti-tumor antibodies and antibody fragments with Tc-99m. Cancer Treat Res. 1990;51:233-44.

Hillman BJ, Neiman HL. Translating molecular imaging research into radiologic practice: summary of the proceedings of the American College of Radiology Colloquium, April 22-24, 2001. Radiology. 2002;222:19-24.

Hillman BJ. Introduction to the special issue on medical imaging in oncology. J Clin Oncol. 2006;24:3223-4.

Hnatowich DJ, Layne WW, Childs RL, et al. Radioactive labeling of antibody: a simple and efficient method. Science. 1983;220:613-5.

Hnatowich DJ. The in vivo use of metallic radioisotopes in cancer detection and imaging. In: Fricker SP (ed). Metal compounds in cancer therapy. London: Chapman & Hall. 1994; 215-47.

Hofer KG. Biophysical aspects of Auger processes. Acta Oncol. 2000;39:651-7.

Holliger P, Hudson PJ. Engineered antibody fragments and the rise of single domains. Nat Biotechnol. 2005;23:1126-36.

Holliger P, Winter G. Engineering bispecific antibodies. Curr Opin Biotechnol. 1993;4:446-9.

Hu S, Shively L, Raubitschek A, et al. Minibody: A novel engineered anti-carcinoembryonic antigen antibody fragment (single-chain Fv-CH3) which exhibits rapid, high-level targeting of xenografts. Cancer Res. 1996;56:3055-61.

Huhalov A, Chester KA. Engineered single chain antibody fragments for radioimmunotherapy. Q J Nucl Med Mol Imaging. 2004;48:279-88.

Hunter WM, Greenwood C. Preparation of iodine-131 labelled human growth hormone of high specific activity. Nature. 1962;194:495-6.

Huston JS, Adams GP, McCartney JE, et al. Tumor targeting in a murine tumor xenograft model with the (sFv')2 divalent form of anti-c-erbB-2 single-chain Fv. Cell Biophys. 1994;24-25:267-78.

Hutson TE, Quinn DI. Cytokine therapy: a standard of care for metastatic renal cell carcinoma? Clin Genitourin Cancer. 2005;4:181-6.

Illidge TM, Brock S. Radioimmunotherapy of cancer: using monoclonal antibodies to target radiotherapy. Curr Pharm Des. 2000;6:1399-418.

Imai K, Takaoka A. Comparing antibody and small-molecule therapies for cancer. Nat Rev Cancer. 2006;6:714-27.

Isobe T, Herbst RS, Onn A. Current management of advanced non-small cell lung cancer: targeted therapy. Semin Oncol. 2005;32:315-28.

Jacene HA, Stearns V, Wahl RL. Lymphadenopathy resulting from acute hepatitis C infection mimicking metastatic breast carcinoma on FDG PET/CT. Clin Nucl Med. 2006;31:379-81.

Jain RK. Transport of molecules across tumor vasculature. Cancer Metastasis Rev. 1987;6: 559-93.

Kaminski MS, Tuck M, Estes J, et al. 131I-tositumomab therapy as initial treatment for follicular lymphoma. N Engl J Med. 2005;352:441-9.

Kassis AI, Adelstein SJ. Radiobiologic principles in radionuclide therapy. J Nucl Med. 2005;46:4S-12S.

Kelloff GJ, Krohn KA, Larson SM, et al. The progress and promise of molecular imaging probes in oncologic drug development. Clin Cancer Res. 2005;11:7967-85.

Kerbel RS. Antiangiogenic therapy: a universal chemosensitization strategy for cancer? Science. 2006;312:1171-5.

Kim JA. Targeted therapies for the treatment of cancer. Am J Surg. 2003;186:264-8.

Kim SJ, Park Y, Hong HJ. Antibody engineering for the developpment of therapeutic antibodies. Mol Cells. 2005;20:17-29.

Kitagawa Y, Nishizawa S, Sano K, et al. Prospective comparison of 18F-FDG PET with conventional imaging modalities (MRI, CT, and 67Ga scintigraphy) in assessment of combined intraarterial chemotherapy and radiotherapy for head and neck carcinoma. J Nucl Med. 2003;44:198-206.

Koppe MJ, Postema EJ, Aarts F, et al. Antibody-guided radiation therapy of cancer. Cancer Metastasis Rev. 2005;24:539-67.

Kostelny SA, Cole MS, Tso JY. Formation of a bispecific antibody by the use of leucine zippers. J Immunol. 1992;148:1547-53.

Lambert JM. Drug-conjugated monoclonal antibodies for the treatment of cancer. Curr Opin Pharmacol. 2005;5:543-9.

Larson SM, Krenning EP. A pragmatic perspective on molecular targeted radionuclide therapy. J Nucl Med. 2005;46:1S-3S.

Larson SM, Pentlow KS, Volkow ND, et al. PET scanning of iodine-124-3F9 as an approach to tumor dosimetry during treatment planning for radioimmunotherapy in a child with neuroblastoma. J Nucl Med. 1992;33:2020-3.

Lee FT, Mountain AJ, Kelly MP, et al. Enhanced efficacy of radioimmunotherapy with 90Y-CHX-A"-DTPA-hu3S193 by inhibition of epidermal growth factor receptor (EGFR) signaling with EGFR tyrosine kinase inhibitor AG1478. Clin Cancer Res. 2005;11:7080s-7086s.

Lehtiö K , Eskola O , Viljanen T , et al. Imaging perfusion and hypoxia with PET to predict radiotherapy response in head-and-neck cancer. *Int*. J. Radiat. Oncol. Biol. Phys. 2004;59:971–82.

Lewis MR, Wang M, Axworthy DB, et al. In vivo evaluation of pretargeted 64Cu for tumor imaging and therapy. J Nucl Med. 2003;44:1284-92.

Libutti SK, Alexander HR Jr, Choyke P, et al. A prospective study of 2-[18F] fluoro-2-deoxy-D-glucose/positron emission tomography scan, 99mTc-labeled arcitumomab (CEA-scan), and blind second-look laparotomy for detecting colon cancer recurrence in patients with increasing carcinoembryonic antigen levels. Ann Surg Oncol. 2001;8:779-86.

Lim JW, Tang CL, Keng GH. False positive F-18 fluorodeoxyglucose combined PET/CT scans from suture granuloma and chronic inflammation: report of two cases and review of literature. Ann Acad Med Singapore. 2005;34:457-60.

Lovqvist A, Humm JL, Sheikh A, et al. PET imaging of (86)Y-labeled anti-Lewis Y monoclonal antibodies in a nude mouse model: comparison between (86)Y and (111)In radiolabels. J Nucl Med. 2001;42:1281-7.

Lowe SW, Lin AW. Apoptosis in cancer. Carcinogenesis. 2000;21:485-95.

Mach JP, Carrel S, Forni M, et al. Tumor localization of radiolabeled antibodies against carcinoembryonic antigen in patients with carcinoma: a critical evaluation. N Engl J Med. 1980;303:5-10.

Mahmood U. Near infrared optical applications in molecular imaging. Earlier, more accurate assessment of disease presence, disease course, and efficacy of disease treatment. IEEE Eng Med Biol Mag. 2004;23:58-66.

Maione P, Rossi A, Airoma G, Ferrara C, Castaldo V, Gridelli C. The role of targeted therapy in non-small cell lung cancer. Crit Rev Oncol Hematol. 2004;51:29-44

Mariani G. New developments in the treatment of metastatic breast cancer: from chemotherapy to biological therapy. Ann Oncol. 2005;16:191-4.

Marmor MD, Yarden Y. Role of protein ubiquitylation in regulating endocytosis of receptor tyrosine kinases. Oncogene. 2004;23:2057-70.

Massarelli E, Herbst RS. Use of novel second-line targeted therapies in non-small cell lung cancer. 1: Semin Oncol. 2006;33:S9-16.

Mattes MJ, Griffiths GL, Diril H, et al. Processing of antibody-radioisotope conjugates after binding to the surface of tumor cells. Cancer. 1994;73:787-93.

Mattes MJ, Shih LB, Govindan SV, et al. The advantage of residualizing radiolabels for targeting B-cell lymphomas with a radiolabeled anti-CD22 monoclonal antibody. Int J Cancer. 1997;71:429-35.

Mattes MJ. Radionuclide-antibody conjugates for single-cell cytotoxicity. Cancer. 2002;94:1215-23.

Maynard J, Georgiou G. Antibody engineering. Annu Rev Biomed Eng. 2000;2:339-76.

McGregor DP, Molloy PE, Cunningham C, et al. Spontaneous assembly of bivalent single chain antibody fragments in Escherichia coli. Mol Immunol. 1994;31:219-26.

Meikle SR, Kench P, Kassiou M, et al. Small animal SPECT and its place in the matrix of molecular imaging technologies. Phys Med Biol. 2005;50:R45-61.

Mendelsohn J, Baselga J. Epidermal growth factor receptor targeting in cancer. Semin Oncol. 2006;33:369-85.

Mertens N, Devos F, Leoen J, et al. New strategies in polypeptide and antibody synthesis: an overview. Cancer Biother Radiopharm. 2004;19:99-109.

Michel RB, Brechbiel MW, Mattes MJ. A comparison of 4 radionuclides conjugated to antibodies for single-cell kill. J Nucl Med. 2003;44:632-40.

Micke P, Ostman A. Exploring the tumour environment: cancer-associated fibroblasts as targets in cancer therapy. Expert Opin Ther Targets. 2005;9:1217-33.

Milenic DE, Brady ED, Brechbiel MW. Antibody-targeted radiation cancer therapy. Nat Rev Drug Discov. 2004;3:488-99.

Milenic DE, Yokota T, Filpula DR, et al. Construction, binding properties, metabolism, and tumor targeting of a single-chain Fv derived from the pancarcinoma monoclonal antibody CC49. Cancer Res. 1991;51:6363-71.

Milenic DE. Monoclonal antibody-based therapy strategies: providing options for the cancer patient. Curr Pharm Des. 2002;8:1749-64.

Mirick GR, Bradt BM, Denardo SJ, et al. A review of human anti-globulin antibody (HAGA, HAMA, HACA, HAHA) responses to monoclonal antibodies. Not four letter words. Q J Nucl Med Mol Imaging. 2004;48:251-7.

Mitra A, Nan A, Papadimitriou JC, et al. Polymer-peptide conjugates for angiogenesis targeted tumor radiotherapy. Nucl Med Biol. 2006;33:43-52.

Molls M, Stadler P, Becker A, et al. Relevance of oxygen in radiation oncology: mechanisms of action, correlation to low hemoglobin levels. J. Strahlenther. Onkol. 1998;174:13–16.

Morris RJ. Antigen-antibody interactions: how affinity and kinetics affect assay design and selection procedures. In: Ritter MA, Ladyman HM, eds. Monoclonal antibodies: Production, engineering and clinical application. New York, NY: Cambridge University Press, 1995; 34-57.

Murray JL, Rosenblum MG, Zhang HZ, et al. Comparative tumor localization of whole immunoglobulin G anticarcinoembryonic antigen monoclonal antibodies IMMU-4 and IMMU-4 F(ab')2 in colorectal cancer patients. Cancer. 1994;73:850-7.

Nelson SJ. Magnetic resonance spectroscopic imaging. Evaluating responses to therapy for gliomas. IEEE Eng Med Biol Mag. 2004;23:30-9.

Newell DR. How to develop a successful cancer drug--molecules to medicines or targets to treatments? Eur J Cancer. 2005;41:676-82.

Niehans G.A., Singleton T.P., Dykoski D., et al. Stability of HER-2/neu expression over time and at multiple metastatic sites. J Natl Cancer Inst. 1993;85:1230-5

O'Donoghue JA, Bardies M, Wheldon TE. Relationships between tumor size and curability for uniformly targeted therapy with beta-emitting radionuclides. J Nucl Med. 1995;36:1902-9.

Olafsen T, Cheung CW, Yazaki PJ, et al. Covalent disulfide-linked anti-CEA diabody allows site-specific conjugation and radiolabeling for tumor targeting applications. Protein Eng Des Sel. 2004;17:21-7.

Ong GL, Mattes MJ. Re-evaluation of the concept of functional affinity as applied to bivalent antibody binding to cell surface antigens. Mol Immunol. 1993;30:1455-62.

Pagani M, Stone-Elander S, Larsson SA. Alternative positron emission tomography with non-conventional positron emitters: effects of their physical properties on image quality and potential clinical applications. Eur J Nucl Med. 1997;24:1301-27.

Pardoll DM. Spinning molecular immunology into successful immunotherapy. Nat Rev Immunol. 2002;2:227-38.

Pastan I, Hassan R, Fitzgerald DJ, Kreitman RJ. Immunotoxin therapy of cancer. Nat Rev Cancer. 2006;6:559-65.

Pavlou AK, Belsey MJ. The therapeutic antibodies market to 2008. Eur J Pharm Biopharm. 2005;59:389-96.

Penichet, ML, Morrison, SL. Design and engineering human forms of monoclonal antibodies. Drug Develop Res. 2004;61:121-136.

Pohlman B, Sweetenham J, Macklis RM. Review of clinical radioimmunotherapy. Expert Rev Anticancer Ther. 2006;6:445-61.

Pomper MG, Hammoud DA. Positron emission tomography in molecular imaging. Could the promise of personalized patient care be reaching fruition? IEEE Eng Med Biol Mag. 2004;23:28-37.

Presta LG. Engineering antibodies for therapy. Curr Pharm Biotechnol. 2002;3:237-56.

Ram S, Buchsbaum DJ. Radioiodination of monoclonal antibodies D612 and 17-1A with 3-iodophenylisothiocyanate and their biodistribution in tumor-bearing nude mice. Cancer. 1994;73:808-15.

Ravi R, Mookerjee B, Bhujwalla ZM, Sutter CH, Artemov D, Zeng Q, et al. Regulation of tumor angiogenesis by p53-induced degradation of hypoxia-inducible factor-1a. Genes Dev 2000;14:34–44.

Reff ME, Heard C. A review of modifications to recombinant antibodies: attempt to increase efficacy in oncology applications. Crit Rev Oncol Hematol. 2001;40:25-35.

Reist CJ, Archer GE, Kurpad SN, et al. Tumor-specific anti-epidermal growth factor receptor variant III monoclonal antibodies: use of the tyramine-cellobiose radioiodination method enhances cellular retention and uptake in tumor xenografts. Cancer Res. 1995;55:4375-82.

Reist CJ, Garg PK, Alston KL, et al. Radioiodination of internalizing monoclonal antibodies using N-succinimidyl 5-iodo-3-pyridinecarboxylate. Cancer Res. 1996;56:4970-7.

Rettig WJ, Garin-Chesa P, Healey JH, et al. Regulation and heteromeric structure of the fibroblast activation protein in normal and transformed cells of mesenchymal and neuroectodermal origin. Cancer Res. 1993;53:3327-35.

Reubi JC, Macke HR, Krenning EP. Candidates for peptide receptor radiotherapy today and in the future. J Nucl Med. 2005;46:67S-75S.

Robinson MK, Weiner LM, Adams GP. Improving monoclonal antibodies for cancer therapy. Drug Develop Res. 2004;61:172-187.

Ross J, Gray K, Schenkein D, et al. Antibody-based therapeutics in oncology. Expert Rev Anticancer Ther. 2003;3:107-21.

Sands H, Jones PL. Methods for the study of the metabolism of radiolabeled monoclonal antibodies by liver and tumor. J Nucl Med. 1987;28:390-8.

Sanz L, Cuesta AM, Compte M, et al. Antibody engineering: facing new challenges in cancer therapy. Acta Pharmacol Sin. 2005;26:641-8.

Sawyers C. Targeted cancer therapy. Nature. 2004;432:294-7.

Schnall M, Rosen M. Primer on imaging technologies for cancer. J Clin Oncol. 2006;24:3225-33.

Schrama D, Reisfeld RA, Becker JC. Antibody targeted drugs as cancer therapeutics. Nat Rev Drug Discov. 2006;5:147-59.

Schubiger PA, Alberto R, Smith A. Vehicles, chelators, and radionuclides: choosing the "building blocks" of an effective therapeutic radioimmunoconjugate. Bioconjug Chem. 1996;7:165-79.

Schuster DM, Halkar RK. Molecular imaging in breast cancer. Radiol Clin North Am. 2004;42:885-908.

Scott AM, Cebon J. Clinical promise of tumour immunology. Lancet. 1997;349:SII19-22.

Seemann MD. Whole-body PET/MRI: the future in oncological imaging. Technol Cancer Res Treat. 2005;4:577-82.

Shan D, Ledbetter JA, Press OW. Apoptosis of malignant human B cells by ligation of CD20 with monoclonal antibodies. Blood. 1998;91:1644-52.

Sharkey RM, Goldenberg DM. Advances in radioimmunotherapy in the age of molecular engineering and pretargeting. Cancer Invest. 2006;24:82-97.

Sharkey RM, Goldenberg DM. Perspectives on cancer therapy with radiolabeled monoclonal antibodies. J Nucl Med. 2005;46:115S-27S.

Sharkey RM, Goldenberg DM. Targeted therapy of cancer: new prospects for antibodies and immunoconjugates. CA Cancer J Clin. 2006;56:226-43.

Sharkey RM, Motta-Hennessy C, Pawlyk D, et al. Biodistribution and radiation dose estimates for yttrium- and iodine-labeled monoclonal antibody IgG and fragments in nude mice bearing human colonic tumor xenografts. Cancer Res. 1990;50:2330-6.

Sharkey RM. Radioimmunotherapy against the tumor vasculature: A new target? J Nucl Med. 2006;47:1070-4.

Sharma SK, Bagshawe KD, Begent RH. Advances in antibody-directed enzyme prodrug therapy. Curr Opin Investig Drugs. 2005;6:611-5.

Sherif ZA, Nakai S, Pirollo KF, Rait A, Chang EH. Downmodulation of bFGF-binding protein expression following restoration of p53 function. Cancer Gene Ther 2001;8:771–82.

Shih LB, Lu HH, Xuan H, et al. Internalization and intracellular processing of an anti-B-cell lymphoma monoclonal antibody, LL2. Int J Cancer. 1994;56:538-45.

Shih LB, Thorpe SR, Griffiths GL, et al. The processing and fate of antibodies and their radiolabels bound to the surface of tumor cells in vitro: a comparison of nine radiolabels. J Nucl Med. 1994;35:899-908.

Smith-Jones PM, Solit DB, Akhurst T, et al. Imaging the pharmacodynamics of HER2 degradation in response to Hsp90 inhibitors. Nat Biotechnol. 2004;22:701-6.

Srinivas U, Tagliabue E, Campiglio M, et al. Antibody-induced activation of p185HER2 in the human lung adenocarcinoma cell line Calu-3 requires bivalency. Cancer Immunol Immunother. 1993;36:397-402.

Steeghs N, Nortier JW, Gelderblom H. Small Molecule Tyrosine Kinase Inhibitors in the Treatment of Solid Tumors: An Update of Recent Developments. Ann Surg Oncol. 2006; Epub ahead of print

Stein R, Goldenberg DM, Thorpe SR, et al. Effects of radiolabeling monoclonal antibodies with a residualizing iodine radiolabel on the accretion of radioisotope in tumors. Cancer Res. 1995;55:3132-9.

Stein R, Govindan SV, Mattes MJ, et al. Improved iodine radiolabels for monoclonal antibody therapy. Cancer Res. 2003;63:111-8.

Sugawara Y, Braun DK, Kison PV, et al. Rapid detection of human infections with fluorine-18 fluorodeoxyglucose and positron emission tomography: prelimin ary results. Eur J Nucl Med. 1998;25:1238-43.

Sundaresan G, Yazaki PJ, Shively JE, et al. 124I-labeled engineered anti-CEA minibodies and diabodies allow high-contrast, antigen-specific small-animal PET imaging of xenografts in athymic mice. J Nucl Med. 2003;44:1962-9.

Tanimoto M, Scheinberg DA, Cordon-Cardo C,et al. Restricted expression of an early myeloid and monocytic cell surface antigen defined by monoclenal antibody M195. Leukemia. 1989;3:339-48.

Tewari KS, Kyshtoobayeva AS, Mehta RS, et al. Biomarker conservation in primary and metastatic epithelial ovarian cancer. Gynecol Oncol. 2000;78:130-6.

Thorpe SR, Baynes JW, Chroneos ZC. The design and application of residualizing labels for studies of protein catabolism. FASEB J. 1993;7:399-405.

Tijink BM, Neri D, Leemans CR, et al. Radioimmunotherapy of head and neck cancer xenografts using 131I-labeled antibody L19-SIP for selective targeting of tumor vasculature. J Nucl Med. 2006;47:1127-35.

Todorovska A, Roovers RC, Dolezal O, et al. Design and application of diabodies, triabodies and tetrabodies for cancer targeting. J Immunol Methods. 2001;248:47-66.

Tolmachev V, Carlsson J, Lundqvist H. A limiting factor for the progress of radionuclide-based cancer diagnostics and therapy-availability of suitable radionuclides. Acta Oncol. 2004;43:264-75.

Townsend DW, Beyer T, Blodgett TM. PET/CT scanners: a hardware approach to image fusion. Semin Nucl Med. 2003;33:193-204.

Van de Wiele C, Revets H, Mertens N. Radioimmunoimaging. Advances and prospects. Q J Nucl Med Mol Imaging. 2004;48:317-25.

van Schaijk FG, Broekema M, Oosterwijk E, et al. Residualizing iodine markedly improved tumor targeting using bispecific antibody-based pretargeting. J Nucl Med. 2005;46:1016-22.

Vanhoefer U. Molecular mechanisms and targeting of colorectal cancer. Semin Oncol. 2005;32:7-10.

Vanholme B. Detectie en zuivering van een cel-substraat antigen betrokken bij de invasie en metastasering bij borstkanker. 2000, Scriptie, Gent, Faculteit Landbouwkundige en Toegepast Biologische Wetenschappen, 108p.

Verel I, Visser GW, Boellaard R, et al. 89Zr immuno-PET: comprehensive procedures for the production of 89Zr-labeled monoclonal antibodies. J Nucl Med. 2003;44:1271-81.

Verel I, Visser GW, Boellaard R, et al. Quantitative 89Zr immuno-PET for in vivo scouting of 90Y-labeled monoclonal antibodies in xenograft-bearing nude mice. J Nucl Med. 2003;44:1663-70.

Verel I, Visser GW, Vosjan MJ, et al. High-quality 124I-labelled monoclonal antibodies for use as PET scouting agents prior to 131I-radioimmunotherapy. Eur J Nucl Med Mol Imaging. 2004;31:1645-52.

Verhaar-Langereis MJ, Zonnenberg BA, de Klerk JM, et al. Radioimmunodiagnosis and therapy. Cancer Treat Rev. 2000;26:3-10.

Vijayakumar V, Blend MJ, Johnson DK, et al. Improved detection of hepatic lesions using MoAb B72.3 and a modified 111In labelling technique in patients with recurrent colon cancer. Nucl Med Commun. 1993;14:658-66.

Vink J, Cloos J, Kaspers GJ. Proteasome inhibition as novel treatment strategy in leukaemia. Br J Haematol. 2006;134:253-62.

von Mehren M, Adams GP, Weiner LM. Monoclonal antibody therapy for cancer. Annu Rev Med. 2003;54:343-69.

von Schulthess GK. Integrated modality imaging with PET-CT and SPECT-CT: CT issues. Eur Radiol. 2005;15:D121-6.

Wagner U, Köhler S, Prietl G, et al. Monoclonal anti-idiotype antibodies in immunotherapy of ovarian carcinoma (MAb ACA125) and breast carcinoma (MAb ACA14C5). Zentralbl Gynakol. 1999;121:190–195.

Wahl RL, Parker CW, Philpott GW. Improved radioimaging and tumor localization with monoclonal F(ab')2. J Nucl Med. 1983;24:316-25.

Waldmann TA. Effective cancer therapy through immunomodulation. Annu Rev Med. 2006;57:65-81.

Wang XM, Yu DM, McCaughan GW, et al. Fibroblast activation protein increases apoptosis, cell adhesion, and migration by the LX-2 human stellate cell line. Hepatology. 2005 Oct;42(4):935-45.

Weiner LM. Fully human therapeutic monoclonal antibodies. J Immunother. 2006;29:1-9.

Weinstein JN, van Osdol W. Early intervention in cancer using monoclonal antibodies and other biological ligands: micropharmacology and the "binding site barrier". Cancer Res. 1992;52:2747s-2751s.

Welch MJ, Redvanly CS. Handbook of radiopharmaceutical: Radiochemistry and applications. West Sussex, England: John Wiley and Sons Ltd; 2003, 848p.

Wessels BW, Rogus RD. Radionuclide selection and model absorbed dose calculations for radiolabeled tumor associated antibodies. Med Phys. 1984;11:638-45.

Willkomm P, Bender H, Bangard M, et al. FDG PET and immunoscintigraphy with 99mTc-labeled antibody fragments for detection of the recurrence of colorectal carcinoma. J Nucl Med. 2000;41:1657-63.

Winter G, Harris WJ. Humanized antibodies. Immunol Today. 1993;14:243-6.

Wu AM, Chen W, Raubitschek A, et al. Tumor localization of anti-CEA single-chain Fvs: improved targeting by non-covalent dimers. Immunotechnology. 1996;2:21-36.

Wu AM, Senter PD. Arming antibodies: prospects and challenges for immunoconjugates. Nat Biotechnol. 2005;23:1137-46.

Yang DJ, Kim EE, Inoue T. Targeted molecular imaging in oncology. Ann Nucl Med. 2006;20:1-11.

Yokota T, Milenic DE, Whitlow M, et al. Microautoradiographic analysis of the normal organ distribution of radioiodinated single-chain Fv and other immunoglobulin forms. Cancer Res. 1993;53:3776-83.

Zalutsky MR, Lewis JS. Radiolabeling antibodies for tumor imaging and therapy. In: Welch MJ, Redvankly CS, Eds. Handbook of radiopharmaceutical: Radiochemistry and applications. West Sussex, England: John Wiley and Sons Ltd; 2003, 685-714.

Zhang L, Yu D, Hu M, Xiong S, Lang A, Ellis LM, et al. Wild-type p53 suppresses angiogenesis in human leiomyosarcoma and synovial sarcoma by transcriptional suppression of vascular endothelial growth factor expression. Cancer Res 2000;60:3655–61.

Chapter 2

SCOPE AND AIMS

2.1 Scope of the thesis

In 2004 in Europe, there were an estimated 2 886 800 incident cases of cancer diagnosed and 1 711 000 cancer deaths. The most common incident form of cancer was lung cancer (13.3% of all incident cases), followed by colorectal cancer (13.2%) and breast cancer (13%). Lung cancer was also the most common cause of cancer death (341 800 deaths), followed by colorectal (203 700), stomach (137 900) and breast cancer (129 900) (Boyle et al., 2005). In the United States the estimates of new cancer cases and deaths follow these European trends (Jemal et al., 2005).

Once patients have been diagnosed with cancer, they are treated with the various modalities of surgery, radiation therapy, chemotherapy, immuno-therapy, or other treatments directed at the eradication of detectable lesions. Despite some spectacular successes in the treatment of relatively rare cancers, this approach has not yet led to a significant decrease in cancer mortality resulting from the common forms of many metastatic epithelial cancers, such as carcinoma of the lung, breast, colon, prostate, pancreas, and other sites. A key explanation in these often disappointing results is that once patients have been diagnosed with cancer, the disease is already in an advanced stage. Therefore, it is needed to intervene with anti-invasive and anti-metastasis diagnosis and therapies much earlier in the cancer progress.

Surgery and external radiation therapy are the major treatment modalities for primary tumours and large metastases. The development and evolution of modern chemotherapy during the second half of the twentieth century has improved the clinical outcome of patients with various forms of cancer. Still, in the far majority of malignancies the efficacy of chemotherapy is very limited. The concept of chemotherapy is non-specific and systemic and is based upon the observation that malignant cells divide at a more rapid rate than the normal cells leading to undesirable side effects. For this reason the

feasibility and efficacy of various forms of targeted therapies have been the subject of investigation on both preclinical and clinical research. These strategies have in common that they start from a target identified as playing an important role in tumour biology and oncogenesis. The targeted agents include monoclonal antibodies (mAbs), small molecules, peptide mimetics and antisense oligonucleotides.

In search of new antibody therapeutics for inhibition of metastatic breast cancer, De Potter et al. (1994) developed several mouse monoclonal antibodies (mAbs) against epitopes on the extracellular membrane of SK-BR-3 human breast cancer cells. In this study, we will focus on one of these mAbs, the IgG1 mAb 14C5, which is possibly involved in the cell-substrate adhesion and invasion of metastatic cancer cells (De Potter et al., 1994; Coene et al., 1997).

2.2 Aims

Our concept of choice is the use of radioiodinated mAb 14C5 as a potential agent for radioimmunodetection (RID) and –therapy (RIT) of lung, colon and breast cancer. As is apparent from the literature, the development of a new antibody drug can be depicted as an iterative design process. Key steps in the development of radioiodinated mAb 14C5 are: target identification and characterization, investigation of the radioiodinated mAb 14C5 properties and synthesis and evaluation of radioiodinated mAb 14C5 derivatives.

2.2.1 Identification and characterization of antigen 14C5

The objective of the first part of the thesis is to identify and characterize the antigen 14C5 (Ag 14C5) by affinity chromatography studies and comparative antigen expression analysis. De Potter et al. (1994) and Coene et al. (1997) already suggested that Ag 14C5 could be related to the family of integrins. Therefore, we will compare the expression of Ag 14C5 with the expression of eight different integrin subunits (α1, α2, α3, αv, β1, β2, β3, and β4) and three

different integrins (αvβ3, αvβ5, and α5β1) by flow cytometry, which possibly could show one integrin which shows high similarity with antigen 14C5 expression. In that case, the integrin similar to antigen 14C5 will be transfected in an Ag 14C5–negative cell line, Colo16. In addition, blocking experiments will be used to show specific Ag 14C5 binding of selected anti-integrin antibodies. These studies are presented in chapter 3.

Coene et al. (1997) demonstrated abundant expression of Ag 14C5 on the tumour surface of *in situ* and invasive breast cancer tissue. Because lung, colon and breast cancer are the most common forms of cancer and causes of cancer deaths, we will further investigate the spectrum of tumour types which might be considered for mAb 14C5 based diagnostic or therapeutic applications. We will analyse different human cancer cell lines for Ag 14C5 expression by immunocytochemistry and flow cytometry. Immunohistochemistry will be performed with human lung cancer and colon cancer tissues. The studies are described in chapter 4.

2.2.2 Targeting properties of radioiodinated monoclonal antibody 14C5 and its fragments Fab and F(ab')$_2$

Potentially suitable for antibody targeting, the second part of the thesis will address the *in vitro* and *in vivo* targeting properties of radioiodinated mAb 14C5, including the development of mAb 14C5 fragments (Fab and F(ab')$_2$), and investigating the process of internalization. Binding affinities will be estimated in a saturation binding assay using radioiodinated antibodies. For blood clearance and tumour uptake, biodistribution of a tumour-bearing mouse model and planar gamma camera imaging studies will be performed. These studies are presented in chapter 5 and chapter 6.

The most important factor influencing the choice of a radionuclide apart from its purpose (i.e. diagnostic or therapeutic) is probably the fate of the target antigen after the labeled mAb-antigen complex is formed. Depending upon

whether the antigen-antibody complex remains on the cell membrane, is shed into the circulation, or is internalized into the tumour cell, the labeled mAb 14C5 will be exposed to different catabolic processes, necessitating different labeling strategies. Therefore, internalization of mAb 14C5 and its fragments will be studied by confocal laser scanning microscopy. Secondly, we will evaluate the fate of radioiodinated mAb 14C5 and its fragments Fab and $F(ab')_2$ in an *in vitro* binding assay. Chapter 7 describes the internalization studies done with these three antibody molecules.

2.2.3 Optimizing the structure of monoclonal antibody 14C5: cloning and sequencing of its variable heavy and light chain genes

In the last part of the thesis, we will continue the process of optimizing the structure of mAb 14C5 in order to obtain improved targeting properties and to reduce the immunogenicity of this murine mAb 14C5. The variable heavy (VH) and light chain genes (VL) of mAb 14C5 will be cloned and sequenced, thereby facilitating further development of multivalent antibody formats of mAb 14C5 with less immunogenicity and more suitable targeting properties. These studies are presented in chapter 8.

2.3 References

Boyle P, Ferlay J. Cancer incidence and mortality in Europe, 2004. Ann Oncol. 2005;16:481-8.

Coene E, Schelfhout AM, De Ridder L, De Potter C. Generation of a monoclonal antibody directed against a human cell substrate adhesion molecule and the expression of the antigen in human tissues. Hybridoma. 1997;16:77–83.

De Potter C, Schelfhout AM, De Smet FH, et al. A monoclonal antibody directed against a human cell membrane antigen prevents cell substrate adhesion and tumor invasion. Am J Pathol. 1994;144:95–103.

Jemal A, Murray T, Ward E, et al. Cancer statistics, 2005. CA Cancer J Clin. 2005;55:10-30.

Chapter 3

IDENTIFICATION OF ANTIGEN 14C5

Burvenich I, Schoonooghe S, Coene E, Mertens N, De Vos F and Slegers G

In preparation

3.1 Introduction

The spread from primary tumours to organs is the life-limiting aspect of most malignant diseases (Ellis et al., 1998; Enns et al., 2005). Having metastasis, the patient can no longer be cured by local treatment. Early detection of metastasis or metastatic potential prior to development of occult disease still lags. Moreover for a physician, being able to detect the metastatic potential is not enough. Offering a patient with a poor prognosis an adequate treatment is mandatory.

Metastatic potential is influenced by the local microenvironment, angiogenesis, stroma-tumour interactions, elaboration of cytokines by the local tissue, and by the molecular phenotype of the tumour and host cells. This underscores the importance of understanding the molecular events of the metastatic process. Using that understanding, biomarker panels can be identified to predict presence and location of metastases, and to identify and develop therapeutic targets (Liotta and Kohn, 2003). Investigation of the molecular basis of invasion can lead to strategies for delaying progression of pre-invasive carcinoma and treatment of primary tumours and established metastasis. Although tumour cell invasion might not be rate limiting for the increase of metastasis, anti-invasive agents can block tumour angiogenesis and thereby indirectly block metastasis. Two classes of molecular anti-invasion targets exist: (a) cell surface and extracellular matrix proteins, which mediate sensing, adhesion, and proteolysis; and (b) signal transduction pathways, which regulate invasion, angiogenesis, and proliferation (Kohn and Liotta, 1995).

The extracellular matrix (ECM) consists of a complex network of macromolecules, such as collagens, glycoproteins, and proteoglycans, which surrounds the connective tissue cells and is mainly being secreted by fibroblasts or other members of the fibroblast family, such as chondroblasts

and osteoblasts (Alberts et al., 1994; Kreis and Vale, 1999). Apart from intercellular adhesion (i.e., cell-to-cell adhesion), the organization of cells within connective tissue is based on adhesion of these cells to ECM components (i.e., cell substrate adhesion) (Jockusch et al., 1995). Subsequently, cell substrate adhesion molecules are considered as essential regulators of cell migration, differentiation, and tissue integrity. They play a role in inflammation, but they also participate in the process of invasion and metastasis of malignant cells in the host tissue (Albelda, 1993; Jiang et al., 1994; Cavallaro and Christofori, 2001). Cell substrate adhesion is a prerequisite for tumour invasion in normal mesenchymal tissue. Invasive tumour cells adhere to the ECM components, such as type IV collagen, laminin, chondroitin and, heparan sulfate proteoglycans, and are guided by them during their permeation through the basal lamina and underlying interstitial stroma of the connective tissue (Anderson, 1992; Yurchenco, 1994). Several ECM adhesion molecules and their protein receptors have been studied extensively for their involvement in tumour invasion and metastasis, including the integrins, lectins, selectins, and cadherins (Dedhar and Saulnier, 1990; Takeichi, 1990; Pignatelli et al., 1992; Behrens, 1993).

In search of new antibody therapeutics for inhibition of metastatic breast cancer, De Potter et al. (1994) developed several mouse monoclonal antibodies (mAbs) against epitopes on the extracellular membrane of SK-BR-3 human breast cancer cells. One of these mAbs is the IgG1 mAb 14C5, which recognizes an extracellular plasma membrane antigen expressed on SK-BR-3 and MCF-7 human breast cancer cells (De Potter et al., 1994; Coene et al., 1997). The antibody is capable of reversibly inhibiting the adhesion of SK-BR-3 cells on both culture-treated plastic and on pronectin-, fibronectin-, osteopontin-, and vibronectin-precoated culture plates. Furthermore, mAb 14C5 has been shown to prevent invasion and, subsequently, metastasis of SK-

BR-3 and MCF-7 cells on host tissue *in vitro* (De Potter et al., 1994). In addition, Giffels et al. (1997) and Wagner et al. (1999) demonstrated that the anti-idiotypic counterpart mAb ACA 14C5 significantly inhibits tumour growth in a dose-dependent way in Sprague–Dawley rats bearing HH-16 clone 1/2 adenocarcinomas or fibrosarcomas overexpressing the antigen 14C5. Therefore, antigen 14C5 offers an interesting target for anti-invasion, anti-angiogenesis or other antibody-based targeted strategies like radioimmunotherapy.

In the past, different studies have failed to identify the antigen 14C5. Immunoprecipitation of the antigen from MCF-7 cells was performed using mAb 14C5 (De Potter et al., 1994). Analysis by SDS-PAGE in the presence of reducing agent demonstrated that mAb 14C5 recognizes two protein fragments with molecular sizes of 50 kDa and 90 kDa respectively. The ratio of both fragments changed from purification to purification, but the 90 kDa fragment was always the predominant fragment, indicating that the latter was recognized by the antibody, whereas the lower molecular weight component was gradually lost during the immunoprecipitation procedure and a substantial amount of the 50 kDa band consisted of the heavy chain of the mAb 14C5, leaking from the column (Coene et al., 1997). Without reducing agent, SDS-PAGE showed a 120 kDa protein band. After transfer of the proteins of the cell lysates and of the immunoprecipitated protein complex on a nitrocellulose membrane and subsequent detection of antigen with mAb 14C5, there was no detection of any interacting component. Immunoprecipitation of radioactive labeled lysate of SK-BR-3 breast cancer cells showed a triplet of approximately 50 kDa and one singlet of approximately 200 kDa (Vanholme, 2000). A similar immunoprecipitation study at the University of Nottingham with biotin-labeled membrane proteins of 719T cells was performed. Two protein fragments of 66 kDa and 70 kDa were purified (data not published).

These contradictory results lead to the investigation of a lambda gt11 cDNA library of SK-BR-3 cells. After prokaryotic expression in *E. coli*, the first screening showed four positive clones. Finally after several screening rounds, one clone was selected for sequencing. The sequence matched the protein proteoglycan decorin, but decorin did not match the expression pattern of the antigen 14C5 (Burvenich, 2001).

The objective of this study was to identify the antigen 14C5 by affinity chromatography studies and comparative antigen expression analysis.

3.2 Materials and methods

3.2.1 Antibodies

The 14C5 antibody-producing hybridoma cells produced mAb 14C5 in Integra CL 350 flasks (Elscolab, Kruibeke, Belgium) containing protein-free hybridoma medium (Invitrogen, Merelbeke, Belgium). MAb 14C5 was protein G purified (Amersham Biosciences Europe, Roosendaal, the Netherlands) from concentrated supernatant and dialyzed against PBS (pH 7.4). The purity of the antibody was evaluated by SDS-PAGE using reducing and non-reducing conditions. Anti-mouse kappa IgG, anti-IgG conjugated to alkaline phosphatase (AP) (1:1000, anti-mouse, Intec ITK diagnostics, Antwerpen, Belgium; 1:7500, anti-goat, Sigma, Bornem, Belgium) were used during western blotting. The 9E10 mAb (anti-*c-myc*, mouse IgG1, Becton Dickinson, BD, Erembodegem-Aalst, Belgium) was used as a control for aspecific Fc-receptor binding during flow cytometric analysis. Alexa Fluor 488-conjugated goat anti-mouse IgG antibody (Invitrogen) was used during flow cytometry. Integrin antibodies (Millipore, Brussels, Belgium) used in flow cytometric analysis were anti-α1 (FB12, mouse IgG1), anti-α2 (P1E6, mouse IgG1), anti-α3 (ASC-1, mouse IgG1), anti-αv (P3G8, mouse IgG1), anti-β1 (P4G11, mouse IgG1), anti-β2 (P4H9-A11, mouse IgG3), anti-β3 (25E3, mouse IgG2a), anti-β4 (ASC-3,

mouse IgG1), anti-α5β1 (HA5, mouse IgG2b), anti-αvβ3 (LM609, mouse IgG1) and anti-αvβ5 (P1F6, mouse IgG1). Anti-β5 (B5-IVF2, mouse IgG1) was obtained from Sigma.

3.2.2 Cell lines

HT-29, Capan-2, and C32 were a kind gift of J&J Pharmaceutical Research & Development (Beerse, Belgium). HT-1080, A2058, and A549 were obtained from the Laboratory of Tumor and Developmental Biology (University of Liège, Belgium). SK-BR-3, Colo16, and MOLT-4, were obtained from the N. Goormaghtigh Institute of Pathology, University of Ghent (Ghent, Belgium). All cell lines were cultured in standard medium with supplements according to the American Type Culture Collection (Manassas, VA) recommendations, except for Colo16, and MOLT-4 grown in RPMI1640 medium containing 10 mmol/l HEPES and 10% fetal bovine serum (Cambrex, Verviers, Belgium). All cells were cultured at 37 °C in a 5% CO_2 humidified incubator and passaged with 0.05% trypsin-0.02% EDTA.

3.2.3 MAb 14C5-affinity chromatography

SK-BR-3 or HT-1080 cells were grown in 500 ml flasks (850 cm^2) to confluence, washed with PBS, detached with cell dissociation buffer (Invitrogen, Merelbeke, Belgium), and washed with PBS. Cells are resuspended in 25 ml NP40 lysis buffer (0.5 % NP40, 50 mM Tris, pH 7.6, 300 mM NaCl, 1 tablet per 10 ml buffer of protease inhibitor cocktail Mini-Complete Roche) following a 30-minute incubation on ice. Lysate is pipetted onto a QIAshredder column sitting in 2 ml collection tube (Qiagen, Venlo, The Netherlands) and centrifuged for 2 min at 14000 rpm to homogenize.

The mAb 14C5 antibody affinity column was prepared using a HiTrap NHS-activated HP column system (GE Healthcare, Brussels, Belgium) according to the directions of the manufacturer. The lysate was diluted (1:2) in PBS before

applying to the column and filtered through a 0.45 µm filter. After passing the clear lysate through the mAb 14C5-HiTrap NHS-activated HP column, the column was washed with 5 ml PBS buffer containing 500 mM NaCl and 0.25 % NP40, followed by 5 ml PBS buffer containing 500 mM NaCl and 0.1 % NP40. The antigen was then eluted from the column with 0.1 M glycine-HCl, pH 2.5, 0.1 % NP40. Fractions were collected in 1 M Tris buffer (pH 9.0) to raise the pH to 7.5.

Prior to SDS-PAGE analysis, antigen was precipitated using 10 % tri-chloroacetic acid and 0.06 % deoxycholate for 1 hour at -20 °C. After centrifugation (20 min, 14000 rpm), pellets were washed twice with 100 % acetone and once with 70 % ethanol. The pellet was re-suspended in Laemmli sample buffer and boiled for 5 min. 10 % SDS-PAGE was performed and the gel was stained with Silver stain and a duplicate gel was blotted and analysed with mAb 14C5 or anti-kappa IgG1 for specific or non-specific protein bands. Anti-IgG conjugated to alkaline phosphatase (AP) (1:1000, anti-mouse; 1:7500, anti-goat) was added, as secondary antibody, and staining was carried out with nitro-blue tetrazolium chloride- 5-Bromo-4-Chloro-3'-Indolylphosphate p-Toluidine Salt (NBT-BCIP, Roche, Vilvoorde, Belgium).

3.2.4 Antigen quantification by BiaCore

Concentration of antigen in crude and purified lysate was analysed using Biacore 2000. MAb 14C5 (1.9 µg in 100 µl of 40 mmol/l sodium acetate, pH 4.5) and an irrelevant mAb 9E10 (8 µg in 100 µl of 40 mmol/l sodium acetate, pH 4.5) were immobilized on a CM5 sensor chip using the amine coupling kit (Biacore, Breda, The Netherlands). The dextran layer of the sensor chip was activated by injecting 50 µl 0.05 mol/l N-hydroxysuccinimide and 0.2 mol/l N-ethyl-N(3-diethylaminopropyl) carbodiimide. Subsequently, antibodies in 40 mmol/l sodium acetate buffer (pH 4.5) were injected until 1499 resonance units (RU) for mAb 14C5 and 1357 RU for mAb 9E10 were realized. Excess

reactive groups were then blocked by injection of 50 µl of 1 mol/l ethanolamine/HCl (pH 8.5). Binding analyses were performed in HBS buffer (10 mmol/l (N-[2-hydroxyethyl]piperazine-N´-[2-ethane sulfonic acid]) (HEPES) (pH 7.4), 0.15 mol/l NaCl, 3 mmol/l EDTA, 0.005% surfactant Tween-20) at a flow rate of 10 µl/min. The surface was regenerated with 0.01 mol/l glycine (pH 2).

3.2.5 Flow cytometry

Confluent cells were harvested using cell dissociation buffer (Invitrogen). Aliquots of 2×10^5 cells were incubated with mAb 14C5 or integrin antibodies under saturating conditions (67 nmol/l) in PBS-0.5% BSA-0.02% (w/v) sodium azide (Sigma) (w/v) on ice for 2 hours. After washing the cells with PBS-0.5% BSA-0.02% sodium azide, cells were incubated with Alexa Fluor 488-conjugated goat anti-mouse on ice for 1 hour. Again, cells were washed with PBS-0.5% BSA-0.02% sodium azide and suspended in a final volume of 300 µl of PBS-0.5% BSA-0.02% sodium azide. In control samples, the primary antibody was omitted. For isotype control, mAb 9E10 (67 nmol/l) was used instead of mAb 14C5.

Flow cytometric analysis was done using a FACScan flow cytometer (Becton Dickinson). Tumour cell populations were gated based on forward and side scatter variables. Data analysis was done using WinMDI (Joseph Trotter).

3.2.6 Nucleotide sequence analyses and quality control of cDNA clones

Full length cDNA encoding the human αv (OriGene Technologies, Maryland, United States) and the human β5 (RZPD, Berlin, Germany) integrin subunits were amplified and purified. cDNA sequences were screened with PCR using 5' and 3' primers delivered with the cDNA clones. Nucleotide sequencing was performed by the dideoxynucleotide chain-termination method using a DNA sequencing kit (Big Dye Terminator version 3.1 cycle sequencing) and

nucleotide sequence homology analyses were performed using Clone Manager 8.0 (Scientific & Educational Software, NC, USA).

Control digests were performed in mixtures of 20 µl, incubated at 37 °C for 2 h containing 2 µl DNA (0.5 µg/µl), 2 µl buffer, 0.5 µl BSA, 1 µl enzyme (Table 3.1). Digests were subjected to 1 % agarose gel electrophoresis, and photographed using an instant positive film (Polaroid Black and White Film Type 667, Sigma).

Tabel 3.1 Restriction digests of human αv or β5 cDNA clones

cDNA clone	Enzyme	Buffer	Restriction fragments (kb)†
αv	ScaI	buf K	5600, 2300, 951, 475
	BsaI	NEB3	4165, 3218, 1041, 902
	PvuII	buf B	5520, 1640, 1069, 1097
β5	ScaI	buf K	2237, 1689, 1265
	BglA	buf D	3628, 1389, 174
	BamI	NEB2, 65°C	2247, 1529, 1008, 407
	NspI	NEB2	4021, 1328, 747, 575, 460, 123
	PstI	buf O	2233, 1457, 1090, 222, 189

†*Restriction fragments formed in restriction digests depending the used enzyme and buffer (Fermentas or New England Biolabs)*

3.2.7 cDNA transfection of Colo16 cells

Full length cDNA encoding the human αv integrin (OriGene Technologies) was ligated into the expression vector pES31 adjusted with a neomycin selection. The neomycin site was derived from a pcDNA3 expression vector by BamHI/PvuI and XhoI restriction digest. Full length cDNA encoding the human β5 integrin (RZPD) was ligated into the expression vector pES31 containing a zeomycin selection site. Full human *αv* clone was amplified by PCR using ALPHAV F (sense) and ALPHAV B (anti-sense) primers, and human *β5* clone was amplified using BETA5 F and BETA5 B primers (Table 3.2).

The sense-primers were designed to contain an EcoRI site and Kozak consensus, the anti-sense primers contained a BamHI restriction site. PCR was performed in 2 % DMSO and 2 mmol/l $MgSO_4$ conditions. After ligation and transformation in *E. coli*, full sequences of selected clones were analysed with primers (*αv*: NM101, 105, 87, ALPHAV F and ALPHAV B; *β5*: NM101, 105, 87, BETA5 F, BETA5 B, BETA5SEQ B1-B4 and F1-F4) by the dideoxynucleotide chain-termination method and nucleotide sequence homology was analysed (Table 3.2). Control digests with ScaI, BsaAI and PvuII for *αv*, and NspI and PstI for *β5* were performed in mixtures of 20 µL, incubated at 37°C for 2 h according to the manufacturer's instructions (Table 3.1). Digests were subjected to 1 % agarose gel electrophoresis, and photographed using an instant positive film (Sigma).

Tabel 3.2 Primer and primer sequences

Primer	Sequence (5' to 3')
ALPHAV F	ATGAATTCGCCACCATGGCTTTTCCGCCGCGGCGACG
ALPHAV B	ATGGATCCTTAAGTTTCTGAGTTTCCTTCACCATTTTCATGAG
BETA5 F	ATGAATTCGCCACCATGCCGCGGGCCC
BETA5 B	ATGGATCCTCAGTCCACAGTGCCATTGTAGGATTTGTTG
BETA5SEQ B1	AAATCCCAACCGGAAGTTGC
BETA5SEQ B2	ACCGTTGTTCCAGGTATCAG
BETA5SEQ B3	CGGCACAGGTTCTGGTACAC
BETA5SEQ B4	CAGCCTCCTGGTCATCTTTC
BETA5SEQ F1	CCGAGCCTGGGCACCAAAC
BETA5SEQ F2	GAGAAATTGGCAGAGAACAAC
BETA5SEQ F3	GGTGCGAGTGCCAGGATG
BETA5SEQ F4	AGACCTGCCACAGCCTATGC
NM101	CAACGTGCTGGTTATTGTGCTGTC
NM105	TCGAGCCACCATGGGTTGGAGCTG
NM87	CAACAGATGGCTGGCAACTAGAAG

____,EcoRI restriction site, ---- ,Kozak consensus, ____,BamHI restriction site

Transfection into antigen 14C5-negative Colo16 squamous carcinoma cells was done using the Saint-Mix lipofectamine reagent (Synvolux Therapeutics, The

Netherlands) according to the manufacturer's instructions. Transfections were done in 6-well dishes with 1 µg DNA per well (1 µg vector containing *αv*, 1 µg vector containing *β5* or 0.5 µg of both *αv* and *β5* containing vectors). After 48 h, flow cytometry analysis was performed using anti-αv (P3G8), anti-β5 (B5-IVF2), and anti-αvβ5 (P1F6) specific antibodies. Selection was performed in duplicate dishes in 800 µg/ml neomycin, zeomycin or, neomycin and zeomycin containing medium.

3.2.8 Blocking experiment

Blocking studies were done with mAb 14C5 or anti-αvβ5, both radio-iodinated with ^{123}I by the Iodo-Gen method. Unbound radio-iodine was removed by gel filtration over a PD-10 desalting column previously equilibrated with 0.5% BSA in PBS. The blocking assay was performed by monitoring loss of the ability of ^{123}I-labeled anti-αvβ5 to bind to target cells in the presence of excess of unlabeled mAb 14C5. Washed target cells (A549, 0.5×10^6) were incubated with 300 nmol/l of the unlabeled mAb 14C5 to block antigen 14C5. Test solutions containing increasing amounts of ^{123}I-labeled mAb 14C5 or ^{123}I-labeled anti-αvβ5 in a total volume of 1 ml cell medium were incubated at 4°C for 2 hours. Then, supernatant was removed by centrifugation (8 minutes, 1200 rpm, 4°C) and cells were washed twice with 1 ml ice-cold PBS and peletted for 8 min at 1200 rpm. For each sample, total binding was determined in the absence of unlabeled mAb 14C5. Radioactivity was counted by a gamma counter (Cobra II, Perkin-Elmer, Jügesheim, Germany). Incubations were performed in triplicate.

3.2.9 Statistical analysis

A nonparametric Mann-Witney test was used for comparisons.

3.3 Results

3.3.1 Isolation of antigen 14C5 by mAb 14C5-affinity chromatography

We tried to purify the antigen 14C5 from HT-1080 fibrosarcoma and SK-BR-3 breast cancer cells (approximately 10^9 cells) by mAb 14C5-affinity-column chromatography. By SDS-PAGE and western blot analyses with anti-kappa and anti-Fc antibodies, only 14C5 antibody fragments leaking from the column could be detected. Therefore, purified lysate was passed over a protein G column (Amersham) to reduce Fc-containing fragments. However, western blot analysis of protein G purified lysate did not show specific protein bands.

The affinity-column protocol was adjusted with three eluting steps prior to loading of crude lysate sample to the column. After three eluting steps, no leaking of mAb 14C5 was detected by SDS-PAGE analysis. However, no specific protein bands attributable to the antigen 14C5 could be detected after western blot analysis.

The amount of soluble antigen in the crude and purified SKBR-3 lysate was determined by Biacore. MAb 14C5 (1499 resonance units, RU) was coated on a CM5 sensor chip. An irrelevant IgG, mAb 9E10 (1357 RU) was coated as negative control. In crude lysate, no interaction with mAb 14C5 was detected. In mAb 14C5 affinity-column purified SKBR-3 lysate, 141 RU bound to the mAb 14C5, whereas only 37 RU interacted with mAb 9E10.

3.3.2 Comparative flow cytometry analysis with integrin antibodies

A comparison of mAb 14C5 and eleven integrin antibodies (anti-α1 (FB12, mouse IgG1), anti-α2 (P1E6, mouse IgG1), anti-α3 (ASC-1, mouse IgG1), anti-αv (P3G8, mouse IgG1), anti-β1 (P4G11, mouse IgG1), anti-β2 (P4H9-A11, mouse IgG3), anti-β3 (25E3, mouse IgG2a), anti-β4 (ASC-3, mouse IgG1), anti-α5β1 (HA5, mouse IgG2b), anti-αvβ3 (LM609, mouse IgG1) and, anti-αvβ5 (P1F6, mouse IgG1)) was performed by flow cytometry analysis.

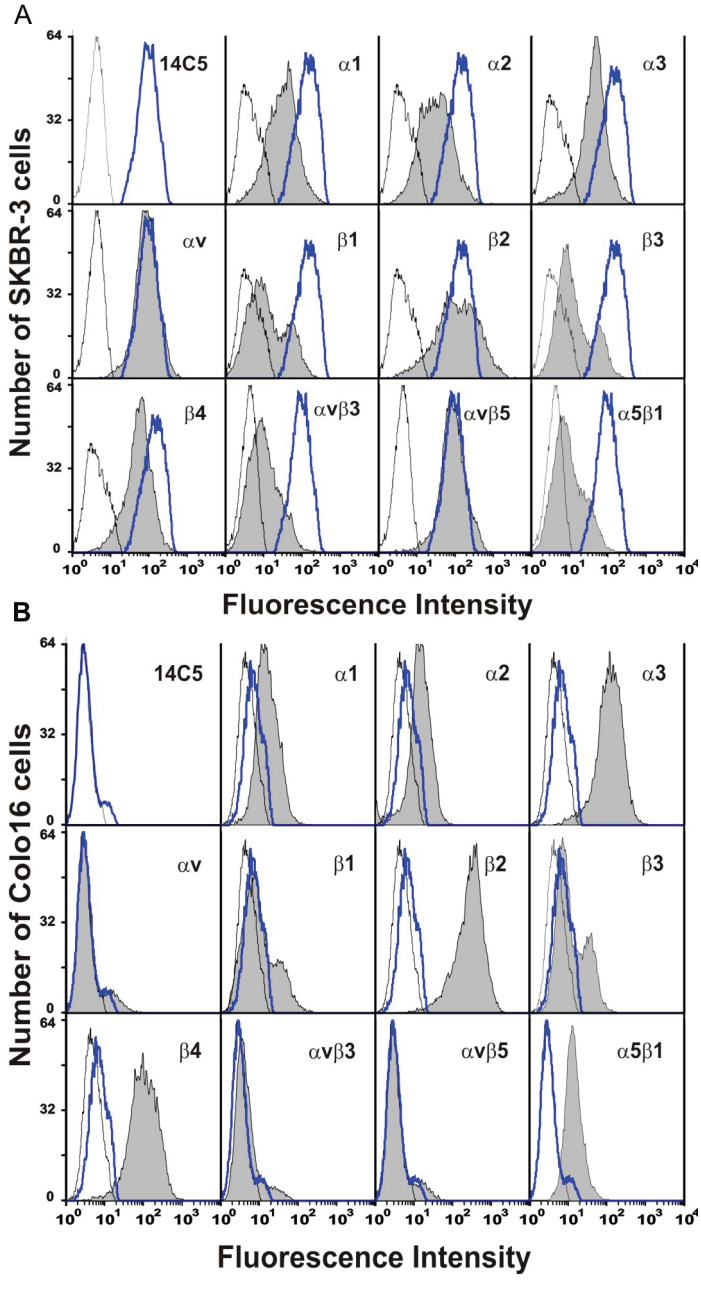

Fig. 3.1. Flow cytometry analysis showing binding of irrelevant anti-c-myc IgG1 (*open histograms*), mAb 14C5 (*blue line*) or integrin antibodies (*grey filled histograms*) under saturating conditions to *(A)* SKBR-3 breast cancer cells and *(B)* Colo16 squamous carcinoma cells.

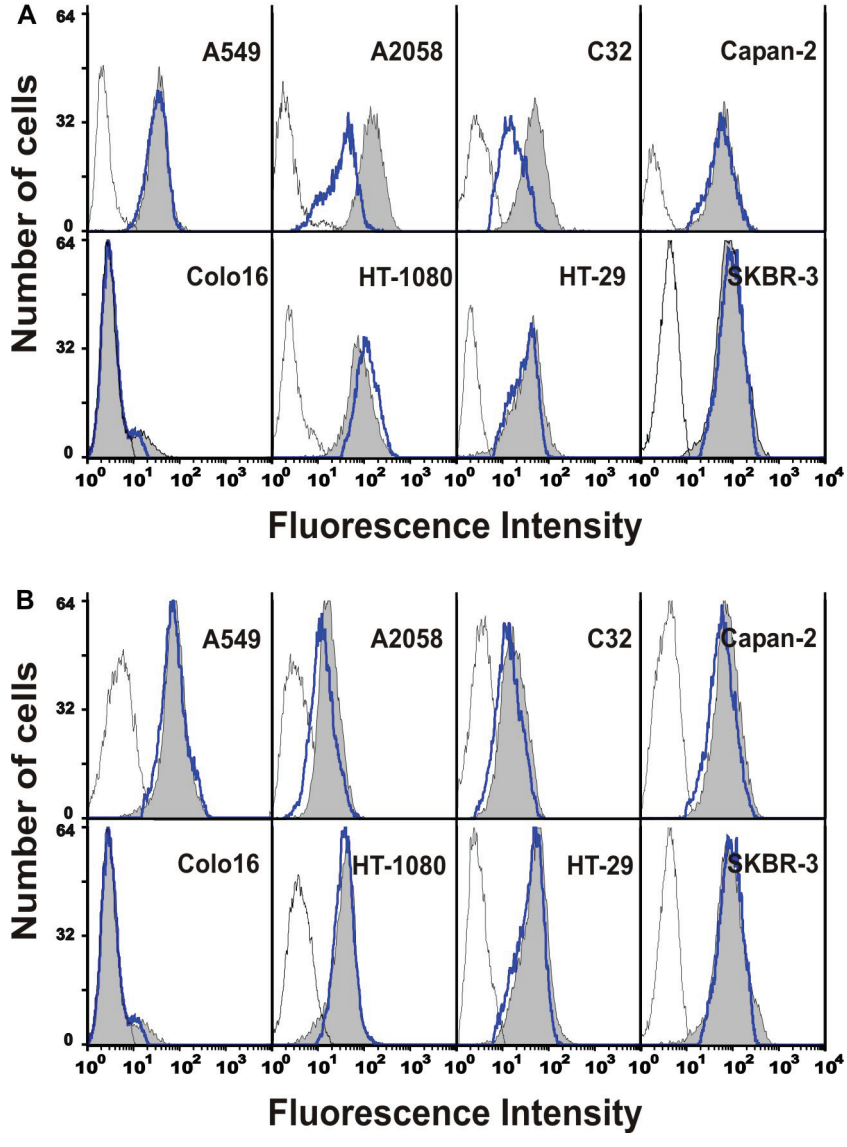

Fig. 3.2. Flow cytometry analysis showing binding of irrelevant anti-c-myc IgG1 (*open histograms*), mAb 14C5 (*blue line*) or integrin antibodies (*grey filled histograms*) under saturating conditions to A549, A2058, C32, Capan-2, Colo16, HT-1080, HT-29, and SKBR-3 cancer cells. *(A)* Comparison between anti-αv and mAb 14C5. *(B)* Comparison between anti-αvβ5 and mAb 14C5.

A total of eight human cell lines were analysed under saturating conditions for a comparison of the reactivity of mAb 14C5 and the eleven anti-integrin antibodies. Figure 3.1A shows the reactivity of mAb 14C5 and anti-integrin

antibodies with the positive control, the SK-BR-3 breast cancer cell line. Figure 3.1B shows the reactivity with the negative control, the Colo16 squamous carcinoma cell line. The expression patterns of the other six cell lines (A2058 skin melanoma, A549 lung carcinoma, C32 melanoma, Capan-2 pancreas carcinoma, HT1080 fibrosarcoma, HT29 colon carcinoma) are shown in the appendix at the end of this chapter.

Two antibodies showed similar reactivity as mAb 14C5, namely anti-αv and anti-αvβ5. However, expression levels of anti-αv differed from expression levels of mAb 14C5 in A2058 and C32 cells (Fig. 3.2A), whereas anti-αvβ5 showed equal reactivity in all tested cell lines (Fig. 3.2B). All other integrin antibodies showed differences in expression levels in more than two cell lines.

3.3.3 Eukaryotic expression of αvβ5 integrin in Colo16 cells

To determine whether antigen 14C5 is in fact the integrin αvβ5 receptor, Colo16 cells were transfected with two expression vectors. One expression vector contained cDNA encoding the human αv integrin subunit and a gene encoding neomycin resistance, a second expression vector contained cDNA encoding the β5 integrin subunit and a gene encoding zeomycin resistance. After drug selection, no stable transfectant sub-lines were established.

However, as shown in figure 3.3, after transfection of Colo16 cells with *αv*, *β5* or co-transfection of *αv* and *β5*, ~30% of transfected cells showed expression of respectively the αv subunit, the β5 subunit or αvβ5. Some overlap is seen between mAb 14C5 binding and the anti-αv sub-unit or anti-β5 sub-unit alone. Only when both integrin sub-units were co-transfected, the expression of mAb 14C5 matched completely with anti-αvβ5 expression levels. These results show that after co-transfection of both *αv* and *β5* genes, the positive transfectant subpopulation binds anti-αvβ5 specific antibody and mAb 14C5 at equivalent levels.

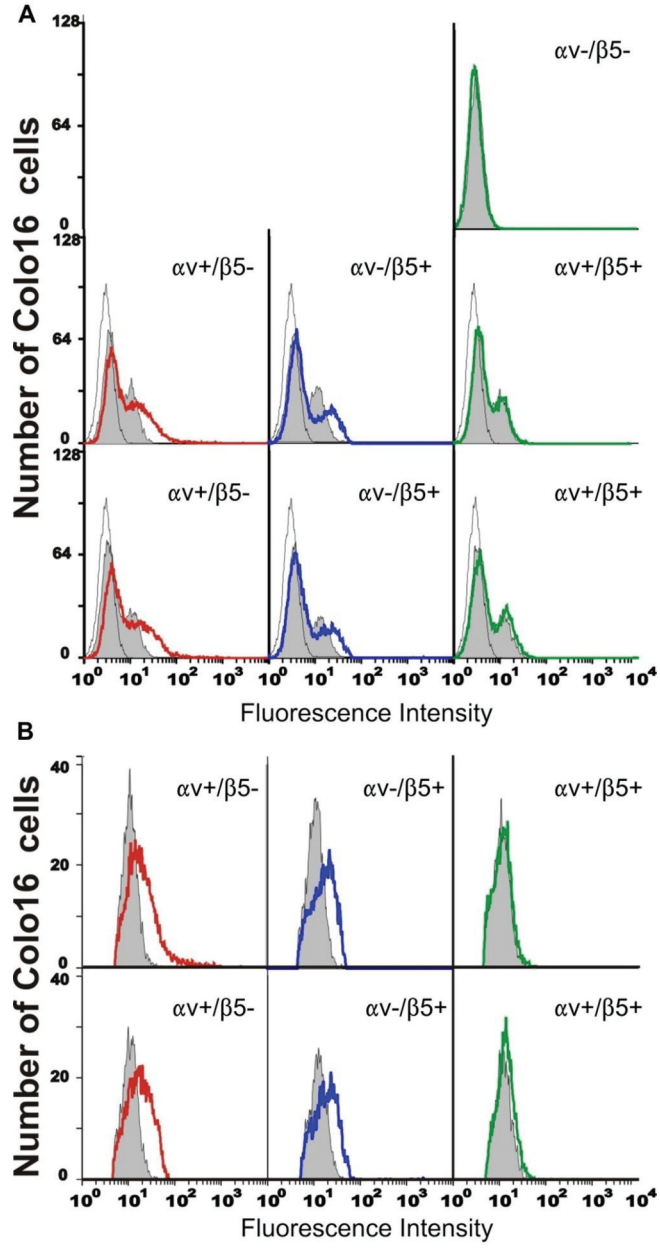

Fig. 3.3. Flow cytometry analysis of Colo16 transfected cells with human *αv* (*αv+/β5-*), *β5* (*αv-/β5+*), or *αvβ5* (*αv+/β5+*). Cell surface expression was analyzed using anti-αv (P3G8, *red line*), anti-β5 (B5-IVF2, *blue line*), and anti-αvβ5 (P1F6, *green line*) specific antibodies and compared with mAb 14C5 (*grey filled histograms*) binding. *(A)* Positive and negative transfectant populations are shown. *(B)* Positive transfected cells were gated.

3.3.4 Blocking experiment with ^{123}I-labeled mAb 14C5 and anti-αvβ5

To confirm that integrin αvβ5 is indeed antigen 14C5, a blocking experiment was performed with ^{123}I-labeled mAb 14C5 and ^{123}I-labeled anti-αvβ5 specific antibody. The blocking agent used in the study represents a 10-fold excess of saturating levels obtained in flow cytometry analysis with mAb 14C5 (300 nmol/l). Figure 3.4 shows the total binding of ^{123}I-labeled mAb 14C5 and anti-αvβ5.

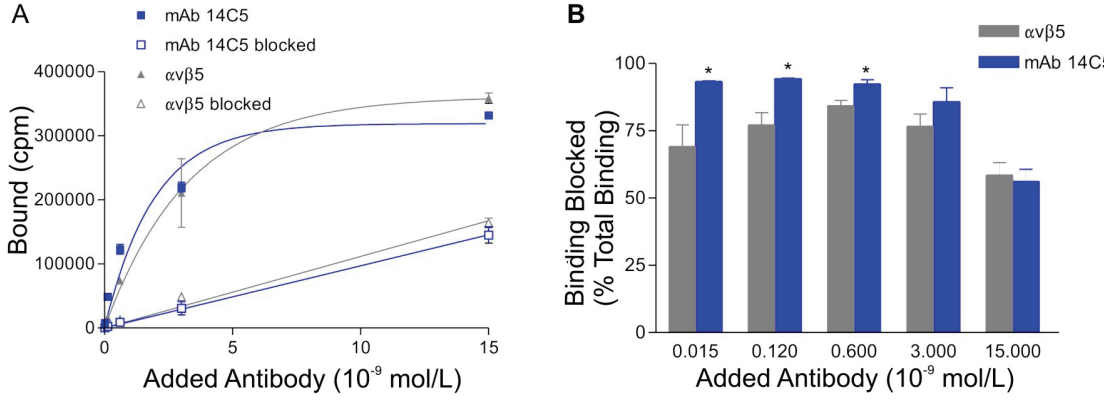

Fig. 3.4. Blocking of αvβ5 specific binding by mAb 14C5. *(A)* Total binding of ^{123}I-labeled mAb 14C5 (*filled squares, blue*) and anti-αvβ5 (filled triangle, grey) and non-specific binding of ^{123}I-mAb 14C5 (*open squares, blue*) and ^{123}I-anti-αvβ5 in the presence of 300 nmol/l of unlabeled mAb 14C5 to SKBR-3 cells is shown. *(B)* The amount of total binding blocked by unlabeled mAb 14C5 of ^{123}I-labeled anti-αvβ5 (*grey*) and ^{123}I-labeled mAb 14C5 (*blue*) expressed as percentage of total binding. Bars, SD (n = 3); *, P < 0.05, significant binding differences between mAb 14C5 and αvβ5

In the presence of 300 nmol/l unlabeled mAb 14C5, this binding was reduced to non-specific binding both for mAb 14C5 and anti-αvβ5 (Fig. 3.4A). The amount of ^{123}I-labeled anti-αvβ5 total binding blocked by unlabeled mAb 14C5 is significant lower than the amount of ^{123}I-labeled mAb 14C5 blocked when non-saturating amounts of radiolabeled antibodies were added to the SKBR-3 cells (n = 3, P < 0.05). On the contrary, at saturating levels (i.e., starting at approximately 5 nmol/l as shown in Fig. 3.4A) there were no significant differences in blocking percentages between mAb 14C5 and anti-αvβ5 specific

antibody (Fig. 3.4B). These results confirm that mAb 14C5 binds to the αvβ5 integrin, probably with higher affinity than anti-αvβ5 specific antibody, which could explain the significant differences in blocking percentages at low antibody concentrations.

3.4 Discussion

The data presented in this chapter reveal for the first time the identity of antigen 14C5 as the integrin αvβ5. In the past, many immunoprecipitation studies failed to purify the antigen and consequently could not deduce the identity of Ag 14C5 by sequence analysis (De Potter et al., 1994; Coene et al., 1997). The studies presented here show that purification of antigen 14C5 by mAb 14C5 affinity-column chromatography did not show specific protein components in the purified SKBR-3 or HT-1080 lysates after western blot analysis. Biacore analysis showed that only little amounts of soluble antigen 14C5 are available in mAb 14C5 affinity-column purified SKBR-3 lysate. Both western blot and Biacore analysis indicate that the conformation of the soluble protein could be altered compared to the cell surface expressed antigen. Therefore, other strategies were explored to identify the antigen.

Based on the immunohistochemical staining of Ag 14C5 on the cell membrane extensions of highly invasive tumour cells, De Potter et al. (1994) and Coene et al. (1997) suggested that Ag 14C5 could be related to the family of integrins. The integrins, a family of related membrane receptors involved in cell-cell and cell-matrix interactions, are heterodimeric complexes of α- and β-subunits. The cell substrate adhesion inhibition after coating with osteopontin and vitronectin suggests that the antigen could be a receptor for these extracellular matrix proteins. According to the literature, osteopontin is recognized by the αvβ3 vitronectin receptor (Reinholt et al., 1990; Miyauchi et al., 1991). Integrins can also bind to other extracellular matrix proteins but with lower affinity. This

might explain the weaker inhibition after coating with fibronectin than osteopontin or vitronectin seen by De Potter et al. (1994) and Coene et al. (1997).

The expression of the antigen 14C5 is compared with the expression of eight different integrin subunits (α1, α2, α3, αv, β1, β2, β3, and β4) and three different integrins (αvβ3, αvβ5, and α5β1). Basically, we selected integrins from literature data involved in cancer pathology and which could possibly block cell-substrate-adhesion (Mizejewski, 1999; Wehrle-Haller and Imhof, 2003; Jin and Varner, 2004; Ruegg et al., 2004). At saturating conditions, anti-αvβ5 specific antibody showed equivalent expression levels as mAb 14C5. By a blocking assay with mAb 14C5, the αvβ5 receptors could be significantly blocked by mAb 14C5, indicating that antigen 14C5 is the αvβ5 receptor.

Flow cytometry analysis of Colo16 cells transfected with human αv and β5 cDNA, indicated that both sub-units are involved in the mAb 14C5 binding. A possible conformation change of the soluble antigen 14C5, i.e. monomeric αv and monomeric β5, could explain why affinity-column chromatography, western blot analysis and Biacore with mAb 14C5 did not work to purify Ag 14C5. However, Wayner et al. (1991) reported immunoprecipitation of the αvβ5 receptor by mAb P5H9 from UCLA-P3 lung carcinoma cells. In the future, we will work on a stable transfection of Colo16 cells with both αv and β5 sub-units and use the immunoprecipitation protocol from Wayner et al. (1991) to purify Ag 14C5.

αvβ5 as tumour associated target is not novel. The cDNA sequence of the human integrin β5 sub-unit was elucidated by McLean et al. (1990). The cDNA sequence of the human integrin αv sub-unit was elucidated by Sims et al. (2000). Smith et al. (1990) reported the purification and functional characterization of integrin αvβ5 as an adhesion receptor for vitronectin.

The role of integrins αvβ3 and its closely related αvβ5 in cancer growth, angiogenesis and metastasis has been widely discussed with pros and contras (Leavesley et al., 1992; Mizejewski, 1999; Kerr et al., 2002; Ruegg et al., 2004; Taverna et al., 2005) and until today remains uncertain and complex. αvβ3 was the first vascular integrin targeted to suppress tumour induced angiogenesis. Evidence indicates that both αvβ3 and αvβ5 promote angiogenesis via distinct pathways, αvβ3 is involved in the response to basic fibroblast growth factor (bFGF) and tumour necrosis factor α (TNFα), and αvβ5 is involved in the response to vascular endothelial growth factor (VEGF) and transforming growth factor α (TGFα; Friedlander et al., 1995). Hynes (2002) hypothesized that these integrins could be in fact negative regulators of angiogenesis and that drugs targeting them may act as agonists rather than antagonists. This hypothesis is based on the fact that although pharmacological agents directed against integrins αvβ3 and αvβ5 have been reported to block angiogenesis, genetic ablations of the genes encoding these integrins fail to block angiogenesis. In a later study, both αvβ3 and αvβ5 did not show to be essential for tumour growth and progression, although they might play some role in mammary gland development (Taverna et al., 2005). Enns et al. (2005) suggested that αvβ5 integrins mediate early steps of metastasis formation, but supports the evidence of Mitjans et al. (2000) that anti-αvβ5 (P1F6) specific binding could not inhibit tumour growth.

RGD peptide inhibitors binding to αvβ3 and αvβ5 have been tested in preclinical (Dechantsreiter et al., 1999; Li et al., 2004; Dayam et al., 2006; Dijkgraaf et al., 2006a) and clinical studies (Eskens et al., 2003). Monoclonal antibodies specific for αv (CNTO 95, fully human; Davis et al., 2004; Jayson et al., 2004; Trikha et al., 2004; Martin et al., 2005) and αvβ3 (LM609, murine; Brooks et al., 1994; Vitaxin, MEDI-522, humanized; Gutheil et al., 2000) have been investigated as therapeutic agents. Cilengitide, a cyclic RGD peptide in

clinical trials for metastatic cancer, has been tested in an aggressive breast cancer model in combination with ^{90}Y-labeled chimeric anti-L6 radioimmunotherapy, which remarkably increased efficacy and increased apoptosis, compared to single-modality therapy with either agent, without additional toxicity (Burke et al., 2002). Noninvasive PET and SPECT imaging of integrin expression have been done with monomeric, dimeric and tetrameric RGD peptides and peptidomimetics (Lewis, 2005; Dijkgraaf et al., 2006b; Haubner, 2006; Zhang et al., 2006). However, the potential role of a radiolabeled anti-mAb αvβ5 specific antibody in radioimmunodetection and radioimmunotherapy has not yet been investigated.

3.5 Conclusion

The studies presented indicate that antigen 14C5 is the αvβ5 receptor. The αvβ5 receptor belongs to the family of integrins. Many integrins have shown to be interesting targets for cancer therapy, and the most investigated target so far is the vascular integrin αvβ3. No research has been conducted to the target potential of αvβ5 for radioimmunodetection and radioimmunotherapy. The fact that the antibody 14C5 can block cell substrate adhesion combined with the ability of mAb 14C5 to deliver a radiotoxic dose to the tumour could provide new treatment possibilities: unlabeled mAb 14C5 could prevent the settlement of undetectable metastatic cells and radiolabeled mAb 14C5 could cause tumour regression of occult secondary tumours. Therefore, further studies to exploit the therapeutic potential of the labeled as well as the unlabeled mAb 14C5 are warranted. Also, imaging αvβ5 integrin expression can be important to evaluate anti-integrin treatment efficacy and drug development of new drugs with favourable tumour targeting.

3.6 References

Albelda SM. Role of integrins and other cell adhesion molecules in tumor progression and metastasis. Lab Invest. 1993;68:4–17.

Alberts B, Bray D, Lewis J, et al. Cell junctions, cell adhesion, and the extracellular matrix. In: Alberts B, Bray D, Lewis J, et al., eds. Molecular Biology of the Cell. 3rd ed. New York, NY: Garland Publishing; 1994.

Anderson JC. Biochemical basis of connective tissue disease. In: Gardner DL, ed. Pathological Basis of the Connective Tissue Diseases. London, UK: Arnold; 1992:173–226.

Behrens J. The role of cell adhesion molecules in cancer invasion and metastasis. Breast Cancer Res Treat. 1993;24:175–184.

Brooks PC, Montgomery AM, Rosenfeld M, et al. Integrin alpha v beta 3 antagonists promote tumor regression by inducing apoptosis of angiogenic blood vessels. Cell. 1994;79:1157-64.

Burke PA, DeNardo SJ, Miers LA, et al. Cilengitide targeting of alpha(v)beta(3) integrin receptor synergizes with radioimmunotherapy to increase efficacy and apoptosis in breast cancer xenografts. Cancer Res. 2002;62:4263-72.

Burvenich I. Karakterisatie van het 14C5 antigeen betrokken bij cel-substraatadhesie, invasie en metastasering van borstcarcinomacellen. 2001, Scriptie, Gent, Faculteit Landbouwkundige en Toegepast Biologische Wetenschappen, 150p.

Cavallaro U, Christofori G. Cell adhesion in tumor invasion and metastasis: loss of the glue is not enough. Biochim Biophys Acta. 2001;1552:39–45.

Coene E, Schelfhout AM, De Ridder L, De Potter C. Generation of a monoclonal antibody directed against a human cell substrate adhesion molecule and the expression of the antigen in human tissues. Hybridoma. 1997;16:77–83.

Davis, HM, Prabhakar, U, Jang, H, et al. A rational approach for a phase I clinical study design to evaluate CNTO 95, a novel, fully human anti-a(v) monoclonal antibody (MAb), in patients with solid tumors. J Clin Oncol. 2004;22:190S-190S.

Dayam R, Aiello F, Deng J, et al. Discovery of small molecule integrin alphavbeta3 antagonists as novel anticancer agents. J Med Chem. 2006 ;49:4526-34.

De Potter C, Schelfhout AM, De Smet FH, et al. A monoclonal antibody directed against a human cell membrane antigen prevents cell substrate adhesion and tumor invasion. Am J Pathol. 1994;144:95–103.

Dechantsreiter MA, Planker E, Matha B, et al. N-Methylated cyclic RGD peptides as highly active and selective alpha(V)beta(3) integrin antagonists. J Med Chem. 1999;42:3033-40.

Dedhar S, Saulnier R. Alterations in integrin receptor expression on chemically transformed human cells: specific enhancement of laminin and collagen receptor complexes. J Cell Biol. 1990;110:481–489.

Dijkgraaf I, Kruijtzer JA, Frielink C, et al. alpha(v)beta(3) Integrin-targeting of intraperitoneally growing tumors with a radiolabeled RGD peptide. Int J Cancer. 2006 *Epub ahead of print*

Dijkgraaf I, Kruijtzer JA, Liu S, et al. Improved targeting of the alpha(v)beta (3) integrin by multimerisation of RGD peptides. Eur J Nucl Med Mol Imaging. 2006 *Epub ahead of print*

Ellis LM, Nicolson GL, Fidler IJ. Concepts and mechanisms of breast cancer metastasis. In: Bland KI and Copeland EM. Comprehensive management of benign and malignant diseases (Volume 1) 2nd edit. Philadelphia, Saunders, 1998.

Enns A, Korb T, Schluter K, et al. Alphavbeta5-integrins mediate early steps of metastasis formation. Eur J Cancer. 2005;41:1065-72.

Eskens FA, Dumez H, Hoekstra R, et al. Phase I and pharmacokinetic study of continuous twice weekly intravenous administration of Cilengitide (EMD 121974), a novel inhibitor of the integrins alphavbeta3 and alphavbeta5 in patients with advanced solid tumours. Eur J Cancer. 2003;39:917-26.

Friedlander M, Brooks PC, Shaffer RW, et al. Definition of two angiogenic pathways by distinct alpha v integrins. Science. 1995;270:1500-2.

Giffels P, Köhler S, De Potter C, et al. MAb 14C5 against a human cell substrate adhesion molecule for inhibition of tumor growth in-vivo. Eur J Cancer. 1997;33:96.

Gutheil JC, Campbell TN, Pierce PR, et al. Targeted antiangiogenic therapy for cancer using Vitaxin: a humanized monoclonal antibody to the integrin alphavbeta3. Clin Cancer Res. 2000;6:3056-61.

Haubner R. alpha(v)beta (3)-integrin imaging: a new approach to characterise angiogenesis? Eur J Nucl Med Mol Imaging. 2006;33 Suppl 13:54-63.

Hynes RO. A reevaluation of integrins as regulators of angiogenesis. Nat Med. 2002;8:918-21.

Jayson, GC, Mullamitha, S, Ton, C, et al. Phase I study of CNTO 95, a fully human monoclonal antibody (mAb) to alpha v integrins, in patients with solid tumors. J Clin Oncol. 2004;22: 224S-224S.

Jiang WG, Puntis MC, Hallett MB. Molecular and cellular basis of cancer invasion and metastasis: implications for treatment. Br J Surg. 1994;81:1576–1590.

Jin H, Varner J. Integrins: roles in cancer development and as treatment targets. Br J Cancer. 2004;90:561-5.

Jockusch BM, Bubeck P, Giehl K, et al. The molecular architecture of focal adhesions. Annu Rev Cell Dev Biol. 1995;11:379–416.

Kerr JS, Slee AM, Mousa SA. The alpha v integrin antagonists as novel anticancer agents: an update. Expert Opin Investig Drugs. 2002;11:1765-74.

Kohn EC, Liotta LA. Molecular insights into cancer invasion: strategies for prevention and intervention. Cancer Res. 1995;55:1856-62.

Kreis T, Vale R. Guidebook to the Extracellular Matrix, Anchor, and Adhesion Proteins. Oxford, UK: Oxford University Press; 1999.

Leavesley DI, Ferguson GD, Wayner EA, et al. Requirement of the integrin beta 3 subunit for carcinoma cell spreading or migration on vitronectin and fibrinogen. J Cell Biol. 1992;117:1101-7.

Lewis MR. Radiolabeled RGD peptides move beyond cancer: PET imaging of delayed-type hypersensitivity reaction. J Nucl Med. 2005;46:2-4.

Li LS, Rader C, Matsushita M, et al. Chemical adaptor immunotherapy: design, synthesis, and evaluation of novel integrin-targeting devices. J Med Chem. 2004;47:5630-40.

Liotta LA, Kohn EC. Invasion and metatasis. In: Kufe DW, Pollock RE, Weichselbaum RR et al. Cancer Medicine 6th edit. Hamilton (Cancada), BC Decker Inc; 2003.

Martin PL, Jiao Q, Cornacoff J, et al. Absence of adverse effects in cynomolgus macaques treated with CNTO 95, a fully human anti-alphav integrin monoclonal antibody, despite widespread tissue binding. Clin Cancer Res. 2005;11:6959-65.

McLean JW, Vestal DJ, Cheresh DA, et al. cDNA sequence of the human integrin beta 5 subunit. J Biol Chem. 1990;265:17126-31.

Mitjans F, Meyer T, Fittschen C, et al. In vivo therapy of malignant melanoma by means of antagonists of alphav integrins. Int J Cancer. 2000;87:716-23.

Miyauchi A, Alvarez J, Greenfield EM, et al. Recognition of osteopontin and related peptides by an alpha v beta 3 integrin stimulates immediate cell signals in osteoclasts. J Biol Chem. 1991;266:20369-74.

Mizejewski GJ. Role of integrins in cancer: survey of expression patterns. Proc Soc Exp Biol Med. 1999 Nov;222(2):124-38.

Pignatelli M, Cardillo MR, Hanby A, Stamp GW. Integrins and their accessory adhesion molecules in mammary carcinomas: loss of polarization in poorly differentiated tumors. Hum Pathol. 1992;23:1159–1166.

Reinholt FP, Hultenby K, Oldberg A, et al. Osteopontin--a possible anchor of osteoclasts to bone. Proc Natl Acad Sci U S A. 1990;87:4473-5.

Ruegg C, Dormond O, Mariotti A. Endothelial cell integrins and COX-2: mediators and therapeutic targets of tumor angiogenesis. Biochim Biophys Acta. 2004;1654:51-67.

Sims MA, Field SD, Barnes MR, et al. Cloning and characterisation of ITGAV, the genomic sequence for human cell adhesion protein (vitronectin) receptor alpha subunit, CD51. Cytogenet Cell Genet. 2000;89:268-71.

Smith JW, Vestal DJ, Irwin SV, et al. Purification and functional characterization of integrin alpha v beta 5. An adhesion receptor for vitronectin. J Biol Chem. 1990;265:11008-13.

Takeichi M. Cadherin cell adhesion receptors as a morphogenetic regulator. Science. 1990;251:1451–1455.

Taverna D, Crowley D, Connolly M, et al. A direct test of potential roles for beta3 and beta5 integrins in growth and metastasis of murine mammary carcinomas. Cancer Res. 2005;65:10324-9.

Trikha M, Zhou Z, Nemeth JA, et al. CNTO 95, a fully human monoclonal antibody that inhibits alphav integrins, has antitumor and antiangiogenic activity in vivo. Int J Cancer. 2004;110:326-35.

Vanholme B. Detectie en zuivering van een cel-substraat antigen betrokken bij de invasie en metastasering bij borstkanker. 2000, Scriptie, Gent, Faculteit Landbouwkundige en Toegepast Biologische Wetenschappen, 108p.

Wagner U, Köhler S, Prietl G, et al. Monoclonal anti-idiotype antibodies in immunotherapy of ovarian carcinoma (MAb ACA125) and breast carcinoma (MAb ACA14C5). Zentralbl Gynakol. 1999;121:190–195.

Wayner EA, Orlando RA, Cheresh DA. Integrins alpha v beta 3 and alpha v beta 5 contribute to cell attachment to vitronectin but differentially distribute on the cell surface. J Cell Biol. 1991;113:919-29.

Wehrle-Haller B, Imhof BA. Integrin-dependent pathologies. J Pathol. 2003;200:481-7.

Yurchenco PD. Assembly of laminin and type IV collagen into basement membrane networks. In: Yurchenco PD, Birk DE, Mecham RP, eds. Extracellular Matrix Assembly and Structure. San Diego, CA: Academic Press; 1994.

Zhang X, Xiong Z, Wu Y, et al. Quantitative PET imaging of tumor integrin alphavbeta3 expression with 18F-FRGD2. J Nucl Med. 2006;47:113-21.

3.7 Appendix

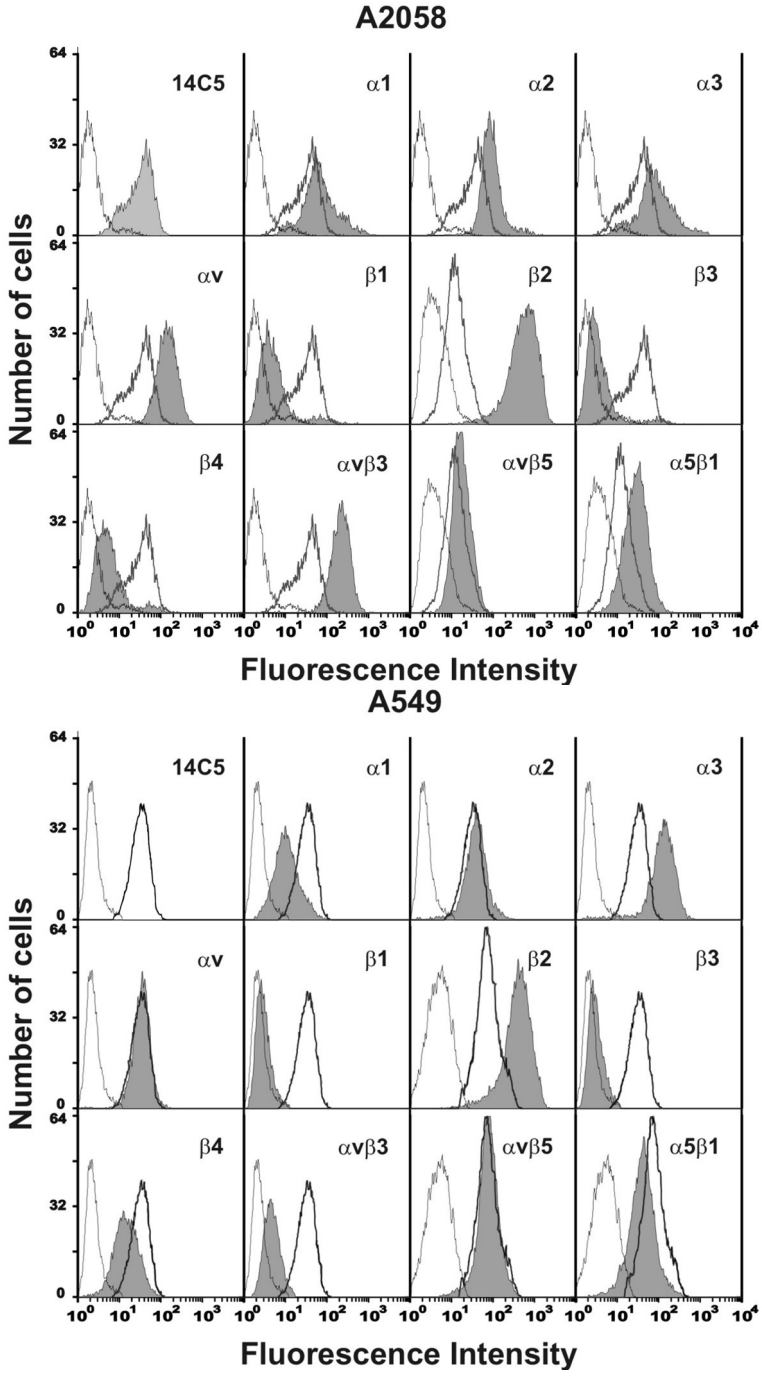
A2058
14C5
α1
α2
α3
αv
β1
β2
β3
β4
αvβ3
αvβ5
α5β1
Number of cells
Fluorescence Intensity
A549
14C5
α1
α2
α3
αv
β1
β2
β3
β4
αvβ3
αvβ5
α5β1
Number of cells
Fluorescence Intensity

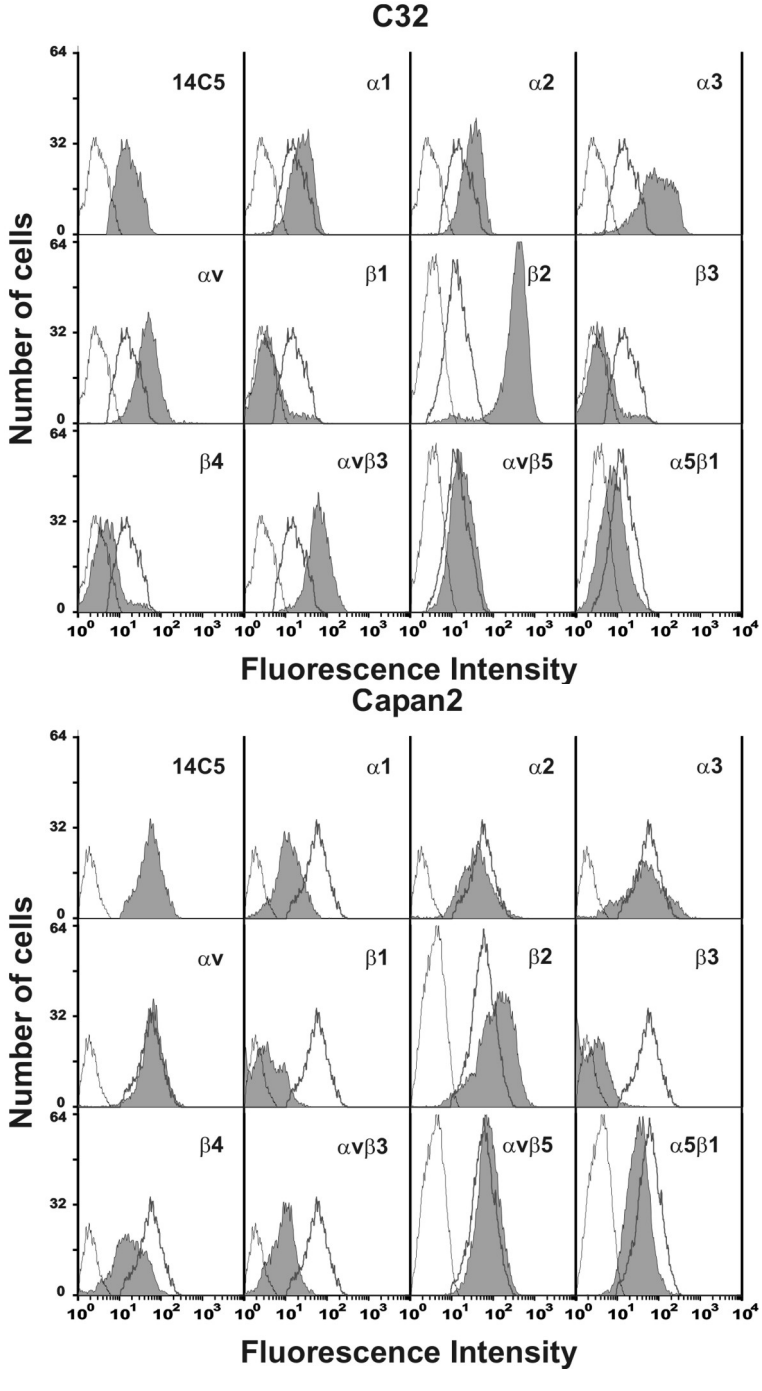
C32
14C5
α1
α2
α3
αv
β1
β2
β3
β4
αvβ3
αvβ5
α5β1
Number of cells
Fluorescence Intensity
Capan2
14C5
α1
α2
α3
αv
β1
β2
β3
β4
αvβ3
αvβ5
α5β1
Number of cells
Fluorescence Intensity

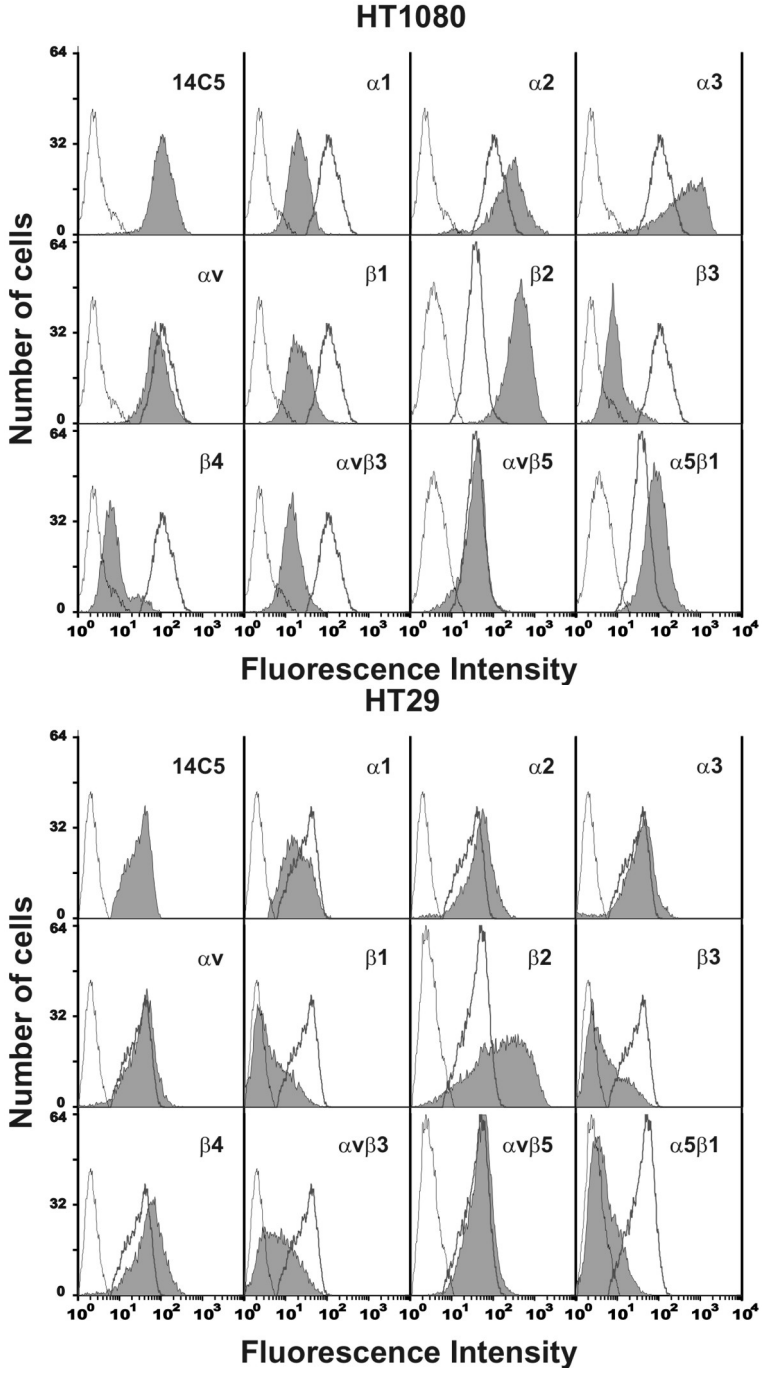
HT1080
14C5
α1
α2
α3
αv
β1
β2
β3
β4
αvβ3
αvβ5
α5β1
Number of cells
Fluorescence Intensity
HT29
14C5
α1
α2
α3
αv
β1
β2
β3
β4
αvβ3
αvβ5
α5β1
Number of cells
Fluorescence Intensity

Chapter 4

IMMUNOCYTOCHEMICAL AND IMMUNOHISTOCHEMICAL ANALYSIS OF ANTIGEN 14C5 AS TUMOUR ASSOCIATED ANTIGEN FOR TARGETED THERAPY

Burvenich I, Vanwallegem L, Vanhuysse J, Coene E, Praet M, Cuvelier C, De Vos F and Slegers G

In preparation

4.1 Introduction

Radioimmunodetection and radioimmunotherapy involve the use of anticancer antibodies conjugated with diagnostic and therapeutic radionuclides, respectively. Intrinsic characteristics of antibody and antigen, as well as the choice of radionuclide, will determine the outcome of these targeted strategies (Goldenberg, 2002). One critical step in the development of a new antibody therapeutic is validation of the antigen (Carter et al, 2004). Because radiotoxicity to normal tissue should be kept as low as possible, high and tumour-associated expression of the target antigen is wanted.

Coene et al. (1997) demonstrated abundant expression of antigen 14C5 (Ag 14C5) on the tumour surface of *in situ* and invasive breast cancer tissue. The antigen was specifically overexpressed in 64 % of invasive ductal adenocarcinomas of the breast (n = 33), in all investigated cases of invasive squamous cell carcinoma (n = 7) and in 40 % of basocellular carcinomas of the skin (n = 5). The antigen 14C5 is located on the cell membrane of the carcinoma cells. When the tumour is characterized by a highly invasive phenotype, 65 % of the cases also show an extensive stromal expression on the fibroblasts between the tumour cells (n = 71). In normal tissues and stroma surrounding in situ carcinomas of the breast (n = 15), no expression of the Ag 14C5 occurred (Coene et al., 1997). Normal epithelial, muscle, and connective tissues that did not show staining with mAb 14C5 were skin, thyroid, parathyroid, colon, stomach, lung, uterine tube, ovary, ureter, urethra, lymph node, nerve, chondroid tissue, skeletal muscle, oesophagus, and artery (De Potter et al., 1994; Coene et al., 1997). Sometimes, low-level staining of myo-epithelial cells was observed in biopsies of breast tissue and in tubular cells of the kidney.

Previous studies demonstrated that antigen 14C5 is most likely the αvβ5 receptor. Table 4.1 shows ligands and cellular tissue distribution of the αv

integrins as described in literature. From this table it is clear that αvβ3 and αvβ5 are capable of recognizing multiple Arg-Gly-Asp(RGD)-containing ligands, whereas the other αv integrins are more restricted in their adhesion functions.

Tabel 4.1 αv Integrins: ligands, cellular and tissue distribution (Kerr et al., 2002; Wehrle-Haller and Imhof, 2003)

αv Integrins	Ligands	Cellular and tissue distribution	Potential implications
αvβ1	Ln, Fn, Opn	Smooth muscle cells, fibroblasts, osteoclasts, tumour cells	Vascular disorders
αvβ3	Opn, Fg, Vn, Tn, Tsp, Fn, PCL, αCol MMP2, vWF	Endothelial cells, smooth muscle cells, osteoclasts, platelets, fibroblasts, tumour cells, epithelial cells, leukocytes	Angiogenesis, restenosis, vascular disorders, osteoporosis
αvβ5	Opn, Fg, Vn, Fn, Tsp, Tat, bone sialoprotein	Endothelial cells, smooth muscle cells, osteoclasts, platelets, fibroblasts, tumour cells, epithelial cells, leukocytes, pancreas	Angiogenesis, vascular disorders
αvβ6	Fn, Fg, Vn, Tn	Epithelial cells, carcinoma cells	-
αvβ8	Vn	Melanoma, kidney, brain, ovary, uterus, placenta	-

Col: Collagen; Fg: Fibrinogen; Fn: Fibronectin; Ln: Laminin; MMP2: Matrix Metalloproteinase 2; Opn: Osteopontin; PCL: perlecan; Tat: HIV tat protein; Tn: Tenascin, Tsp: Thrombospondin; Vn: Vitronectin: vWF: von Willebrand factor

In pancreatic cancer cell lines, the integrin subunit β5 was associated with adenocarcinomas and ampullary tumours, whereas highly differentiated cell lines showed variable loss of one or more of the integrin chains (Mizejewski et al., 1999). In breast cancer, the αvβ5 and αvβ1 integrins were widely distributed among a variety of breast cancer cell lines (Meyer et al., 1998). Kemperman et al. (1997) reported high expression of αvβ5 on HT-29 colon carcinoma cells. Wayner et al. (1991) reported high expression of αvβ5 on different lung carcinoma cell lines and melanoma cells, and demonstrated that although αvβ3 and αvβ5 bind to the same ligand vitronectin, αvβ3 associates with focal contacts, whereas αvβ5 forms small patches distributed over most of the cell surface. This finding let to another study reported by the same research group, showing that the inability to form focal contacts inhibits spread and

migration of a human pancreatic cell line. This cell line fails to express αvβ3, but binds to vitronectin in an αvβ5 dependent way (Leavelsley et al., 1992). These results demonstrated that two homologous integrins, expressed on the same cells and recognizing the same ligand, can promote distinct signals potentiating diverse biological activities in response to a given extracellular matrix. Finally, increased levels of integrin αvβ5 were shown on the fibroblasts of scleroderma (Asano et al. 2004).

In this study, we address the antigen 14C5 expression and look for possible discrepancies between Ag 14C5 binding of mAb 14C5 and the anti-αvβ5 specific antibody (P1F6). To investigate expression, we performed immunocytochemistry on twenty-one human cancer cell lines from different origin. Levels of antigen expression were analysed with flow cytometry. In addition, with respect to possible imaging and therapy with radiolabeled mAb 14C5, we investigated the expression of Ag 14C5 on 20 human colon carcinoma tissues and 16 human lung carcinoma tissues both with mAb 14C5 and anti-αvβ5 antibody (P1F6).

4.2 Materials and methods

4.2.1 Antibodies

The 14C5 antibody-producing hybridoma cells produced mAb 14C5 in Integra CL 350 flasks (Elscolab, Kruibeke, Belgium) containing protein-free hybridoma medium (Invitrogen, Merelbeke, Belgium). MAb 14C5 was protein G purified (Amersham Biosciences Europe, Roosendaal, the Netherlands) from concentrated supernatant and dialyzed against PBS (pH 7.4). The purity of the antibody was evaluated by SDS-PAGE using reducing and non-reducing conditions. The anti-αvβ5 (P1F6, mouse IgG1, Millipore, Belgium) was used for comparison in immunohistochemical studies. The 9E10 mAb (anti-*c-myc*, mouse IgG1, Becton Dickinson, BD, Erembodegem-Aalst, Belgium) was used

as a control for aspecific Fc-receptor binding during flow cytometric analysis. Alexa Fluor 488-conjugated goat anti-mouse IgG antibody (Invitrogen) was used during flow cytometry.

4.2.2 Cell lines

HT-29, LoVo, Capan-1, Capan-2, and C32 were a kind gift of J&J Pharmaceutical Research & Development (Beerse, Belgium). HT-1080, A2058, A549, AsPC-1, and MDA-MB-231 were obtained from the Laboratory of Tumor and Developmental Biology (University of Liège, Belgium). OVCAR-3, HeLa, K-562 and BT-20 were obtained from the Department of Molecular Biomedical Research (Flanders Institute for Biotechnology, Ghent, Belgium). SK-BR-3, MCF-7, T-47D, LN-229, Colo16, 791T and MOLT-4, were obtained from the N. Goormaghtigh Institute of Pathology, University of Ghent (Ghent, Belgium). All cell lines were cultured in standard medium with supplements according to the American Type Culture Collection (Manassas, VA) recommendations, except for Colo16, K-562 and MOLT-4 grown in RPMI1640 medium containing 10 mmol/l HEPES and 10% fetal bovine serum (Cambrex, Verviers, Belgium) and 791T grown in DMEM medium containing 10% fetal bovine serum. All cells were cultured at 37 °C in a 5% CO_2 humidified incubator and passaged with 0.05% trypsin-0.02% EDTA.

4.2.3 Immunocytochemical studies

Confluent tumour cell lines were harvested by cell scraping and washing twice with PBS. Cells were cytocentrifuged for 5 minutes at 180 × g and fixed in acetone for 10 minutes. For immunocytochemical detection, an avidin-biotin system was applied (DakoCytomation, Heverlee, Belgium). MAb 14C5 (1 µg/ml) was incubated for 1 hour in PBS 5% bovine serum albumin (BSA; Sigma-Aldrich, Bornem, Belgium) at room temperature. The cells were washed twice with PBS. Then, the sample was incubated with biotinylated anti-mouse

immunoglobulins for 15 minutes; the avidin-peroxidase complex was added for 15 minutes followed by 3-amino-9-ethylcarbozole (DakoCytomation) for 10 minutes as chromogen. Between each step, cells were washed twice with PBS. Cells were counterstained with Mayer's hematoxylin and mounted in Aquatex mounting medium (VWR International, Leuven, Belgium). Negative control cells were obtained by omitting the primary antibody.

4.2.4 Flow cytometry

Confluent cells were harvested using cell dissociation buffer (Invitrogen). Aliquots of 2×10^5 cells were incubated with mAb 14C5 (10 nmol/l) in PBS-0.5% BSA-0.02% (w/v) sodium azide (Sigma-Aldrich)(w/v) on ice. After washing the cells with PBS-0.5% BSA-0.02% sodium azide, cells were incubated with Alexa Fluor 488-conjugated goat anti-mouse on ice for 1 hour. Again, cells were washed with PBS-0.5% BSA-0.02% sodium azide and suspended in a final volume of 300 µL of PBS-0.5% BSA-0.02% sodium azide. In control samples, the primary antibody was omitted. For isotype control, mAb 9E10 (10 nmol/l) was used.

Flow cytometric analysis was done using a FACScan flow cytometer (Becton Dickinson). Tumour cell populations were gated based on forward and side scatter variables. Data analysis was done using WinMDI (Joseph Trotter).

4.2.5 Immunohistochemical study

4.2.5.1 Patient tumour tissue

As described by Coene et al. (1997), biopsy specimens from human colon and lung epithelial tumours, and normal colon and lung tissues were investigated for the expression of the antigen 14C5. Therefore, 5-µm sections from fresh frozen material were cut and fixed in acetone for 1 min at 4°C. For immunohistochemical detection, an avidin-biotin system was applied as

described previously for the immunocytochemical study (DakoCytomation, Heverlee, Belgium).

4.2.5.2 Animal tumour tissue

Male athymic mice (*nu/nu*; 5 weeks; Charles River, Brussels, Belgium) were injected s.c. into the right flank with A549 (*lung*), LoVo (*colon*), HT1080 (*fibrosarcoma*), Capan-2 (*pancreas*) or SKOV3 (*ovarium*) cells (1×10^7) in 200 µl fetal bovine serum-free culture medium. When tumours achieved a size of 0.2 to 0.5 g, 6-µm sections from fresh frozen material were cut and fixed in acetone for 1 min at 4°C. For immunohistochemical detection, an avidin-biotin system was applied as described previously for the immunocytochemical study (DakoCytomation, Heverlee, Belgium).

4.3 Results

4.3.1 Immunocytochemical analysis of human cancer cell lines

Twenty-one human cell lines were examined by immunocytochemical analysis and/or flow cytometry analysis for expression of the antigen 14C5 (Table 4.2). Ag 14C5 is ubiquitously expressed in the investigated cell lines (18 of 21). Not all cells stained equally, but the positive cells had a membrane-associated staining (Fig. 4.1). No obvious correlation was observed between the level of immunostaining and the tissue origin of the neoplastic cells.

4.3.2 Quantitative expression analysis with FACS

Fifteen cell lines were investigated by flow cytometric analysis (Fig. 4.2). Significant binding of mAb 14C5 was observed with C32, OVCAR-3, A2058, LoVo and HeLa cells. The highest reactivity was found with SK-BR-3, HT-1080, A549, BT-20, HT-29, Capan-1 and Capan-2 cells.

Table 4.2 Results of the immunoperoxidase staining for antigen 14C5 of 21 different human cancer cell lines

Cell line	14C5 reactivity
Carcinoma Breast	
SK-BR-3	Positive
MCF-7	Positive
BT-20	Positive
T-47D	Positive
MDA-MB-231	Positive
Carcinoma Ovary	
OVCAR-3	Positive
SKOV-3	Positive
Carcinoma Cervix	
HeLa	Positive
Carcinoma Lung	
A549	Positive
Carcinoma Colon	
HT-29	Positive
LoVo	Positive
Carcinoma Squamous Cell	
Colo16	Negative
Carcinoma Pancreas	
Capan-1	Positive
Capan-2	Positive
AsPC-1	Positive
Fibrosarcoma	
HT-1080	Positive
Osteosarcoma	
791T	Positive
Glioblastoma	
LN-229	Negative
Leukemia	
MOLT-4	Negative
Melanoma	
C32	Positive
A2058	Positive

As isotype control, an irrelevant mAb 9E10 was used. This antibody binds an intracellular epitope (c-myc) and therefore cannot bind to the cell membrane unless the antigen 14C5 is an Fc receptor or the mAb 9E10 is bound to the membrane by other Fc receptors. All plots of mAb 9E10 binding, matched the auto-fluorescence plots of unbound cells in the presence of secondary antibody.

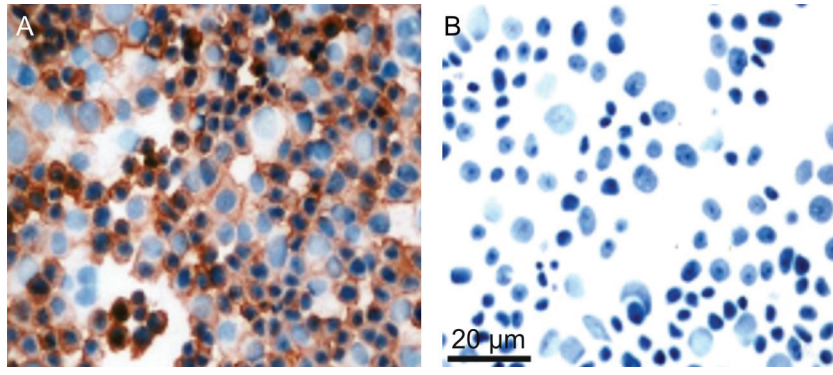

Fig. 4.1. Immunocytochemistry with mAb 14C5 on A549 lung carcinoma cells (200×). *(A)* Membrane-associated staining with mAb 14C5 (1:500; 1 mg/ml). *(B)* Negative control, mAb 14C5 was omitted.

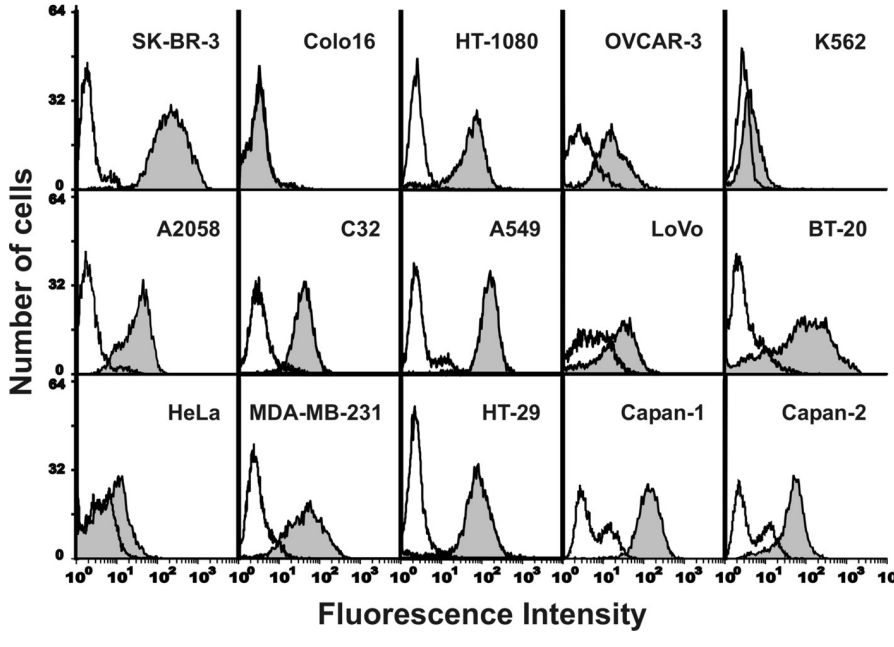

Fig. 4.2. Histogram of fluorescence-activated cell sorting analysis showing the binding of mAb 14C5 with various neoplastic cell lines. Cells were stained with mAb 14C5 (filled histograms) or anti-c-myc-IgG1 (open histograms) isotope control mAb. Bound mAbs were detected with Alexa488-conjugated anti-mouse IgG

4.3.3 Immunohistochemical analysis

4.3.3.1 Patient study

The results of the immunohistochemical staining with human colon cancer tissues (n = 20) are shown in Table 4.3 and Table 4.5. The carcinoma cells stained positive in 50% of carcinoma tumours. This staining was weak to focal strong positive (Fig. 4.3A). Sometimes, only apical staining of tumour cell membrane was observed (Fig. 4.3B). However, fibroblasts in the stroma surrounding the tumour cells showed extensive expression of the antigen 14C5.

Table 4.3 Antigen 14C5 expression with human colon cancer tissue

Patient			Ag 14C5 expression		
			Tumour		Normal
Nr	Diagnose	Figure	Stroma	Cells	
1	rectum CA		+/-	-	NA
2	colon CA		+	-	NA
3	colon CA		+++	-	NA
4	rectum CA		++	-	NA
5	rectum CA		++	+/-	NA
6	rectum CA		+	-	NA
7	colon CA		+++	-	NA
8	rectum CA		+	+	NA
9	colon CA		+	-	NA
10	rectum CA		+++	+	NA
11	colon CA		+++	+	-
12	rectum CA		++	+	NA
13	rectum CA	Fig. 4.3A	+++	++	NA
14	colon CA		+	-	-
15	rectum CA		+	-	NA
16	colon CA		+	+	NA
17	colon CA		+++	+/++	NA
18	colon CA	Fig. 4.3B	+++	+/++	NA
19	recto sigmoid		+	+	NA
20	colon CA		+	-	NA

NA, not available; CA, carcinoma; +/-, weak positive; +, positive; ++, strong positive; +++, very strong positive; -, negative

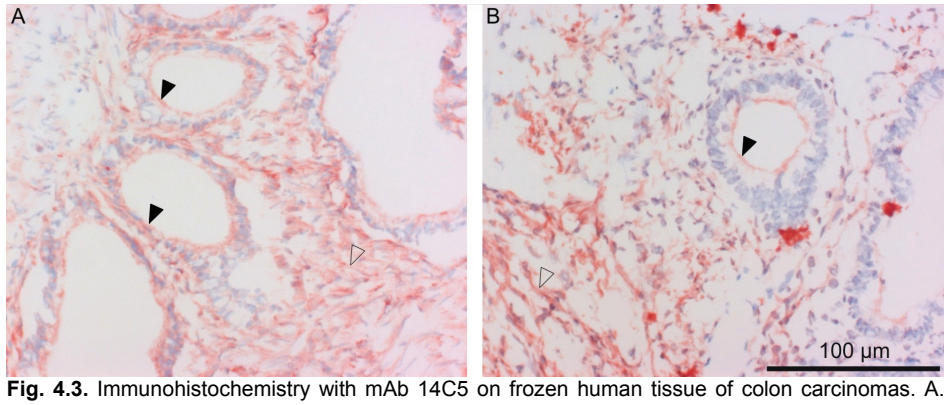

Fig. 4.3. Immunohistochemistry with mAb 14C5 on frozen human tissue of colon carcinomas. A. Adenocarcinoma of the rectum. There is a distinct expression on the cytoplasmic membrane of the carcinoma cells. The surrounding fibrous tissue and the fibroblasts express the antigen 14C5 at high level (200×). B. Colon adenocarcinoma with apical expression on the cytoplasmic membrane of the carcinoma cells. There is also a distinct expression of the antigen 14C5 on the surrounding fibrous tissue and the fibroblasts (200×). *Filled arrows*, tumour cell membrane staining; *Open arrows*, stroma

The results of the immunohistochemical staining with human non-small cell lung cancer (NSCLC) tissues (n = 16) are shown in Table 4.4 and Table 4.5. In bronchoalveolar carcinoma (BAC), which tends to be more inclined to stay within the lung and is less likely to spread to other organs, the carcinoma cells stained negative and stroma surrounding BAC stained only weakly positive in one case (n = 4). Typical carcinoid represents another uncommon group of pulmonary neoplasms. They are well differentiated and represent the least biologically aggressive type of pulmonary neuroendocrine tumour. These tumours characteristically grow slowly and tend to metastasize infrequently. The investigated carcinoid did not show staining with mAb 14C5. The more common types of NSCLC, i.e. squamous (n = 5) and adenocarcinoma (n = 3) stained focal positive in 2 of 5 squamous carcinomas (Fig. 4.4A and 4.4D) and in 1 of 3 investigated adenocarcinoma (Fig. 4.4C). Fibroblasts in the stroma surrounding the tumour cells showed positive to very strong positive staining in all squamous and adenocarcinoma samples (n = 8) (Fig. 4.4B-D).

Table 4.4 Antigen 14C5 expression with human lung cancer tissue

Patient			Ag 14C5 expression		
			Tumour		Normal tissue
Nr	Diagnose	Figure	Stroma	Cells	
1	md squamous		+	-	NA
2	md adeno		++	-	NA
3	pd squamous		+++	-	NA
4	BAC		-	-	NA
5	md squamous	Fig. 4.4A	+++	+	NA
6	BAC		-	-	NA
7	md-wd adeno		+++	-	NA
8	pd giant-cell adeno		+	-	NA
9	BAC		-	-	NA
10	md squamous	Fig. 4.4D	+++	+	NA
11	Carcinoid		-	-	NA
12	BAC		+/-	-	NA
13	md squamous	Fig. 4.4B	+++	-	-
15	adeno	Fig. 4.4C	+++	+	NA
16	LCUC		++	-	NA

NA, not available; adeno: adenocarcinoma; BAC, bronchoalveolar adenocarcinoma; LCUC: Large Cell Undifferentiated Carcinoma; md: moderately differentiated; pd: poorly differentiated; RCC: renal cell carcinoma; wd: well differentiated +/-, weak positive; +, positive; ++, strong positive; +++, very strong positive; -, negative

Table 4.5 gives a summary of the immunohistochemical investigation of human lung and colon carcinoma tissues and their surrounding stroma.

Tabel 4.5 Summary of the immunohistochemical investigation of human lung and colon carcinomas and their surrounding stroma

		Stroma		Tumour cells	
Tumour type	n	+	-	+	-
Lung					
Squamous Cell carcinoma	5	5 (100 %)	0 (0 %)	2 (40 %)	3 (60 %)
Adenocarcinoma	3	3 (100 %)	0 (0 %)	1 (33 %)	2 (67 %)
BAC	4	1 (25 %)	3 (75 %)	0 (0 %)	4 (100 %)
Large Cell Cancer	1	1 (100 %)	0 (0 %)	0 (0 %)	1 (100 %)
Carcinoid	1	0 (0 %)	1 (100%)	0 (0 %)	1 (100%)
Colon					
Adenocarcinoma	20	19 (95 %)	1 (5 %)	10 (50 %)	10 (50 %)

BAC, bronchoalveolar adenocarcinoma

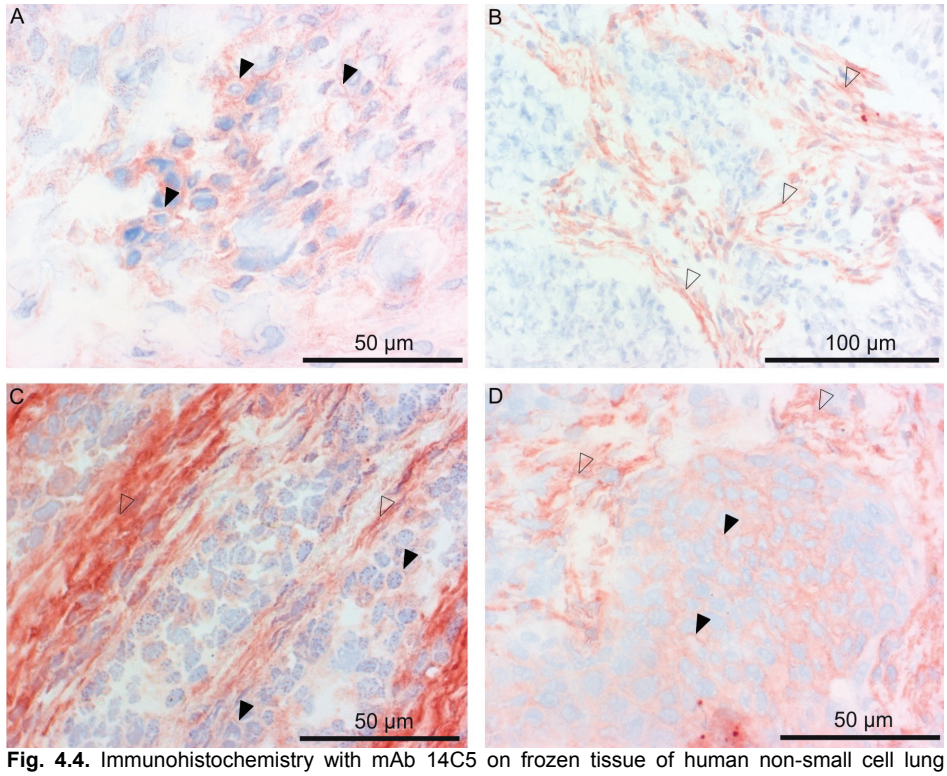

Fig. 4.4. Immunohistochemistry with mAb 14C5 on frozen tissue of human non-small cell lung carcinomas. *(A)* Moderately differentiated squamous carcinoma. Focal positive staining of cell membranes (400×). *(B)* Moderately differentiated squamous carcinoma. No staining of tumour cell membranes was observed. The surrounding fibrous tissue and the fibroblasts express the antigen 14C5 at high level (200×). *(C)* Adenocarcinoma. A weak staining of the tumour cell membranes and strong to very strong expression of the antigen 14C5 on the surrounding fibrous tissue and the fibroblasts (400×). *(D)* Moderately differentiated squamous carcinoma. Focal positive staining of tumour cell membranes with high expression in surrounding stroma (400×). *Filled arrows*, tumour cell membrane staining; *Open arrows*, stroma

Normal tissues of lung (n = 5) and colon (n = 5) were analyzed for expression of the antigen 14C5. No expression was detected on normal lung tissues. On colon tissues, sometimes small blood vessels and mucous secreting cells showed staining with mAb 14C5.

This study was also performed with the αvβ5 specific antibody (P1F6). The location of the staining on the tissues was identical, but staining was more intense with P1F6 antibody. However, aspecific staining with normal tissue was higher with P1F6 than with mAb 14C5.

4.3.3.2 Animal study

Immunohistochemical studies were done with mAb 14C5 on human A549 (*lung*), LoVo (*colon*), HT1080 (*fibrosarcoma*), Capan-2 (*pancreas*) and SKOV3 (*ovarium*) carcinoma tissues grown in athymic mice. Two tissue types, A549 and SKOV-3, showed specific binding of mAb 14C5 (Fig. 4.5 and Fig. 4.6). On the other tumour tissues, staining with the anti-mouse IgG specific antibody showed too much background on the negative control samples, and therefore comparison between positive and negative samples was not possible.

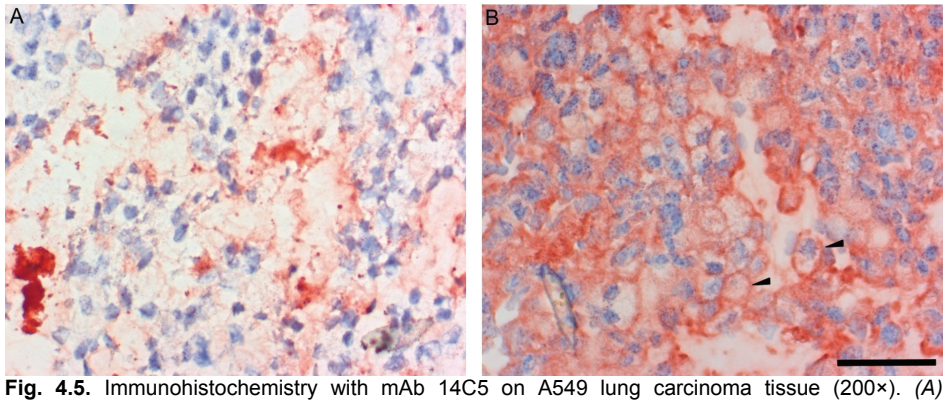

Fig. 4.5. Immunohistochemistry with mAb 14C5 on A549 lung carcinoma tissue (200×). *(A)* Negative control, mAb 14C5 was omitted. *(B)* Membrane-associated staining with mAb 14C5 (1:500; 1 mg/ml). *bar*, 20 µm

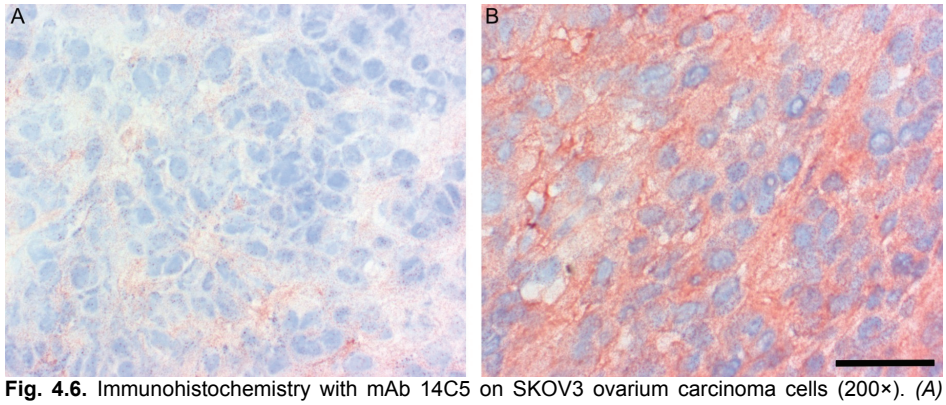

Fig. 4.6. Immunohistochemistry with mAb 14C5 on SKOV3 ovarium carcinoma cells (200×). *(A)* Negative control, mAb 14C5 was omitted. *(B)* Membrane-associated staining with mAb 14C5 (1:500; 1 mg/ml). Stroma between the tumour cells showed high level expression of Ag 14C5. *bar*, 20 µm

A549 tissue showed very strong staining of cell membranes. SKOV-3 tissue showed strong staining of the cell membranes and equivalent staining of the stroma between the tumour cells.

4.4 Discussion

Prior work has shown that mAb 14C5 recognizes a cell surface antigen on mammary tumours. No antigen 14C5 could be detected in normal tissues as well as in the stroma surrounding *in situ* carcinomas of the breast. Sometimes, low-level staining of myoepithelial cells was observed in biopsies of breast tissue and in tubular cells of the kidney (De Potter et al., 1994; Coene et al., 1997).

The present data show that the expression of antigen 14C5 is not restricted to the breast cancer cell lines but is also present in varying degrees on other neoplastic human cell lines from different origins: carcinomas of ovary, cervix, lung, colon, and pancreas, sarcomas, and melanomas. Flow cytometric results showed that 9 out of 15 of the investigated cell lines showed high expression of antigen 14C5. Moreover, the A549 lung cancer cells showed the highest antigen 14C5 expression, providing a possible new target for non-small cell lung cancer (NSCLC) therapy. Although breast cancer is currently second as the leading cancer causing death in women in Europe and the United States, lung cancer is the leading cause of cancer-related mortality in both men and women, followed by colorectal (Boyle and Ferlay, 2005). NSCLC accounts for ~80% of all lung cancers (Ghambir et al. 2001; Gridelli, 2004; Maione et al., 2004). Today, the therapy of NSCLC has reached a plateau in improving patient survival (Maione et al., 2004). Investigation on NSCLC-related antigen 14C5 expression may result in antigen 14C5 as a novel target for NSCLC therapy.

Therefore, the expression of the antigen 14C5 was investigated in human lung carcinoma and human colon carcinoma. In these tumour types, Ag 14C5 expression occurred mainly in the stroma surrounding the tumour cells and on the stromal fibroblasts (squamous cell carcinoma, 5/5; adenocarcinoma of lung, 3/3; large cell carcinoma, 1/1; colon adenocarcinoma, 19/20) and was less localized at the tumour cells themselves (squamous cell carcinoma, 2/5; adenocarcinoma of lung, 1/3; large cell carcinoma, 0/1; colon adenocarcinoma 10/20). The mechanisms that regulate fibroblast activation and their accumulation in cancer are not fully understood. Kalluri and Zeisberg (2006) showed in their review that it is conceivable that fibroblasts might serve as novel therapeutic targets. Such therapies can be given alone or in combination with chemotherapy, radiation or surgery. Fibroblast-directed therapy can be envisioned as either to ablate or to normalize the cancer-associated fibroblasts. One such a target that has already been associated with cancer fibroblasts is fibroblast-activating protein (FAP) (Garin-Chesa et al., 1990). A phase I dose-escalation study with sibrotuzumab (anti-FAP IgG) in patients with advanced colorectal carcinoma or non-small-cell lung carcinoma showed that sibrotuzumab specifically binds to the tumour sites with no apparent side effects (Scott et al., 2003). Further investigation on the expression of antigen 14C5 and its possible role as cancer-associated fibroblast target is necessary to fully understand the therapeutic and diagnostic potential of mAb 14C5.

To further characterize the antigen 14C5, immunohistochemical staining with mAb 14C5 was compared with αvβ5 specific staining. No discrepancy was found in the expression patterns between the two antibodies. However, staining with anti-αvβ5 was more intense, as well as non-specific staining with this antibody.

In the near future the expression of Ag 14C5 on normal tissues will be investigated in more detail. Normal epithelial, muscle, and connective tissues

that did not show staining with mAb 14C5 were skin, thyroid, parathyroid, colon, stomach, lung, uterine tube, ovary, ureter, urethra, lymph node, nerve, chondroid tissue, skeletal muscle, oesophagus, and artery (De Potter et al., 1994; Coene et al., 1997). Sometimes, low-level staining of myo-epithelial cells was observed in biopsies of breast tissue and in tubular cells of the kidney. In this study, sometimes small blood vessels and mucous secreting cells of colon tissue showed staining with mAb 14C5. According to the FDA guidelines concerning the manufacturing and testing of monoclonal antibody products for human use, 32 tissues should be tested for cross reactivity. The following tissues remain to be tested with mAb 14C5: adrenal, bladder, blood cells, bone marrow, cerebellum, cerebral cortex, endothelium, eye, heart, liver, pancreas, pituitary, placenta, prostate, spinal cord, spleen, testis, and thymus.

4.5 Conclusion

The antigen 14C5 could be an interesting new target for radioimmunodetection and radioimmunotherapy. The localization in human breast, lung and colon carcinoma tissues is high on stromal fibroblasts surrounding invasive carcinomas. Therefore, staining for the antigen 14C5 receptor offers a possible diagnostic tool in predicting the metastatic potential of malignant tumours originating in the breast, lung and colon. Further investigation is necessary to understand its possible role as cancer-associated fibroblast target. A comparison between the expression of Ag 14C5 and αvβ5, confirms studies presented in chapter 3 that αvβ5 might be the receptor of mAb 14C5. Further studies to exploit the therapeutic potential of the labeled as well as the unlabeled mAb 14C5 are warranted.

4.6 References

Asano Y, Ihn H, Yamane K, et al. Increased expression levels of integrin alphavbeta5 on scleroderma fibroblasts. Am J Pathol. 2004;164:1275-92.

Boyle P, Ferlay J. Cancer incidence and mortality in Europe, 2004. Ann Oncol. 2005;16:481-8.

Carter P, Smith L, Ryan M. Identification and validation of cell surface antigens for antibody targeting in oncology. Endocr Relat Cancer. 2004;11:659-87.

Coene E, Schelfhout AM, De Ridder L, De Potter CR. Generation of a monoclonal antibody directed against a human cell substrate adhesion molecule and the expression of the antigen in human tissues. Hybridoma 1997;16:77-83.

De Potter CR, Schelfhout AM, De Smet FH, et al. A monoclonal antibody directed against a human cell membrane antigen prevents cell substrate adhesion and tumor invasion. Am J Pathol 1994;144:95-103.

Gambhir SS, Czernin J, Schwimmer J, Silverman DH, Coleman RE, Phelps MEJ. A tabulated summary of the FDG PET literature. J Nucl Med 2001;42:1S-93S.

Garin-Chesa P, Old LJ, Rettig WJ. Cell surface glycoprotein of reactive stromal fibroblasts as a potential antibody target in human epithelial cancers. Proc Natl Acad Sci U S A. 1990;87:7235-9.

Goldenberg DM. Targeted therapy of cancer with radiolabeled antibodies. J Nucl Med 2002;43:693-713.

Gridelli C. Targeted therapies in the treatment of non small cell lung cancer: reality and hopes. Curr Opin Oncol 2004;16:126-9.

Kalluri R, Zeisberg M. Fibroblasts in cancer. Nat Rev Cancer. 2006;6:392-401.

Kemperman H, Wijnands YM, Roos E. alphaV Integrins on HT-29 colon carcinoma cells: adhesion to fibronectin is mediated solely by small amounts of alphaVbeta6, and alphaVbeta5 is codistributed with actin fibers. Exp Cell Res. 1997;234:156-64.

Kerr JS, Slee AM, Mousa SA. The alpha v integrin antagonists as novel anticancer agents: an update. Expert Opin Investig Drugs. 2002;11:1765-74.

Leavesley DI, Ferguson GD, Wayner EA, et al. Requirement of the integrin beta 3 subunit for carcinoma cell spreading or migration on vitronectin and fibrinogen. J Cell Biol. 1992;117:1101-7.

Maione P, Rossi A, Airoma G, Ferrara C, Castaldo V, Gridelli C. The role of targeted therapy in non-small cell lung cancer. Crit Rev Oncol Hematol 2004;51:29-44.

Meyer T, Marshall JF, Hart IR. Expression of alphav integrins and vitronectin receptor identity in breast cancer cells. Br J Cancer. 1998;77:530-6.

Mizejewski GJ. Role of integrins in cancer: survey of expression patterns. Proc Soc Exp Biol Med. 1999 Nov;222(2):124-38.

Scott AM, Wiseman G, Welt S, et al. A Phase I dose-escalation study of sibrotuzumab in patients with advanced or metastatic fibroblast activation protein-positive cancer. Clin Cancer Res. 2003;9:1639-47.

Wayner EA, Orlando RA, Cheresh DA. Integrins alpha v beta 3 and alpha v beta 5 contribute to cell attachment to vitronectin but differentially distribute on the cell surface. J Cell Biol. 1991;113:919-29.

Wehrle-Haller B, Imhof BA. Integrin-dependent pathologies. J Pathol. 2003;200:481-7.

Chapter 5

IN VITRO AND IN VIVO TARGETING PROPERTIES OF IODINE-123 OR IODINE-131 LABELED MONOCLONAL ANTIBODY 14C5 IN A NON-SMALL CELL LUNG CANCER AND COLON CARCINOMA MODEL

Burvenich I, Schoonooghe S, Cornelissen B, Blanckaert P, Coene E, Cuvelier C, Mertens N and Slegers G

Clin Can Res **2005**;11:7288-96

5.1 Introduction

An important future role of mAb 14C5 may lie in the ability of this antibody to prevent the spread of tumour cells in the patient's body. MAb 14C5 recognizes an epitope at the extracellular domain of a membrane antigen, which plays a role in cell substrate adhesion. This could be deduced from the inhibition of adhesion of SK-BR-3 and MCF-7 breast cancer cells to culture plastic, pronectin-, osteopontin-, and vitronectin-coated wells (De Potter et al., 1994). The inhibition on fibronectin-coated wells was weaker. In addition, a confrontation experiment with precultured embryonic heart fragments showed that the cell substrate adhesion of breast cancer cells could be inhibited or at least delayed (De Potter et al., 1994; Coene et al., 1997).

The localization of antigen (Ag) 14C5 in human breast, lung and colon carcinoma tissues is often high on stromal fibroblasts surrounding invasive carcinomas. Some studies have indicated that activated fibroblasts play a role at the initiation of cancer, as well as in the progression and in metastasis. Therefore these cancer associated fibroblasts might serve as targets for fibroblast-targeted therapy (Kalluri and Zeisberg, 2006). MAb 14C5 may offer a new tool for radioimmunodetection (RID) and radioimmunotherapy (RIT) of these fibroblasts. ^{123}I-labeled mAb 14C5 could be used for tumour diagnosis or to evaluate chemotherapy response (RID), whereas ^{131}I-labeled mAb 14C5 could be used to ablate primary tumour cells, metastatic cells and possibly cancer-associated fibroblasts (RIT).

Lahorte et al.(2004) reported on the radioiodination of mAb 14C5 with ^{123}I. High radiochemical yields and purities were obtained, while maintaining good *in vitro* and *in vivo* stability, as well as *in vitro* binding properties. In this study, the targeting properties of radioiodinated mAb 14C5 with A549 lung and LoVo colon cells will be explored. *In vitro*, binding properties of ^{125}I-labeled mAb 14C5 will be examined with both A549 and LoVo cells. *In vivo*,

biodistribution and gamma camera imaging studies are shown with respectively ^{131}I- and ^{123}I-labeled mAb 14C5.

5.2 Materials and methods

5.2.1 Antibodies

The 14C5 antibody-producing hybridoma cells produced mAb 14C5 in Integra CL 350 flasks (Elscolab, Kruibeke, Belgium) containing protein-free hybridoma medium (Invitrogen, Merelbeke, Belgium). MAb 14C5 was protein G purified (Amersham Biosciences Europe, Roosendaal, the Netherlands) from concentrated supernatant and dialyzed against PBS (pH 7.4). The purity of the antibody was evaluated by SDS-PAGE using reducing and non-reducing conditions. The anti-integrin β_1 mAb, anti-α1, anti-α2, and anti-α3 IgG1 (Millipore, Belgium) were used for comparison or as a control for nonspecific binding in biodistribution studies.

5.2.2 Cell lines

LoVo cells were a kind gift of J&J Pharmaceutical Research & Development (Beerse, Belgium). A549 cells were obtained from the Laboratory of Tumor and Developmental Biology (University of Liège, Belgium). All cell lines were cultured in standard medium with supplements according to the American Type Culture Collection (Manassas, VA) recommendations. All cells were cultured at 37 °C in a 5% CO_2 humidified incubator and passaged with 0.05% trypsin-0.02% EDTA.

5.2.3 Radioiodination and quality control

MAb 14C5, anti-integrin β1, anti-α1, anti-α2, and anti-α3 IgG1 were labeled with ^{123}I, ^{125}I, or ^{131}I. Isotopes were obtained from Bristol-Myers Squibb (Brussels, Belgium). Radioiodination was done using the Iodo-Gen method (Fraker and Speck, 1978). Coating of the Iodo-Gen iodination reagent was

done according to the manufacturer's instructions (Perbio, Erembodegem, Belgium).

For radioiodination, iodide and mAb 14C5 dissolved in 0.1 mol/l potassium phosphate buffer (pH 8.5) were added to an Iodo-Gen-coated reaction vial for 10 minutes at room temperature. Protein-bound iodine was separated from free iodide by passing over a PD-10 column (Amersham Biosciences Europe) equilibrated with PBS-1% BSA. Quality control of radiolabeled antibody was done by size exclusion high-performance liquid chromatography using an Ultrahydrogel 120 6-µm column (7.8 × 300 mm GPC; Waters, Brussels, Belgium) and 0.01 mol/l potassium phosphate buffer (pH 7.4) eluant at a flow rate of 0.8 ml/min. Stability of the radiolabeled antibodies in PBS at 4°C or in murine serum (50% in PBS) was analysed by iTLC and 50 mmol/l citric acid as eluant at 2 h, 15 h, 24 h and 48 h after radiosynthesis.

5.2.4 Saturation binding study

Saturation binding studies were done with ^{125}I-labeled mAb 14C5 using LoVo and A549 cells. Twelve test solutions (in duplicate), containing increasing amounts of radiolabeled mAb 14C5 and 0.5 x 10^6 cells in a total volume of 3 ml cell medium were incubated at 4°C for 2.5 hours. Then, supernatant was removed by centrifugation (8 minutes, 180 × g, 4°C) and cells were washed with 3 ml ice-cold PBS. For each sample, nonspecific binding was determined in the presence of 167 nmol/l of the unlabeled mAb 14C5. Radioactivity was counted by a gamma counter (Cobra II, Perkin-Elmer, Jügesheim, Germany). K_d values were determined with Graphpad Prism 3.1 software (San Diego, CA).

5.2.5 In vivo studies

5.2.5.1 Animal model

Male athymic mice (*nu/nu*; 5 weeks; Charles River, Brussels, Belgium) were injected s.c. into the right flank with A549 or LoVo cells (1×10^7) in 200 µl fetal bovine serum-free medium. When tumours achieved a size of 0.5 to 1 g (i.e., after 3 weeks for A549 tumours and 5 weeks for LoVo tumours), biodistribution studies were initiated. Male NMRI mice (5 weeks) were obtained from an in-house breeding program. All animal studies are in agreement with the Belgian laws and approved by the local ethical committee for animal experiments (ECP 02/54).

5.2.5.2 Biodistribution studies

Biodistribution studies were done with athymic mice bearing A549 (0.648 ± 0.469 g) or LoVo (0.888 ± 0.468 g) tumours or with non-tumour-bearing NMRI mice. Mice were injected in the tail vein with 5 to 10 µCi ^{131}I-labeled mAb 14C5 (2.5-5 µg). Typically, groups of three were sacrificed at 1, 3, 6, 24, 48, and 168 h after injection of radiolabeled antibody. Tumours and organs (brain, heart, liver, spleen, kidney, lung, intestine, muscle, blood, and stomach) were immediately removed, blotted dry, and weighed. Samples were counted in a gamma counter (Cobra II). Standards prepared from the injected tracer material were counted each time with tissues and tumours, enabling calculations to be corrected for physical decay of the isotope. Radiolabeled antibody distribution over time was expressed as the percentage of injected dose per gram [%ID/g; (counts/min tissue sample per counts/min standard) × 100 / weight (g)] and as tumour-to-blood ratios.

5.2.5.3 Planar gamma camera imaging

Scintigraphic imaging was done on LoVo and A549 tumour-bearing mice on a Toshiba GCA-9300A/hg single photon emission computed tomography camera

in the planar mode equipped with a low-energy high-resolution parallel-hole collimator. At 30 minutes, 6 hours, 24 hours and 48 hours after injection of 500 µCi of ^{123}I-labeled antibody (20 µg), 10-min images were acquired in a 1,024 × 1,024-pixel matrix (field of view, 23.5 × 12.46 cm) with a photopeak window set at 15% around 159 keV. Animals were anesthetized by i.p. injection of 75 µl (1.5 mg) of a pentobarbital solution (Nembutal, 20 mg/ml, Ceva Santé Animale, Brussels, Belgium).

5.2.6 Statistical analysis

A nonparametric Mann-Whitney test was used for comparison.

5.3 Results

5.3.1 Radioiodination and quality control

The radioiodination yield for mAb 14C5 and anti-integrin control antibodies (β1, α1, α2, and α3) was typically 70% to 80%. The amounts of free iodide (^{125}I, ^{123}I, or ^{131}I) in the purified iodinated mAb 14C5 was <2% and <5% for anti-integrin antibodies (β1, α1, α2, and α3) even after 24 hours at room temperature.

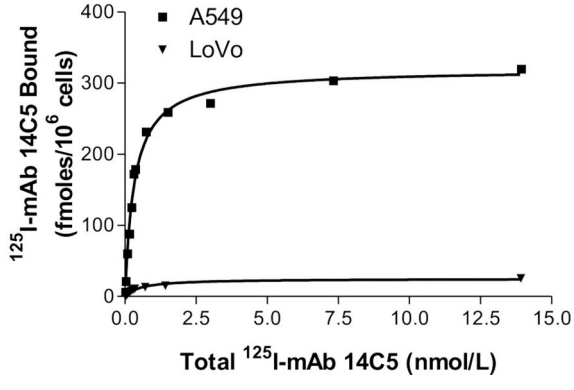

Fig. 5.1. Saturation binding of ^{125}I-labeled mAb 14C5 to A549 or LoVo cells. Increasing concentrations of ^{125}I-labeled mAb 14C5 were incubated with 0.5 x 10^6 cells at 4°C for 2.5 hours. Bound activity was isolated by centrifuging the cells and washing them twice with ice-cold PBS buffer.

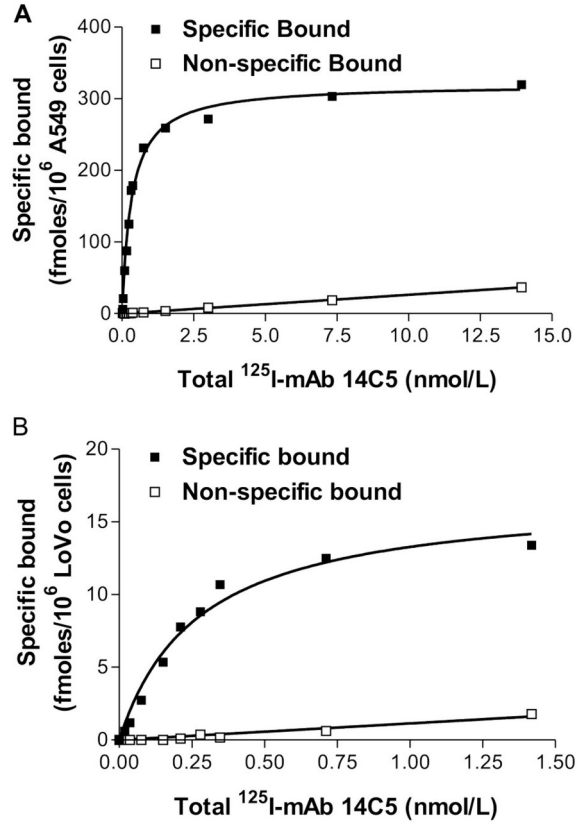

Fig. 5.2. Saturation binding of ^{125}I-labeled mAb 14C5 to A549 (*A*) and LoVo cells (*B*). Increasing concentrations of ^{125}I-labeled mAb 14C5 were incubated with 0.5 x 10^6 cells at 4°C for 2.5 h. Non-specific binding was determined in the presence of 167 nmol/l unlabeled mAb 14C5.

5.3.2 Affinity properties

The dissociation constant (K_d) of the radiolabeled mAb 14C5 was determined for A549 and LoVo cell lines by a saturation binding assay. Figure 5.1 shows the saturation plot of ^{125}I-labeled mAb 14C5 to A549 and LoVo cells. Under saturated conditions, A549 cells showed higher expression of antigen 14C5 than LoVo (Bmax 319.4 ± 7.8 and 16.9 ± 1.1 fmoles/10^6 cells) , which agrees with the results previously obtained by flow cytometric analysis also showing higher expression of Ag 14C5 in A549 cells compared with LoVo cells. Figure 5.2 shows the nonspecific binding of ^{125}I-labeled mAb 14C5 to A549 and LoVo. Nonspecific binding was determined in the presence of 167 nmol/l

unlabeled mAb 14C5. MAb 14C5 bound to A549 and LoVo cells with similar affinity (K_d 0.19 ± 0.07 and 0.20 ± 0.05 nmol/l). The saturation binding curves generated were characteristics of high affinity binding of an antibody to its antigen and merits further evaluation of the radiolabeled mAb 14C5 in a tumour model.

5.3.3 Biodistribution

LoVo cells with a low antigen 14C5 expression were compared with A549 cells with a high expression in a tumour model for the *in vivo* evaluation of ^{131}I-labeled mAb 14C5. In a first series of experiments, pharmacokinetic properties of ^{131}I-labeled mAb 14C5 were studied in mice bearing a LoVo tumour versus untreated NMRI mice. All tissues of LoVo-bearing mice, except for the stomach, showed significantly lower accumulation of ^{131}I-labeled mAb 14C5 than tissues of NMRI mice (Fig. 5.3).

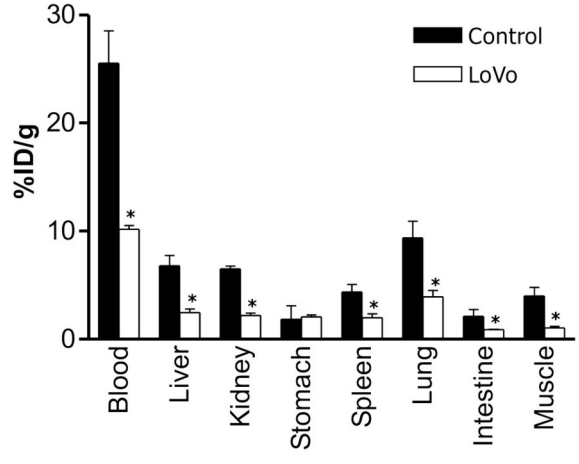

Fig. 5.3. Biodistribution of 5 to 10 µCi ^{131}I-labeled mAb 14C5 (2.5-5 µg) at 24 hours after injection in NMRI mice without tumour (control; filled columns) and nude mice bearing a LoVo colon tumour (LoVo; open columns). Columns, mean %ID/g (n = 3); *bars*, SD. *, P < 0.05, significant differences between control and mice bearing a tumour.

After 24 h, 9 %ID/g accumulated in the LoVo tumours. This tumour uptake is reflected in a decrease in radioactivity in the blood pool and other organs in the tumour-bearing mice (LoVo) compared with the non-tumour-bearing NMRI

mice (control; Fig. 5.3). The low accumulation of radioactivity in the stomach indicates a low dehalogenation of the tracer.

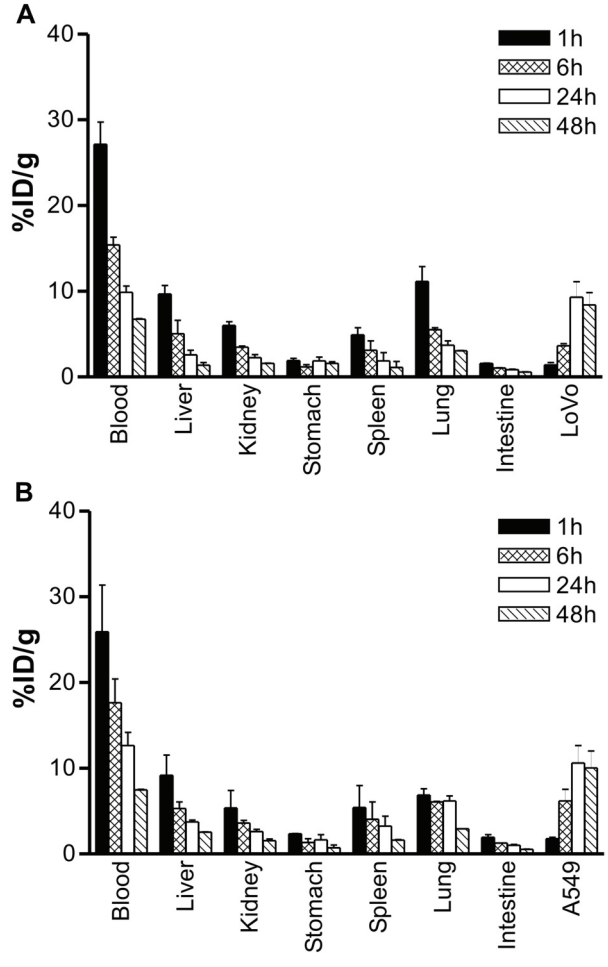

Fig. 5.4. Biodistribution of 5 to 10 µCi ^{131}I-labeled mAb 14C5 (2.5-5 µg) in nude mice bearing A549 (*A*) or LoVo (*B*) tumours at 1, 6, 24 and 48 hours after injection. Columns, mean %ID/g normal tissues and tumours; *bars*, SD (n = 3).

The biodistribution of ^{131}I-labeled mAb 14C5 in the normal organs showed no significant differences between mice bearing either A549 or LoVo tumours (Fig. 5.4). The highest tumour uptake was observed within A549 tumours at 24 hours after injection (10.4 ± 0.8%ID/g, n = 5), but was not significantly higher than LoVo tumours (9.3 ± 0.8%ID/g, n = 5) at 24 hours after injection (Fig. 5.5).

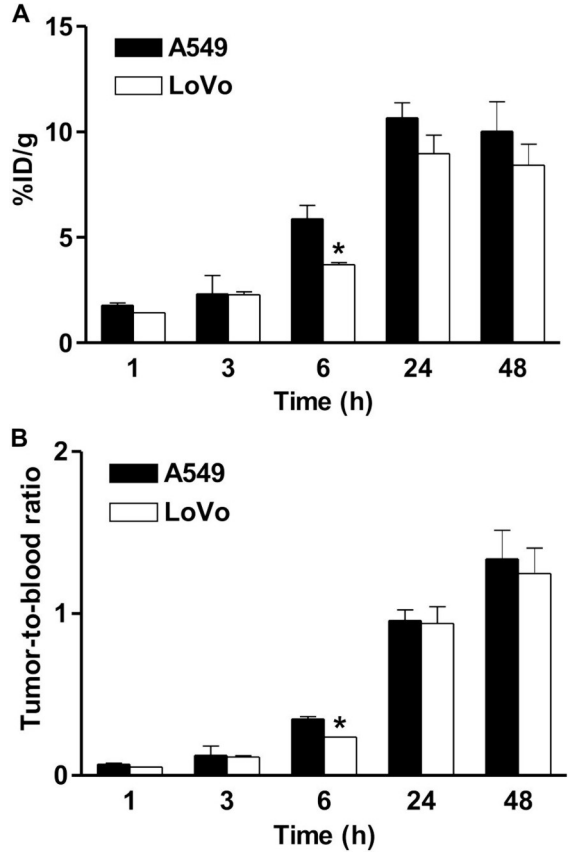

Fig. 5.5. Tumour uptake (*A*) and tumour-to-blood ratios (*B*) of ^{131}I-labeled mAb 14C5 in nude mice bearing an A549 lung tumour or a LoVo colon tumour at 1, 3, 6, 24 and 48 h after injection. The data are expressed as the mean percentages of injected dose per gram of normal tissues and tumours; *bars*, SD (n = 3). *, data showing significant differences between A549 or LoVo tumour ($P < 0.05$).

Radioactive counts varied greatly with tumour size, whereas tumour-to-blood ratios showed less variation with tumour size. To investigate the factors influencing the antibody pharmacokinetics of ^{131}I-labeled mAb 14C5, the tumour uptake of mAb 14C5 versus an irrelevant anti-integrin β1 antibody in relation to the tumour mass was studied. To reduce the number of animals needed, we focused this experiment on mice bearing A549 lung tumours.

The biodistribution results of 13 mice with tumour masses varying from 0.027 to 1.9 g are shown in Fig. 5.6A. As a control, tumour uptake of the irrelevant

IgG1 anti-integrin β1 was measured in five mice bearing tumours varying from 0.053 to 1.2 g. Figure 5.6A shows a high dependency of tumour uptake on tumour mass (the smaller the tumour, the higher the uptake), whereas no such relation was seen with the nonspecific control IgG1.

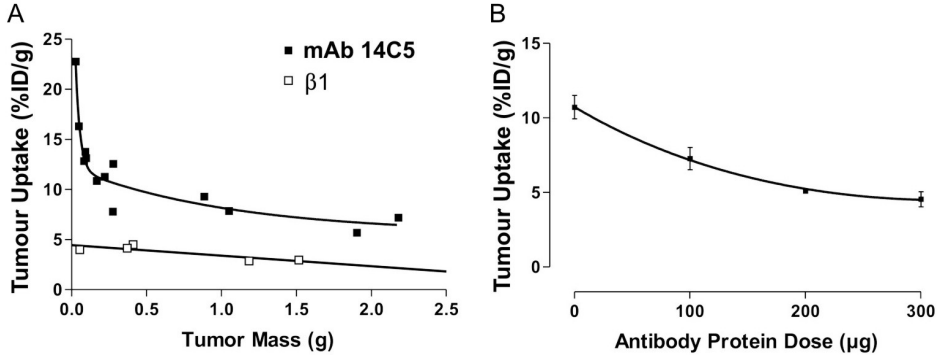

Fig. 5.6. Factors influencing antibody pharmacokinetics of mAb 14C5 in A549 tumour-bearing mice. (*A*) Tumour uptake of tumour-specific antibody, mAb 14C5, vs. an irrelevant anti-β1 antibody in relation to tumour mass at 24 h p.i. (*B*) Antibody accumulation in the A549 tumour (%ID/g at 24h p.i.) in relation to protein dose. Tumour weights used varied between 0.5 and 1 g. All mice were injected with 1 µg of radiolabeled mAb 14C5, supplemented with unlabeled mAb 14C5 to yield the protein amounts indicated.

In a second experiment, the antibody accretion in the tumour (%ID/g at 24 hours after injection) in relation to the cold mAb 14C5 protein dose was investigated. Mice were injected with 1 µg radiolabeled mAb 14C5 supplemented with an increasing amount of unlabeled mAb 14C5. Figure 5.6B shows that when 300 µg of unlabeled mAb 14C5 is added, the uptake of ^{131}I-labeled 14C5 at 24 hours after injection is decreased from 10% to 5%ID/g. This indicates the specific uptake of mAb 14C5.

5.3.4 Imaging

The planar gamma camera images of tumour-bearing mice at different time intervals post injection of ^{131}I-labeled mAb 14C5 are shown in Fig. 5.7A-D (1, 6, 24, and 48 hours, respectively). Tumours were visible within 6 hours after

tracer injection in both LoVo and A549 tumour models (Fig. 5.7B). The tumour-to-background contrast improved at later time points (Fig. 5.7C and D).

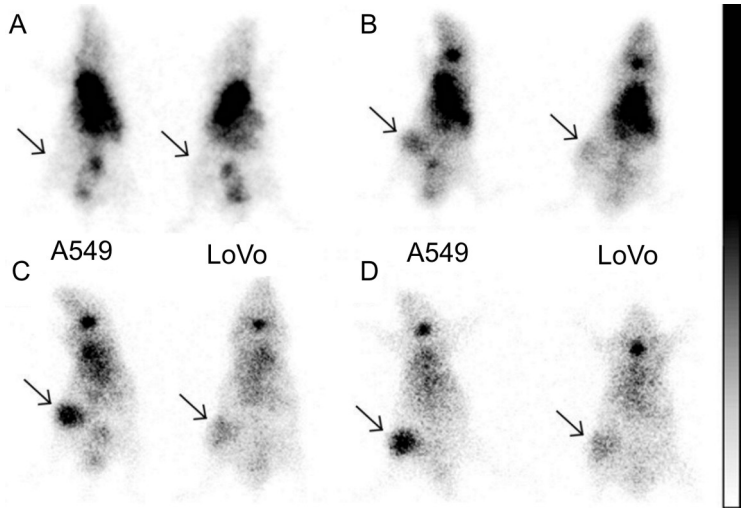

Fig. 5.7. Whole-body planar gamma images of 500 µCi ^{123}I-labeled mAb 14C5 (20 µg) in mice bearing a LoVo or an A549 tumour (arrows). Images were taken at 30 minutes *(A)*, 6 hours *(B)*, 24 hours *(C)* and 48 hours *(D)* after injection of radiolabeled mAb 14C5.

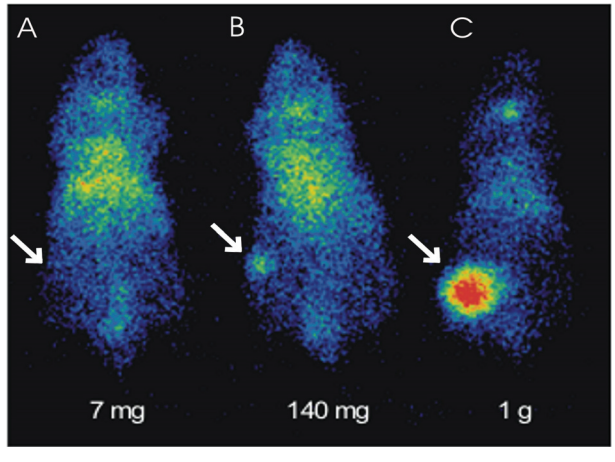

Fig. 5.8. Influence of tumour mass on the visibility of A549 tumours with planar gamma imaging. Whole-body planar gamma images were taken of three mice bearing an A549 tumour (arrows) with different size (*A*, 7 mg; *B*, 140 mg; *C*, 1 g) at 24 hours after injection of 500 µCi ^{123}I-labeled mAb 14C5 (20 µg).

As background value, a region of interest was drawn round the contralateral flank. Highest tumour-to-flank ratios were obtained at 48 hours after injection. (A549 5.2 ± 1.8 and LoVo 2.0 ± 0.3: $n = 3$) for tumours weighing 1.3 ± 0.2 g.

The planar imaging results varied greatly with tumour size as seen in the biodistribution data. Figure 5.8 shows the influence of tumour size on the visibility of A549 tumours at 48 hours after injection. A549 tumours in the right flank of nude mice, as small as 0.140 g (6 × 7 mm), could be clearly visualized.

5.4 Discussion

The targeting properties of mAb 14C5 bound to ^{123}I and ^{131}I in nude mice bearing an A549 lung or a LoVo colon tumour were investigated. In RID and RIT, high-affinity binding with a long residence time on the specific target antigen is considered to be one of the most important properties of antibodies for achieving efficient tumour targeting. Although mAb 14C5 has not yet been evaluated in a clinical phase, the results in this chapter concerning the targeting properties of the ^{123}I- and ^{131}I-labeled antibody 14C5 are promising. The high affinity of mAb 14C5 for LoVo (K_d 0.20 ± 0.05 nmol/l) and A549 (K_d 0.19 ± 0.07 nmol/l) and the ubiquitous expression of the antigen 14C5 in human cancer cell lines provide a potentially useful antibody for radioimmunodetection and radioimmunotherapy.

The high antigen 14C5-expressing A549 lung tumours and even the low antigen 14C5-expressing LoVo colon tumours showed good tumour uptake with ~10 %ID/g tumour tissue at 24 hours after injection. This finding is in agreement with other high-affinity antibodies that bind effectively both high- and low-density antigen, whereas a low-affinity antibody only binds appreciably to high-density antigen because of its requirement for divalent attachment (Zuckier et al., 2000). This uptake is high enough to merit further evaluation in therapeutic trials (Behr et al., 2000; Clarke et al., 2000; Smith-Jones et al., 2000; Zuckier et al., 2000; Popkov et al., 2001; Smith-Jones et al., 2003). Via planar gamma camera imaging, A549 lung tumours as well as the LoVo colon tumours could be clearly visualized when tumours weighed ~1 g.

Even when A549 lung tumours were as small as 0.14 g, they were still clearly visible by planar gamma camera imaging.

These results are encouraging, although modifications to mAb 14C5 are still possible to improve the targeting properties in patients. Many articles report on modifications that retain specificity but alter pharmacokinetics, involving the development of fragments of antibodies (e.g., $F(ab')_2$, Fab, and scFv; refs. Goldenberg, 2002; Winthrop et al., 2003; Adams et al., 2004) or recombinant multivalent antibodies (Goel et al., 2000; Schoonjans et al., 2000; Reff and Heard, 2001; Todorovska et al., 2001, Power et al., 2003; Olafsen et al., 2004). Also, the development of humanized antibodies should reduce the antigenicity of murine mAb 14C5 (Reff and Heard, 2001; Goldenberg, 2002). In addition, the choice of the radionuclide can be beneficial for radioimmunodetection and radioimmunotherapy. Development of radiolabeled mAb 14C5 with ^{99m}Tc or ^{111}In compared with ^{123}I for radioimmunodetection and ^{90}Y, ^{177}Lu or ^{186}Re compared with ^{131}I for radioimmunotherapy could result in higher tumour uptake and therefore better tumour-targeting properties of radiolabeled mAb 14C5 (Adams et al., 2004; Koppe et al., 2004).

5.5 Conclusion

The antigen 14C5 could be an interesting new target for radioimmunodetection and radioimmunotherapy. Therefore targeting properties of radioiodinated mAb 14C5 were investigated in this study. Radioiodinated mAb binds its antigen with high affinity. Tumour uptake in mice bearing an A549 lung tumour or a LoVo colon tumour was high and specific. Antibody fragments and other radioisotopes than iodide can improve targeting properties of mAb 14C5 and therefore must be further explored. Furthermore, because antigen 14C5 is highly expressed on a variety of tumour cells, it offers great potential for a variety of cancer therapies, including non-small cell lung cancer and colon

carcinoma. Therefore, further studies to exploit the therapeutic potential of the labeled as well as the unlabeled mAb 14C5 are warranted.

5.6 References

Adams GP, Shaller CC, Dadachova E et al. A single treatment of yttrium-90-labeled CHX-A"-C6.5 diabody inhibits the growth of established human tumor xenografts in immunodeficient mice. Cancer Res 2004;64:6200-6.

Behr TM, Blumenthal RD, Memtsoudis S, et al. Cure of metastatic human colonic cancer in mice with radiolabeled monoclonal antibody fragments. Clin Cancer Res 2000;6:4900-4907.

Clarke K, Lee FT, Brechbiel MW, et al. Therapeutic efficacy of anti-Lewis(y) humanized 3S193 radioimmunotherapy in a breast cancer model: enhanced activity when combined with taxol chemotherapy. Clin Cancer Res. 2000;6:3621-8.

Coene E, Schelfhout AM, De Ridder L, et al. Generation of a monoclonal antibody directed against a human cell substrate adhesion molecule and the expression of the antigen in human tissues. Hybridoma 1997;16:77-83.

De Potter CR, Schelfhout AM, De Smet FH, et al. A monoclonal antibody directed against a human cell membrane antigen prevents cell substrate adhesion and tumor invasion. Am J Pathol 1994;144:95-103.

Fraker PJ, Speck JC Jr. Protein and cell membrane iodinations with a sparingly soluble chloroamide,1,3,4,6-tetrachloro-3a,6a-diphrenylglycoluril. Biochem Biophys Res Commun 1978;80:849-57.

Goel A, Colcher D, Baranowska-Kortylewicz J, et al. Genetically engineered tetravalent single-chain Fv of the pancarcinoma monoclonal antibody CC49: improved biodistribution and potential for therapeutic application. Cancer Res 2000;60:6964-71.

Goldenberg DM. Targeted therapy of cancer with radiolabeled antibodies. J Nucl Med 2002;43:693-713.

Kalluri R, Zeisberg M. Fibroblasts in cancer. Nat Rev Cancer. 2006;6:392-401.

Koppe MJ, Bleichrodt RP, Soede AC et al. Biodistribution and therapeutic efficacy of (125/131)I-, (186)Re-, (88/90)Y-, or (177)Lu-labeled monoclonal antibody MN-14 to carcinoembryonic antigen in mice with small peritoneal metastases of colorectal origin. J Nucl Med 2004;45:1224-32.

Lahorte CM, Bacher K, Burvenich I, et al. Radiolabeling, biodistribution, and dosimetry of (123)I-mAb 14C5: a new mAb for radioimmunodetection of tumor growth and metastasis in vivo. J Nucl Med 2004;45:1065-73.

Olafsen T, Tan GJ, Cheung CW, et al. Characterization of engineered anti-p185HER-2 (scFv-CH3)2 antibody fragments (minibodies) for tumor targeting. Protein Eng Des Sel 2004;17:315-23.

Popkov M, Sidrac-Ghali S, Lusignan Y, et al. Inhibition of tumour growth and metastasis of human fibrosarcoma cells HT-1080 by monoclonal antibody BCD-F9. Eur J Cancer 2001;37:2484-92.

Power BE, Doughty L, Shapira DR, et al. Noncovalent scFv multimers of tumor-targeting anti-Lewis(y) hu3S193 humanized antibody. Protein Sci 2003;12:734-47.

Reff ME, Heard C. A review of modifications to recombinant antibodies: attempt to increase efficacy in oncology applications. Crit Rev Oncol Hematol 2001;40:25-35.

Schoonjans R, Willems A, Schoonooghe S, et al. Fab chains as an efficient heterodimerization scaffold for the production of recombinant bispecific and trispecific antibody derivatives. J Immunol 2000;165:7050-7.

Smith-Jones PM, Vallabahajosula S, Goldsmith SJ, et al. In vitro characterization of radiolabeled monoclonal antibodies specific for the extracellular domain of prostate-specific membrane antigen. Cancer Res 2000;60:5237-43.

Smith-Jones PM, Vallabhajosula S, Navarro V, et al. Radiolabeled monoclonal antibodies specific to the extracellular domain of prostate-specific membrane antigen: preclinical studies in nude mice bearing LNCaP human prostate tumor. J Nucl Med 2003;44:610-7.

Todorovska A, Roovers RC, Dolezal O, et al. Design and application of diabodies, triabodies and tetrabodies for cancer targeting. J Immunol Methods 2001;248:47-66.

Winthrop MD, DeNardo SJ, Albrecht H, et al. Selection and characterization of anti-MUC-1 scFvs intended for targeted therapy. Clin Cancer Res 2003;9:3845S-53S.

Zuckier LS, Berkowitz EZ, Sattenberg RJ, et al. Influence of affinity and antigen density on antibody localization in a modifiable tumor targeting model. Cancer Res 2000;60:7008-13.

Chapter 6

BIODISTRIBUTION AND PLANAR GAMMA CAMERA IMAGING OF IODINE-123 OR IODINE-131 LABELED F(ab')$_2$ AND Fab FRAGMENTS OF MONOCLONAL ANTIBODY 14C5 IN A NON-SMALL CELL LUNG CANCER MODEL

Burvenich I, Schoonooghe S, Blanckaert P, Bacher C, Coene E, Mertens N, De Vos F and Slegers G

Nuc Med Biol **2007**, *accepted for publication*

6.1 Introduction

Prior work has demonstrated that ^{125}I-labeled monoclonal antibody (mAb) 14C5 binds its antigen with high affinity (A549, K_d 0.19 ± 0.07 nmol/l; LoVo, K_d 0.20 ± 0.05 nmol/l) and tumours as small as 0.14 g could be clearly visualized by planar gamma imaging when using ^{123}I-labeled mAb 14C5. However, the highest tumour-to-blood ratio (~ 3.0) was obtained only 168 hours after injection (Burvenich et al., 2005).

Compared to the use of ^{123}I and ^{131}I, ^{99m}Tc has some advantages: its ready availability, short physical half-life ($t_{½}$, 6 h) and ideal γ energy (140 keV) (Zalutsky and Lewis, 2003). Intact monoclonal antibodies (~150 kDa) show rather slow antibody kinetics. As a result, short-lived radionuclides (e.g. SPECT, ^{99m}Tc ($t_{½}$, 6 h); PET, ^{18}F ($t_{½}$, 1.8 h)) fall beyond imaging possibilities for radioimmunodetection when using intact antibodies. Also, the slow kinetics of intact mAbs limits their use in radioimmunotherapy (RIT). Their long persistence in circulation exhibits toxic radiation to normal tissues with limited quantities delivered to the tumours (Carter, 2006). Furthermore, intact mAbs show poor diffusion from the vasculature into and through the tumour (Jain, 1987; Goel et al., 2000). While micrometastases offer an interesting target for RIT, these lesions often show high interstitial pressure and low vascularization, in which only low sensitivities have been observed (Bock et al. 1992; Vijayakumar et al. 1993, Goldenberg et al. 2002). Another problem when using a murine mAb is that patients frequently develop an immune response to these murine proteins in the form of human anti-mouse antibodies (HAMA). In the worst case, this response leads to serious allergic hypersensitivity, but at best limits antibody efficacy by resulting in very rapid clearance. A gradual decrease in half-life with repeated dosage of injected murine antibodies has been demonstrated, limiting the use of multiple doses in RIT (Maynard and Georgiou, 2000).

To minimize these limitations of intact mAbs, many efforts of various groups have been undertaken in increasing the tumour-to-background ratio, tumour penetration and lowering HAMA response. A common approach is the development of smaller antibody fragments and genetically engineered single-chain Fv (scFv) constructs of antibody molecules (Reff, 2001; Goldenberg, 2002; Batra et al., 2002). The evaluation of the enzymaticly derived Fab and $F(ab')_2$ fragments may be useful to evaluate the potential of 14C5 mAb-derived fragments. Indeed, enzymaticly derived bivalent $F(ab')_2$ and monovalent Fab fragments have shown promising tumour penetration and good therapeutic results in animal (Wahl et al., 1983; Sharkey et al., 1990; Hansen et al., 1990; Blumenthal et al., 1992; Behr et al., 2000) and clinical studies (Murray et al., 1994; Willkomm et al., 2000; Libutti et al., 2001; Goldenberg, 2002). Disadvantages seen with these fragments are lower tumour uptake and high renal uptake particularly when a radiometal is used, which raises concern for renal toxicity. However, studies have shown that a high predose of cationic amino acids (e.g. L-lysine) could significantly reduce renal tubular reabsorption of radiometal-labeled Fab (Behr et al, 1995; Behr et al., 1998).

The objective of this study was to examine the biodistribution and elimination from the blood of ^{123}I-labeled Fab and $F(ab')_2$ 14C5 fragments and to compare with parental mAb 14C5 for the detection and possible therapy of non-small cell lung cancer. Additionally, we have explored the *in vitro* characteristics of ^{125}I-$F(ab')_2$ and ^{125}I-Fab fragments of mAb 14C5, i.e., their stability, specificity and affinity.

6.2 Materials and methods

6.2.1 Antibodies

The mAb 14C5 was produced and purified as described previously (Burvenich et al., 2005). Fab and F(ab')$_2$ fragments were derived from murine mAb 14C5 using the Immunopure IgG1 Fab and F(ab')$_2$ preparation kit (Perbio) according to the manufacturer's instructions. IgG and Fc fragments were removed using a protein A sepharose column (Perbio). For concentration and exchange of buffer with PBS (pH 7.4), Centricon YM-30 (Millipore) was used. Fragments were evaluated by SDS-PAGE without reduction. When purity was <90%, fragments were further purified using a HiPrep 26/60 Sephacryl S-200 HR column (GE Healthcare Europe) on an Akta purifier, with PBS as eluant (pH 7.5, 0.5 ml/min).

PH2, an irrelevant anti-muc bivalent scFv-Fab dimer (75 kDa), was used as control antibody in biodistribution studies.

6.2.2 Cell lines

A549 cells, a human lung carcinoma cell line, were obtained from the Laboratory of Tumor and Developmental Biology (University of Liège, Liège, Belgium). A549 cells were cultured in DMEM (Cambrex), containing 2 mmol/l L-glutamine (Cambrex) and 10% fetal bovine serum (Cambrex).

6.2.3 Radioiodination and quality control

Fab, F(ab')$_2$ and mAb 14C5 were labeled with ^{123}I, ^{125}I, or ^{131}I. Isotopes were obtained from Bristol-Myers Squibb. Radioiodination was performed using the Iodo-Gen method as previously described. In brief, sodium iodide and protein dissolved in 0.1 mol/l potassium phosphate buffer (pH 8.5) were added to an Iodo-Gen-coated reaction vial and reacted for 10 minutes at room temperature. Protein-bound iodine was separated from free iodide by passing over a PD-10

column (GE Healthcare Europe) equilibrated with 1% BSA in PBS. Quality control of radioiodinated protein was performed by size-exclusion high-performance liquid chromatography using a Shodex KW 802.5 column (7.8 mm × 300 mm; Thomson Instrument Company). Protein was eluted with 0.1 mol/l potassium phosphate buffer (pH 7.4) at a flow rate of 0.8 ml/min. ^{125}I-labeled fragments were analyzed by SDS-PAGE followed by phosphor imager analysis for integrity. Samples of 2 µCi labeled protein were loaded on SDS-PAGE, and SDS-PAGE gel was exposed to MultiSensitive Phosphor Screens (medium) for 5 minutes. In order to assess *in vitro* stability, radioiodinated fragments were incubated for 24 hours at 4°C in PBS with 1% BSA or at 37°C in PBS with 50% mouse serum in PBS. Samples were taken periodically for iTLC analysis (ITLC SG strips, Pall Corporations), using 20 mmol/l citric acid (pH 5.0) as eluant. Strips were divided in ten parts and radioactivity of each part was counted with a gamma counter (Cobra II; Perkin Elmer).

6.2.4 Saturation binding study

The affinities of ^{125}I-F(ab')$_2$ and ^{125}I-Fab were analyzed by a saturation binding assay using A549 cells. Specific activities of 1 µCi ^{125}I/µg protein were typically used. Twelve duplicate test samples containing increasing amounts of ^{125}I-F(ab')$_2$ or ^{125}I-Fab fragments and 0.5 x 10^6 A549 cells in a total volume of 2 ml cell medium were incubated at 4°C for 2.5 hours. Supernatant was removed by centrifugation (8 minutes, 180 ×g, 4°C) and cells were washed with 2 ml ice-cold PBS. Nonspecific binding was estimated in the presence of 300 nmol/l (i.e. approximately 1000-fold excess of K_d value of mAb 14C5) unlabeled mAb 14C5 for ^{125}I-F(ab')$_2$. For ^{125}I-Fab, no monovalent blocking agent was available. Therefore, nonspecific binding was not determined experimentally, but estimated by fitting total binding results using following equations: Specific = $X \times B_{max}/(K_d + X)$; Nonspecific = $NS \times X$, Y = Specific +

Nonspecific. Nonlinear regression and K_d values were determined using Graphpad Prism Software (San Diego, CA).

6.2.5 In vivo studies

6.2.5.1 Animal model

Athymic mice (*nu/nu*; female, 5 weeks; Charles River) were used for the *in vivo* biodistribution and imaging studies. A549 cells (1×10^7) were injected subcutaneously. When tumours reached a size of 0.5 to 1.0 g, approximately 3 weeks after injection, biodistribution studies were performed. All animal experiments were approved by the local ethics committee for animal experiments.

6.2.5.2 Biodistribution studies

For biodistribution studies, mice were injected in the tail vein with 5 to 10 µCi ^{131}I-labeled F(ab')$_2$ or Fab fragments (2.5-5.0 µg in 100 µl PBS). Typically, groups of three mice were sacrificed 0.02, 1, 3, 6, 24, and 48 hours after injection. Tumours and organs (brain, heart, liver, spleen, kidney, lung, intestine, muscle and stomach) were removed immediately, blotted dry and weighed. Also, a blood sample was taken. Tumour, organ and blood activities were counted in a gamma counter (Cobra II). Standards, prepared from the same tracer solution that was injected, were counted each time with tissues and tumours. Tissue radioactivity concentrations were expressed as the percentage of injected dose per gram of organ (% ID/g).

The blood clearance studies were performed in non-tumour-bearing mice (NMRI; female, 4-6 weeks old). Blood samples (30 µL, n = 3) were drawn from the tail vein at various time points following the injection of 370 kBq of ^{131}I-labeled Fab, F(ab')$_2$ or mAb 14C5. The half-lives were calculated using

SPSS 12.0 for Windows. The data for Fab, $F(ab')_2$ and IgG were analyzed by a two-phase exponential curve fit.

6.2.5.3 Planar gamma camera imaging

Planar gamma camera imaging was done on a Toshiba GCA-9300A/hg single-photon emission computed tomography camera equipped with a low-energy high-resolution parallel-hole collimator. Animals with an A549 tumour were anesthetized by intraperitoneal injection of 75 µl of a sodium pentobarbital solution (Nembutal, 20 mg/ml, Ceva Santé Animale). Images were acquired 1, 6, 24 and 48 hours after injection of 500 µCi ^{123}I-labeled $F(ab')_2$ or ^{123}I-labeled mAb 14C5 (20 µg in 200 µl PBS). Ten-minute images were obtained in a 256 × 256-pixel matrix (field of view, 23.5 × 12.46 cm) with a photopeak window set at 15% around 159 keV. For imaging of A549 tumours with 1 mCi ^{123}I-labeled Fab fragments (20 µg), 10-minute images were acquired 1, 6, 12 and 30 hours after injection.

6.2.6 Statistical analysis

Comparison between mAb 14C5 and its fragments, $F(ab')_2$ and Fab was performed using nonparametric Mann-Witney test.

6.3 Results

6.3.1 Preparation of $F(ab')_2$ and Fab fragments

The product of the ficin-treated mAb 14C5 (150 kDa) was evaluated by SDS-PAGE (Fig. 6.1A). Pure $F(ab')_2$ fragments (> 90%, ~100 kDa) were generated in the presence of 1 mmol/l cysteine after 20 h of incubation at 37°C. Highest production of Fab fragments (~50 kDa) was obtained in the presence of 10 mmol/l cysteine after 15 h of incubation at 37°C. MAb 14C5 was also run in parallel under nonreducing conditions and migrated at ~150 kDa. Fab and

F(ab')$_2$ migrated at ~50 and ~100 kDa, respectively. For Fab, purity of > 90% could only be obtained after separation of high-molecular-weight impurities (mAb and F(ab')$_2$) on a Sephacryl S-200 high-resolution column.

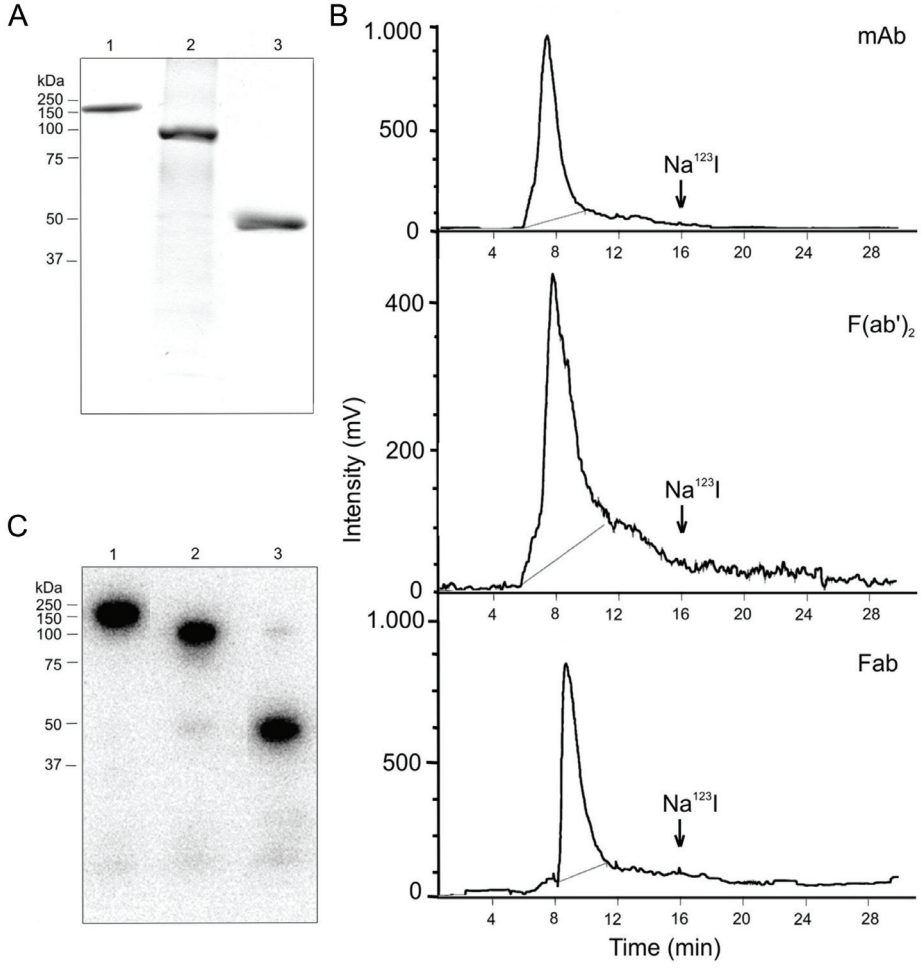

Fig. 6.1. Quality control of F(ab')$_2$ and Fab 14C5 fragments. (*A*) Gel showing Coomassie Blue R-250 staining of unlabeled mAb 14C5 (*lane* 1), F(ab')$_2$ (*lane* 2) and Fab (*lane* 3). (*B*) Quality control of ^{123}I-labeled mAb 14C5, ^{123}I-labeled F(ab')$_2$ and ^{123}I-labeled Fab was done with size-exclusion high-performance liquid chromatography using an Ultrahydrogel 120 6-µm column (7.8 × 300 mm GPC) and 0.01 mol/l potassium phosphate buffer (pH 7.4) eluant at a flow rate of 0.8 ml/min. (*C*) Phosphorescence image of ^{125}I-labeled mAb 14C5 (*lane 1*), ^{125}I-labeled F(ab')$_2$ (*lane 2*) and ^{125}I-labeled Fab 14C5 (*lane 3*) fragments.

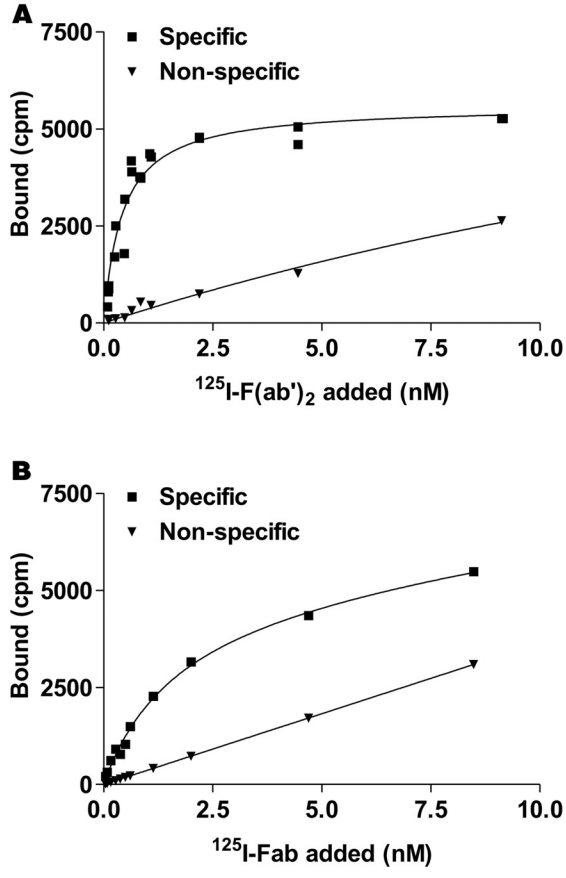

Fig. 6.2. Saturation binding of ^{125}I-F(ab')$_2$ (*A*) or ^{125}I-Fab (*B*) to A549 cells. Increasing concentrations of ^{125}I-labeled fragments were incubated with 0.5 × 10^6 cells at 4°C for 2.5 hours. For ^{125}I-F(ab')$_2$, nonspecific binding was determined in the presence of 300 nmol/L unlabeled mAb 14C5. For ^{125}I-Fab, nonspecific binding was estimated using nonlinear regression of total binding data with Graphpad.

6.3.2 Radio-iodination and Binding Capacity of ^{125}I-F(ab')$_2$ and ^{125}I-Fab 14C5

The radioiodination yield for F(ab')$_2$ and Fab fragments was typically 70-80%. ^{125}I-Radiolabeling of Fab, F(ab')$_2$ and mAb 14C5 was analyzed by ITLC, SDS-PAGE and HPLC to check the integrity of the radioiodinated molecules. The amount of free iodide (^{125}I, ^{123}I, or ^{131}I) in the purified iodinated products was < 5% as determined by HPLC (Fig. 6.1B). ^{123}I-Labeled Fab, F(ab')$_2$, and mAb

eluted at 9.1, 8.0, and, 7.5 minutes, respectively, as single peaks. Even after 48 hours at 37°C in the presence of murine serum, the amount of free iodide remained < 5% as determined with ITLC. Electrophoresis of the labeled products under nonreducing conditions and autoradiography showed the ~150-kDa protein band of mAb (Fig. 6.1C, lane 1), the ~100-kDa protein band of F(ab')$_2$ (Fig. 6.1C, lane 2) and, the ~50-kDa band of Fab (Fig. 6.1C, lane 3).
To investigate the binding capacity of iodinated fragments, the dissociation constants (K_d) of ^{125}I-labeled F(ab')$_2$ and ^{125}I-labeled Fab were estimated for A549 cells by a saturation binding assay. Figure 6.2 shows the saturation binding plots of ^{125}I-labeled F(ab')$_2$ (Fig. 6.2A) and ^{125}I-labeled Fab (Fig. 6.2B) to A549 cells. F(ab')$_2$ bound to A549 cells with higher affinity than Fab (K_d 0.37 ± 0.10 nmol/l and 2.25 ± 0.44 nmol/l, respectively; $P < 0.05$). The obtained saturation binding curves were characteristic of high-affinity specific binding of a ligand to its receptor.

6.3.3 Pharmacokinetic properties of ^{131}I-labeled mAb 14C5 and its F(ab')$_2$ and Fab fragments in NMRI mice

Figure 6.3 shows the results of the pharmacokinetic studies performed to determine the blood clearance of ^{131}I-labeled Fab, F(ab')$_2$ and intact mAb 14C5. The data were analyzed using a bi-exponential model for Fab, F(ab')$_2$ and mAb 14C5, showing an α-phase $t_{½}$ (clearance of immunoconjugates from the central compartment (blood) to the peripheral compartments) and β-phase $t_{½}$ (clearance of immunoconjugates from the blood out of the body) (Wen et al., 1999). The alpha half-life ($t_{½}\alpha$) value for Fab, F(ab')$_2$ and mAb 14C5 was 14.9, 21 and 118 min, respectively. The beta half-life $t_{½}\beta$ value for Fab, F(ab')$_2$ and mAb 14C5 was 439, 627 and 4067 min, respectively. Thus, ^{123}I-labeled Fab and F(ab')$_2$ showed markedly lower $t_{½}\alpha$ (respectively 7.9 and 5.5 times lower) and $t_{½}\beta$ (respectively 9.3 and 6.5 times lower) values than intact mAb 14C5.

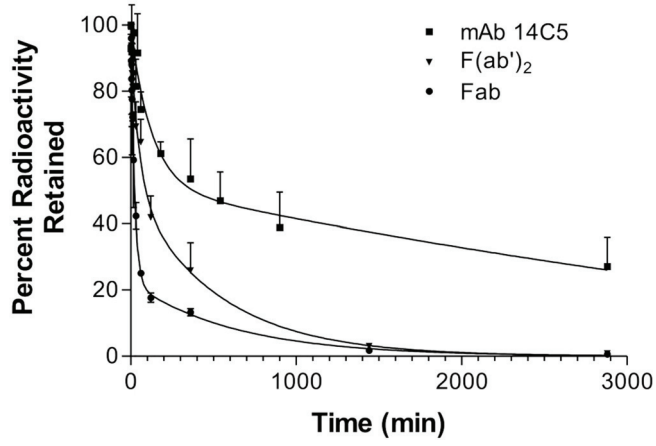

Fig. 6.3. Blood clearance of ^{131}I-labeled Fab, F(ab')$_2$ and mAb 14C5 in NMRI mice. An average of three mice per group is presented. Values are corrected for the decay of the radionuclide.

6.3.4 Biodistribution of ^{131}I-labeled mAb 14C5 and its F(ab')$_2$ and Fab fragments in Swiss nu/nu mice bearing an A549 lung tumour

Biodistribution studies were performed in athymic mice bearing A549 lung tumours. Although ^{131}I-labeled mAb 14C5 showed 10.7 ± 2.2 %ID/g in tumours at 24 h post injection, the nonspecific retention of radiolabeled mAb 14C5 in the liver, kidneys, spleen, heart, lungs and blood was higher than that of Fab and F(ab')$_2$ (Table 6.1).

The highest tumour uptake was observed for Fab as early as 3 hours after injection, after 6 hours for F(ab')$_2$, and was specific ($P < 0.05$) (Fig. 6.4). Tumour uptake (% ID/g) was highest for mAb 14C5 (10.7 ± 2.23% ID/g, $n = 5$) and lowest for Fab (2.4 ± 0.8% ID/g, $n = 3$), with an intermediate value for F(ab')$_2$ (4.7 ± 0.7% ID/g, $n = 3$). After 6 hours, uptake of fragments in all other organs (except kidneys, stomach and lung) remained significantly lower than in tumour and blood. The kidneys showed an initially high uptake of both fragments (34.3 ± 3.8 % ID/g 1 h after injection for ^{131}I-Fab, 23.9 ± 3.5% ID/g for ^{131}I-F(ab')$_2$ versus 5.6 ± 1.5 % ID/g for ^{131}I-mAb).

Tabel 6.1 Biodistribution of ^{131}I-labeled mAb 14C5, F(ab')$_2$ and Fab 14C5 (%ID/g) in athymic mice bearing an A549 tumour

	Time (h)					
Tissue	0.02	1	3	6	24	48
mAb						
Tumour	0.61 ± 0.17	1.67 ± 0.24	2.74 ± 0.65	5.35 ± 1.75	10.66 ± 2.23	9.49 ± 1.68
Blood	37.44 ± 8.97	26.32 ± 3.93	19.74 ± 2.35	16.91 ± 2.35	10.48 ± 0.95	7.25 ± 0.43
Liver	13.21 ± 2.31	9.36 ± 1.69	7.31 ± 0.97	5.23 ± 0.57	3.43 ± 0.73	2.16 ± 0.68
Kidneys	7.68 ± 2.00	5.59 ± 1.49	4.92 ± 0.72	3.57 ± 0.22	2.59 ± 0.30	1.56 ± 0.13
Intestine	0.86 ± 0.37	2.28 ± 0.40	2.46 ± 0.42	2.06 ± 0.18	1.42 ± 0.19	0.89 ± 0.05
Stomach	0.62 ± 0.19	2.21 ± 0.27	1.99 ± 1.64	1.29 ± 0.33	1.53 ± 0.19	1.00 ± 0.56
Spleen	3.07 ± 1.87	5.25 ± 0.59	4.35 ± 0.46	3.75 ± 0.54	2.60 ± 0.71	1.44 ± 0.29
Lungs	13.02 ± 9.71	8.30 ± 3.06	6.68 ± 0.93	5.89 ± 1.47	4.91 ± 1.05	2.99 ± 0.09
F(ab')$_2$						
Tumour	1.16 ± 0.35	2.30 ± 1.07	4.25 ± 1.21	4.74 ± 0.66	3.54 ± 2.10*	1.97 ± 0.66*
Blood	40.45 ± 5.05	17.92 ± 2.51	13.55 ± 3.84	8.91 ± 2.17	1.63 ± 0.78	0.56 ± 0.53
Liver	10.03 ± 0.54	5.39 ± 0.62	4.29 ± 2.02	3.07 ± 1.31	0.64 ± 0.22	0.37 ± 0.23
Kidneys	9.29 ± 3.06	23.89 ± 3.52	8.95 ± 1.78	5.51 ± 0.90	0.81 ± 0.30	0.29 ± 0.27
Intestine	1.19 ± 0.17	2.36 ± 0.18	2.89 ± 0.90	2.19 ± 0.80	0.57 ± 0.38	0.12 ± 0.07
Stomach	1.19 ± 1.07	6.26 ± 3.33	5.25 ± 3.33	5.70 ± 3.17	1.15 ± 0.14	0.20 ± 0.19
Spleen	3.09 ± 0.30	3.31 ± 0.24	3.22 ± 1.10	3.06 ± 1.70	0.46 ± 0.11	0.13 ± 0.02
Lungs	14.43 ± 3.12	6.92 ± 1.66	4.84 ± 1.31	4.00 ± 1.47	0.87 ± 0.44	0.27 ± 0.21
Fab						
Tumour	0.69 ± 0.54	1.86 ± 1.19	2.40 ± 0.79	1.62 ± 0.86*	0.74 ± 0.25*	0.24 ± 0.06*
Blood	33.71 ± 6.38	5.58 ± 0.64	2.77 ± 1.65	1.50 ± 0.83	0.30 ± 0.06	0.10 ± 0.02
Liver	5.93 ± 1.12	1.74 ± 0.21	0.96 ± 0.60	0.52 ± 0.28	0.11 ± 0.06	0.04 ± 0.01
Kidneys	8.66 ± 3.33	34.30 ± 3.84	12.69 ± 1.04	4.20 ± 1.52	0.34 ± 0.24	0.14 ± 0.10
Intestine	0.72 ± 0.65	1.35 ± 1.26	1.68 ± 1.56	1.07 ± 1.03	0.15 ± 0.17	0.03 ± 0.03
Stomach	0.71 ± 0.15	9.41 ± 4.99	12.20 ± 5.01	3.32 ± 2.81	0.40 ± 0.13	0.09 ± 0.06
Spleen	3.38 ± 1.03	1.34 ± 0.21	0.80 ± 0.52	0.41 ± 0.43	0.10 ± 0.06	0.06 ± 0.04
Lungs	11.87 ± 1.03	2.69 ± 0.27	1.62 ± 0.96	0.95 ± 0.51	0.17 ± 0.09	0.06 ± 0.01

*, significant differences between tumour uptake of fragments and tumour uptake of mAb 14C5, $P < 0.05$

Tumour-to-blood ratios increased up to 2.6 ± 0.7 for Fab and 3.5 ± 2.5 for F(ab')$_2$, compared to 1.3 ± 0.2 for ^{131}I-labeled mAb 14C5 48 h after injection (Table 6.2). Tumour-to-contralateral muscle ratios increased up to 46.8 ± 7.7 for Fab and 13.0 ± 2.1 for F(ab')$_2$ 24 h after injection, compared to 7.6 ± 2.3 for ^{131}I-labeled mAb 14C5 ($P < 0.05$). Tumour-to-liver ratios were significantly lower for ^{131}I-labeled mAb (0.3 ± 0.1) at early time points than for Fab (2.0 ± 0.9; $P < 0.05$) and F(ab')$_2$ (1.2 ± 0.7; $P < 0.1$).

6.3.5 Planar Gamma Camera Imaging

Figure 6.5 shows the planar gamma camera images of tumour-bearing mice at different time intervals after injection of ^{123}I-labeled mAb 14C5 (Fig. 6.5A), ^{123}I-labeled F(ab')$_2$ (Fig. 6.5B) and ^{123}I-labeled Fab 14C5 fragments (Fig. 6.5C). Fab and F(ab')$_2$ show improved tumour-to-background contrast compared to tumour imaging with ^{123}I-labeled mAb 14C5.

Tabel 6.2 Biodistribution of ^{131}I-labeled mAb 14C5, F(ab')$_2$ and Fab 14C5 (tumour-to-tissue ratios) in athymic mice bearing an A549 tumour

	Time (h)					
Tissue	0.02	1	3	6	24	48
mAb						
Blood	0.02 ± 0.01	0.06 ± 0.01	0.12 ± 0.06	0.31 ± 0.07	0.90 ± 0.21	1.31 ± 0.19
Liver	0.08 ± 0.06	0.18 ± 0.04	0.31 ± 0.10	1.04 ± 0.41	2.92 ± 1.02	4.65 ± 1.36
Kidneys	0.12 ± 0.08	0.31 ± 0.10	0.46 ± 0.12	1.49 ± 0.42	3.84 ± 0.89	6.16 ± 1.59
Intestine	0.83 ± 0.55	0.73 ± 0.05	0.92 ± 0.21	2.59 ± 0.81	6.54 ± 1.40	10.69 ± 2.28
Stomach	1.09 ± 0.61	0.75 ± 0.04	1.45 ± 0.58	4.40 ± 2.19	6.10 ± 0.50	12.09 ± 6.82
Spleen	0.27 ± 0.22	0.32 ± 0.03	0.53 ± 0.19	1.40 ± 0.30	3.83 ± 1.60	6.69 ± 1.18
Lungs	0.07 ± 0.07	0.23 ± 0.10	0.36 ± 0.17	0.91 ± 0.24	1.98 ± 0.76	3.18 ± 0.54
Muscle	1.64 ± 0.50	2.90 ± 1.58	3.16 ± 1.70	9.59 ± 4.07	7.57 ± 2.30	n.d.
F(ab')$_2$						
Blood	0.03 ± 0.01	0.13 ± 0.08	0.33 ± 0.15*	0.55 ± 0.09*	1.04 ± 0.15	3.52 ± 2.48*
Liver	0.12 ± 0.03	0.43 ± 0.21	1.15 ± 0.66	1.41 ± 1.07	2.89 ± 1.14	5.80 ± 3.71
Kidneys	0.13 ± 0.05	0.17 ± 0.15	0.50 ± 0.22	0.63 ± 0.47	2,15 ± 0.55	5.43 ± 4.11
Intestine	0.96 ± 0.22	0.99 ± 0.49	1.58 ± 0.72	1.64 ± 1.27	3.57 ± 2.01	12.33 ± 4,43
Stomach	1.50 ± 1.05	0.40 ± 0.13	1.21 ± 0.84	0.88 ± 0.94	1.61 ± 0.84	9,68 ± 2.05
Spleen	0.37 ± 0.09	0.70 ± 0.35	1.48 ± 0.78	1.65 ± 1.18	4.08 ± 2.19	8.66 ± 1.84
Lungs	0.08 ± 0.03	0.36 ± 0.21	0.72 ± 0.56	1.06 ± 0.80	2.22 ± 0.44	5.16 ± 3.41
Muscle	1.83 ± 0.60	3.42 ± 1.07	6.40 ± 2.40	6.78 ± 1.55	13.03 ± 2.07	n.d.
Fab						
Blood	0.02 ± 0.01	0.35 ± 0.27*	0.68 ± 0.29*	1.11 ± 0.46*	1.95 ± 0.97*	2.55 ± 0.73*
Liver	0.11 ± 0.07	1.04 ± 0.57	1.98 ± 0.87	3.07 ± 0.83	5.27 ± 1.72	6.31 ± 3.23
Kidneys	0.07 ± 0.03	0.05 ± 0.04	0.13 ± 0.06	0.38 ± 0.15	1.91 ± 0.95	1.97 ± 1.44
Intestine	0.63 ± 0.35	0.88 ± 0.35	1.04 ± 0.44	1.54 ± 0.48	3.41 ± 1.41	5.28 ± 1.39
Stomach	0.96 ± 0.69	0.19 ± 0.03	0.24 ± 0.23	0.59 ± 0.30	1.61 ± 1.24	3.03 ± 2.23
Spleen	0.19 ± 0.11	1.33 ± 0.64	2.51 ± 1.36	3.69 ± 1.18	6.20 ± 2.13	4.52 ± 3.07
Lungs	0.06 ± 0.04	0.69 ± 0.43	1.13 ± 0.40	1.73 ± 0.65	3.60 ± 1.58	3.77 ± 1.74
Muscle	1.14 ± 0.96	2.98 ± 1.42	4.57 ± 0.40	11.16 ± 1.88	46.80 ± 7.71	n.d.

n.d., data not determined; *, tumour-to-blood ratios of fragments that are significantly higher than tumour-to-blood ratios of mAb 14C5, $P < 0.05$

Imaging with ^{123}I-labeled mAb 14C5 and ^{123}I-labeled F(ab')$_2$ showed retention in the liver region, whereas imaging with ^{123}I-labeled Fab fragments showed high uptake in the kidney region, stomach and bladder. Despite the higher

background contrast with ^{123}I-F(ab')$_2$, imaging with ^{123}I-labeled mAb 14C5 could provide superior quality images due to higher sensitivity. Imaging with ^{123}I-F(ab')$_2$ and ^{123}I-mAb in patients is necessary to conclude which radiopharmaceutical is superior for imaging.

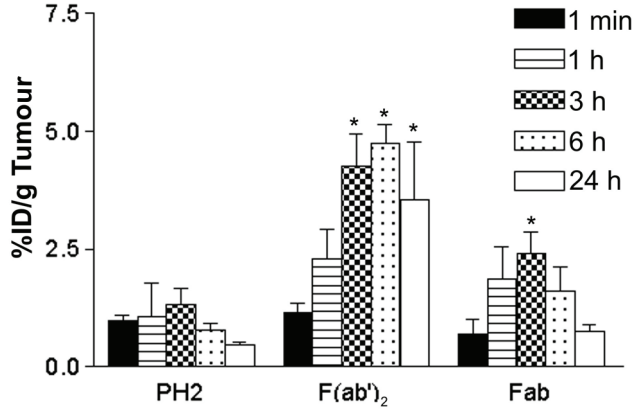

Fig. 6.4. Antigen specificity of *in vivo* tumour binding. Tumour uptake of tumour-specific mAb 14C5 fragments, Fab and F(ab')$_2$, versus an irrelevant PH2 anti-MUC1 dimer (75 kDa, scFv-Fab dimer). Bars, SD (n = 3). *, P < 0.05, significant differences between Fab or F(ab')$_2$ and irrelevant PH2.

6.4 Discussion

When optimizing RID and RIT, it is a challenge to improve the tumour uptake while reducing the uptake in normal tissues (Wahl et al., 1983; Reff, 2001; Goldenberg, 2002; Batra et al., 2002; Koppe et al., 2005; Sharkey and Goldenberg, 2005). Although ^{123}I-labeled mAb 14C5 clearly showed A549 lung tumours of 0.14 g by planar gamma imaging, the use of enzymatically digested antibody fragments (Fab and F(ab')$_2$) or engineered antibodies (e.g., scFv, sc(Fv)$_2$, diabodies, etc) may offer advantages such as improved tumour penetration (Wu et al., 2005) and rapid blood clearance (Goldenberg, 2002; Koppe et al., 2005). As a consequence, tumour uptake of Fab fragments is often low, although some authors support the efficacy of Fab in RIT (Behr et al., 2000; Goldenberg, 2002).

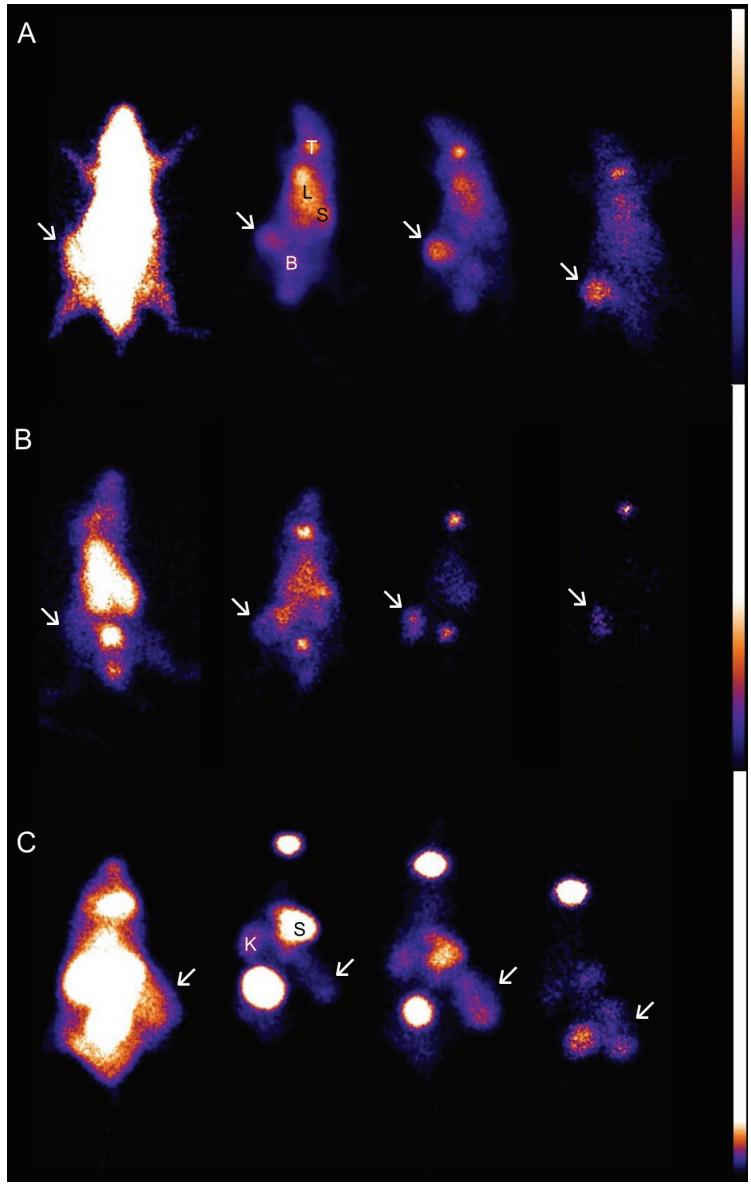

Fig. 6.5. Planar images of athymic mice bearing A549 tumours, using 500 µCi ^{123}I-labeled mAb 14C5 (A), 500 µCi F(ab')$_2$ (B), and 1 mCi Fab (C) (20 µg protein in 200 µL PBS). Animals were anesthetized by intraperitoneal injection of 75 µl of a sodium pentobarbital solution (Nembutal, 20 mg/ml, Ceva Santé Animale). Ten-minute images were obtained in a 256 × 256-pixel matrix (field of view, 23.5 × 12.46 cm) with mAb and F(ab')$_2$. Thirty-minute images were obtained with Fab. Tumours are indicated by arrows. B = Bladder, K = Kidney, L = Liver, T = Thyroid, S = Stomach.

Larger fragments (e.g. [sc(Fv)$_2$]$_2$ and F(ab')$_2$) show intermediate clearance rates, and higher tumour uptake is observed (Goldenberg, 2002; Wu et al., 2005). Therefore, the aims of this study were to develop radioiodinated F(ab')$_2$ and Fab 14C5 fragments and to perform a first preclinical evaluation of 14C5 antibody-derived fragments to improve pharmacokinetics in a mouse model with an A549 lung tumour. These classic mono- and bivalent antibody fragments are easy to produce with fast enzymatic proteolysis, although genetically engineered antibodies can be produced more economically and possess other unique and superior properties for a range of diagnostic and therapeutic applications (Schoonjans et al., 2000; Goel et al., 2000; Todorovska et al., 2001; Power et al., 2003; Olafsen et al., 2004; Holliger et al., 2005).

The receptor-binding capacity of both fragments was tested. ^{125}I-F(ab')$_2$ showed excellent receptor binding (K_d 0.37 ± 0.10 nmol/l). These properties are comparable with the data previously obtained with mAb 14C5 (e.g., K_d 0.19 ± 0.07 nmol/l) (Burvenich et al., 2005). Faster blood clearance *in vivo* combined with preservation of good binding properties resulted in improved tumour-to-background contrast images at 24 and 48 h postinjection when using radioiodinated F(ab')$_2$ 14C5 fragments instead of intact mAb 14C5. The thyroid activity demonstrates dehalogenation, but blocking the thyroid with 0.1% NaI before injection of radioactive agents can reduce this uptake. Nevertheless, deiodination *in vivo* will diminish the tumour signal and increase normal tissue uptake (i.e. in stomach, salivary glands, intestines and bladder). Using other labeling strategies may improve the targeting potential of F(ab')$_2$ and Fab 14C5 fragments. Radiometals such as ^{99m}Tc or ^{111}In have shown better tumour retention compared to ^{123}I, especially when internalizing agents were used (Steffens et al., 1999; Smith-Jones et al., 2000).

Compared with mAb 14C5 and F(ab')$_2$ 14C5 fragments, *in vitro* binding properties of Fab 14C5 fragments were less favourable (K_d 2.25 ± 0.44 nmol/l).

In vivo, ^{131}I-labeled Fab 14C5 showed the fastest blood clearance. Six hours after injection, ^{123}I-Fab 14C5 activity was higher in the tumour than in the blood, which agrees with the improved tumour-to-background imaging using this fragment compared to imaging with ^{123}I-mAb 14C5. However, tumour uptake of ^{123}I-labeled Fab 14C5 is much lower compared to ^{123}I-mAb 14C5 and ^{123}I-F(ab')$_2$ 14C5. High uptake in bladder, kidneys, and stomach is visible, which could interfere with tumour imaging in patients. However, tumour retention is still visible at 30 h postinjection, making it possible to visualize breast, lung, liver and, possibly, colon tumours at that time.

Preclinical therapeutic studies with ^{131}I-F(ab')$_2$ and ^{131}I-Fab are necessary to demonstrate the therapeutic potential. These results warrant the further development of mAb 14C5-derived multivalent engineered antibodies.

6.5 Conclusion

This study showed that ^{123}I-F(ab')$_2$ and ^{123}I-Fab fragments of mAb 14C5 have improved characteristics as tumour imaging agents compared to the intact mAb 14C5: the fragments accumulate more rapidly in the tumour, and clear faster from the blood and nontumour tissues. However, tumour uptake remains highest for mAb 14C5. Preclinical RIT studies with ^{131}I-mAb 14C5 and its fragments, ^{131}I-F(ab')$_2$ and ^{131}I-Fab, will demonstrate which immunoconjugate has the highest therapeutic potential. Further improvements may be obtained with bioengineering techniques for the development of a 14C5-scFv-based radiopharmaceutical for imaging and therapy.

6.6 References

Batra SK, Jain M, Wittel UA, et al. Pharmacokinetics and biodistribution of genetically engineered antibodies. Curr Opin Biotechnol 2002;13:603-8.

Behr TM, Blumenthal RD, Memtsoudis S, et al. Cure of metastatic human colonic cancer in mice with radiolabeled monoclonal antibody fragments. Clin Cancer Res 2000;6:4900-7.

Behr TM, Goldenberg DM, Becker W. Reducing the renal uptake of radiolabeled antibody fragments and peptides for diagnosis and therapy: present status, future prospects and limitations. Eur J Nucl Med. 1998;25:201-12.

Behr TM, Sharkey RM, Juweid ME, et al. Reduction of the renal uptake of radiolabeled monoclonal antibody fragments by cationic amino acids and their derivatives. Cancer Res 1995;55:3825-34.

Blumenthal RD, Sharkey RM, Haywood L, et al. Targeted therapy of athymic mice bearing GW-39 human colonic cancer micrometastases with 131I-labeled monoclonal antibodies. Cancer Res 1992;52:6036-44.

Bock E, Becker W, Scheele J, et al. Diagnostic accuracy of 99mTc-anti-CEA immunoscintigraphy in patients with liver metastases from colorectal carcinoma. Nuklearmedizin. 1992;31:80-3.

Burvenich I, Schoonooghe S, Cornelissen B, et al. In vitro and in vivo targeting properties of iodine-123- or iodine-131-labeled monoclonal antibody 14C5 in a non-small cell lung cancer and colon carcinoma model. Clin Cancer Res 2005;11:7288-96.

Carter PJ. Potent antibody therapeutics by design. Nat Rev Immunol. 2006;6:343-57.

Goel A, Colcher D, Baranowska-Kortylewicz J, et al. Genetically engineered tetravalent single-chain Fv of the pancarcinoma monoclonal antibody CC49: improved biodistribution and potential for therapeutic application. Cancer Res 2000;60:6964-71.

Goldenberg DM. Targeted therapy of cancer with radiolabeled antibodies. J Nucl Med 2002;43:693-713.

Hansen HJ, Jones AL, Grebenau R, et al. Labeling of anti-tumor antibodies and antibody fragments with Tc-99m. Cancer Treat Res 1990;51:233-44.

Holliger P, Hudson PJ. Engineered antibody fragments and the rise of single domains. Nat Biotechnol. 2005;23:1126-36.

Jain RK. Transport of molecules across tumor vasculature. Cancer Metastasis Rev. 1987;6:559-93.

Koppe MJ, Postema EJ, Aarts F, et al. Antibody-guided radiation therapy of cancer. Cancer Metastasis Rev 2005;24:539-67.

Libutti SK, Alexander HR Jr, Choyke P, et al. A prospective study of 2-[18F] fluoro-2-deoxy-D-glucose/positron emission tomography scan, 99mTc-labeled arcitumomab (CEA-scan), and blind second-look laparotomy for detecting colon cancer recurrence in patients with increasing carcinoembryonic antigen levels. Ann Surg Oncol 2001;8:779-86.

Maynard J, Georgiou G. Antibody engineering. Annu Rev Biomed Eng. 2000;2:339-76.

Murray JL, Rosenblum MG, Zhang HZ, et al. Comparative tumor localization of whole immunoglobulin G anticarcinoembryonic antigen monoclonal antibodies IMMU-4 and IMMU-4 F(ab')2 in colorectal cancer patients. Cancer 1994;73:850-7.

Olafsen T, Tan GJ, Cheung CW, et al. Characterization of engineered anti-p185HER-2 (scFv-CH3)2 antibody fragments (minibodies) for tumor targeting. Protein Eng Des Sel 2004;17:315-23.

Power BE, Doughty L, Shapira DR, et al. Noncovalent scFv multimers of tumor-targeting anti-Lewis(y) hu3S193 humanized antibody. Protein Sci 2003;12:734-47.

Reff ME. A review of modifications to recombinant antibodies: attempt to increase efficacy in oncology applications. Crit Rev Oncol Hematol 2001;40:25-35.

Schoonjans R, Willems A, Schoonooghe S, et al. Fab chains as an efficient heterodimerization scaffold for the production of recombinant bispecific and trispecific antibody derivatives. J Immunol 2000;165:7050-7.

Sharkey RM, Goldenberg DM. Perspectives on cancer therapy with radiolabeled monoclonal antibodies. J Nucl Med 2005;46:115-27S.

Sharkey RM, Motta-Hennessy C, Pawlyk D, et al. Biodistribution and radiation dose estimates for yttrium- and iodine-labeled monoclonal antibody IgG and fragments in nude mice bearing human colonic tumor xenografts. Cancer Res 1990;50:2330-6.

Smith-Jones PM, Vallabahajosula S, Goldsmith SJ, et al. In vitro characterization of radiolabeled monoclonal antibodies specific for the extracellular domain of prostate-specific membrane antigen. Cancer Res. 2000;60:5237-43.

Steffens MG, Oosterwijk E, Kranenborg MH, et al. In vivo and in vitro characterizations of three 99mTc-labeled monoclonal antibody G250 preparations. J Nucl Med. 1999;40:829-36.

Todorovska A, Roovers RC, Dolezal O, et al. Design and application of diabodies, triabodies and tetrabodies for cancer targeting. J Immunol Methods 2001;248:47-66.

Vijayakumar V, Blend MJ, Johnson DK, et al. Improved detection of hepatic lesions using MoAb B72.3 and a modified 111In labelling technique in patients with recurrent colon cancer. Nucl Med Commun. 1993;14:658-66.

Wahl RL, Parker CW, Philpott GW. Improved radioimaging and tumor localization with monoclonal F(ab')2. J Nucl Med 1983;24:316-325.

Wen YH, Kalff J, Peters RH. Pharmacokinetic modeling in toxicology: a critical perspective. Environ Rev 1999;7:1-18.

Willkomm P, Bender H, Bangard M, et al. FDG PET and immunoscintigraphy with 99mTc-labeled antibody fragments for detection of the recurrence of colorectal carcinoma. J Nucl Med 2000;41:1657-63.

Wu AM, Senter PD. Arming antibodies: prospects and challenges for immunoconjugates. Nat Biotechnol 2005;23:1137-46.

Zalutsky MR, Lewis JS. Handbook of radiopharmaceuticals. Eds. Welch JW, Redvanly CS. John Wiley & Sons, West Sussex, 2003; 685-714.

Chapter 7

INTERNALIZATION AND CELLULAR RETENTION OF IODINATED MONOCLONAL ANTIBODY 14C5 AND ITS FRAGMENTS F(ab')$_2$ AND Fab

Burvenich I, Schoonooghe S, Coene E, Mertens N, De Vos F and Slegers G

In preparation

7.1 Introduction

In the development of an antibody-based diagnostic or therapeutic radiopharmaceutical, intrinsic properties of the antigenic target, the molecular form of the antibody and the characteristics of the radionuclide of choice will influence the potential of the radiopharmaceutical (Goldenberg, 2002; Goldenberg, 2003; Milenic et al., 2004).

The most important factor influencing the choice of the radionuclide apart from its purpose (i.e. diagnostic or therapeutic) is probably the fate of the target antigen after the labeled mAb-antigen complex is formed. Depending upon whether the antigen-antibody complex remains on the cell membrane, is shed into the circulation, or is internalized into the tumour cell, the labeled mAb will be exposed to different catabolic processes, necessitating different labeling strategies (Zalutsky and Lewis, 2003).

Previously, we have shown that Ag 14C5 most likely is the integrin αvβ5 receptor. Integrin-mediated internalization is exploited by bacterial and viral intracellular pathogens and, the integrin αvβ5 receptor mediates the internalization of vitronectin (Memmo and McKeown-Longo, 1998; Hart, 1999). Therefore, it is possible that the mAb 14C5-Ag complex will internalize. Internalization can lead to a rapid loss of the radiolabel from the tumour cell, because this process exposes the labeled mAb to intracellular catabolic processes in the lysosomes. Labeling internalizing mAbs with radiometals (e.g. ^{111}In) results in higher retention. Also, several approaches have been developed for residualizing radioiodine activity in the tumour: oligosaccharide conjugates, positively charged templates, and D-amino-acid peptides (Zalutsky and Lewis, 2003).

In this study we will investigate the fate of the ^{125}I-labeled mAb-Ag 14C5 complex. Internalization of mAb 14C5 and its fragments F(ab')$_2$ and Fab was evaluated by confocal laser scanning microscopy. Internalization and cellular

catabolism of the molecules was also monitored using ^{125}I-labeled antibody and its fragments.

7.2 Materials and methods

7.2.1 Antibodies

The mAb 14C5 was produced and purified as described before (Burvenich et al., 2005). Fab and F(ab')$_2$ fragments were derived from murine mAb 14C5 using the Immunopure IgG1 Fab and F(ab')$_2$ preparation kit (Perbio) according to the manufacturer's instructions. IgG and Fc fragments were removed using a protein A sepharose column (Perbio). For concentration and exchange of buffer with PBS (pH 7.4), Centricon YM-30 (Millipore) was used. Fragments were evaluated without reduction by SDS-PAGE. When purity was <90%, fragments were further purified using a HiPrep 26/60 Sephacryl S-200 HR column (GE Healthcare Europe) on an Akta purifier, with PBS as eluant (pH 7.5, 0.5 ml/min). Alexa Fluor 488-conjugated goat anti-mouse IgG antibody (Invitrogen) was used during flow cytometry.

7.2.2 Cell lines

A549 cells were obtained from the Laboratory of Tumour and Developmental Biology (University of Liège, Belgium). Cells were cultured in standard medium with supplements according to the American Type Culture Collection (Manassas, VA) recommendations. All cells were cultured at 37 °C in a 5% CO_2 humidified incubator and passaged with 0.05% trypsin-0.02% EDTA.

7.2.3 Confocal laser scanning microscopy

A549 cells were confluently grown in 8-well confocal chamber slides (Lab-Tek Chamber CVG, Nalge Nunc International, Neerijse, Belgium) and incubated with 10 µg of mAb 14C5, F(ab')$_2$ or Fab in 200 µl of medium at 0 °C or at

37 °C for various time periods. Subsequently, the cells were washed with PBS and the surface-bound antibody was removed by treatment with low-pH medium (pH 2.25) to improve visibility of the intracellular fraction. Cells were fixed with 3.7% formaldehyde for 20 min at room temperature, incubated with 0.4% Triton in PBS for 5 min and finally with 50 mM NH_4Cl in PBS for 5 min. Cells were incubated overnight in PBS 1% BSA 0.02% NaN_3 until incubation with Alexa Fluor 488-labeled secondary antibody was performed for 1 h at 37 °C. After washing cells once with PBS and once with 50 mM Tris (pH 8), 80 % glycerol in 50 mM Tris (pH 8) was added. Nuclei were stained by using propidium iodide. The cells were analyzed with a Zeiss LSM-410 confocal laser scanning microscope (CLSM, Carl Zeiss, Zaventem, Belgium). Control samples were obtained by omitting the acidic wash step.

7.2.4 Radioiodination and quality control

Fab, $F(ab')_2$ and mAb 14C5 were labeled with ^{125}I. Isotopes were obtained from Bristol-Myers Squibb. Radioiodination was performed using the Iodo-Gen method as previously described. In brief, iodide and protein dissolved in 0.1 mol/l potassium phosphate buffer (pH 8.5) were added to an Iodo-Gen-coated reaction vial and reacted for 10 minutes at room temperature. Protein-bound iodine was separated from free iodide by passing over a PD-10 column (GE Healthcare Europe) equilibrated with 1% BSA in PBS. Quality control of radioiodinated protein was performed by size-exclusion high-performance liquid chromatography using a Shodex KW 802.5 column (7.8 mm × 300 mm; Thomson Instrument Company). Protein was eluted with 0.1 mol/l potassium phosphate buffer (pH 7.4) at a flow rate of 0.8 ml/min. ^{125}I-labeled fragments were analyzed by SDS-PAGE followed by phosphor imager analysis for integrity. Samples of 2 µCi labeled protein were loaded on SDS-PAGE and SDS-PAGE gel was exposed to MultiSensitive Phosphor Screens (Medium) for 5 minutes. In order to assess *in vitro* stability, radioiodinated fragments were

incubated for 24 hours at 4°C in PBS with 1% BSA or at 37°C in PBS with 50% mouse serum in PBS. Samples were taken periodically for ITLC analysis (ITLC SG strips, Pall Corporations), using 50 mmol/l citric acid (pH 5.0) as eluant. Strips were divided in ten parts and radioactivity of each part was counted with a gamma counter (Cobra II; Perkin Elmer).
Specific activities of 10 µCi/µg protein were used in radioimmunoassays.

7.2.5 Internalization of ^{125}I-labeled mAb 14C5 and its fragments

Confluently grown A549 in 10 cm²-dishes were incubated with 1 µCi ^{125}I-labeled mAb 14C5, corresponding to 0.1-0.2 µg mAb 14C5, in 1 ml of medium at 4 °C for 2 hours. Cells were washed twice with ice-cold medium to remove unbound mAbs. Two ml of ice-cold medium was added, and the cells were incubated at 4°C (no internalization) or at 37°C (allowing internalization). Triplicate samples were removed at different time points, and the medium was isolated. The ^{125}I-labeled antibodies still present on the cell surface were stripped by washing the cells twice with ice-cold low-pH culture medium (pH 2.25) for 1 min. Cell surface bound and intracellular activity were determined by measuring the activity of the acid washes and cell-associated radioactivity after treatment with low-pH medium. The different fractions were counted with a gamma counter (Cobra II). The fraction of internalized antibody was calculated from the intracellular activity divided by the initially bound radioactivity.
Analogously, studies were conducted with ^{125}I-labeled F(ab')$_2$ and Fab fragments and with acetone-fixed cells and non-fixed cells.

7.2.6 Cellular retention and catabolism

The cellular retention of radioactivity was studied after 2 hours of incubation at 4°C with ^{125}I-mAb or its fragments. At the end of incubation the cells were washed thoroughly to eliminate unbound conjugate, and the incubation was

continued in fresh medium at 37°C (allowing internalization) or at 4°C (inhibiting internalization). After 0.25-2.0 h, the cells were washed with fresh medium and counted for radioactivity. Supernatants of samples incubated at 37°C for 2 hours were passed over a PD-10 column. Fractions of 500 µl were obtained. Fractions 3-9, containing labeled antibody or antibody fragments, were pooled, concentrated with centricon YM-30 for ^{125}I-mAb 14C5 and ^{125}I-F(ab')$_2$, and with YM-10 for ^{125}I-Fab, and analyzed with SDS-PAGE and Cyclone Phosphor Imager (PerkinElmer).

7.2.7 Statistical analysis

Comparison between mAb 14C5 and its fragments, F(ab')$_2$ or Fab was performed using a nonparametric Mann-Witney test.

7.3 Results

7.3.1 Confocal laser scanning microscopy

In a first experiment, internalization of mAb 14C5, F(ab')$_2$ and Fab was monitored by CLSM. A549 cells incubated on ice showed no internalized antibody (Fig. 7.1A). A549 cells incubated with mAb 14C5 at 37°C, showed both membrane and intracellular fluorescence (Fig. 7.1C), whereas cells treated with an acid wash after incubation at 37°C with mAb 14C5 showed only intracellular fluorescence (Fig. 7.1E). The intracellular fluorescence detected in Fig. 7.1C and E, indicates the presence of internalized mAb 14C5. To improve visibility, the nuclei of the cells are included in Fig. 7.1 B, D and F. Similar results were obtained with F(ab')$_2$ (data not shown). No internalization was seen with Fab.

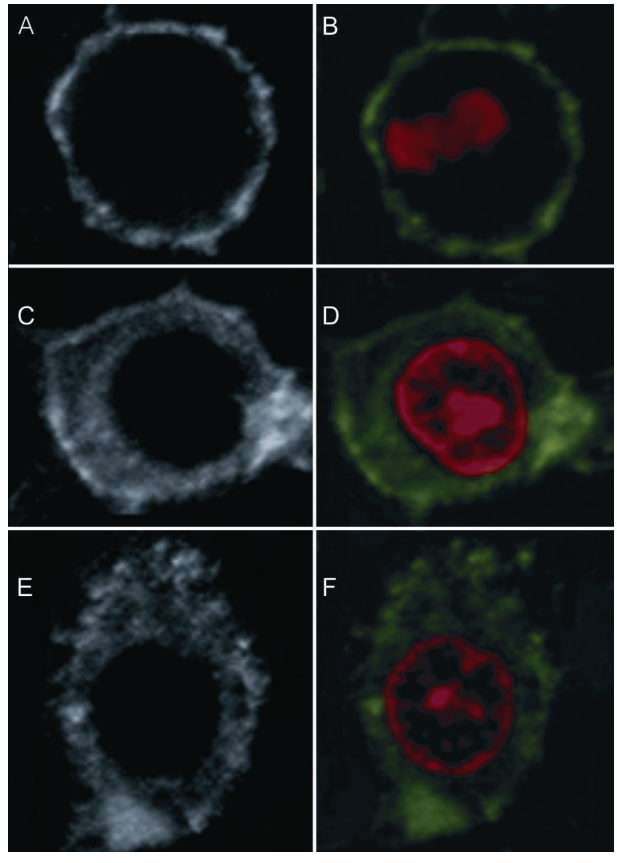

Fig. 7.1. Confocal laser scanning immunofluorescence images of A549 cells incubated with mAb 14C5 and Alexa-fluor 488-conjugated anti-mouse IgG. The cells shown in (A, B) were incubated with mAb 14C5 on ice for 1 h. After incubation with Alexa Fluor 488-conjugated anti-mouse IgG, no intracellular fluorescence was detected, indicating there is no internalization of mAb 14C5 at 0°C. The cells shown in (C, D) and (E, F) were incubated with mAb 14C5 at 37°C for 1 h. After incubation with Alexa Fluor 488-conjugated anti-mouse IgG, intracellular fluorescence was detected, indicating internalization of mAb 14C5 at 37°C. To improve the visibility of the intracellular fluorescence, an acid wash was used to remove the membrane-bound mAb 14C5 of cells shown in (E, F). Also to improve the visibility, the nucleus is shown by propidium iodide in images (B), (E) and (F). cell diameter, 5-10μm

7.3.2 Internalization of ^{125}I-mAb 14C5, ^{125}I-F(ab')$_2$ and ^{125}I-Fab 14C5 fragments

In a second experiment, the degree of internalization was investigated in a radioimmunoassay with A549 cells. Cells were incubated with ^{125}I-labeled mAb 14C5, F(ab')$_2$ or Fab at 4°C for 2 h. After removing unbound mAb,

$F(ab')_2$ or Fab 14C5 the cells were incubated at 37°C for various time periods to allow internalization.

The fraction of ^{125}I-labeled mAb 14C5 that remained associated with the cells after treatment with a low-pH buffer, increased with longer incubation periods from 12.1 ± 1.4 % (t = 0 min) to 32.5 ± 0.1 % for A549 cells (t = 120 min) (Fig. 7.2A). The fraction of ^{125}I-labeled $F(ab')_2$ that remained associated with the cells after treatment with a low-pH buffer increased with longer incubation periods at 37°C from 3.9 ± 0.3 % (t = 0 minute) to 24.5 ± 0.3 % (t = 120 minutes) (Fig. 7.2C). In contrast, the fraction of ^{125}I-labeled Fab associated with A549 cells varied with time only from 3.0 ± 0.6 % (t = 0 minute) to 5.6 ± 0.3 % (t = 120 minutes) (Fig. 7.2E).

Because internalization is an energy-dependent process it takes place at 37°C, but will be inhibited at 4°C. Figure 7.2 shows no increase of radioactivity associated with A549 cells after placing the cells at 4°C. The 10% intracellular ^{125}I-labeled mAb 14C5 at the start of the internalization assay or 3% intracellular for $F(ab')_2$ and Fab (t = 0 h, T = 37°C), can be considered as the acid-resistant fraction.

As a negative control, studies were repeated with acetone-fixed cells (Fig. 7.2B, mAb; Fig. 7.2D, $F(ab')_2$; Fig. 7.2F, Fab). These cells only present target epitopes for binding, but no internalization can occur. Figure 7.2 shows no increase in intracellular activity with acetone-fixed cells, both at 4°C and 37°C with neither mAb, $F(ab')_2$ nor Fab. Because the acid-resistant fraction was higher with the acetone-fixed target cells, a control test with mAb 14C5 was performed to test the efficiency of the acid wash in function of time both for non-fixed and acetone-fixed A549 cells (Fig. 7.3).

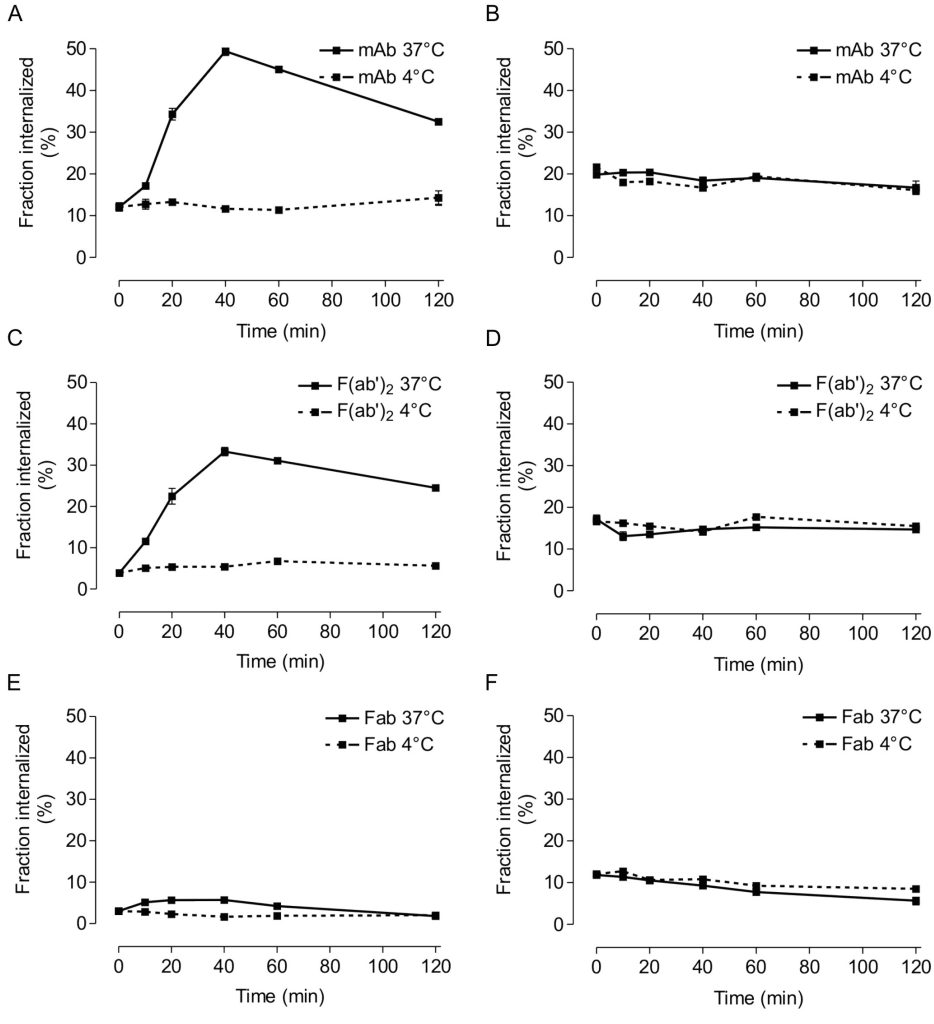

Fig. 7.2. Internalization of ^{125}I-mAb, ^{125}I-F(ab')$_2$ and ^{125}I-Fab with A549 cells. Petri dishes (10 cm^2) with confluent cells were incubated with 1 µCi of ^{125}I-labeled mAb or its fragments at 4°C for 2 h. Supernatant containing unbound antibody was removed. Fresh medium was added and samples were incubated at 37°C (*full lines*) to allow internalization or at 4°C (*dashed lines*) to inhibit internalization. At various time points, the ^{125}I-labeled antibodies still present on the cell surface were stripped by washing the cells with ice-cold low-pH buffer (pH 2.25) for 1 min. The remaining radioactivity (fraction internalized) was counted as a fraction of the initially bound radioactivity (%). Studies were done with non-fixed A549 cells (A, mAb; C, F(ab')$_2$; E, Fab) and acetone-fixed A549 cells (B, mAb; D, F(ab')$_2$; F, Fab). *Bars*, SD.

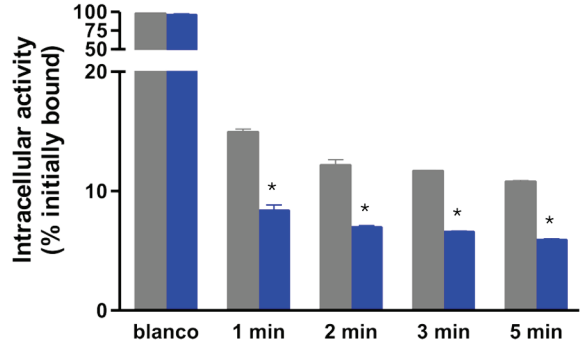

Fig. 7.3. Efficiency of acid wash for both acetone-fixed (*grey*) and non-fixed (*blue*) A549 cells. Petri dishes (10 cm^2) with confluent cells were incubated with 1 µCi of ^{125}I-labeled mAb at 4°C for 2 h. Supernatant containing unbound ^{125}I-mAb 14C5 was removed. Cells were washed twice with PBS (*blanco*, 1 min) or with culture medium (pH 2.25) for the indicated time. *, $P < 0.05$, significant differences between acetone and non-acetone conditions; *Bars, SD*.

Figure 7.3 shows a significant influence of the fixation on washing efficiency. The efficiency increased in function of time both for acetone and non-acetone conditions, but at each amount of time remained significantly lower for acetone conditions ($P < 0.05$). As fixatives can have an impact on the conformation of the antigen, it could be possible that ^{125}I-labeled mAb 14C5 or its fragments, can bind its epitope stronger after acetone-fixation.

7.3.3 Intracellular catabolism and cellular retention

In order to get additional information for the processing of mAb 14C5 and its fragments, the catabolism of this antibody and its fragments by target A549 cells were studied. The processing of the antibody and fragments was followed over a period of 2 h. Radioactivity associated with the cells (which includes the activity both on the cell surface and within the cell, which were not separated in this study), or released into the supernatant was determined. In addition, the radioactivity released into the supernatant was analysed further on a PD-10 column to determine the percentage of free ^{125}I or ^{125}I-monoiodotyrosine. Fractions 3 to 9 (500 µL) were considered to contain the ^{125}I-labeled antibodies

and were further analyzed for the presence of metabolites using SDS-PAGE and autoradiography.

As shown in figure 7.4, the radioactivity was released gradually into the supernatant. ^{125}I-labeled mAb 14C5 and ^{125}I-labeled F(ab')$_2$ demonstrated similar cellular retention of radioactivity with A549 cells (Fig. 7.4A en 7.4C). Placed at 37°C for 2 h, A549 released 43.7 ± 1.4 % of ^{125}I-mAb and 49.5 ± 1.0 % of ^{125}I-F(ab')$_2$. At 4°C this could be reduced to 8.3 ± 0.2 % for ^{125}I-mAb and 7.2 ± 0.5 % for ^{125}I-F(ab')$_2$. ^{125}I-labeled Fab showed poor cellular retention. Placed at 37°C for 2 hours, the cells released 92.7 ± 0.3 % of initially bound ^{125}I-labeled Fab (Fig. 7.4E). At 4°C, with no internalization occurring, this was reduced to 40.6 ± 0.5 % for ^{125}I-labeled Fab. As a control, studies were repeated with ^{125}I-labeled mAb (Fig. 7.4B), ^{125}I-F(ab')$_2$ (Fig. 7.4D) and ^{125}I-Fab (Fig. 7.4F) with acetone-fixed cells. Since no internalization will take place with these fixed cells, release of radioactivity into the supernatant will only be a result of dissociation or dehalogenation processes. As shown in figure 7.4, a high portion of released radioactivity of ^{125}I-mAb, ^{125}I-F(ab')$_2$ and ^{125}I-Fab with non-fixed cells could be attributed to dissociation of the antibodies.

Figure 7.5 shows the amount of free ^{125}I (possibly ^{125}I-monoiodotyrosine and other small metabolites) in the supernatant by eluting the supernatants over a PD-10 column. For the three immunoconjugates, the percentage free ^{125}I was higher for non-fixed cells than acetone-fixed cells (Fig. 7.5A, mAb 14C5; Fig. 7.5C, F(ab')$_2$; Fig. 7.5E, Fab). However, the percentages are very low, indicating that mAb 14C5 and its fragments are slowly degraded after internalization. Also, after PD-10 purification, pure radioiodinated mAb 14C5, F(ab')$_2$ and Fab (i.e. fractions 3 to 9) showed no metabolites attributable to internalization by SDS-PAGE and autoradiography (Fig. 7.5B, mAb 14C5; Fig. 7.5D, F(ab')$_2$; Fig. 7.5F, Fab).

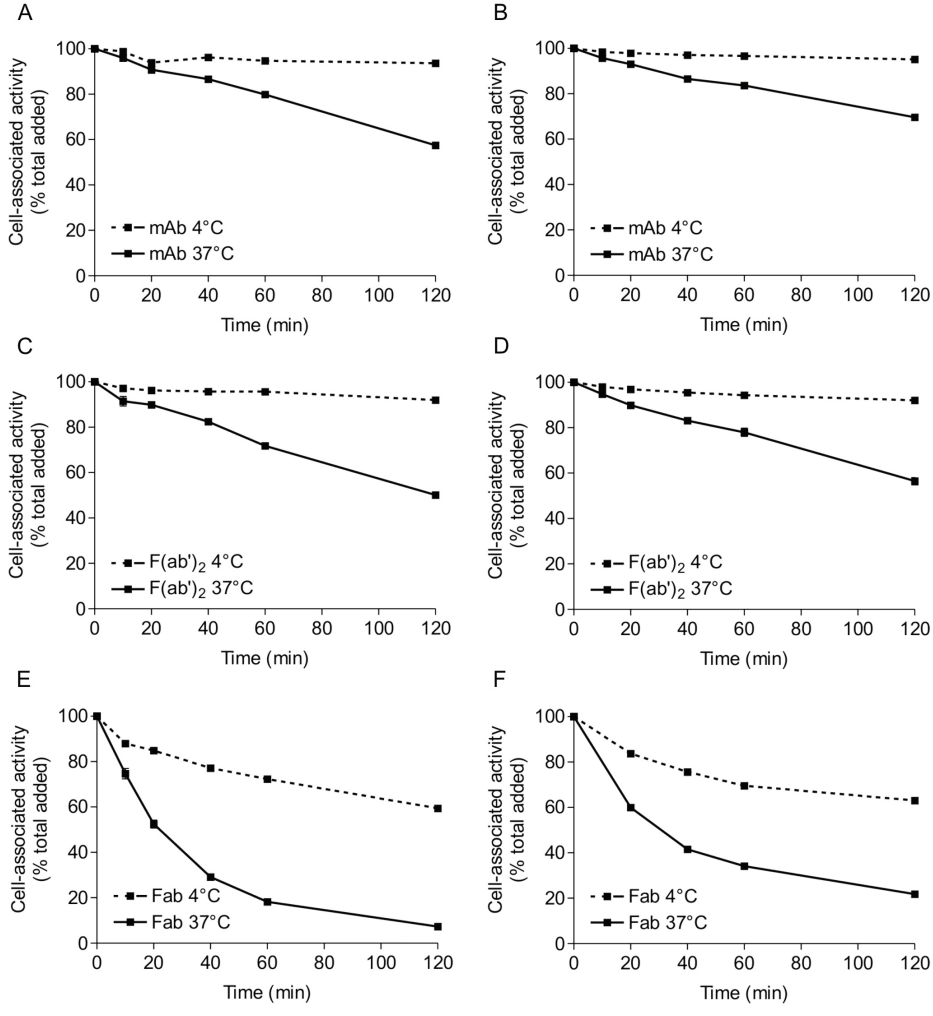

Fig. 7.4. Cellular retention of ^{125}I-mAb, ^{125}I-F(ab')$_2$ and ^{125}I-Fab with A549 cells. Petri dishes (10 cm^2) with confluent cells were incubated with 1 µCi of ^{125}I-labeled mAb or its fragments at 4°C for 2 h. Supernatant containing unbound ^{125}I-mAb 14C5 or its fragments was removed. Fresh medium was added and samples were incubated at 37°C to allow internalization (*full lines*) or at 4°C to inhibit internalization (*dashed lines*). At various time points, supernatants were removed and cells were washed twice with 1 ml fresh medium. The remaining radioactivity (cell-associated activity) was counted as a fraction of the initially bound radioactivity (% total added). Studies were done with non-fixed A549 cells (*A*, mAb; *C*, F(ab')$_2$; *E*, Fab) and acetone-fixed A549 cells (*B*, mAb; *D*, F(ab')$_2$; *F*, Fab). *Bars*, SD.

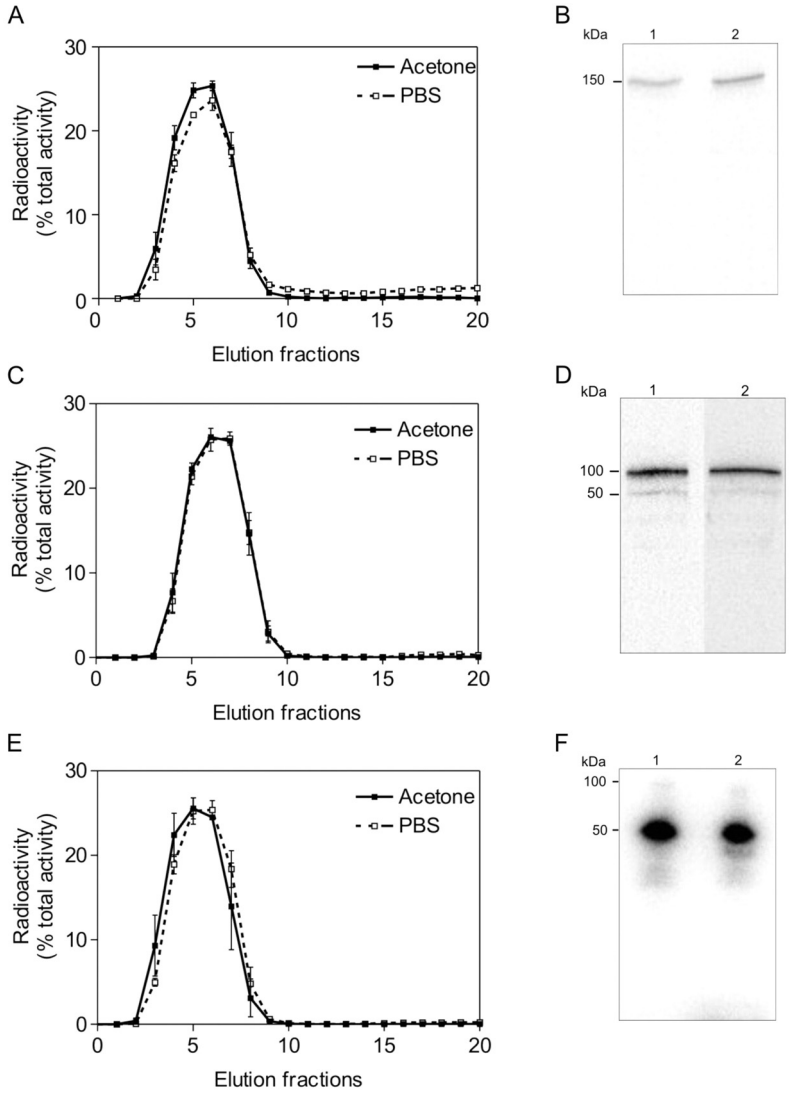

Fig. 7.5. Analysis of metabolites released to the supernatant during internalization. Studies were done with acetone-fixed A549 cells (*full lines, lanes 1*) and non-fixed A549 cells (*dashed lines, lanes 2*) and with ^{125}I-mAb 14C5 (*A*, *B*), ^{125}I-F(ab')$_2$ (*C*, *D*) and ^{125}I-Fab (*E*, *F*). Petri dishes (10 cm^2) with confluent A549 cells were incubated with 1 µCi of ^{125}I-labeled antibody or fragments at 4°C for 2 h. Supernatant containing unbound antibody or fragments was removed. Fresh medium was added and samples were incubated at 37°C to allow internalization. At various time points, the supernatant was removed and free ^{125}I or ^{125}I-monoiodotyrosine (fraction 10 to 20) were separated from ^{125}I-labeled antibody and fragments (fraction 3 to 9) with a PD-10 column (*A*, mAb 14C5; *C*, F(ab')$_2$; *E*, Fab). Subsequently, fraction 3 to 9 of each protein was concentrated and evaluated for metabolites with autoradiography after separating possible metabolites with SDS-PAGE (*B*, mAb; *D*, F(ab')$_2$; *F*, Fab; *lane 1*, acetone-fixed cells; *lane 2*, non-fixed cells). *Bars*, SD.

7.4 Discussion

Antibody internalization into the cell is required for many targeted therapeutics, such as antibody-toxin conjugates (Altenschmidt et al., 1997), immunoliposomes (Mamot et al., 2003), antibody-drug conjugates and for targeted delivery of genes or viral DNA into cells (Fominaya and Wels, 1996). In radioimmunodetection and radioimmunotherapy, radioisotope (e.g., γ and β^-) conjugates can exert their toxic effect without having to be inside or even bound to the cells. Therefore antibody internalization is less important in this situation. However, internalization might be advantageous in α- and Auger-therapy because of the short range of α-particles (40-100 μm) and Auger electrons (a few Å) (Hofer, 2000; Mattes, 2002; Milenic et al., 2004). On the other hand, with respect to pretargeting strategies, internalization might be unwanted (Sharkey and Goldenberg, 2006).

Moreover, after internalization, the majority of the antibody will be delivered to the lysosomal compartment for degradation (Geissler et al., 1991; Geissler et al., 1992). Therefore, after internalization, cell-associated radio-iodine can rapidly decrease due to the escape of iodotyrosine from the cells. Many research groups have investigated the importance of different labeling strategies with respect to internalization (Mattes et al., 1994; Press et al., 1996; Yao et al., 2001). Labeling of internalizing mAbs with radiometals results in higher retention of the radionuclide in tumour cells due to the intracellular retention of metal containing catabolic products. However, three approaches have been developed for residualizing radioiodine activity in tumour cells after mAb internalization: oligosaccharide conjugates, positively-charged templates, and D-amino acid peptides (Zalutsky and Lewis, 2003). Using radiometals or residualizing radioiodine strategies, internalization may offer a therapeutic advantage in RIT because it traps these isotopes into the cell.

Our studies have demonstrated the internalization of mAb 14C5 and its $F(ab')_2$ fragment by A549 cells. No protein metabolites attributable to the internalization process are shown within the first 2 hours of internalization, but some authors have reported antibody degradation starting at 2 h (Shih et al., 1994). The amount of free ^{125}I or ^{125}I-monoiodotyrosine released into the supernatant was < 5% of initially bound radioactivity. These data suggest that mAb 14C5 and $F(ab')_2$ are slowly catabolized. ^{125}I-Fab 14C5 fragments were almost not internalized, suggesting that there might be a need of bivalency for internalization. For many antibodies, bivalency seems to be mandatory for internalization (Nielsen and Marks, 2000), although this is not seen with every antibody (Shih et al., 1994; Poul et al., 2000). Further studies using recombinant Fab and bispecific multivalent fragments will be conducted to investigate the role of bivalent epitope binding. Also, subcellular fractionation studies of A549 cells can show where catabolism of the investigated fragments takes place. In addition, it is suggested by some authors that antibodies binding the same antigen might demonstrate a different way of intracellular trafficking after internalization (Shih et al., 1994). Since $F(ab')_2$ and mAb show similar intracellular uptake and cellular retention different from Fab, it could be possible that the monovalent epitope binding of Fab is responsible for these differences (Press et al., 1988).

In comparison, mAb and $F(ab')_2$ show better retention of radioactivity than Fab both at 4°C and 37°C. Using acetone-fixed cells or non-acetone fixed cells at 4°C, no internalization takes place. Under these conditions, the amount of activity released in the supernatant is due to the dissociation of membrane-bound antibody or fragments. This agrees with the lower affinity measured with Fab (K_d 2.25 ± 0.44 nmol/l) compared to $F(ab')_2$ (K_d 0.37 ± 0.10 nmol/l) and mAb 14C5 (K_d 0.19 ± 0.08 nmol/l). Also, the loss of cell-associated radioactivity for mAb 14C5 and both fragments is higher at 37°C than at 4°C.

This could be explained by an effect of temperature on the dissociation rate (Ong and Mattes, 1993; Xavier et al., 1999). Xavier et al. (1999) showed an increase in k_{diss} of monoclonal antibody HyHEL-5 from 0.10 s^{-1} at 10°C to 2.7 s^{-1} at 32°C.

7.5 Conclusion

Internalization was seen with mAb 14C5 and its $F(ab')_2$ fragment, but to a much lesser extent with Fab. This offers the possibility of using Auger electrons and α-particles with mAb 14C5 and $F(ab')_2$, and possibly other targeted strategies than radioimmunotherapy such as the use of immunotoxins. The rapid dissociation seen with the Fab 14C5 fragment may limit its use in clinical practice.

7.6 References

Altenschmidt U, Schmidt M, Groner B, et al. Targeted therapy of schwannoma cells in immunocompetent rats with an erbB2-specific antibody-toxin. Int J Cancer. 1997;73:117-24.

Fominaya J, Wels W. Target cell-specific DNA transfer mediated by a chimeric multidomain protein. Novel non-viral gene delivery system. J Biol Chem. 1996;271:10560-8.

Geissler F, Anderson SK, Press O. Intracellular catabolism of radiolabeled anti-CD3 antibodies by leukemic T cells. Cell Immunol. 1991;137:96-110.

Geissler F, Anderson SK, Venkatesan P, et al. Intracellular catabolism of radiolabeled anti-mu antibodies by malignant B-cells. Cancer Res. 1992;52:2907-15.

Goldenberg DM. Advancing role of radiolabeled antibodies in the therapy of cancer. Cancer Immunol Immunother. 2003;52:281-96.

Goldenberg DM. Targeted therapy of cancer with radiolabeled antibodies. J Nucl Med. 2002;43:693-713.

Hart SL. Integrin-mediated vectors for gene transfer and therapy. Curr Opin Mol Ther. 1999;1:197-203.

Hofer KG. Biophysical aspects of Auger processes. Acta Oncol. 2000;39:651-7.

Mamot C, Drummond DC, Hong K, et al. Liposome-based approaches to overcome anticancer drug resistance. Drug Resist Updat. 2003;6:271-9.

Mattes MJ, Griffiths GL, Diril H, et al. Processing of antibody-radioisotope conjugates after binding to the surface of tumor cells. Cancer. 1994;73:787-93.

Mattes MJ. Radionuclide-antibody conjugates for single-cell cytotoxicity. Cancer. 2002;94:1215-23.

Memmo LM, McKeown-Longo P. The alphavbeta5 integrin functions as an endocytic receptor for vitronectin. J Cell Sci. 1998;111:425-33.

Milenic DE, Brady ED, Brechbiel MW. Antibody-targeted radiation cancer therapy. Nat Rev Drug Discov. 2004;3:488-99.

Nielsen UB, Marks JD. Internalizing antibodies and targeted cancer therapy: direct selection from phage display libraries. Pharm. Sci. Technol. Today. 2000;3:282-291.

Ong GL, Mattes MJ. Re-evaluation of the concept of functional affinity as applied to bivalent antibody binding to cell surface antigens. Mol Immunol. 1993;30:1455-62.

Poul MA, Becerril B, Nielsen UB, et al. Selection of tumor-specific internalizing human antibodies from phage libraries. J Mol Biol. 2000;301:1149-61.

Press OW, Martin PJ, Thorpe PE, Vitetta ES. Ricin A-chain containing immunotoxins directed against different epitopes on the CD2 molecule differ in their ability to kill normal and malignant T cells. J Immunol. 1988;141:4410-7.

Press OW, Shan D, Howell-Clark J, et al. Comparative metabolism and retention of iodine-125, yttrium-90, and indium-111 radioimmunoconjugates by cancer cells. Cancer Res. 1996 ;56:2123-9.

Sharkey RM, Goldenberg DM. Advances in radioimmunotherapy in the age of molecular engineering and pretargeting. Cancer Invest. 2006;24:82-97.

Shih LB, Lu HH, Xuan H, et al. Internalization and intracellular processing of an anti-B-cell lymphoma monoclonal antibody, LL2. Int J Cancer. 1994;56:538-45.

Xavier KA, McDonald SM, McCammon JA, et al. Association and dissociation kinetics of bobwhite quail lysozyme with monoclonal antibody HyHEL-5. Protein Eng. 1999;12:79-83.

Yao Z, Garmestani K, Wong KJ, et al. Comparative cellular catabolism and retention of astatine-,bismuth-, and lead-radiolabeled internalizing monoclonal antibody. J Nucl Med. 2001;42:1538-44.

Zalutsky MR, Lewis JS. Handbook of radiopharmaceuticals. Eds. Welch JW, Redvanly CS. John Wiley & Sons, West Sussex, 2003; 685-714.

Chapter 8

CLONING, SEQUENCING AND EXPRESSION OF IMMUNOGLOBULIN VARIABLE REGIONS OF MURINE MONOCLONAL ANTIBODY 14C5

Burvenich I, Schoonooghe S, Coene E, Mertens N,
De Vos F and Slegers G

In preparation

8.1 Introduction

Maximal tumour targeting with minimal background or minimal exposure to normal organs is the goal for the clinical application of monoclonal antibodies (mAbs) in cancer diagnosis and therapy. In that regard, Fab and $F(ab')_2$ fragments of intact mAb 14C5 were developed and targeting properties were evaluated. Although improved background clearance was obtained at early time points compared with intact mAb 14C5, tumor uptake of fragments was significantly lower than that of intact mAb 14C5. These classic mono- and bivalent antibody fragments are easy to produce with fast enzymatic proteolysis, and can be evaluated within a short time frame. However, enzymatical proteolysis has a low efficiency and therefore is not economically interesting for clinical applications.

Genetic engineering provides powerful tools for manipulating the structure and pharmacokinetic properties of antibodies. One useful strategy has been the production of single chain fragments (scFv) containing the variable regions of the immunoglobulin heavy chain and light chain, covalently connected by a flexible peptide linker (Colcher et al., 1990). Several scFvs have been evaluated for their specific in vivo tumour targeting to antigens such as TAG-72, carcinoembryonic antigen (CEA) and the HER2/neu receptor. They demonstrated more rapid clearance and higher tumour-to-normal tissue ratios than the corresponding IgG or Fab fragments (Milenic et al., 1991; Adams GP et al., 1993; Wu AM et al., 1996). Furthermore, penetration of scFv into a tumor from the vasculature, as demonstrated with autoradiography, was superior to that of corresponding intact IgG, $F(ab')_2$ or Fab (Yokota et al., 1993).

Because of the rapid clearance of 25 kDa proteins from the blood pool, the maximum tumor uptake of a monomeric scFv is limited. Multivalent antibody constructs have demonstrated improved tumour uptake and intermediate blood

clearance ratios compared with scFv and intact antibodies. Different strategies have been described in literature for the formation of multivalent antibodies with altered pharmacokinetics and improved tumour uptake. Adams et al. (1993) described an improvement in *in vivo* tumour targeting using divalent forms of anti-*neu*-scFv with a C-terminal Gly_4Cys joined by a disulfide bond (Huston et al., 1994). Another antibody fragment, a minibody, was produced by fusion of T84.66 anti-CEA scFv to the human IgG1 CH3 domain (Hu et al. 1996). Others have fused scFvs to protein domains capable of multimerization, e.g., leucine zipper proteins (Kostelny et al., 1992), streptavidin (Dubel et al., 1995), or the κ-constant region (McGregor et al. 1994). The easiest approach for the production of dimeric scFvs is based on spontaneous formation of noncovalent dimers such as 50 kDa diabodies (Holliger, 1993). A recent overview of alternative antibody formats based on the scFv as building block is given by Carter (2006).

Except for altering pharmacokinetics, genetic engineering has another advantage. Mouse monoclonal antibodies have shown limited use as therapeutic agents in humans as a result of the production of human anti-mouse-antibodies (HAMA response). In an attempt to reduce the immunogenicity of mouse antibodies, genetic engineering was also used to generate chimeric antibodies, that is, antibodies with human constant regions and mouse variable regions. However, anti-chimeric antibody responses (HACAs) have been observed. Further minimization of the mouse component of antibodies can be achieved through complement determining region (CDR) grafting. In these humanized antibodies, only the CDR loops are inserted into the human variable framework.

Manipulating the structure and pharmacokinetic properties of mAb 14C5, increases the clinical usefulness of mAb 14C5 as novel agent for radioimmuno-

detection and radioimmunotherapy. The aim of this study was to clone and characterize Fv 14C5.

8.2 Materials and methods

8.2.1 Cell lines

HEK293T, a human embryonic kidney cell line transfected with SV40 large T-Ag ($SV40T^{tsA1609}$), was used for transient eukaryotic expression of recombinant Fab 14C5.

A549 cells, a human lung carcinoma cell line, were obtained from the Laboratory of Tumor and Developmental Biology (University of Liège, Liège, Belgium). A549 cells were cultured in DMEM (Cambrex), containing 2 mmol/l L-glutamine (Cambrex) and 10% fetal bovine serum (Cambrex).

8.2.2 scFv 14C5 cDNA synthesis and cloning with Recombinant Phage Antibody System

Purified mRNA was isolated from total RNA of 1×10^8 14C5 hybridoma cells (De Potter et al., 1994) by oligo(dT)-cellulose affinity chromatography. cDNA was synthesized using oligodT primers and avian myeloblastosis virus reverse transcriptase (AMV RT) (Promega) or Moloney murine leukaemia virus (MMLV) RT (Promega). The resulting cDNA was subjected to PCR using the primers (Heavy Primer 1, Heavy Primer 2, Light Primer Mix) of the Recombinant Phage Antibody System (Amersham Biosciences) for the isolation of the VH (340 bp) and VL (325 bp) domain. Both Taq and Vent polymerase conditions were used. Hot start PCR was carried out (5 min at 95°C, followed with 35 cycles under conditions of denaturing at 94°C for 1 min, annealing at 52°C for 1.5 min, and extension at 72°C for 1 min). 5 µl of PCR reaction was evaluated on a 1% agarose gel. VH and VL were sliced and purified with Qiaex II gel extraction kit (Qiagen). The antibody heavy chain

and light chain DNA are joined into a single chain using the Linker-Primer mix with Taq polymerase and Vent polymerase conditions (7 cycles as follows: 94°C for 1 minute, 63°C for 4 minutes). Reaction is analysed on a 1.5% agarose gel, sliced and purified with Qiaex II gel extraction kit. Following assembly, the amplified product (~750 bp) is digested with Sfi I and Not I for subsequent cloning into the pCANTAB 5 E phagemid. cDNA sequences were screened with PCR using 5' and 3' pCANTAB5 sequencing primer set (GE Healthcare). Nucleotide sequencing was performed by dideoxynucleotide chain-termination method using a DNA sequencing kit (BigDye terminator version 3.1 cycle sequencing) and nucleotide sequence homology analyses were performed using Clone Manager (Professional Suite 8, Scientific & Educational Software, NC, USA).

8.2.3 Fab 14C5 cDNA synthesis and cloning

Light and heavy chain of mAb 14C5 were separated with SDS-PAGE and transferred to a PVDF membrane. Protein bands were stained with Ponceau S before direct N-terminal sequence analysis (Edman degradation).

Purified mRNA was isolated from total RNA of 1×10^8 14C5 hybridoma cells by oligo(dT)-cellulose affinity chromatography. cDNA was synthesized using oligodT primers and avian myeloblastosis virus reverse transcriptase (AMV RT) (Promega) or Moloney murine leukaemia virus (MMLV) RT (Promega). The resulting cDNA was subjected to PCR using degenerate primers designed for VH (VH1-4 F) and VL (VL F) ends deduced from the N-terminal amino acid sequences obtained by the Edman degradation (Table 8.1).

Based on the alignment of different mouse IgG1 constant domain sequences, primers were designed for CH1 (CH1 B) and CL (CL B) Fab 14C5 ends. The CH1 B and CL B primers were designed to contain a BamHI, a BspEI and an ApaI restriction site.

Hot start touchdown PCR was carried out using Vent polymerase: 5 min at 95°C, followed with 9 cycles under conditions of denaturing at 95°C for 1 min, annealing starting at 57°C for 1 min (for every subsequent cycle, the temperature is decreased with 0.5°C), extension at 72°C for 2 min, and 25 cycles under conditions of denaturing at 95°C, annealing starting at 52°C for 1 min, extension at 72°C for 2 min. A final elongation step of 10 min at 72°C was used at the end.

Tabel 8.1 Primers and primer sequences for PCR with cDNA Fab 14C5

Name	Primers (5´ to 3´)
VH1 F	GARGTRAGYCTNGTKGARTCTGGDGGMG
VH2 F	GARGTRAGYTTRGTKGARTCTGGDGGMG
VH3 F	GARGTRTCNCTNGTKGARTCTGGDGGMG
VH4 F	GARGTRTCNTTRGTKGARTCTGGDGGMG
VL F	AGYATYGTGATGACHCAGACTCCMAAATTC
CH1 B	ATGGATCCTTATCCGGAGGGCCCAATTTTCTTGTCCACCTTGGTGCTGCTG
CL B	ATGGATCCTTATCCGGAGGGCCCACACTCATTCCTGTTGAAGCTCTTG
NM101	CAACGTGCTGGTTATTGTGCTGTC
NM105	TCGAGCCACCATGGGTTGGAGCTG
NM87	CAACAGATGGCTGGCAACTAGAAG

A, deoxyadenine; C, Deoxycytosine; G, deoxyguanidine; T; deoxythymidine; D, A+T+G; H, A+T+C; K, T+G; M, A+C; Y, C+T ; R, A+G ; N, A+G+C+T
restriction sites : _____, BamHI, ------, BspEI; _____,ApaI

The resulting PCR products were gel-purified in agarose and extracted using Qiaex II (Qiagen). The light chain VL-CL (L) was then cloned into a combination of pES33 (Eco47III/PvuI digest) 2030 bp fragment and pES31PH1LEZeo (BspEI/PvuI and Xho I digest) 3900 bp expression vector fragment containing a zeomycin selection site and E-tag. Similarly, the heavy chain fragment VH-CH1 (Fd) was cloned into a combination of pES33 (Eco47III/PvuI digest) 2030 bp fragment and pES31PH1HHisNeo (BspEI/PvuI and Xho I digest) 3535 bp expression vector fragment containing a neomycin selection site and $(His)_6$-tag. The L and Fd fragments were kinated with T4 kinase and introduced into the expression vectors by BspEI digest. cDNA

sequences were screened with PCR using 5' and 3' primers VH1 F, VH2 F, VH4 F, CH1 B, CL B, NM101, NM105, and NM87 (Table 8.1).
Nucleotide sequencing was performed by the dideoxynucleotide chain-termination method using a DNA sequencing kit (BigDye terminator version 3.1 cycle sequencing) and nucleotide sequence homology analyses were performed using Clone Manager.

8.2.4 Production of recombinant Fab 14C5 fragment

For transient expression, HEK293T cells were transfected according to the $Ca_3(PO_4)_2$ precipitation method (O'Mahoney et al., 1994). Twenty hours before transfection, HEK293T cells were seeded at 4×10^6 cells/175 cm^2. 1 µg DNA of each expression plasmid was added to the cells for 24 h, after which the cells were covered with supplemented DMEM containing 5 mg/l bovine insulin, 5 mg/l transferrin, and 5 µg/l selenium (ITS) replacing FCS. Medium was harvested every 48 hours after transfection. 200 µl Fab 14C5 of concentrated (40×) supernatant was applied to 2×10^5 A549 breast cancer cells and Fab 14C5 binding was analysed by flow cytometry. Secondary goat anti-mouse (H+L) Alexa-488 antibody was used (Invitrogen).

8.3 Results

8.3.1 cDNA cloning of the scFv 14C5 by Recombinant Phage Antibody System

The Recombinant Phage Antibody System (Amersham Biosciences) was used in a first attempt to isolate VH and VL cDNA of mAb 14C5. The amplified VH, VL and scFv DNAs were about 340 bp, 320 bp and 750 bp respectively. Following assembly, the amplified scFv product (~750 bp) was digested with Sfi I and Not I for subsequent cloning into the pCANTAB 5 E phagemid vector (Fig. 8.1).

After transformation, formed colonies were PCR screened and cDNA sequences were analyzed. After homology analyses, none of the analyzed sequences matched with sequences of heavy and light chain variable domains of a murine IgG1 antibody.

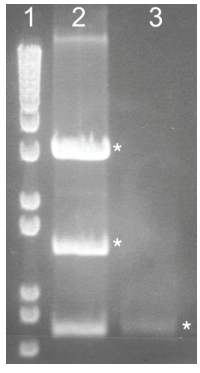

Fig. 8.1. Digest of scFv amplified product from hybridoma 14C5 cells. *lane 1*, 1 kb Plus DNA Ladder; *lane 2*, SfiI/NotI/BsaI digest of pCANTAB5 E phagemid vector (3070 bp, 1401 bp, 748 bp); *lane 3*, SfiI/NotI digest of amplified scFv 14C5 product; *, restriction fragments used in ligation

8.3.2 Fab 14C5 cDNA synthesis and cloning based on N-terminal amino acid sequences of mAb 14C5

Edman degradation of pure mAb 14C5 generated nine amino acid sequences (Glu-Val-Ser-Leu-Val-Glu-Ser-Gly-Gly) for the heavy chain and fifteen amino acid sequences (Ser-Ile-Val-Met-Thr-Gln-Thr-Pro-Lys-Phe-Leu-Leu-Val-Ser-Ala) for the light chain of mAb 14C5.

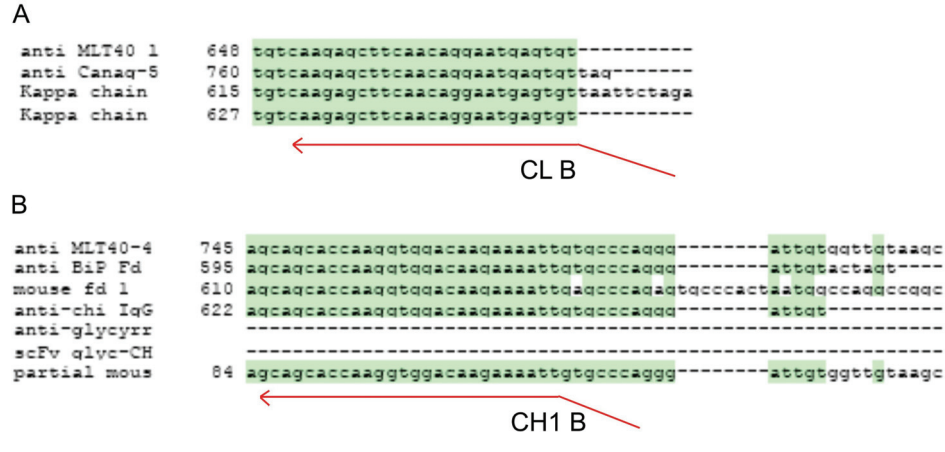

Fig. 8.2. Primer design for constant domains of light and heavy chain of mAb 14C5

Degenerate primers were designed (Table 8.1) based on these amino acids. In order to reduce degeneracy, N-terminal sequences of homologous IgG1 antibodies were compared to select the most common used codons. Based on the alignment of different mouse IgG1 constant domain sequences, primers were designed for CH1 (CH1 B) and CL (CL B) Fab 14C5 ends (Fig. 8.2). These primers were designed to contain a BamHI, a BspEI and an ApaI restriction site (Table 8.1). Touchdown PCR resulted in Fd chains when VH1, VH2, VH4 F and CH1 B primers were used, but not when the combination of VH3 F and CH1 B primers was used (Fig. 8.3). Light chain PCR fragment was formed when VL F and CL B primers were used.

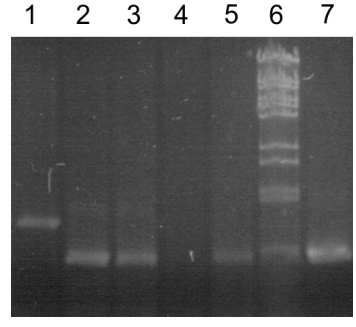

Fig. 8.3. PCR of 14C5 hybridoma cDNA with designed Fab primers. *Lane 1*, positive control, *β-actine* PCR product; *lane 2*, PCR fragment with VH1 F and CH1 B primer; *lane 3*, PCR fragment with VH2 F and CH1 B primer; lane 4, PCR fragment with VH3 F and CH1 B primer; lane 5, PCR fragment with VH4 F and CH1 B primer; lane 6, 1 kb Plus DNA Ladder (Invitrogen); lane 7, PCR fragment with VL F and CL B primer

The resultant PCR products (VH1, VH2, VH4, L) were introduced into a pES31 vector. After transformation, formed colonies were PCR screened and cDNA sequences were analyzed.

8.3.3 cDNA sequence analysis of variable domains of Fab 14C5

The DNA sequence and amino acid sequence of the heavy and light chain variable regions were deduced from the heavy chain and light chain sequences of the positive clones. As shown in Fig. 8.4, amino acid numbering and complementary determining regions (CDRs) of the VH (H1, H2 and H3) and

VL (L1, L2, and L3) domains were determined according to Kabat et al. (1991). The VH gene of mAb 14C5 belongs to the VH3d family. The Vκ gene fragments belong to the Vκ5 family (Kabat et al., 1991).

A

```
  1  AGT ATT GTG ATG ACC CAG ACT CCC AAA TTC CTG CTT GTA TCA GCA GGA GAC AGG GTT ACC ATA ACC
  1    S   I   V   M   T   Q   T   P   K   F   L   L   V   S   A   G   D   R   V   T   I   T

 67  TGC AAG GCC AGT CAG AGT GTG TAT AAT GAT GTA GCT TGG TAC CAA CAG AAG CCA GGG CAG TCT CCT
 23    C   K   A   S   Q   S   V   Y   N   D   V   A   W   Y   Q   Q   K   P   G   Q   S   P
         >>.................L1..................>>

133  AAA CTG CTG ATA TAC TAT GTA TCC AAT CGC TAC ACT GGA GTC CCT GAT CGC TTC ACT GGC AGT GGA
 45    K   L   L   I   Y   Y   V   S   N   R   Y   T   G   V   P   D   R   F   T   G   S   G
                       >>.........L2..........>>

199  TAT GGG ACG GAT TTC ACT TTC ACC ATC AGC ACT GTG CAG GCT GAA GAC CTG GCA GTT TAT TTC TGT
 67    Y   G   T   D   F   T   F   T   I   S   T   V   Q   A   E   D   L   A   V   Y   F   C

265  CAG CAC GAT TAT AGC TCT CCG TGG ACG TTC GGT GGA GGC ACC AAG CTG GAA ATC AAA
 89    Q   H   D   Y   S   S   P   W   T   F   G   G   G   T   K   L   E   I   K
       >>.............L3..............>>
```

B

```
  1  GAG GTG AGT CTT GTG GAG TCT GGG GGA GGC TTA GTG AAG CCT GGA GGG TCC CTG AAA CTC TCC TGT
  1    E   V   S   L   V   E   S   G   G   G   L   V   K   P   G   G   S   L   K   L   S   C

 67  GCA GCC TCT GGA TTC ACT TTC AAT ACC TAT GCC ATG TCT TGG GTT CGC CAG AGT CCA GAG AAG AGG
 23    A   A   S   G   F   T   F   N   T   Y   A   M   S   W   V   R   Q   S   P   E   K   R
                               >>.....H1.....>>

133  CTG GAG TGG GTC GCA TCC ATT AGT AGT GGT GGT ACC ACC TAT TTT CCA GAC AGT GTG CAG GGC CGA
 45    L   E   W   V   A   S   I   S   S   G   G   T   T   Y   F   P   D   S   V   Q   G   R
                       >>.........................H2.........................>>

199  TTC ACC ATC TCC AGA GAT AAT GCC AGG AAC ATC CTG TAC CTG CAA ATG AGC AGT CTG AGG TCT GAG
 67    F   T   I   S   R   D   N   A   R   N   I   L   Y   L   Q   M   S   S   L   R   S   E

265  GAC ACG GCC ATA TAT TAC TGT ACA AGA GGC ACG ACG GGC AGG TCG TAT ACT ATG GAC TAC TGG GGT
 89    D   T   A   I   Y   Y   C   T   R   G   T   T   G   R   S   Y   T   M   D   Y   W   G
                           >>..........H3..........>>

331  CAA GGA ACC TCA GTC ACC GTC TCC TCA
111    Q   G   T   S   V   T   V   S   S
```

Fig. 8.4. The amino acid sequences are aligned and organized into different complement determining regions (CDR) and framework regions, as defined by Kabat et al. (1991). *(A)* Vκ gene of mAb 14C5 with L1, L2, and L3 showing CDR regions of kappa light chain. *(B)* VH gene of mAb 14C5 with H1, H2, and H3 showing CDR regions of heavy chain.

8.3.4 Quantitative analysis of the recombinant Fab 14C5

Co-expression of L and Fd chains is expected to yield Fab 14C5 fragments in the supernatant. Supernatant was concentrated and analysed for binding with A549 lung cancer cells. The antigen-binding of the concentrated recombinant Fab proteins by flow cytometry is shown (Fig. 8.5).

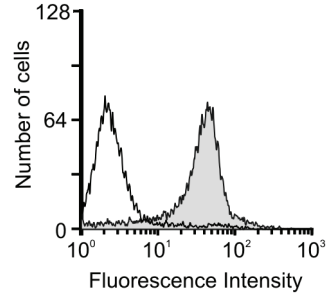

Fig. 8.5. Histogram of flow cytometric analysis of recombinant Fab 14C5 binding to A549 lung cancer cells. Open histograms, negative control; filled histograms, recombinant Fab 14C5

8.4 Discussion

In this study, we described the cloning and sequencing of the variable (V) genes of mAb 14C5. Following Kabat et al. (1991) the CDR regions were deduced. The VH gene of mAb 14C5 belongs to the VH3a/d family. The Vκ gene belongs to the Vκ5 family (Kabat et al., 1991). Flow cytometry study with recombinant Fab 14C5 demonstrated binding with the antigen 14C5. This indicates that the cloned variable genes encode the variable domains of a functional anti-Ag 14C5 antibody fragment.

These results offer opportunities for further optimization of mAb 14C5 with antibody engineering for applications in radioimmunodetection and -therapy. The V-genes can be used to construct a functional scFv fragment. Based on the V-gene sequences, primers can be designed hybridizing to the flanking regions of the Vκ and VH gene. After amplification of V genes, the two variable regions can be artificially joined using a single 15-amino acid linker $(Gly_4Ser)_3$. This flexible peptide linker is specifically designed to bridge the 3.5 nm gap between the carboxy-terminus of the VH chain and the amino-terminus of the VL chain (Huston et al., 1988). The affinity and stability of scFv antibodies containing the $(Gly_4Ser)_3$ linker are generally comparable to those of the native antibody (Huston et al., 1988; Glockshuber et al., 1991; Takkinen et al., 1991).

Altering pharmacokinetics of mAb 14C5, the recombinant Fab chain can be used as heterodimerization scaffold for the construction of multivalent anti-mAb 14C5 antibodies (Schoonjans et al., 2000) or the resulting scFv molecules can be linked with polypeptide linkers resulting in multivalent scFv constructs (Carter, 2006). Tags can be added such as $(His)_6$ which facilitates radiolabeling with other isotopes than radioiodine, i.e. ^{99m}Tc can be used by the tricarbonyl system (Willuda et al., 2001).

Moreover, to reduce the immunogenicity of murine mAb 14C5, the 14C5 V genes can be used to construct chimeric antibodies (Imai et al., 2006). Secondly, although labour-intensive, grafting the CDR regions into the most closely related human antibody framework is an established technique. Ewert et al. (2004) reviewed two methods for knowledge-based improvement of antibody stability and folding efficiency. Hereby, CDR grafting is done in more distantly related, but stable acceptant frameworks and secondly, improving a suboptimal framework is done by the introduction of point mutations designed to optimize key residue interactions.

Also, a broader range of applications of mAb 14C5 is now possible. Toxins and drugs instead of isotopes can be coupled to mAb 14C5 and guided to the tumour. Bispecific antibodies can be designed and used to activate the immune system or to be employed in pretargeting strategies (Sharkey and Goldenberg, 2006).

8.5 Conclusion

In this study, mAb 14C5 was characterized by cloning and sequencing its variable genes. This opens the way to a broad range of applications including altering pharmacokinetics, reducing immunogenicity, the use of a variety of isotopes, conjugation of drugs or toxins, the design of bispecific antibodies and pretargeting strategies.

8.6 References

Adams GP, McCartney JE, Tai MS, et al. Highly specific in vivo tumor targeting by monovalent and divalent forms of 741F8 anti-c-erbB-2 single-chain Fv. Cancer Res. 1993;53:4026-34.

Burvenich I., Schoonooghe S., Blanckaert P., et al. Biodistribution and planar gamma camera imaging of ^{123}I- and ^{131}-I-labeled F(ab')$_2$ and Fab fragments of monoclonal antibody 14C5 in nude mice bearing an A549 lung tumor. Nuc Med Biol 2007, *in press*.

Carter PJ. Potent antibody therapeutics by design. Nat Rev Immunol. 2006;6:343-57.

Colcher D, Bird R, Roselli M, et al. In vivo tumor targeting of a recombinant single-chain antigen-binding protein. J Natl Cancer Inst. 1990;82:1191-7.

Dubel S, Breitling F, Kontermann R, et al. Bifunctional and multimeric complexes of streptavidin fused to single chain antibodies (scFv). J Immunol Methods. 1995;178:201-9.

Ewert S, Honegger A, Pluckthun A. Stability improvement of antibodies for extracellular and intracellular applications: CDR grafting to stable frameworks and structure-based framework engineering. Methods. 2004;34:184-99.

Glockshuber R, Malia M, Pfitzinger I, et al. A comparison of strategies to stabilize immunoglobulin Fv-fragments. Biochemistry. 1990;29:1362-7.

Holliger P, Prospero T, Winter G. "Diabodies": small bivalent and bispecific antibody fragments. Proc Natl Acad Sci U S A. 1993;90:6444-8.

Hu S, Shively L, Raubitschek A, et al. Minibody: A novel engineered anti-carcinoembryonic antigen antibody fragment (single-chain Fv-CH3) which exhibits rapid, high-level targeting of xenografts. Cancer Res. 1996;56:3055-61.

Huston JS, Adams GP, McCartney JE, et al. Tumor targeting in a murine tumor xenograft model with the (sFv')2 divalent form of anti-c-erbB-2 single-chain Fv. Cell Biophys. 1994;24-25:267-78.

Huston JS, Levinson D, Mudgett-Hunter M, et al. Protein engineering of antibody binding sites: recovery of specific activity in an anti-digoxin single-chain Fv analogue produced in Escherichia coli. Proc Natl Acad Sci U S A. 1988;85:5879-83.

Kostelny SA, Cole MS, Tso JY. Formation of a bispecific antibody by the use of leucine zippers. J Immunol. 1992;148:1547-53.

McGregor DP, Molloy PE, Cunningham C, et al. Spontaneous assembly of bivalent single chain antibody fragments in Escherichia coli. Mol Immunol. 1994;31:219-26.

Milenic DE, Yokota T, Filpula DR, et al. Construction, binding properties, metabolism, and tumor targeting of a single-chain Fv derived from the pancarcinoma monoclonal antibody CC49. Cancer Res. 1991;51:6363-71.

O'Mahoney JV, Adams TE. Optimization of experimental variables influencing reporter gene expression in hepatoma cells following calcium phosphate transfection. DNA Cell Biol. 1994;13:1227-32.

Schoonjans R, Willems A, Schoonooghe S, et al. Fab chains as an efficient heterodimerization scaffold for the production of recombinant bispecific and trispecific antibody derivatives. J Immunol. 2000;165:7050-7.

Sharkey RM, Goldenberg DM. Advances in radioimmunotherapy in the age of molecular engineering and pretargeting. Cancer Invest. 2006;24:82-97.

Takkinen K, Laukkanen ML, Sizmann D, et al. An active single-chain antibody containing a cellulase linker domain is secreted by Escherichia coli. Protein Eng. 1991;4:837-41.

Willuda J, Kubetzko S, Waibel R, et al. Tumor targeting of mono-, di-, and tetravalent anti-p185(HER-2) miniantibodies multimerized by self-associating peptides. J Biol Chem. 2001;276:14385-92.

Wu AM, Chen W, Raubitschek A, et al. Tumor localization of anti-CEA single-chain Fvs: improved targeting by non-covalent dimers. Immunotechnology. 1996;2:21-36.

Yokota T, Milenic DE, Whitlow M, et al. Microautoradiographic analysis of the normal organ distribution of radioiodinated single-chain Fv and other immunoglobulin forms. Cancer Res. 1993;53:3776-83.

Chapter 9

GENERAL DISCUSSION AND FUTURE PERSPECTIVES

GENERAL DISCUSSION AND FUTURE PERSPECTIVES

In the first part of this thesis (Chapter 3 and Chapter 4), we tried to identify and characterize antigen 14C5 as a new tumour associated antigen for antibody targeting. We found that antigen 14C5 is likely to be the integrin αvβ5 receptor and that the antigen is highly expressed on a variety of human cancer cell lines. Analysing the expression levels on human lung and colon cancer tissues by immunohistochemistry showed that the location of antigen 14C5 in patients is often associated with fibroblasts in the stroma surrounding the tumour cells and to a lesser extent associated at the tumour cell surface. This was also reported by Coene et al. (1997) for the expression of Ag 14C5 on human breast cancer tissues. Interestingly, Kalluri et al. (2006) discuss the potential role of fibroblast as cancer targets. A promising candidate for specifically targeting cancer associated fibroblasts is sibrotuzumab, an antibody to human fibroblast-activation protein (FAP). A phase I dose-escalation study with sibrotuzumab in patients with advanced colorectal or non-small cell lung cancer showed that sibrotuzumab specifically binds to the tumour sites without apparent site effects (Scott et al., 2003). Preclinical therapeutic studies with mAb 14C5 have to show whether our antibody is capable of showing similar or better therapeutic effects. Further studies on the expression of Ag 14C5 and αvβ5 have to show whether αvβ5 is an indicator of the fibroblast phenotype (Scaffidi et al., 2001).

Because antigen 14C5 is expressed on epithelial cancer cells as well as in the surrounding tumour stroma, Ag 14C5 is potentially suitable for antibody targeting. For many years, all of the efforts to treat cancer have been concentrated on the inhibition or destruction of tumour cells. Recently, many research groups start to believe that strategies to treat the tumour cell and to

modulate the host microenvironment could provide a better approach for the treatment of cancer. Therefore, many recent reviews discuss the role of the tumour microenvironment as potential target for targeted therapies (Fidler et al., 2002; Fidler et al., 2003; Hofmeister et al., 2006; Kalluri et al., 2006). The different strategies involve anti-angiogenesis and anti-vascularization (Folkman, 2006; Kerbel, 2006), anti-fibroblast (Micke et al., 2005; Kalluri et al., 2006), and anti-integrin therapeutics (Pasqualini et al., 1997; Paulhe et al., 2005). This supports the potential of antigen 14C5 as target and warrants its further investigation.

Comparing the binding of mAb 14C5 with another αvβ5 antibody (P1F6), we showed similar expression patterns, although specific as well as non-specific staining of the latter was more intense. Also, blocking studies with mAb 14C5 could block the specific binding of ^{125}I-labeled anti-αvβ5 to A549 lung cancer cells, confirming that the identity of antigen 14C5 most likely is the integrin αvβ5 receptor. Integrin αvβ5 belongs to a widely expressed family of cell adhesion receptors that recognise extracellular matrix proteins and cell surface antigens. Different integrin members have been associated with tumour progression (Mizejewski et al., 1999; Hynes et al., 2002; Kerr et al., 2002; Wehrle-Haller et al., 2003; Jin et al., 2004; Haubner, 2006; Serini et al., 2006). Moreover, antibodies targeting similar integrins are currently under clinical investigation, including CNTO95 (a fully human anti-αv antibody, binds αvβ3 and αvβ5) (Davis et al., 2004; Jayson et al., 2004; Trikha et al., 2004; Martin et al., 2005) and Vitaxin (a humanized anti-αvβ3 antibody). The high-affinity humanized anti-αvß3 antibody (Vitaxin) is in clinical development as an anti-angiogenic therapeutic (Gutheil et al., 2000); unfortunately, so far its tumour-targeting performance for cancer imaging and therapy has been unsatisfactory (Posey et al., 2001; Cai and Chen, 2006). Cilengitide, a cyclic RGD peptide in clinical trials for metastatic cancer has been tested in an aggressive breast

cancer model in combination with ^{90}Y-labeled chimeric anti-L6 radioimmunotherapy, which remarkably increased efficacy and apoptosis, compared to single-modality therapy with either agent, without additional toxicity (Burke et al., 2002). Noninvasive PET and SPECT imaging of integrin expression have been done with monomeric, dimeric and tetrameric RGD peptides and peptidomimetics (Lewis, 2005; Dijkgraaf et al., 2006a-b; Haubner, 2006; Zhang et al., 2006).

In the near future, the most important challenge will be the novelty or lack of novelty regarding antigen 14C5 as a new cancer associated target from an intellectual property perspective, limiting its potential application in the clinic. Therefore, distinguishing antigen 14C5 and/or mAb 14C5 from the already existing targets and antibodies must be the highest priority in further mAb 14C5 development. Secondly, priority must be given to the non-specific targets in normal tissues. De Potter et al. (1994) and Coene et al. (1997) reported no expression of Ag 14C5 on normal epithelial, muscle, and connective tissues including skin, thyroid, parathyroid, colon, stomach, lung, uterine tube, ovary, ureter, urethra, lymph node, nerve, chondroid tissue, skeletal muscle, oesophagus, and artery. Sometimes, low-level staining of myo-epithelial cells was observed in biopsies of breast tissue and in tubular cells of the kidney. In this thesis, sometimes small blood vessels and mucous secreting cells on normal colon tissue were stained with mAb 14C5. The FDA guidelines (1997) concerning the development of antibody drugs suggest sampling of 32 different normal tissue types to look for expression on normal tissue for risk assessment. However, it is not necessary to fully satisfy all of these criteria as evidenced by clinical approval of antibodies targeting HER2 (Herceptin), CD20 (Rituxan, Zevalin and Bexxar), CD33 (Mylotarg), CD52 (Campath) and epidermal growth factor receptor (EGFR) (Erbitux) (Carter et al., 2004). To conclude antigen 14C5 expression, the involvement of Ag 14C5 in the cancer

associated fibroblasts should be further explored, as it might lead to an interesting antibody-based therapeutic concept for mAb 14C5.

Potentially suitable for antibody targeting, the second part of the thesis investigated the *in vitro* and *in vivo* targeting properties of radioiodinated mAb 14C5 (Chapter 5) and optimization strategies including mAb 14C5 fragments Fab and $F(ab')_2$ (Chapter 6), the possibility of internalization (Chapter 7) and finally the cloning and sequencing of scFv 14C5 (Chapter 8).

Few validated surface antigens have demonstrated robust anti-tumour activity using so-called 'naked' antibodies. Fortunately, the potency of anti-cancer antibodies can be improved in numerous ways including arming with potent drugs (Payne, 2003) or radionuclides (Goldenberg, 2003). These arming technologies have lead to the regulatory approval of the antibody drugs, Mylotarg, Zevalin, and Bexxar, conjugated with the drug calicheamicin, and the radionuclides ^{90}Y and ^{131}I, respectively (Carter, 2006). For this reason and working at a radiopharmaceutical lab, our first antibody-based therapeutic concept of choice was investigating the potency of radioimmunotherapy with mAb 14C5. However, given the anti-substrate adhesion function of mAb 14C5, we can not exclude that the naked antibody itself could have a significant therapeutic activity. Initial steps are made to investigate the blocking function of mAb 14C5 *in vivo* by a model which uses HT-1080 fibrosarcoma cells transfected with the *lacZ* gene (Schweinitz et al., 2004).

The studies presented in this thesis showed that radioiodinated mAb 14C5 binds its antigen with high affinity (K_d, 0.2 nmol/l), showed good and specific tumour uptake *in vivo* and good planar gamma camera imaging quality. However, the blood clearance is slow which is typical for a 150 kDa sized intact antibody. Many efforts of various groups have been undertaken in increasing the tumour-to-background ratio and to increase tumour penetration.

A common approach is the development of smaller antibody fragments by enzymatic digestion (papain, pepsin or ficin) and genetically engineered single-chain Fv (scFv) constructs of antibody molecules (Reff, 2001; Goldenberg, 2002; Batra et al., 2002). Being able to provide Fab and $F(ab')_2$ fragments of mAb 14C5 in an easy and short way, we investigated targeting properties of these both fragments. Biodistribution results showed increased tumour-to-blood and tumour-to-muscle ratios, but the overall tumour uptake of both fragments was significantly reduced, necessitating the further optimization of mAb 14C5.

Genetic engineering provides powerful tools for manipulating structure and pharmacokinetic properties of antibodies. One useful strategy has been the production of single chain fragments (scFv) containing the variable regions of the immunoglobulin heavy chain and light chain, covalently connected by a flexible peptide linker (Colcher et al., 1990). Although a scFv is too small (25 kDa) and therefore often not suitable for targeting due to rapid clearance, it can be used as a building block for multivalent molecules which have intermediate sizes above the exclusion limit for kidney filtration. Moreover, genetic engineering can be used to reduce the immunogenicity of mouse antibodies, generating chimeric antibodies or through complement determining region (CDR) grafting. In chapter 8, the VH and VL chain genes of mAb 14C5 were identified, which makes it now possible to develop a multivalent intermediate of mAb 14C5 with less immunogenicity and more suitable targeting properties.

REFERENCES

Batra SK, Jain M, Wittel UA, et al. Pharmacokinetics and biodistribution of genetically engineered antibodies. Curr Opin Biotechnol. 2002;13:603-8.

Burke PA, DeNardo SJ, Miers LA, et al. Cilengitide targeting of alpha(v)beta(3) integrin receptor synergizes with radioimmunotherapy to increase efficacy and apoptosis in breast cancer xenografts. Cancer Res. 2002;62:4263-72.

Cai W, Chen X. Anti-angiogenic cancer therapy based on integrin alphavbeta3 antagonism. Anticancer Agents Med Chem. 2006;6:407-28

Carter P, Smith L, Ryan M. Identification and validation of cell surface antigens for antibody targeting in oncology. Endocr Relat Cancer. 2004;11:659-87.

Carter P. Potent antibody therapeutics by design. Nat Rev Immunol. 2006;6:343-57.

Coene E, Schelfhout AM, De Ridder L, De Potter CR. Generation of a monoclonal antibody directed against a human cell substrate adhesion molecule and the expression of the antigen in human tissues. Hybridoma 1997;16:77-83.

Colcher D, Bird R, Roselli M, et al. In vivo tumor targeting of a recombinant single-chain antigen-binding protein. J Natl Cancer Inst. 1990;82:1191-7.

Davis, HM, Prabhakar, U, Jang, H, et al. A rational approach for a phase I clinical study design to evaluate CNTO 95, a novel, fully human anti-a(v) monoclonal antibody (MAb), in patients with solid tumors. J Clin Oncol. 2004;22:190S-190S.

De Potter CR, Schelfhout AM, De Smet FH, et al. A monoclonal antibody directed against a human cell membrane antigen prevents cell substrate adhesion and tumor invasion. Am J Pathol 1994;144:95-103.

Dijkgraaf I, Kruijtzer JA, Frielink C, et al. alpha(v)beta(3) Integrin-targeting of intraperitoneally growing tumors with a radiolabeled RGD peptide. Int J Cancer. 2006 *Epub ahead of print*

Dijkgraaf I, Kruijtzer JA, Liu S, et al. Improved targeting of the alpha(v)beta (3) integrin by multimerisation of RGD peptides. Eur J Nucl Med Mol Imaging. 2006 *Epub ahead of print*

Fidler IJ. The organ microenvironment and cancer metastasis. Differentiation. 2002;70:498-505.

Fidler IJ. The pathogenesis of cancer metastasis: the 'seed and soil' hypothesis revisited. Nat Rev Cancer. 2003;3:453-8.

Folkman J. Angiogenesis. Annu Rev Med. 2006;57:1-18.

Goldenberg DM. Targeted therapy of cancer with radiolabeled antibodies. J Nucl Med. 2002;43:693-713.

Goldenberg DM. Advancing role of radiolabeled antibodies in the therapy of cancer. Cancer Immunology Immunotherapy 2003;52:281–96.

Gutheil JC, Campbell TN, Pierce PR, et al. Targeted antiangiogenic therapy for cancer using Vitaxin: a humanized monoclonal antibody to the integrin alphavbeta3. Clin Cancer Res. 2000;6:3056-61.

Haubner R. alpha(v)beta (3)-integrin imaging: a new approach to characterise angiogenesis? Eur J Nucl Med Mol Imaging. 2006;33 Suppl 13:54-63.

Hofmeister V, Vetter C, Schrama D, et al. Tumor stroma-associated antigens for anti-cancer immunotherapy. Cancer Immunol Immunother. 2006;55:481-94.

Hynes RO. A reevaluation of integrins as regulators of angiogenesis. Nat Med. 2002;8:918-21.

Jayson, GC, Mullamitha, S, Ton, C, et al. Phase I study of CNTO 95, a fully human monoclonal antibody (mAb) to alpha v integrins, in patients with solid tumors. J Clin Oncol. 2004;22: 224S-224S.

Jin H, Varner J. Integrins: roles in cancer development and as treatment targets. Br J Cancer. 2004;90:561-5.

Kalluri R, Zeisberg M. Fibroblasts in cancer. Nat Rev Cancer. 2006;6:392-401.

Kerbel RS. Antiangiogenic therapy: a universal chemosensitization strategy for cancer? Science. 2006;312:1171-5.

Kerr JS, Slee AM, Mousa SA. The alpha v integrin antagonists as novel anticancer agents: an update. Expert Opin Investig Drugs. 2002;11:1765-74.

Lewis MR. Radiolabeled RGD peptides move beyond cancer: PET imaging of delayed-type hypersensitivity reaction. J Nucl Med. 2005;46:2-4.

Martin PL, Jiao Q, Cornacoff J, et al. Absence of adverse effects in cynomolgus macaques treated with CNTO 95, a fully human anti-alphav integrin monoclonal antibody, despite widespread tissue binding. Clin Cancer Res. 2005;11:6959-65.

Micke P, Ostman A. Exploring the tumour environment: cancer-associated fibroblasts as targets in cancer therapy. Expert Opin Ther Targets. 2005;9:1217-33.

Mizejewski GJ. Role of integrins in cancer: survey of expression patterns. Proc Soc Exp Biol Med. 1999 Nov;222(2):124-38.

Pasqualini R, Koivunen E, Ruoslahti E. Alpha v integrins as receptors for tumor targeting by circulating ligands. Nat Biotechnol. 1997;15:542-6.

Paulhe F, Manenti S, Ysebaert L, et al. Integrin function and signaling as pharmacological targets in cardiovascular diseases and in cancer. Curr Pharm Des. 2005;11:2119-34.

Payne G. Progress in immunoconjugate cancer therapeutics. Cancer Cell 2003;3:207–12.

Posey JA, Khazaeli MB, DelGrosso A, et al. A pilot trial of Vitaxin, a humanized anti-vitronectin receptor (anti alpha v beta 3) antibody in patients with metastatic cancer. Cancer Biother Radiopharm. 2001;16:125-32.

Reff ME, Heard C. A review of modifications to recombinant antibodies: attempt to increase efficacy in oncology applications. Crit Rev Oncol Hematol. 2001;40:25-35.

Scaffidi AK, Moodley YP, Weichselbaum M, et al. Regulation of human lung fibroblast phenotype and function by vitronectin and vitronectin integrins. J Cell Sci. 2001;114:3507-16.

Schweinitz A, Steinmetzer T, Banke IJ, et al. Design of novel and selective inhibitors of urokinase-type plasminogen activator with improved pharmacokinetic properties for use as antimetastatic agents. J Biol Chem. 2004;279:33613-22.

Scott AM, Wiseman G, Welt S, et al. A Phase I dose-escalation study of sibrotuzumab in patients with advanced or metastatic fibroblast activation protein-positive cancer. Clin Cancer Res. 2003;9:1639-47.

Serini G, Valdembri D, Bussolino F. Integrins and angiogenesis: a sticky business. Exp Cell Res. 2006;312:651-8.

Trikha M, Zhou Z, Nemeth JA, et al. CNTO 95, a fully human monoclonal antibody that inhibits alphav integrins, has antitumor and antiangiogenic activity in vivo. Int J Cancer. 2004;110:326-35.

Wehrle-Haller B, Imhof BA. Integrin-dependent pathologies. J Pathol. 2003;200:481-7.

Zhang X, Xiong Z, Wu Y, et al. Quantitative PET imaging of tumor integrin alphavbeta3 expression with 18F-FRGD2. J Nucl Med. 2006;47:113-21.

Chapter 10

SUMMARY
SAMENVATTING

SUMMARY

In search of new antibody therapeutics for inhibition of metastatic breast cancer, De Potter et al. (1994) developed several mouse monoclonal antibodies (mAbs) against epitopes on the extracellular membrane of SK-BR-3 human breast cancer cells. One of these mAbs is the IgG1 mAb 14C5, which recognizes an extracellular plasma membrane antigen expressed on SK-BR-3 and MCF-7 human breast cancer cells. The antibody is capable of reversibly inhibiting the adhesion of SK-BR-3 cells on both culture-treated plastic and on pronectin-, fibronectin-, osteopontin-, and vibronectin-precoated culture plates. Furthermore, mAb 14C5 has been shown to prevent invasion and, subsequently, metastasis of SK-BR-3 and MCF-7 cells on host tissue in vitro. In addition, mAb 14C5 and its anti-idiotypic counterpart (mAb ACA 14C5) was able to significantly inhibit tumor growth in a dose-dependent way in Sprague–Dawley rats bearing HH-16 clone 1/2 adenocarcinomas or fibrosarcomas overexpressing the 14C5 antigen. In the past, different strategies have failed to identify the antigen 14C5. Therefore, the foci of this research were to identify and further characterize antigen 14C5 as potential target for mAb 14C5-based immunotherapies and to explore the targeting properties of radioiodinated mAb 14C5 for radioimmunodetection and –therapy.

First, we tried to purify antigen 14C5 by mAb 14C5 affinity-column chromatography. No specific protein components in the purified SKBR-3 or HT-1080 lysates were found after western blot analysis. Biacore analysis showed that only little amounts of soluble antigen 14C5 are available in mAb 14C5 affinity-column purified SKBR-3 lysate. A possible explanation for both western blot and Biacore analysis failure could be a conformation change of the soluble protein as compared to the cell surface expressed antigen. Therefore, other strategies were explored to identify the antigen.

It was already suggested by De Potter et al. (1994) and Coene et al. (1997) that antigen 14C5 could be related to the family of integrins. We further explored this idea by comparing the expression of the antigen 14C5 with the expression

of eight different integrin subunits (α1, α2, α3, αv, β1, β2, β3, and β4) and three different integrins heterodimers (αvβ3, αvβ5, and α5β1). Basically, we selected integrins involved in cancer pathology which could possibly block cell-substrate-adhesion, since these are both characteristics of mAb 14C5. By flow cytometry at saturating conditions, anti-αvβ5 specific antibody (P1F6) showed equivalent expression levels to mAb 14C5. In a blocking assay with mAb 14C5, the αvβ5 receptors could be significantly blocked by mAb 14C5, indicating that antigen 14C5 is the αvβ5 receptor. Flow cytometry analysis of Colo16 cells transfected with human *αv* and *β5* cDNA, demonstrated that subpopulations expressing both sub-units bind mAb 14C5.

Immunocytochemical analysis and flow cytometry analysis show that the expression of antigen 14C5 is not restricted to the breast cancer cell lines but is also present in varying degrees on other neoplastic human cell lines from different origins: carcinomas of ovary, cervix, lung, colon, and pancreas, sarcomas, and melanomas. Flow cytometric results showed that 9 out of 15 of the investigated cell lines showed high expression of antigen 14C5. Among these, the A549 lung cancer cells showed the highest antigen 14C5 expression, providing a possible new target for non-small cell lung cancer (NSCLC) therapy. Further expression analysis of the antigen 14C5 was done by immunohistochemistry of human lung carcinoma and human colon carcinoma. In both these tumour types, Ag 14C5 expression mainly occurred in the stroma and on stromal fibroblasts surrounding the tumour cells and to a lesser extent at the tumour cells. Further studies on the expression of antigen 14C5 have to show whether antigen 14C5 is an indicator of the fibroblast cancer-associated phenotype.

To further characterize the antigen 14C5, immunohistochemical staining with mAb 14C5 was compared with αvβ5 specific (P1F6) staining. No discrepancy

was found in the expression patterns between the two antibodies. However, staining with anti- αvβ5 was more intense, specific as well as non-specific.

The second part of the thesis explored the potential of radioiodinated mAb 14C5 as agent for radioimmunodetection and –therapy. Saturation binding analysis showed that radioiodinated mAb 14C5 binds its antigen with high affinity (K_d, 0.2 ± 0.1 nmol/l, A549 lung carcinoma cells), showed good and specific tumour uptake *in vivo* and good planar gamma camera imaging quality. However, the blood clearance was slow, which is typical for a 150 kDa sized intact antibody.

Fab and F(ab')$_2$ fragments of intact mAb 14C5 were generated with a ficin column. Saturation binding analysis showed that radioiodinated F(ab')$_2$ still binds antigen 14C5 with high affinity (K_d, 0.4 ± 0.1 nmol/l), while radioiodinated Fab looses affinity due to its monomeric binding (K_d, 2.3 ± 0.4 nmol/l). Clearance from the blood was faster with Fab and F(ab')$_2$ fragments. The alpha half-life ($t_{½}\alpha$) values for Fab, F(ab')$_2$ and mAb 14C5 were 14.9 min, 21 min and 118 min, respectively. The beta half-life ($t_{½}\beta$) values for Fab, F(ab')$_2$ and mAb 14C5 were 439 min, 627 min and 4067 min, respectively. Biodistribution results showed increased tumour-to-blood and tumour-to-muscle ratios, but the overall tumour uptake of both fragments was significantly reduced, necessitating further optimization of mAb 14C5.

Internalization can lead to a rapid loss of the radiolabel from the tumor cell, because this process exposes the labelled mAb to intracellular catabolic processes in the lysosomes. We investigated the fate of the ^{125}I-labelled mAb 14C5-antigen complex. Studies were also conducted with ^{125}I-labeled F(ab')$_2$ and Fab fragments. Internalization of mAb 14C5 and its F(ab')$_2$ fragment was seen in A549 cells, both with confocal laser scanning microscopy and using radioiodinated antibodies. No protein metabolites attributable to the

internalization process are shown within the first 2 hours of internalization, although some authors have reported antibody degradation starting at 2 hours. Also, the amount of free ^{125}I or ^{125}I-monoiodotyrosine released into the supernatant was <5% of initially bound radioactivity. These data suggest that mAb 14C5 and F(ab')$_2$ are slowly catabolized. ^{125}I-Fab 14C5 fragments were almost not internalized, suggesting that there might be a need of bivalency for internalization of the antibody-antigen 14C5 complex. However, ^{125}I-Fab showed a rapid dissociation, which can limit its use in patients.

Genetic engineering provides powerful tools for manipulating the structure and pharmacokinetic properties of antibodies. It offers the opportunity to change the antibody characteristics (structure, size, valence, immunogenicity, etc.) in order to obtain optimal targeting properties. In this context, the variable heavy and variable light chain genes were sequenced and the complement determining regions characterizing mAb 14C5 were identified. This opens the way to a broad range of applications including altering pharmacokinetics, reducing immunogenicity, the use of a variety of isotopes, conjugation of drugs or toxins, the design of bispecific antibodies and pretargeting strategies.

SAMENVATTING

In een poging om nieuwe therapeutische antilichamen te maken voor de inhibitie van borstkankermetastasen, ontwikkelden De Potter et al. (1994) verschillende monoklonale muisantilichamen (MALs) gericht tegen epitopen gelegen op het extracellulaire membraan van SK-BR-3 humane borstkankercellen. Eén van deze antilichamen, het IgG1 MAL 14C5, herkent een extracellulair membraanantigeen dat voorkomt op SK-BR-3 en MCF-7 borstkankercellen. Dit antilichaam heeft als eigenschap dat het de adhesie kan inhiberen van SK-BR-3 cellen op een celcultuurplaat en op cultuurplaten waarop pronectine, fibronectine, osteopontine of vibronectine werd gebonden. Bovendien toonden in vitro testen aan dat het MAL 14C5 invasie en metastasering in gastweefsel kon verhinderen. Significante tumorgroei-inhibitie werd waargenomen in Sprague-Dawley ratten met een anti-idiotypische tegenhanger van MAL 14C5 (MAL ACA 14C5). Deze groei-inhibitie was dosis afhankelijk en werd aangetoond met HH-16 kloon ½ adenocarcinomas of fibrosarcomas die beide het antigeen 14C5 tot overexpressie brachten. Ondanks vele pogingen, kon men het antigeen 14C5 nog niet identificeren. De doelstellingen van deze studie waren de identificatie en verdere karakterisatie van het antigeen als mogelijk doelwit voor immunotherapie met MAL 14C5 en onderzoek naar de targeting eigenschappen van radiogejodeerd MAL 14C5 voor radioimmunodetectie en -therapie.

In eerste instantie probeerden we het antigeen 14C5 op te zuiveren via affiniteitschromatografie waarbij 14C5 MAL werd geïmmobiliseerd op een kolom. Met western blot analyse konden geen specifieke eiwitten worden aangetoond, noch in het opgezuiverde SK-BR-3 borstkanker cellysaat, noch in HT-1080 fibrosarcoma cellysaten. Biacore-analyse toonde bovendien aan dat er slechts weinig oplosbaar antigeen 14C5 beschikbaar was in de opgezuiverde SK-BR-3 lysaten (~140 RU). Een mogelijke verklaring voor het falen van deze proeven, is een conformatiewijziging van het antigeen in oplossing ten

opzichte van het membraangebonden antigeen. Daarom werd een andere identificatiestrategie toegepast.

De idee dat het antigeen kon behoren tot de integrine eiwitfamilie werd al aangebracht door De Potter et al. (1994) en Coene et al. (1997). Dit idee werkten we verder uit in een vergelijkende expressiestudie, waarbij met flowcytometrie onder verzadigde condities de expressie van acht verschillende integrine subeenheden (α1, α2, α3, αv, β1, β2, β3, and β4) en drie verschillende integrine heterodimeren (αvβ3, αvβ5, and α5β1) werd vergeleken met die van antigeen 14C5. Deze integrines werden geselecteerd omdat ze betrokken zijn bij kankerpathologie en beschikken over een celadhesie blokkering functie. Enkel anti-αvβ5 specifiek antilichaam (P1F6) toonde een gelijkaardig bindingspatroon als MAL 14C5. MAL 14C5 kon de αvβ5 receptoren significant blokkeren in een blokkeringsstudie. Flowcytometrie met humaan αv and β5 getransfecteerde Colo16 cellen toonde aan dat enkel een subpopulatie waarin beide subeenheden tot expressie werden gebracht, 100% in staat was om MAL 14C5 te binden.

Immunocytochemie en/of flowcytometrie toonde hoge expressie van het antigeen 14C5 in een grote variëteit van kankercellen: ovarium-, baarmoeder-, long-, darm- en pancreascarcinoma, sarcomas en melanomas. De A549 longkanker cellijn toonde de hoogste expressie. Dit biedt de mogelijkheid dat antigeen 14C5 een nieuw doelwit kan zijn voor niet-kleincellige longkankertherapiën. Immunohistochemie van longkanker en darmkanker weefsels toonde aan dat het antigeen 14C5 voornamelijk tot expressie komt in het stroma en op de stromale fibroblasten die de tumorcellen omringen. Momenteel verkennen vele onderzoeksgroepen de mogelijkheid om de ruimte rondom de tumor als doelwit te kiezen voor diverse therapieën, in plaats van de tumorcellen zelf en dit kan eveneens een mogelijke strategie worden met MAL

14C5. Verder onderzoek moet uitwijzen of het antigeen 14C5 een indicator kan zijn voor het kankergeassocieerde fibroblast fenotype.
Voor verder karakterisatie van het antigeen werd de immunohistochemische studie van longkanker en darmkankerweefsels eveneens uitgevoerd met het αvβ5 specifieke antilichaam (P1F6). Er werd geen verschil gevonden in het expressiepatroon, wel was de aankleuring met P1F6 sterker zowel voor de specifieke binding, als voor de niet-specifieke binding.

In het tweede deel van de thesis werd het gebruik van radiogejodeerd MAL 14C5 als een radiotherapeutisch en/of een radiodiagnostisch farmacon onderzocht. Verzadigingsexperimenten toonden een hoge affiniteit tussen MAL 14C5 en zijn antigeen (K_d, 0.2 ± 0.1 nmol/l, A549 longkanker cellen). Een hoge specifieke tumoropname en een kwalitatieve planaire beeldvorming werden aangetoond in tumordragende naakte muizen. Echter, de bloedklaring van het farmacon was traag en typisch voor een 150 kDa monoklonaal antilichaam.
Fab en $F(ab')_2$ fragmenten werden gemaakt met behulp van een ficine geïmmobiliseerde kolom. Verzadigingsexperimenten met radiogejodeerd $F(ab')_2$ toonden een hoge affiniteit (K_d, 0.4 ± 0.1 nmol/l), terwijl radiogejodeerd Fab meer affiniteit verloor door zijn enkelvoudige binding (K_d, 2.3 ± 0.4 nmol/l). De bloedklaring was sneller met de Fab and $F(ab')_2$ fragmenten. Alfa halflevens ($t_{½}\alpha$) van Fab, $F(ab')_2$ en MAL 14C5 waren respectievelijk 14.9 min, 21 min and 118 min. De beta halflevens ($t_{½}\beta$) van Fab, $F(ab')_2$ en mAb 14C5 waren respectievelijk 439 min, 627 min and 4067 min. Biodistributies toonden verhoogde tumor-bloed en tumor-spier verhoudingen, maar de absolute tumoropname van beide fragmenten lag beduidend lager dan dat van MAL 14C5. Hierdoor is een verdere optimalisatie van het antilichaam noodzakelijk, vooraleer klinische toepassingen met dit antilichaam mogelijk worden.

Internalisatie kan leiden tot snelle afbraak van een radiogejodeerd antilichaam door blootstelling aan lysosomale afbraak in de cel. Daarom onderzochten we wat er gebeurt met het radiogejodeerde mAb 14C5-antigeen complex na binding van MAL 14C5. Deze studies werden eveneens uitgevoerd met de radiogejodeerde $F(ab')_2$ en Fab fragmenten. Internalisatie van MAL 14C5 en zijn $F(ab')_2$ fragmenten werd aangetoond in A549 cellen, zowel indirect met confocale microscopie als direct met radiogejodeerde eiwitten. Twee uur na internalisatie konden geen afbraakprodukten als gevolg van het internalisatie-proces worden waargenomen. Bovendien bleef de hoeveelheid ongebonden jood en jood-monotyrosine vrijgesteld in het supernatans lager dan 5%. Deze data suggereren dat zowel MAL als $F(ab')_2$ fragmenten internalizeren, maar dat hun afbraak traag verloopt. Internalisatie met radiogejodeerd Fab fragmenten werd nauwelijks waargenomen. Dit doet denken dat een bivalente binding van het antilichaam met zijn antigeen noodzakelijk blijkt vooraleer internalisatie kan doorgaan. Hoewel evenmin afbraakprodukten met radiogejodeerd Fab werden waargenomen, vertoonde dit fragment een snelle dissociatie. Dit kan verdere toepassingen van Fab 14C5 bij patiënten limiteren.

Genetische manipulatie maakt het mogelijk om de structuur en de karakteristieken van een volledig antilichaam te wijzigen, zodat gunstige farmacokinetische eigenschappen worden behaald die optimaal zijn voor gebruik bij patiënten. Om deze mogelijkheid te onderzoeken werden de variabele lichte keten en variabele zware keten genen van MAL 14C5 gesequentieerd. De complementaire determinerende regio's die karakteristiek zijn voor MAL 14C5 werden geïdentificeerd. Dit opent de weg naar de constructie van alternatieve antilichaamfragmenten met gunstigere farmacokinetische eigenschappen en verminderde immunogeniciteit. Dit laat eveneens toe een bredere waaier radioisotopen te gebruiken en andere componenten, zoals toxines en therapeutische stoffen, aan MAL 14C5 te

koppelen. Bispecifieke antilichamen kunnen worden aangemaakt, waardoor ook pretargeting strategieën en andere immunotherapeutische strategieën tot de nabije toekomst van het 14C5 antilichaam kunnen behoren.